Les isotopes du fer en tant que traceur des cycles biogéochimiques dans l'océan et à ses interfaces

F. Lacan

Université Toulouse III –Paul Sabatier
Ecole doctorale Sciences de l'Univers, de l'Environnement et de l'Espace

Thèse
Présentée par

Francois Lacan

En vue de l'obtention du diplôme d'Habilitation à Diriger des Recherches

Les isotopes du fer en tant que traceur des cycles biogéochimiques dans l'océan et à ses interfaces

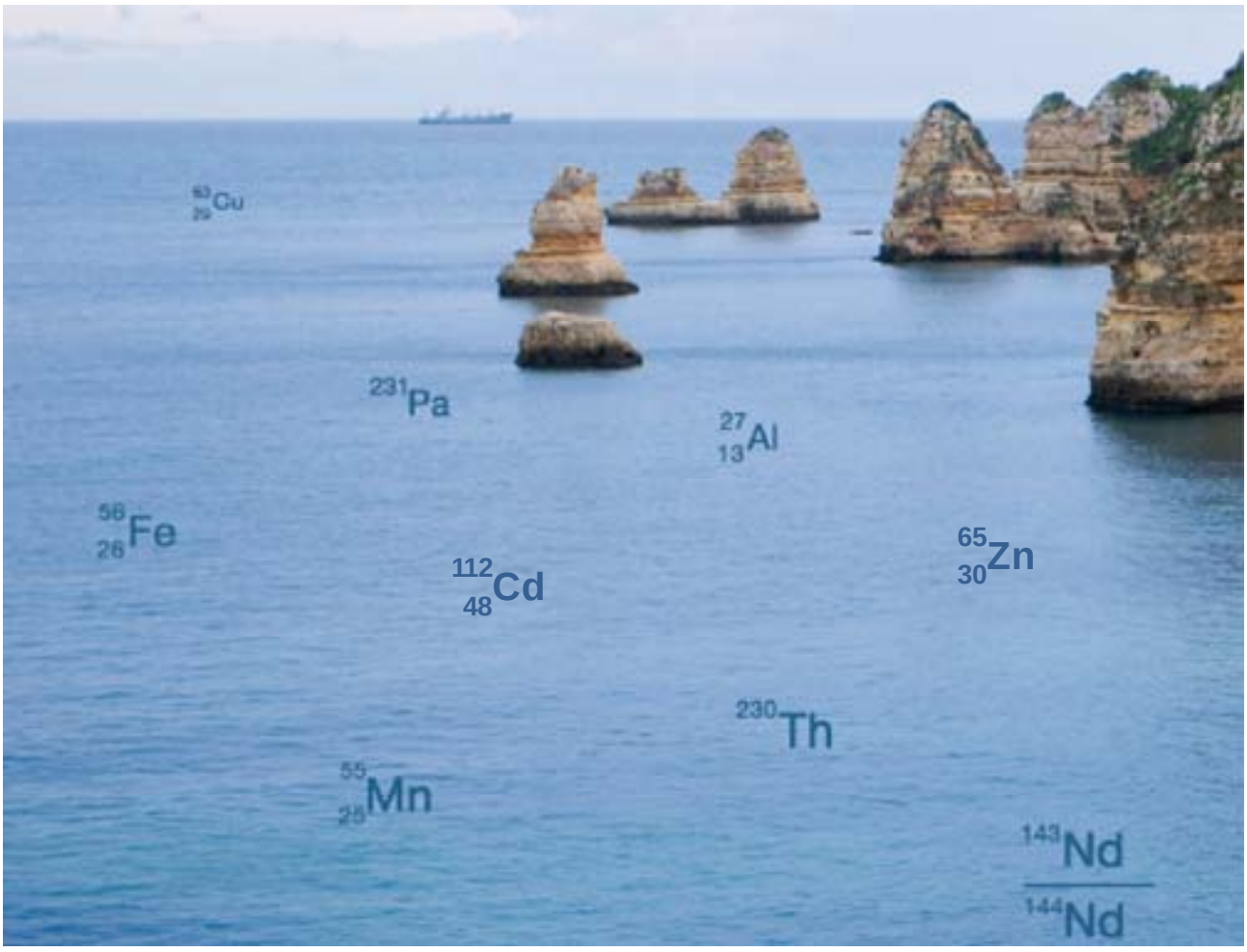

A ma mère et à mon père

Remerciements

Je remercie en 1er lieu tout particulièrement Kathy Pradoux et Marc Souhaut. Tous deux assistants ingénieur dans l'équipe de géochimie marine du LEGOS, ils réalisent quotidiennement un travail qui force l'admiration et sont pour moi un soutien de tous les instants.

Merci à Catherine Jeandel qui m'a formé à la recherche, qui m'a fait confiance et qui n'a céssé de me soutenir depuis maintenant quinze ans. Je ne serais pas là sans elle.

Je remercie mes trois étudiants à ce jour, Amandine Radic, Marie Labatut et Cyril Abadie, compagnons de recherches.

Merci à Pieter van Beek, Tristan Rousseau, Mélanie Grenier, Ester Garcia-Solsona, Virginie Sanial, Michael Bourquin, Elena Masferrer-Dodas, Bruno Lansard, Thomas Arsouze, Yan Zhang, Célia Venchiarutti, Erika Sternberg, Matthieu Roy-Barman, Laurent Coppola, Kazuyo Tachikawa, Roseanna Arraes-Mescoff et Géraldine Sarthou, tous passés par ou encore à l'équipe de géochimie marine du LEGOS et qui ont contribué au travail et à la joie au travail.

Un énorme merci aux secrétaires et gestionaires du LEGOS, Martine Mena, Nadine Lacroux, Brigitte Cournou et Agathe Baritaud.

Merci aux membres du service ICPMS de l'Observatoire Midi Pyrénées et aux personnes qui gravitent autour, Jerôme Chmeleff, Fred Candaudap, Aurélie Lanzanova, mais aussi, Franck Poitrasson, Jeroen Sonke, Jonathan Prunier et Manu Henry. Merci aussi à Michel Valadon et Remi Freydier.

Je remercie aussi très sincèrement les membres du service informatique du LEGOS, Bruno Buisson, Mathieu Pourcel, Philippe Techine et Christian Naskas.

Et un gros merci aussi aux membres du service entretient de l'Observatoire, Didier Papais, Jean-Marc le Dantec, Bertrand Sautereau, et aujourd'hui Tiphaine Jolivet.

MERCI A TOUS !!!!

Enfin, un grand merci du fond du coeur à ma femme Paula et mes filles Pauli et Jeanne, qui m'ont soutenu et qui ont accepté mes absences notamment pendant les campagnes en mer ou un investissement parfois excessif au travail à leur détriment.

Table des matières

Liste des Figures

LISTE DES FIGURES

Drôle d'exercice que de rédiger une thèse d'Habilitation à Diriger des Recherches. Quoi faire ? J'ai entendu plusieurs sons de cloches. Il y aurait 2 possibilités. L'une consisterait à faire une synthèse de ses propres travaux, alors que l'autre consisterait à faire une synthèse de l'état actuel des connaissances sur le sujet central de ses recherches. Dans les deux cas, des perspectives sont attendues. Il me semble que ces deux options sont très différentes.

Afin de trancher, je m'en réfère aux textes de références sur le sujet et aux recommandations du Conseil Scientifique de l'Université Toulouse 3, qui écrit je cite:

L'habilitation à diriger des recherches "sanctionne la reconnaissance d'un haut niveau scientifique, le caractère original d'une démarche, la maitrise d'une stratégie de recherche dans un domaine large et la capacité à encadrer de jeunes chercheurs" (arrêté du 23 novembre 1988, modifié par les arrêtés des 13 février 1992 et 13 juillet 1995, interprété par les circulaires des 5 janvier 1989 et 16 novembre 1992).

Le document doit […] revêtir une dimension personnelle. […] Ces deux parties devront être contextualisées et présenter un itinéraire original. […] Le document fera apparaitre une réflexion sur le cheminement scientifique du candidat, sa cohérence, sa stratégie autonome de recherche, sa capacité de synthèse […], sa compétence pour l'encadrement de jeunes chercheurs. Il devra inclure une perspective scientifique.

Je vais m'efforcer de suivre ces lignes directrices, et donc centrer ce manuscrit sur mes propres travaux, tout en les contextualisant.

I. Eléments de contexte

1. Parcours

a. Genèse

S'il est question de démarche personnelle alors allons-y. Enfant et adolescent, j'ai passé la plupart de mes vacances, en famille, au bord de la mer, sur une ile de la Manche. Petit à petit s'est créé en moi un amour de la mer. Parallèlement, nul dans toutes les disciplines littéraires, j'ai aimé dès le départ les sciences dures, physique, chimie, biologie et géologie, surtout la physique. J'ai donc suivi une formation universitaire de physicien, à l'Université Paris 6. En maîtrise de physique, je me suis naturellement orienté vers l'océanographie, suivant les conseils de ma mère.

Mes premiers travaux de recherche ont porté sur l'assimilation de données, plus précisément *l'Adaptation d'algorithmes variationnels à la restitution des champs de traceurs et de vitesses d'écoulements intervenant dans les phénomènes d'advection et de diffusion* (mémoire de maîtrise, sous la direction du Professeur Gueorgui Khomenko). Ce travail, faisait intervenir des notions mathématiques assez complexes, multiplicateurs de Lagrange, notion d'espace dual (je vous assure qu'un bouquin sur les théories de Lagrange écrit en russe, c'est ardu). Je me dirigeais donc tout droit vers une carrière d'océanographe physicien, si je n'avais été ébloui par le cours de physico-chimie de l'atmosphère de Monsieur Gérard Mégie (alors pour moi un illustre inconnu; j'appris plus tard la dimension de la personne). Ce cours fascinant m'a fait prendre conscience que la physique ne régit pas tout, et que par exemple le climat sur terre est largement contrôlé – à certaines échelles de temps du moins - par la composition chimique de l'atmosphère.

La synthèse que je pouvais faire de ce que j'avais appris jusque là me poussait à définir ma thématique de recherche d'intérêt de la manière suivante:

Les grands cycles de la matière au sein de l'océan

Cet objectif ne m'a jamais quitté, il reste au centre de mes motivations scientifiques aujourd'hui.

J'ai donc choisi de m'orienter vers les cycles biogéochimiques lors de mon année de préparation du Diplôme d'Etude Approfondie "Océan Atmosphère Biosphère", à Toulouse. Au moment de choisir mon stage, j'ai donc naturellement postulé pour le seul sujet proposé concernant à la fois l'océan et les cycles biogéochimiques. Il s'agissait d'un stage sur les isotopes du néodyme dans l'océan Pacifique Equatorial, encadré par C. Jeandel. L'idée étant de tracer les origines du fer, potentiellement apporté par la Papouasie Nouvelle Guinée, jusqu'au centre de l'Océan Pacifique. A partir de cet instant les choses étaient parties, je n'ai plus quitté le domaine de la géochimie marine, avec une forte dominante isotopique.

Si je raconte ce parcours initial, ce n'est pas par pure nostalgie. Il expose mes motivations profondes et ma formation initiale. Ce virage de la physique vers la géochimie implique que je pratique la géochimie, sans avoir suivi de formation sérieuse en chimie. C'est un handicap qui limite certains aspects de mes recherches. D'un autre coté, je suis particulièrement à l'aise (pour un géochimiste) pour ce qui est de la physique participant à nos objets d'étude.

Le cheminement de mes activités de recherche fait l'objet de la partie majeure de ce manuscrit, Chapitre II, ci-après. Je ne rentrerai pas dans les détails ici, mais je vais expliquer brièvement ce parcours et son articulation.

b. Cheminement scientifique

J'ai entamé mes recherches en géochimie marine au Laboratoire d'étude en Géophysique et Océanographie Spatiales (LEGOS, CNES, CNRS, IRD, Univ. Toulouse 3), sur les isotopes du néodyme, en stage de DEA. Ce stage était dirigé par Catherine Jeandel, responsable de l'équipe de géochimie marine. A la suite de ce stage, j'ai poursuivi en doctorat sur la même thématique, les isotopes du néodyme, mais cette fois-ci dans l'océan Nord Atlantique. En deux mots, ce travail m'a montré **l'intérêt de l'outil isotopique pour étudier les questions de flux de matière à l'interface continent/océan**, et le devenir de ces apports de matière au sein de la colonne d'eau. Ces questions sont notamment pertinentes pour l'étude du cycle du fer qui joue un rôle particulièrement important sur les grands cycles océaniques.

Ensuite, j'ai réalisé un premier postdoc à la Woods Hole Oceanographic Institution (Etats Unis d'Amérique), sur la thématique des isotopes du cadmium dans l'océan, en collaboration avec Roger François. Ce travail m'a familiarisé aux questions des cycles biologiques océaniques (le Cd étant impliqué dans la production primaire) et m'a montré que j'étais capable de réaliser des **développements analytiques de tout premier plan** (ayant réalisé les 1ères mesures d'isotope du Cd dans l'eau de mer).

Ces deux expériences m'ont permis de construire mon projet de recherche pour le CNRS. Plutôt que d'utiliser les isotopes du néodyme pour tracer les flux de matière, notamment de fer, des continents vers l'océan et au sein de l'océan, il était opportun (compte tenu des développements instrumentaux) de développer **un nouveau tracer du cycle du fer, la composition isotopique du fer lui-même**. Ce nouveau traceur devait permettre de répondre à des questions sur les sources de fer qui faisaient débat, j'y reviendrai.

Avant de pouvoir réaliser ce projet, j'ai effectué un 2nd postdoc au Laboratoire des Sciences de l'Environnement (LSCE, CEA-CNRS-UVSQ), sur la modélisation des traceurs ^{231}Pa et ^{230}Th dans un modèle global couplé circulation océanique / biogéochimie, en collaboration avec Jean-Claude Dutay. Ce travail a **renforcé mon intérêt pour l'étude des interactions dissous/particules** dans le cadre d'études des cycles biogéochimiques marins.

J'ai interrompu ce postdoc au LSCE ayant été admis chargé de recherche au CNRS (en 2005, à 30 ans). J'ai ainsi commencé le projet de recherche évoqué ci-dessus sur les isotopes du fer, de retour

au LEGOS, dans l'équipe de géochimie marine, où je retrouvais (parmi d'autres) Catherine Jeandel. Je suis ensuite passé chargé de recherche de 1ère classe au CNRS en 2009.

Ainsi, même si mes thématiques de recherche ont varié depuis mes débuts, isotopes du Nd, puis du Cd, puis modélisation du $^{231}Pa/^{230}Th$ et aujourd'hui isotope du fer, je considère ce cheminement tout à fait logique. Ma thématique de recherche sur les isotopes du fer s'est construite sur un trépied constitué de mon doctorat et de mes 2 postdocs. Cette diversité alimente aujourd'hui constamment mes travaux centrés sur le fer, que je conduis donc depuis près de 8 ans.

2. Cadre des travaux

Cette partie décrit le cadre dans lequel j'effectue mes recherches.

a. Contexte local, national et international

L'équipe de géochimie marine, "GEOMAR", du LEGOS comprend, pour ce qui concerne les chercheurs, une directrice de recherche, Catherine Jeandel, dont la thématique principale est centrée sur l'usage des isotopes du néodyme et Pieter van Beek, maître de conférences, dont la thématique principale est centrée sur l'usage des isotopes du radium. L'équipe comprend aussi 3 assistant ingénieurs, Marc Souhaut, Kathy Pradoux et, depuis mi 2011, Vincent Bouvier. Nous sommes donc 6 personnels permanents à ce jour. Une douzaine de personnes en tout. C'est une petite équipe, très liée, dont les différents membres travaillent en synergie très forte. La majorité de notre travail est structurée par des grands projets, la plupart du temps internationaux, centrée sur une campagne océanographique de grande envergure. La

Figure 1 illustre les campagnes auxquelles l'équipe a participé depuis mon recrutement.

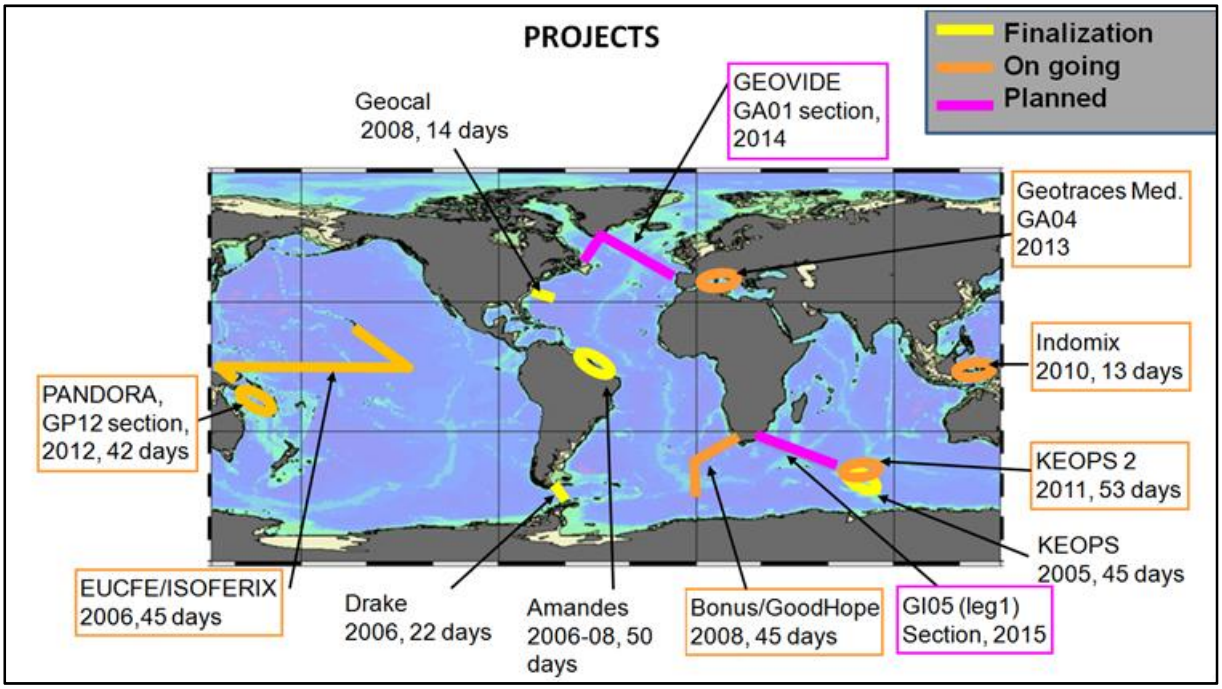

Figure 1: Campagnes en mer de l'équipe GEOMAR, depuis 2005.

Bien que chaque chercheur de l'équipe ait ses thématiques propres, ces campagnes nous permettent de nous retrouver sur des questions communes et ainsi de mettre en œuvre une **approche multi-traceurs, à l'échelle de l'équipe**. Pour illustrer cette stratégie, je vais prendre l'exemple du projet KEOPS (P.I. S. Blain) dont l'objectif principal était de comprendre les mécanismes de fertilisation naturelle de l'océan austral dans la région des îles Kerguelen. Alors que les isotopes du néodyme nous ont permis de quantifier les apports de matière érodée depuis les îles de la région, les isotopes du radium nous ont fourni des informations sur le transport de ces apports au sein de la colonne d'eau (advection horizontale versus mélange vertical), tandis que les isotopes du fer nous ont apporté des contraintes sur l'impact des sources sédimentaires profondes vers la surface. Naturellement ce travail d'équipe s'intègre plus largement dans le cadre de ces projets nationaux et internationaux, dont certains impliquent nos collègues physiciens du LEGOS.

Je dirais donc que mon activité de recherche est en partie dictée par mes choix, mais résulte aussi en partie d'une **dynamique d'équipe, d'une dynamique de laboratoire, d'une dynamique nationale et d'une dynamique internationale**. J'apprécie beaucoup cette situation, qui me semble équilibrée. Ces grands projets collaboratifs sont extrêmement riches, en ce que les échanges de connaissances qu'ils génèrent permettent de tirer le maximum des mesures de chacun. Aujourd'hui et dans la décennie à venir, mon activité va être fortement liée au programme **GEOTRACES** (Scientific Committee on Oceanic Research), dont je suis aussi un acteur.

Bien qu'il soit très clair dans mon esprit, et dans mon activité quotidienne, que ma thématique de recherche est centrée sur les isotopes du fer, le fait est que je travaille dans la même équipe que mon ex-directrice de doctorat, qui poursuit ses travaux sur les isotopes du néodyme (sujet de mon doctorat). Il va de soi que mes collaborations avec Catherine Jeandel sont extrêmement étroites. Par le biais de cette **collaboration privilégiée, je garde un contact continu avec les recherches sur la thématique des isotopes du néodyme et des concentrations de terres rares**.

b. Projets

Ci-dessous la liste des projets (appels d'offres nationaux) dans le cadre desquels j'ai travaillé.

SIGNATURE/GINS (INSU, PI C. Jeandel, LEGOS). 1999-2002. Neodymium isotopic composition in the North Atlantic

OceanicCdIC (NSF, WHOI, PI. R. Francois). 2003. Cadmium isotopic composition in the ocean

MOZAIQUE (INSU, PI. J-C Dutay, LSCE). 2006-2009. Modeling of trace elements in the ocean: Neodymium (Nd), Protactinium (Pa) and Thorium (Th)

KEOPS (INSU, PI. S. Blain. LOB). 2005-2007. KErguelen: compared study of the Ocean and the Plateau in Surface water

ISOFERIX (INSU, PI. F. Lacan, LEGOS). 2006-2008. ISOtopic tracing of Fe sources in the Equatorial Pacific: impact on new primary production and nitRogen fIXation (EUCFE cruise)

BONUS-GOODHOPE (LEFE, ANR, PIs M. Boyé LEMAR, S. Speich LPO, **responsable LEGOS F. Lacan**). 2007-2012. Interactions between the dynamic, circulation, biogeochemistry and geochemistry in the Atlantic sector of the Southern Ocean and its exchanges with the Indo-Atlantic connection.

GEOCAL (INSU, PI. F. Lacan, LEGOS). 2008-2010. A French contribution to the GEOTRACES intercalibration effort (Fe, Nd and Ra isotopes, 231Pa, 230Th)

INDOMIX (INSU, PI. A. Koch-Larrouy, LEGOS). 2010-2012. Physical and geochemical transformations within the Indonesian throughflow.

KEOPS2 (INSU-ANR, PI. S. Blain, LOMIC, responsable LEGOS P. van Beek). 2011-2014. Kerguelen Ocean and plateau compared study 2.

SOLWARA (INSU-ANR, PI. A. Ganachaud, LEGOS, responsable géochimie C. Jeandel). 2008-2013. Physical and geochemical transformations within the Salomon Sea.

OPTIMISP (INSU, PI. F. Lacan, LEGOS). 2012. Optimization of In Situ Pumps.

Je viens par ailleurs de déposer un projet à l'ERC (European Research Council) en tant que PI, et je suis partenaire de 2 ARN qui viennent d'être déposées (**GEOVIDE** une section GEOTRACES dans l'Atlantique Nord en collaboration avec le LEMAR, et **ISOFEREXT** sur les isotopes du fer dans les enveloppes superficielles, en collaboration avec le GET)…

c. Campagnes

Ci-dessous la liste des campagnes auxquelles j'ai participé, avec ou sans embarquement (voir aussi Figure 1).

Depuis mon recrutement, j'essaie de planifier environ 1 campagne tous les 2 ans. S'agissant de métaux traces, la préparation des campagnes est très lourde. De plus les mesures prévues étant extrêmement délicates, elles sont aussi très demandeuses en temps et énergie. Compte tenu de cela, ce rythme est largement suffisant.

TIP2000 : R/V Marion Dufresne, IFRTP, France, Sep. 2000, Indonésie – Australie, embarquement de 21 jours.

KEOPS : R/V Marion Dufresne, IPEV, France, Jan. Fev. 2005, Région des Kerguelen, participation sans embarquement.

EUCFe - ISOFERIX : R/V Kilo Moana, Univ of Hawaii, Sept. Oct. 2006, Hawaii – Papouasie Nouvelle Guinée, embarquement de 45 jours.

BONUS-GOODHOPE (GIPY4): R/V Marion Dufresne, IPEV, Fév. Mar. 2008, Afrique du Sud – Océan Austral, embarquement de 42 jours.

Intercalibration GEOTRACES : R/V Knorr, Jun-July 2008, Atlantique Nord, participation sans embarquement.

INDOMIX : R/V Marion Dufresne, IPEV, July 2010, Indonésie, embarquement de 13 jours.

KEOPS 2 (GIpr01): R/V Marion Dufresne, IPEV, France, Nov. Déc. 2011, Région des Kerguelen, participation sans embarquement.

PANDORA (GP12): R/V Atalante, Ifremer, July August 2012, Mer des Salomon, embarquement de 42 jours.

GEOTRACES Méditerranée (GA04): R/V Pelagia, Pays Bas, Mai-Juil. 2013, Mer Méditerranée et Mer Noire, participation sans embarquement.

3. Responsabilités collectives

J'ai pris la responsabilité de l'équipe de géochimie marine du LEGOS au 1er janvier 2011 (il y a un peu plus de 2 ans). L'équipe compte aujourd'hui 13 personnes, dont 3 chercheurs, enseignants chercheurs, 3 assistant ingénieurs, 1 CDD *international project officer* du programme GEOTRACES qui n'est pas sous ma responsabilité, 1 postdoc et 5 doctorants. En termes de management, j'ai instauré 2 choses qui me semblent importantes.

J'organise des réunions d'équipe régulières, toutes les 2 semaines à horaire fixe (autant que possible). Ces réunions comportent 2 parties, une partie scientifique qui n'a lieu qu'une fois sur 2, donc une fois par mois, et une partie gestion, qui a lieu à chaque fois. Les parties scientifiques permettent de discuter en équipe (et parfois avec des invités) des résultats obtenus au sein de l'équipe, ou encore d'articles publiés par la communauté. Ces discussions scientifiques mensuelles au sein de l'équipe permettent d'entretenir une **forte dynamique scientifique d'équipe**. Les parties de gestion, auxquelles assiste principalement le personnel permanent de l'équipe, nous permettent de gérer les questions logistiques, financières, d'infrastructures (qui sont très lourdes dans l'équipe, avec une salle blanche et un laboratoire souterrain), mais aussi stratégiques telles que par exemple les réponses aux divers appels d'offre (LEFE, ANR…), les demandes de bourses de thèses, ou encore la gestion des ressources humaines au sein du groupe, notamment le travail demandé aux assistants ingénieurs.

Cela me mène au 2ème point important. J'ai mis en place (même si à l'époque je n'étais pas responsable d'équipe) une **gestion trimestrielle des tâches et de leurs priorités demandées aux assistants ingénieurs**. La diversité de ses tâches, de la comptabilité à la gestion d'infrastructures lourdes, en passant par les travaux scientifiques avait conduit à une surcharge de demande provenant des chercheurs, enseignants chercheurs, qui avait 2 conséquences néfastes: i) les assistants ingénieurs étaient soumis à une pression excessive, ii) la gestion des priorités des tâches était défaillante. Nous établissons donc désormais tous les 3 mois, en concertation entre chercheurs enseignants chercheurs et assistants ingénieurs, un bilan de l'activité du trimestre passé et un projet d'activité pour le trimestre à venir. Les priorités y sont clairement définies. Cette période de 3 mois est suffisamment longue pour permettre à l'assistant ingénieur d'organiser son travail et de faire face aux imprévus, et suffisamment courte pour conserver une bonne dynamique.

En juillet 2011, l'arrivée d'un 3ème assistant ingénieur, a conduit à une redistribution des tâches et à un allègement de la pression sur les 2 assistants ingénieurs qui étaient déjà présents.

J'ai pris la **responsabilité scientifique du service commun de spectrométrie de masse à source plasma (ICPMS) de l'Observatoire Midi Pyrénées** en novembre 2012. Il s'agit d'une responsabilité importante. Ce service est extrêmement actif et joue un rôle majeur sur le rayonnement et l'attractivité de l'Observatoire Midi Pyrénées. **L'acquisition d'un second ICPMS à multi-collection (Neptune Plus) est prévue courant 2013**.

Je suis membre du comité de gestion de ce service depuis 2006.

Depuis mon recrutement en 2005, j'ai pris la **responsabilité des salles blanches du LEGOS**. C'est une tâche qui s'est avérée très lourde. Les infrastructures associées sont importantes et étaient dans un état de vétusté problématique, consécutif à un désengagement progressif de l'UMS OMP dans la gestion de ces infrastructures (lui-même consécutif à un déficit criant en personnel sur ce segment). Quelques exemples. L'humidité dans les salles pouvait atteindre 100%, ce qui provoquait une condensation sur les plafonds d'où des gouttes tombaient ensuite sur les paillasses. La pureté de l'air n'était pas contrôlée, et s'est avérée peu satisfaisante pour des travaux sur le fer dans l'océan. Par temps particulièrement froid, les températures en salle n'étaient plus maintenues, elles descendaient jusqu'à ~13°C, ou pire, le système entier de traitement d'air s'arrêtait de sorte que les salles n'étaient plus en surpression d'air filtré. Les pieds de paillasse rouillaient. Je pourrais continuer la liste.

De gros travaux ont été réalisés (~150k€), avec l'aide très importante de nos 3 assistants ingénieurs. Aujourd'hui, la pression, la température et l'hygrométrie des salles blanches sont précisément maîtrisées en toute saison. La pureté de l'air est améliorée et contrôlée périodiquement. L'ensemble du système est sous surveillance électronique; nous sommes automatiquement prévenus par email ou téléphone du moindre problème. Je pense que ce gros effort est derrière nous et que la gestion à venir sera plus légère.

Je suis membre élu du conseil scientifique de l'Observatoire Midi Pyrénées, depuis 2009 (mon mandat devrait arriver à terme prochainement).

Je suis membre de la commission informatique du LEGOS, représentant l'équipe GEOMAR depuis 2006.

Je suis webmaster du site de l'équipe GEOMAR depuis 2010 (http://www.legos.obs-mip.fr/recherches/equipes/geomar).

4. Formation, encadrement et enseignement

Je n'ai jamais été particulièrement attiré par l'enseignement académique. Depuis 2011, je donne 10h par an de cours magistraux sur les éléments traces et isotopes en tant que traceurs de processus océanique, en master 2 Océanographie Physique et Biogéochimique à l'Université d'Aix Marseille (j'ai aussi donné ce cours ponctuellement en 2005). J'ai donné 56h de TD/TP en tant que vacataire lorsque j'étais doctorant, et 2 formations au logiciel Ocean Data View, dont l'une dans le cadre de la formation permanente CNRS. C'est peu. C'est un choix. On ne peut pas tout faire. Je tiens néanmoins à conserver un minimum d'enseignements régulièrement. Cela m'aide notamment à garder un certain recul sur mes activités. Ces 10h à Marseille me conviennent parfaitement.

Mon activité de formation consiste donc principalement en l'encadrement de stagiaires, doctorants, postdocs, mais aussi de nos assistants ingénieurs. Je classerais ces activités en 4 catégories: a) l'encadrement direct de mes étudiants (M1, M2, doctorants), b) l'encadrement direct d'étudiants qui me sont confiés lors de campagnes en mer, c) l'encadrement d'étudiants et postdocs, en collaboration (co-encadrement) et d) l'encadrement des ingénieurs et techniciens. Ci dessous la liste de ces encadrements.

Encadrement direct de mes étudiants (M1, M2, doctorants)

3 doctorants sur la thématique des isotopes du fer (cf. ci-dessous):

- Amandine Radic (2007-2011). 100%
- Marie Labatut (2010-2013, thèse en cours), co-encadrement, 90%.
- Cyril Abadie (2011-2014, thèse en cours), co-encadrement, 90%.

1 master 2 :

- Marie Labatut (6 mois en 2010), thématique des isotopes du fer. 100%

1 master 1 :

- Marie Labatut (2 mois en 2009), thématique des particules en suspension. 100%

1 stagiaire BTS chimie 1ère année :

-Manuel Maille (2 mois en 2007), sur du développement analytique de mesures ICPMS. 100%

Thèse d'Amandine Radic:

Amandine à commencé sa thèse en octobre 2007. Elle a soutenu en janvier 2011. Amandine a tout d'abord terminé le travail de développement analytique permettant, pour la 1ère fois, la mesure des isotopes du fer dans l'océan. Elle a ensuite travaillé sur des échantillons naturels en provenance du Pacifique Equatorial et de l'Océan Austral. Au cours de sa thèse elle a publié 1 article en 1er auteure

et 3 articles en co-auteure (Rang A); elle a 2 talks en 1er auteure et 8 talks en co-auteurs (congrès internationaux), 2 posters en 1er auteure et 2 posters en co-auteure (congrès internationaux). Elle a participé à une campagne en mer importante (Bonus/GoodHope, 42j embarqués). Elle a passé 3 mois au CALTECH (USA) en visite chez Seth John (qui est le seul autre chercheur dont le groupe produit aujourd'hui des mesures d'isotopes du fer dans l'océan ouvert), financé par une bourse ATUPS (Univ. Paul Sabatier). Je retiens la conclusion du président du jury: "c'est une thèse qui fera date". Suite à son doctorat, Amandine a souhaité réfléchir à son avenir et ne pas foncer tête baissé vers un postdoc. Elle hésitait avec le métier d'institutrice. Je l'ai naturellement prévenu de l'handicap que constituerait une durée prolongée sans activité si elle optait finalement pour la recherche. Elle a néanmoins préféré prendre le temps de réfléchir. Elle passe actuellement les concours d'instituteurs. De ce fait elle n'a pas publié ses derniers travaux. Je le ferai, ou ils seront repris par Cyril Abadie (thèse en cours).

Thèse de Marie Labatut (en cours, à ce jour, mars 2013, il reste 6 mois):

J'ai encadré Marie en M1 puis en M2, puis en thèse. Elle a commencé cette dernière en octobre 2010. Sa soutenance est prévue en septembre 2013. Son sujet de thèse porte sur le cycle des isotopes du fer dans le Pacifique Equatorial. Amandine Radic n'avait mesuré que 2 des 15 profils prélevés au cours de la campagne EUCFe. Au cours de ses 2,5 année de thèse, Marie a publié 3 articles en co-auteure, elle a 2 talks en 1er auteure et 3 talks en co-auteurs (congrès internationaux), 1 posters en 1er auteure et 4 posters en co-auteure (congrès internationaux). Elle a participé à 2 campagnes en mer importantes (Indomix et Pandora, respectivement 13 et 42 jours embarqués). Nous avons rencontré de très grosses difficultés avec les instruments de mesures à Toulouse qui était hors service pendant environ la moitié de sa thèse. Cela nous a conduit à aller faire des mesures à Strasbourg (LHyGeS) et à Gif sur Yvette (LSCE). Marie n'a pu utiliser avec succès le MC-ICPMS de Toulouse qu'en février 2013 ! Malgré cela, elle a aujourd'hui l'ensemble de ses mesures, et dispose donc de ses 6 derniers mois de thèse pour interpréter ses données et rédiger son manuscrit. Son travail soutenu depuis qu'elle a commencé (en M1) permet d'envisager au moins 2, si ce n'est 3 publications en 1er auteure.

Cyril Abadie (en cours, à ce jour, mars 2013, il en est à mi-thèse)

Le sujet de Cyril porte sur les isotopes du fer dans l'Atlantique Sud ainsi que dans le secteur Atlantique de l'Océan Austral. De même que dans le Pacifique, Amandine n'avait analysé qu'une partie des échantillons. Le sujet de Cyril comporte aussi une partie expérimentale. Il s'agira de mesurer des échantillons d'incubation de phytoplancton afin d'estimer les fractionnements isotopiques associés à la consommation du fer par le phytoplancton. Les incubations ont été réalisées au cours de la campagne KEOPS2, en collaboration avec le LEMAR (Brest). A mi thèse, le bilan en terme de production scientifique est forcément léger, 1 poster en 1er auteur lors d'un Workshop international (à Londres), et en co-auteur, 1 talk en conférence internationale, 1 talk au Workshop de Londres et un talk à un après midi Scientifiques de la Sociétés Françaises des Isotopes Stables. Il est prévu que Cyril embarque sur la campagne GEOVIDE, qui nous l'espérons aura lieu en 2014.

<u>Encadrement direct d'étudiants qui me sont confiés lors de campagnes en mer</u>

2 doctorants réalisant des prélèvements en vue de mesures d'isotopes du néodyme et de concentrations de terres rares (pendant le temps de la campagne à 100%) :

- Thomas Arsouze, campagne Bonus/GoodHope, 42 jours de mer (2008).
- Célia Venchiarutti, campagne EUCFe/ISOFERIX, 45 jours de mer (2006).

Il va sans dire que j'encadre aussi mes propres étudiants (ci-dessus) lors des campagnes en mer.

Encadrement d'étudiants et postdocs, en collaboration (co-encadrement)

Comme je l'ai indiqué plus haut, je collabore étroitement avec Catherine Jeandel sur la thématique des isotopes du néodyme et des concentrations de terres rares (REE). Dans ce cadre, même si je n'ai pas officiellement co-encadré les étudiants et postdocs ci-dessous, j'ai, en pratique, supervisé directement leurs mesures de concentration de REE sur ICPMS, et de ce fait, en pratique participé à des degrés variables à leur encadrement.

2 postdocs :

- Yan Zhang (2 ans, 2006-2008), co-encadrement à 60%.
- Ester Garcia-Solsona (2 ans et 7 mois, 2010-2013), co-encadrement, 15%.

1 doctorant :

- Mélanie Grenier (3 ans, 2009-2012), co-encadrement, 10%.

4 masters 2 :

- Hélène Delattre (5 mois en 2010), co-encadrement, 15%
- Mélanie Grenier (5 mois en 2009), co-encadrement officiel, 20%.
- Alexandre Cros (5 mois en 2008), co-encadrement officiel, 20%.
- Olivier Lauret (4 mois en 2001), co-encadrement, 20%.

1 master 1

Olivier Lauret (2 mois, 2000), co-encadrement, 20%.

Encadrement des ingénieurs et techniciens

Il ne s'agit pas ici de former de potentiels jeunes chercheurs, mais il s'agit tout de même d'une formation scientifique ou technique ou sur d'autres aspects.

3 IT dans le cadre de l'équipe de géochimie marine du LEGOS

- Catherine Pradoux, AI CNRS, permanente de l'équipe. Co-encadrement (50%) de 2005 à 2011 sur les mesures de concentrations de REE par ICPMS et la gestion de la salle blanche du LEGOS puis encadrement complet (100%) depuis 2011 sur les questions de fonctionnement de la salle blanche et la thématique des isotopes du fer.
- Marc Souhaut, AI CNRS, permanent de l'équipe. Co-encadrement (50%) depuis 2005, sur les questions d'infrastructure salle blanche et depuis 2011 de gestion comptable de l'équipe (20%).
- Vincent Bouvier, AI CNRS, permanent de l'équipe. Co-encadrement depuis 2011, sur la gestion des infrastructures et fonctionnement des salles blanches (50%).

Je voudrais revenir maintenant sur l'encadrement de mes propres étudiants et dire deux ou trois mots sur la manière dont j'envisage l'encadrement de jeunes chercheurs. On m'a expliqué assez tôt, au cours de l'encadrement de ma 1ère doctorante, que "diriger n'était pas materner" (ce que j'avais tendance à faire). C'est facile à comprendre, pas forcément facile à mettre en œuvre. Il faut pour cela accepter que l'étudiant fasse des erreurs. Dans nos thématiques, cela conduit parfois à perdre des échantillons uniques. En d'autres termes, laisser la liberté nécessaire à ce que l'étudiant s'épanouisse – ne pas utiliser un étudiant comme un ingénieur – est à double tranchant : cela peut conduire à des choses excellentes (si l'étudiant est bon) ou au contraire produire un résultat décevant. Quoi qu'il en soit **ce risque doit être pris, car il est une condition nécessaire à ce que l'étudiant se forme à la recherche**. Je l'ai accepté et mis en œuvre dès le début de l'encadrement de ma 2nd doctorante (et a fortiori pour mon 3ème doctorant). J'avoue avoir certainement trop materné ma 1ère doctorante.

Maintenant, deux ou trois règles que je m'impose.

La première, je m'efforce de rester très disponible pour les étudiants. Je pense y parvenir, je suis finalement assez peu fréquemment en déplacement.

On ne peut pas devenir géochimiste marin sans avoir participé à une campagne en mer. Dans l'équipe, nous nous efforçons donc dans la mesure du possible d'envoyer les étudiants en campagne avant leur soutenance. A ce jour, à ma connaissance, cela a toujours été le cas depuis que je suis dans cette équipe. Les candidats aux bourses de thèses sont d'ailleurs prévenus. Ma 1ère doctorante a passé 42 jours en mer sur la campagne Bonus/GoodHope, la 2nde 55 jours en mer entre les campagnes Indomix et Pandora, et le 3ème a un embarquement prévu sur le projet GEOVIDE (classé A+ par la commission flotte et soutenu par l'INSU).

Les étudiants doivent se confronter au plus tôt à la communauté internationale lors de grands congrès (AGU etc…). En moyenne 1 congrès international par an. Je les encourage, dès que possible, à solliciter une présentation orale plutôt qu'un poster.

Ils doivent naturellement rédiger de la manière la plus autonome possible leurs articles en 1er auteur. Vu le contexte actuel, je les encourage à en rédiger le plus grand nombre possible. Ca n'est pas toujours facile.

J'essaie de les encourager à interagir avec le maximum de personnes dans leur entourage scientifique, ou de ne pas hésiter à contacter tel ou tel chercheur étranger, pour répondre à leurs questions. Je n'ai pas toutes les réponses ! Loin s'en faut !

Si le contexte le permet, je les encourage à aller faire un court séjour chez un collègue à l'étranger.

Je les encourage à monter des petits projets (appels d'offres internes au labo, à l'Université, à GEOTRACES)

Enfin, lorsque l'heure du postdoc arrive (s'ils souhaitent poursuivre en postdoc), je leur recommande fermement de ne pas poursuivre sur un sujet trop proche de celui de leur doctorat, mais au contraire d'explorer de nouvelles thématiques, pour élargir leur vision des choses.

5. Liste de communications

Mise à jour en mars 2013.

Les communications de mes doctorants sont indiquées en **vert.**

Articles dans revues à comités de lecture

xx. Garcia-Solsona, E., Jeandel, C. **Labatut** M., **Lacan F.**, Vance D., Chavagnac V. Rare Earth Elements and Nd isotopes tracing water mass mixing and particle-seawater interactions in the SE Atlantic. *Geochimica et Cosmochimica Acta*, *Submitted*.

27. Yeghicheyan D., C. Bossy, M. Bouhnik-Le Coz, C. Douchet, G. Granier, A. Heimburger, **Lacan F.**, Lanzanova A. Rousseau T., Seidel JL., Tharaud M., Candaudap F., Chmeleff J., Cloquet C., Delpoux S., **Labatut** M., Losno R., Pradoux C., Sivry Y. Sonke J. 2013. A compilation of silicon, rare earth element and twenty one other trace element concentrations in the natural river water standard SLRS-5 (NRC-CNRC), Geostandards and Geoanalytical Research. in press.

26. Rousseau T. , Sonke J.E., Chmeleff J., Candaudap F., **Lacan F.**, Boaventura G., Seyler P., Jeandel C. (2013) Rare earth element analysis in natural waters by multiple isotope dilution - sector field ICP-MS. *Journal of Analytical Atomic Spectrometry*, doi:10.1039/C3JA30332B.

25. Jeandel C., Delattre M., Grenier M., Pradoux C. and **Lacan F.** 2013. Rare Earth Concentrations and Nd isotopes reveal exchange processes along the East Pacific Rise, South East Pacific Ocean. *Geochemistry, Geophysics, and Geosystems*. doi:10.1029/2012GC004309

24. Grenier M., Jeandel C., **Lacan F.**, Vance D., Venchiarutti C., Cros A., Cravatte S. 2012. From the subtropics to the central equatorial Pacific Ocean: neodymium isotopic composition and rare earth element concentration variations. *Journal of Geophysical Research Oceans.*, doi:10.1029/2012JC008239.

23. Boyle E.A., John S., Abouchami W., Adkins J.F., Echegoyen-Sanz Y., Ellwood M., Flegal R., Fornace K., Gallon C., Galer S., Gault-Ringold M., **Lacan F.**, **Radic** A., Rehkamper M., Rouxel O., Sohrin Y., Stirling C., Thompson C., Vance D., Xue Z., Zhao Y. 2012. GEOTRACES IC1 (BATS) contamination-prone trace element isotopes Cd, Fe, Pb, Zn, Cu, and Mo intercalibration. *Limnology and Oceanography Methods*, 10:653-665, DOI: 10.4319/lom.2012.10.653.

22. van de Flierdt, T., Pahnke, K., Amakawa, H., Andersson, P., Basak, C., Coles, B., Colin, C., Crocket, K., Frank, M., Frank, N., Goldstein, S.L., Goswami, V., Haley, B.A., Hathorne, E.C., Hemming, S.R., Henderson, G.M., Jeandel, C., Jones, K., Kreissig, K., **Lacan, F.**, Lambelet, M., Martin, E.E., Newkirk, D.R., Obata, H., Pena, L., Piotrowski, A.M., Pradoux, C., Scher, H.D., Schöberg, H., Singh, S.K., Stichel, T., Tazoe, H., Vance, D., Yang, J. 2012. GEOTRACES intercalibration of neodymium isotopes and rare earth elements in seawater and marine particulates - Part 1: international intercomparison, *Limnology and Oceanography Methods*. 10, 2012, 234–251. DOI 10.4319/lom.2012.10.234.

21. Lacan F, Tachikawa K, Jeandel C. 2012. Neodymium isotopic composition of the oceans: a compilation of seawater data. *Chemical Geology* 300-301, 177-184, 10.1016/j.chemgeo.2012.01.019.

20. Jeandel C., Peucker Ehrenbrink B., Jones M., Pearce C., Oelkers E., Godderis Y., **Lacan F.**, Aumont O., and Arsouze T. 2011. Ocean margins: the missing term for oceanic element budgets? *EOS*, 92, 217–219. PDF

19. Bown J., Boye M., Baker A., Duvieilbourg E., **Lacan F.**, Le Moigne F., Planchon F., Speich S., Nelson D.M. 2011. The biogeochemical cycle of dissolved cobalt in the Atlantic and the Southern Ocean south off the coast of South Africa. *Marine Chemistry*, doi:10.1016/j.marchem.2011.03.008. PDF

18. Radic A., **Lacan F.**, Murray J. 2011. Iron isotope composition of seawater in the Equatorial Pacific Ocean: new constraints for the oceanic iron cycle. *Earth and Planetary Science Letters* 306 1–10, doi:10.1016/j.epsl.2011.03.015. PDF

17. Jeandel, C., Venchiarutti, C., Bourquin, M., Pradoux, C., **Lacan, F**., van Beek, P. and Riotte, J. (2011), Single Column Sequential Extraction of Ra, Nd, Th, Pa and U from a Natural Sample. *Geostandards and Geoanalytical Research*, 35: doi: 10.1111/j.1751-908X.2010.00087.x. PDF

16. Arsouze T., Treguier A.M., Peronne S., Dutay J.-C., **Lacan F.**, Jeandel C. 2010. Modeling the Nd isotopic composition in the North Atlantic basin using an eddy-permitting model. *Ocean Sciences* 6, 789–797, doi:10.5194/os-6-789-2010. PDF

15. Lacan F., Radic A., Labatut, M, Jeandel C., Poitrasson F., Sarthou G., Pradoux C., Chmeleff J., Freydier R. 2010 High precision determination of the isotopic composition of dissolved iron in iron depleted seawater by double spike MC-ICPMS. *Analytical chemistry,* 82, 7103–7111. PDF

14. Arsouze T., Dutay J.-C., **Lacan F.**, Jeandel C. 2009 Reconstructing the Nd oceanic cycle using a coupled dynamical – biogeochemical model. *Biogeosciences, 6, 2829-2846*. PDF

13. Dutay J.-C., **Lacan F**., Roy Barman M., Bopp L. 2009. Influence of particle size and type on ^{231}Pa and ^{230}Th simulation with a global coupled biogeochemical-ocean general circulation model: A first approach. *Geochemistry, Geophysics, and Geosystems*, *10*, Q01011, doi:10.1029/2008GC002291. PDF

12. Lacan, F., A. Radic, C. Jeandel, F. Poitrasson, G. Sarthou, C. Pradoux, and R. Freydier. 2008. Measurement of the isotopic composition of dissolved iron in the open ocean, *Geophys. Res. Lett., 35*, L24610, doi:10.1029/2008GL035841. PDF

11. Arsouze T., Dutay J.-C., Kageyama M., **Lacan F.**, Alkama R., Marti O., Jeandel C. 2008. A modeling sensitivity study of the influence of the Atlantic meridional overturning circulation on neodymium isotopic composition at the Last Glacial Maximum. *Climate of the Past* 4, 191-203. PDF

10. Zhang Y., **Lacan F.** Jeandel C. 2008. Dissolved Rare Earth Elements Trace Terrigeneous Inputs in the Wake of the Kerguelen Island (Southern Ocean). *Deep Sea Research II* 55, 638-652, doi:10.1016/j.dsr2.2007.12.029. PDF

9. Arsouze T., Dutay J.-C., **Lacan F.**, Jeandel C. 2007. Modeling the neodymium isotopic composition with a global ocean circulation model. *Chemical Geology*, 239 165–177, doi:10.1016/j.chemgeo.2006.12.006. PDF

8. Jeandel C., Arsouze T., **Lacan F.**, Dutay J.-C., Téchiné P. 2007. Isotopic Nd compositions and concentrations of the lithogenic inputs into the ocean: A compilation, with an emphasis on the margins. *Chemical Geology* 239, 156–164, doi:10.1016/j.chemgeo.2006.11.013. PDF

7. Lacan F., Francois R., Ji Y. and Sherell R.M. 2006. Cadmium isotopic composition in seawater and phytoplankton culture experiments, *Geochim. Cosmochim. Acta*, 70, 5104-5118, doi:10.1016/j.gca.2006.07.036. PDF

6. Lacan F. and Jeandel C. 2005. Acquisition of the neodymium isotopic composition of the North Atlantic Deep Water, *Geochemistry, Geophysics, and Geosystems*, 6, Q12008, doi:10.1029/ 2005GC000956. PDF

5. Lacan F. and Jeandel C. 2005. Neodymium isotopes as a new tool for quantifying exchange fluxes at the continent-ocean interface. *Earth and Planetary Sciences Letters*, 232, 245-257, doi:10.1016/ j.epsl.2005.01.004 PDF

4. Lacan F. and Jeandel C. 2004. Neodymium isotopic composition and rare earth element concentration in the deep and intermediate Nordic Seas: constraints on the Iceland Scotland Overflow Water signature. *Geochemistry, Geophysics and Geosystems,* 5, Q11006, doi:10.1029/2004GC000742. PDF

3. Lacan F. and Jeandel C. 2004. Subpolar Mode Water formation traced by neodymium isotopic composition. *Geophysical Research Letters*, 31, L14306, doi:10.1029/2004GL019747. PDF

2. Lacan F. and Jeandel C. 2004. Denmark Strait water circulation traced by heterogeneity in neodymium isotopic compositions. *Deep Sea Research I*, 51, 71 –82. PDF

1. Lacan F. and Jeandel C. 2001. Tracing Papua New Guinea imprint on the central Equatorial Pacific Ocean using neodymium isotopic compositions and Rare Earth Element patterns. *Earth and Planetary Science Letters* 186, 497-512. PDF

Thèses

Lacan F. 2002. Nordic Sea and Subarctic Atlantic Water Masses Traced by neodymium Isotopes (*Masses d'eau des Mers Nordiques et de l'Atlantique Subarctique tracées par les isotopes du néodyme*) PhD Thesis. Toulouse III University, France. PDF

Lacan F. 1999. A study of the Neodymium Isotopic Composition in the Equatorial Pacific Ocean (*Etude de la Composition Isotopique du Néodyme dans l'Océan Pacifique Equatorial*). Master Thesis. Toulouse III University, France.

Lacan F. 1998. Adaptation of variational algorithms for the restitution of tracer and flow intensity fields in advection and diffusion processes (*Adaptation d'algorithmes variationnels à la restitution des champs de traceurs et de vitesses d'écoulements intervenant dans les phénomènes d'advection et de diffusion*). Bachelor Thesis. Paris VI University, France.

Autres articles

1. Poitrasson F., Sonke J., **Lacan F.**, Dupre B. 2011. Les isotopes non-traditionnels, nouvelle frontière en géochimie. *Elements*, Volume 7, Number 1, p. 64.

Exposés oraux (talks) dans des conférences internationales ***(invités en violet)***

29. Heimbürger L-E, Sonke J. E., Point D., Labaut M., Pradoux C., Lagane C., **Lacan** F., Jeandel C., Ganachaud A., Eldin G. Methylmercury production and marine boundary exchange – results of the 2012 GEOTRACES West Pacific PANDORA cruise. 11th International Conference on Mercury as a Global Pollutant. Edinburgh, UK, July 2013.

28. Point D., Lorrain A., Heimbürger L-E, Lagane C., Menkes C., Masboul J., Allain V., Sonke J. E., Labaut M., **Lacan** F., Pradoux C., Jeandel C., Eldin G. Methylmercury origin, accumulation and distribution in tuna and swordfish from the southwestern Pacific Ocean. 11th International Conference on Mercury as a Global Pollutant. Edinburgh, UK, July 2013.

27. de Brauwere A., Jeandel C., **Lacan F.**, van Beek P., Venchiarutti C., Fripiat F.. Putting the pieces together: A multi-tracer model to quantitatively identify the major processes related to the fertilized bloom on the Kerguelen Plateau. Submitted to ASLO, New Orleans, USA, February 2013.

26- **Lacan F.**, Labatut M., Radic A., C. Abadie. **Invited talk.** Fe isotopic signatures in the seawater and suspended particles from the Equatorial Pacific and the Southern Ocean. AGU. San Francisco, USA, December 2012.

25- Labatut M., Radic A., **Lacan F.**, Poitrasson F. and Murray J. Oceanic cycle of Fe in the western equatorial Pacific: Insights from its isotopic composition in the dissolved and particulate fractions. Ocean Sciences Meeting, Abstract ID: 10247. Salt Lake City, USA, February 2012.

24- **Lacan F**, Radic A, Labatut M. **Invited talk**. Iron isotopes in seawater, a new effective tool for studying the iron oceanic cycle. International Congress on Analytical Sciences, Kyoto (Japan). May 2011

23- Bown J., Boye M., Baker A., Duvieilbourg E., **Lacan F.**, Le Moigne F., Planchon F., Speich S., Nelson D.M. The biogeochemical cycle of dissolved cobalt in the Atlantic and the Southern Ocean south off the coast of South Africa. 43rd International Liege Colloquium on Ocean Dynamics "Traces & Tracers", Liege (Belgium). May 2011.

22- Jeandel C., Pradoux C., Zhang Y., Van Beek P., **Lacan F**. Land-to-ocean processes on and along the Kerguelen plateau traced by the REE concentrations and Nd isotopic composition. 43rd International Liege Colloquium on Ocean Dynamics "Traces & Tracers", Liege (Belgium). May 2011.

21- Labatut M., Grenier M., Radic A., **Lacan F.**, Poitrasson F. and Jeandel C. Studying the Fe oceanic cycle in the western equatorial Pacific with Fe and Nd isotopes. 43rd International Liege Colloquium on Ocean Dynamics "Traces & Tracers", Liege (Belgium). May 2011.

20- **Lacan F.**, Radic A. And Labatut M. Iron isotopes in the ocean: new constrains on the Fe oceanic cycle. 43rd International Liege Colloquium on Ocean Dynamics "Traces & Tracers", Liege (Belgium). May 2011.

19- **Lacan F**, Radic A, Jeandel C. **Invited talk**. Iron Isotopes in Seawater: First Results from High Nutrient Low Chlorophyll Areas. *Eos Trans. AGU, 91(26), Ocean Sci. Meet. Suppl , Abstract CO14A-01*, Ocean Science Meeting, Portland (USA). February 2010.

18- Rouxel O, John S, Radic A, **Lacan F**, Adkins J, Boyle E. Intercalibration study of the Fe isotope composition of seawater: Results from Geotraces. *Eos Trans. AGU, 91(26), Ocean Sci. Meet. Suppl , Abstract CO21A-06*, Portland (USA). February 2010.

17- Boyle E, Eschgoyan-Sanz Y, Zhang J, Abouchami W, **Lacan F**, John S, Adkins J, Rehkamper M, Xiu Z, Rouxel O, Vance D. Pb and other Trace Element Isotopes in the GEOTRACES CP-TEI Intercalibration, and an Update on the Evolution of Anthropogenic Lead in the Western North Atlantic. *Eos Trans. AGU, 91(26), Ocean Sci. Meet. Suppl , Abstract CO21A-05*, Ocean Science Meeting, Portland (USA). February 2010.

16- Jeandel C, Godderis Y, Peucker-Ehrenbrink B, **Lacan F** & Arsouze T. Impact of the Boundary Processes on Si, Ca and Mg Inputs to the Ocean. Goldschmidt Conference, Davos (Switzerland). June 2009.

15- Radic A, **Lacan F**, Jeandel C, Poitrasson F & Sarthou G. Dissolved Iron Isotopes in the Southern and Equatorial Pacific Oceans. Goldschmidt Conference, Davos (Switzerland). June 2009.

14- Radic A, **Lacan F**, Jeandel C, Sartou G. & Poitrasson F. Dissolved iron isotopic composition in the world ocean. ASLO aquatic Science Meeting 2009, Nice (France), January 2009.

13- **Lacan F**, Radic A, Jeandel C, Pradoux C, Freydier R, Poitrasson F & Sartou G. Measurement of the Isotopic Composition of Dissolved Fe in Seawater. Goldschmidt Conference, Vancouver. July 2008.

12- Zhang Y, Jeandel C and **Lacan F**. Boundary Exchange Processes on and along the Kerguelen Plateau. Goldschmidt Conference, Vancouver. July 2008.

11- Zhang, Y, **Lacan, F**, Jeandel, C. Dissolved Rare Earth Elements in the Southern Ocean: Chemical Tracers of Terrigeneous Inputs and Water Masses in the Wake of Kerguelen. Eos Trans. AGU, 87(52), Fall Meet. Suppl., Abstract OS32B-04. dec 2006.

10- **Lacan F.** , Francois R, Ji, Y., Sherrell, R. **Invited talk**. Does oceanic primary production lead to a cadmium isotopic fractionnation? Field vs. culture data. EGU, Vienna, Austria. April 2005

9- Arsouze T., Jeandel C., **Lacan F.**, Ayoub N. and Dutay J-C. Modelling the oceanic Nd isotopic composition on a global scale. International Conference on Isotopes in Environmental Studies – Aquatic Forum Monte-Carlo, Monaco, October 2004.

8- **Lacan F.** and Francois, R. Cadmium isotopic composition: a new tracer in oceanography? Ocean Science Meeting, Portland, OR, USA, OS31L-04. January 2004.

7- Jeandel C. and **Lacan F**. Boundary processes traced by neodymium isotopes. EGS-AGU-EUG Joint Assembly Nice, France. April 2003.

6- **Lacan F.** and Jeandel C. NADW formation traced by Nd isotopic ratios. Goldschmidt Conference, S42. Davos (Suisse). August 2002.

5- Jeandel C., Lauret O., **Lacan F.**, Candaudap F., Usbeck R. and Rutgers Van Der Loeff M. Neodymium Isotopes Trace the Water Mass Mixing in the Argentine Basin : Implications for the Proxy of Past and Present Circulation. American Geophysical Union, OS31C-0466. December 2001.

4- **Lacan F.**, Jeandel C. and Gascard J.C. Atlantic Water Traced up to the Nansen Fjord (East Greenland) by Hydrological Parameters and Neodymium Isotopic Composition. American Geophysical Union, OS21D-04. December 2001.

3- Jeandel C., Lauret O., **Lacan F.**, Candaudap F. and Rutgers Van Der Loeff M. Neodymium Isotopic Signatures of Water Masses along the Argentinean Slope. 2001 an Ocean Odyssey (IAPSO - IABO), WS01-11. October 2001.

2- **Lacan F.**, Jeandel C. and Candaudap F. Rare Earth Element Patterns and Neodymium Signature along the Greenland Slope and in the Denmark Strait. European Union of Geosciences XI, CC04-10. April 2001.

1- Jeandel C. and **Lacan F.** Neodymium Isotopic Composition Tracing the Equatorial Undercurrent at 0°-140°W (EqPAC Section). 2000 Ocean Sciences Meeting (AGU), OS32R-03. January 2000.

Posters dans des conférences internationales

29. Labatut M., Radic A., **Lacan F.**, Poitrasson F. and Murray J. Oceanic cycle of Fe in the western equatorial Pacific: A story of Fe in the western equatorial Pacific : Insights from its isotopic composition in the dissolved and particulate fractions of seawater and in potential sources. Submitted to ASLO. New Orleans, USA, February 2013.

28- de Brauwere A., Jeandel C., **Lacan F.**, van Beek P., Venchiarutti C., Fripiat F. Putting the Pieces Together: A Multi-Tracer Model to Quantitatively Identify the Major Processes Related to the

Fertilized Bloom on the Kerguelen Plateau (Southern Ocean). AGU. San Francisco, USA, December 2012.

27- Grenier M., Jeandel C., **Lacan F.**, Cravatte C., Durand F. From the subtropics to the Equatorial Pacific: along the route, the neodymium relates. Ocean Sciences Meeting, Abstract ID: 11009. Salt Lake City, USA, February 2012.

26- Garcia-Solsona E., **Labatut** M., **Lacan F.**, Pradoux C., Vance D., Jeandel C., Distribution of REE and Nd isotopes along the Bonus Goodhope section in the Southeast Atlantic Ocean. Ocean Sciences Meeting, Abstract ID: 9695. Salt Lake City, USA, February 2012.

25- Garcia-Solsona E., **Labatut** M., **Lacan F.**, Pradoux C., Jeandel C. Dissolved and particulate REE patterns and Nd isotopes along the Bonus GoodHope (BGH) section. 43rd International Liege Colloquium on Ocean Dynamics "Traces & Tracers", Liege (Belgium). May 2011.

24- Grenier M, Jeandel C, Durand F, Cravatte S, **Lacan F**. Original study of the Equatorial Pacific Ocean fertilization based on a lagrangian simulation of the circulation coupled to Nd isotopic composition and Rare Earth Element concentration data. *Eos Trans. AGU, 91(26), Ocean Sci. Meet. Suppl , Abstract PO45Y-08*, Ocean Sciences Meeting, Portland. February 2010.

23- Jeandel C., **Lacan F**, **Labatut** M. Trace element concentrations of the suspended particles in the Southern Ocean (Bonus/GoodHope transect). *Eos Trans. AGU, 91(26), Ocean Sci. Meet. Suppl , Abstract CO15C-10*, Ocean Sciences Meeting, Portland. February 2010.

22- Boye M., Achterberg E., Bown J., Bucciarelli E., Cardinal D., Cassar N., Cavagna A.-J., Chever F., Dehairs F., Fine R.A., Happell J., Jeandel C., Joubert W., **Labatut** M., **Lacan F**., Le Moigne F., Masqué P., Monteiro P., Planchon F., **Radic** A., Sarthou G., Speich S., Verdeny E., Wake B., Waldron. A First synthesis of the GEOTRACES issues from the IPY BONUS GOODHOPE cruise in the Southern Ocean. *Eos Trans. AGU, 91(26), Ocean Sci. Meet. Suppl , Abstract CO15C-08*, Ocean Science Meeting, Portland (USA). February 2010.

21- **Radic** A, **Lacan F**, Jeandel C, Poitrasson F & Sarthou G. Isotopic composition of dissolved iron in the Equatorial Pacific and the Southern oceans. Eos Trans. AGU, 90(52), Fall Meet. Suppl., Abstract PP23A-1381. AGU Fall Meeting, San Francisco. December 2009.

20- **Radic** A, **Lacan F**, Jeandel C, Poitrasson F & Sartou G. Isotopic Composition of Dissolved Iron in Different Oceanic Basins. AGU fall meeting. San Francisco. December 2008.

19- Arsouze T., Dutay J-C, F. **Lacan F**; and C. Jeandel Modelling the Nd Oceanic Cycle Using a Fully Prognostic Dynamical/Biogeochemical Coupled Model. AGU fall meeting. San Francisco. December 2008.

18- Jeandel C, Pradoux K, **Lacan F** & Provost C. Nd Isotopic Signatures of the Drake Strait Water Masses. Goldschmidt Conference, Vancouver. July 2008.

17- Arsouze T., J-C. Dutay, M. Kageyama, C. Jeandel, R. Alkama, O., Marti, **F. Lacan**. Influence of the Atlantic thermohaline circulation on neodymium isotopic composition at the last glacial maximum, a modelling sensitivity test. Geophysical Research Abstracts, Vol. 10, EGU2008-A-00000, 2008, EGU General Assembly, Vienna, April 2008

16- C. Pradoux, C. Jeandel, C. Venchiarutti , **F. Lacan**, M. Bourquin, P. Van Beek, And J. Riotte. 2007. Extracting sequentially Ra, Nd, Pa, Th and U from a unique natural sample, on the same column. Goldschmidt Conference, Cologne. August 2007.

15- Y. Zhang, **F. Lacan** and C. Jeandel. Lithogenic inputs over the Kerguelen Plateau (Southern Ocean) traced by the dissolved and particulate REE concentrations, and Nd isotopic compositions. Goldschmidt Conference, Cologne. August 2007.

14- Arsouze, T, Dutay, J, **Lacan, F**, Jeandel, C, Alkama, R, Kageyama, M, Piotrowski, A. A Nd Isotopic Composition Modeling Approach of the Oceanic Thermohaline Circulation Change During LGM. Eos Trans. AGU, 87(52), Fall Meet. Suppl., Abstract OS51C-1060. dec 2006.

13- Peronne, S, Treguier, A, Arsouze, T, Dutay, J, **Lacan, F**, Jeandel, C. Modelling the Oceanic Nd Isotopic Composition With a North Atlantic Eddy Permitting Model. Eos Trans. AGU, 87(52), Fall Meet. Suppl., Abstract OS51C-1065. dec 2006.

12- Zhang, Y, **Lacan, F**, Jeandel, C. Dissolved Rare Earth Elements in the Southern Ocean: Chemical Tracers of Terrigeneous Inputs and Water Masses in the Wake of Kerguelen. Eos Trans. AGU, 87(36), West. Pac. Geophys. Meet. Suppl., Abstract B41A-0051. July 2006

11- Dutay, JC; **Lacan, F**; Roy-Barman, M; Bopp, L. Simulation of the cycle of trace elements (PA, Th) with the coupled Ocean-biogeochemistry model ORCA-PISCES. Implementation of a reversible scavenging model. Geophysical Research Abstracts, Vol. 8, 04337, 2006. European Geosciences Union, Vienna (Austria) EGU06-A-04337. April 2006.

10- Dutay JC, **F Lacan**, M Roy-Barman, L Bopp. $^{231}Pa/^{230}Th$ Cycles Simulated in the Oceanic General Circulation Model ORCA-2 Coupled With The Biogeochemistry Model PISCES. Eos Trans. AGU, 87(36), Ocean Sci. Meet. Suppl., Abstract OS16M-02. Feb. 2006.

9- Venchiarutti, C, Jeandel, C, Roy-Barman, M, Pradoux, C, Van Beek, P, Souhaut, M, **Lacan F**. ^{230}Th and ^{231}Pa: tracers of water masses and export fluxes in the wake of Kerguelen. Eos Trans. AGU, 87(36), Ocean Sci. Meet. Suppl., Abstract OS35M-05. Feb. 2006.

8- **Lacan, F**., Dutay, J-C., Roy-Barman, M., Bopp, L. $^{231}Pa/^{230}Th$ cycles simulated in the oceanic general circulation model ORCA-2 coupled with the biogeochemistry model PISCES. International Ocean Research Conference (The Oceanography Society's), Paris (France), June 2005.

7- Arsouze, T., C. Jeandel, **F. Lacan** and J-C Dutay. Modelling of the oceanic Nd signature distribution with the ORCA model: comparison with field measurements. International Ocean Research Conference (The Oceanography Society's), Paris (France), June 2005. Best student paper award-winner.

6- Arsouze, T., Jeandel, C., **Lacan, F**., Dutay, J-C. Simulation of the Oceanic Nd Isotopic Composition with the ORCA Model. EGU, Vienna, Austria. April 2005.

5- **Lacan F.**, R. Francois, M. Bothner, J. Crusius and C. Jeandel. No Evidence of any Cadmium Isotopic Fractionation in the Ocean. International Conference on Isotopes in Environmental Studies – Aquatic Forum Monte-Carlo, Monaco, October 2004.

4- **Lacan F.** and Jeandel C. Water masses of the first 1000 meters of the North Atlantic Subpolar Gyre traced by neodymium isotopes. Gordon Research Conference, Tilton, USA. August 2003.

3- **Lacan F**. and Jeandel C. Water masses of the first 1000 meters of the North Atlantic Subpolar Gyre traced by neodymium isotopes. EGS-AGU-EUG Joint Assembly Nice, France. April 2003.

2- Jeandel C. , **Lacan F**, Henry F , Thouron D., Lauret O. , Minster B. , Usbeck R. , Provost C .and Garçon V Water mass pathways off the Argentine coast traced by REE concentrations and Nd isotopic composition. Mineralogical Magazine, A367, Cambridge Publications, 2002

1- **Lacan F.** and Jeandel C. Rare Earth Element Patterns and Neodymium Signature in the Arctic Seas. 2001 an Ocean Odyssey (IAPSO - IABO), IA02-9. October 2001.

Séminaires et autres (invités ou organisateur en violet)

47. **Lacan F.,** Radic A., Labatut M., C. Abadie, C. Pradoux. Les isotopes du fer pour l'étude des cycles biogéochimiques océaniques. Après-Midi Scientifique de la Société Francaise des Isotopes Stables, Toulouse, Nov. 2012.

46. **Lacan** F., Van Beek P. Iron isotopes, Particle chemical composition and Natural radioactive tracers in GEOTRACES-OVIDE. GEOTRACES-OVIDE Workshop, Brest, March 2012.

45- Grenier M., Jeandel C., Delattre H., **Lacan F**., Cravatte S. REE et isotopes du Nd dans le Pacifique Sud. NEOSYMPA Workshop. Paris 6 University, Oct. 2012.

44- Abadie C., Radic A., Labatut M., Pradoux C., **Lacan F**., Poitrasson F. Particulate Iron Concentrations and Isotopic Compositions in the Southern Ocean, Atlantic Sector. GEOTRACES Workshop, Stable isotopes of biologically important trace metals. Imperial College London, UK. Sept. 2012. Poster

43- **Lacan F**., Labatut M., C. Abadie., Radic A. – Iron isotopes in the dissolved and particulate phases of seawater: sources and processes. GEOTRACES Workshop, Stable isotopes of biologically important trace metals. Imperial College London, UK. Sept. 2012.

42- Radic A., **Lacan F**., Iron isotopes in seawater : a new tracer of the oceanic biogeochemistry. Seminar at the Max Plank Institute for Chemistry, Mainz (Germany), April 2012.

41- Jeandel C., Eldin G. Cravatte S., Ganachaud A., **Lacan F**. van Beek P. The Pandora cruise, July 2011 : an integrated approach of the circulation and geochemistry in the Solomon Sea. Journées de Paleoceanographie IMAGES-France. Aix-en-Provence (France). November 2011.

40- Jeandel C., **Lacan F**., van Beek P. **Invited talk.** Land to ocean fluxes: insights from isotopic tracers. Scientific Steering Committee GEOTRACES. Xiamen (China). September 2011.

39- **Lacan F.** and Jeandel C. **Invited talk.** Fluxes of matter at the continent/ocean interface: insights from isotopic tracers. Kyoto University (Japan). May 2011.

38- **Lacan F**. Neodymium isotopes and trace elements for tracing continent/ocean fluxes. 1rst Indomix post cruise meeting. Toulouse (France), June 2011.

37- **Lacan F**., Radic A., Labatut M. Les isotopes du fer dans l'océan traceur de sources et de processus. Les Journées Scientifiques de l'Observatoire Midi Pyrénées : Les isotopes non traditionnels nouvelle frontière en géochimie. Toulouse (France). October 2010. **Meeting Convener**.

36- Jeandel C, Sarthou G., Tachikawa K., Sternberg, E. Roy-Barman M., van Beek P., **Lacan, F**. Coppola L. **Invited talk**. How TEI can help us to better constrain some processes in the Mediterranean Sea. GEOTRACES Mediterranean Meeting, Nice (France). October 2010.

35- **Lacan F.**, Jeandel C., Radic A., Grenier M., Labatut M., Delattre H., Cros A., Pradoux C., Cravatte S., Durand F. and Murray J. **Invited talk**. Lithogenic inputs into the western Equatorial Pacific: combining neodymium and iron isotope observations with Lagrangian modeling. 2010 GEOTRACES Asia Planning Workshop, Taipei (Taiwan). October 2010.

34- Grenier M., Jeandel C., Durand F., **Lacan F**. Original study of the Equatorial Pacific Ocean fertilization based on a lagrangian simulation of the circulation coupled to Nd isotopic composition and Rare Earth Element concentration data. 2nd GEOTRACES data/model synergy workshop, ENS, Paris, December 2009.

33- Radic A. **Lacan F**. and Jeandel C. Iron isotopes in seawater: a new tracer for the oceanic iron cycle ? 2nd GEOTRACES data/model synergy workshop, ENS, Paris, December 2009.

32- **Lacan F**. and Labatut M. Trace element concentrations of the suspended particles in the Southern Ocean (Bonus/GoodHope transect). 2nd GEOTRACES data/model synergy workshop, ENS, Paris, December 2009.

31- **Labatut** M., **Lacan F**., Jeandel C. Chemical composition of suspended particules during the BonusGoodHope cruise, preliminary results. Bonus/GoodHope Trace elements and Physics workshop, IUEM, Brest (France), Novembre 2009.

30- **Radic** A., **Lacan F**. Isotopic composition of dissolved Fe during the Bonus/GoodHope cruise, preliminary results. Bonus/GoodHope Trace elements and Physics workshop, IUEM, Brest (France), Novembre 2009.

29- **Radic**, A., **Lacan F**. Measurements of Dissolved Iron Isotopes in the Southern and Equatorial Pacific Oceans. California Institue of Technology, Pasadena (USA), November 2009.

28- **Lacan F.**, **Labatut** M., Jeandel. Some particulate element contents from the Niskin samplings in the whole water column. Particles in the PISCES model workshop, LSCE, Gif sur Yvette (France), September 2009.

27- **Lacan F.**, **Labatut** M. Some particulate element contents from the Niskin samplings in the whole water column. Bonus/GoodHope particles in the whole water column workshop, LSCE, Gif sur Yvette (France), September 2009. **Workshop Convener**

26- Jeandel C., Grenier M., Durand F. et **Lacan F**. Intérêt du couplage traceur virtuel/traceur réel pour quantifier les apports côte-large. CYBER Prospective workshop, Paris, June 2009

25- A. **Radic**, **F. Lacan**, C. Jeandel, F. Poitrasson, G. Sarthou. Composition isotopique du Fer dissous dans l'océan ouvert : Méthodes et premières mesures. Journées bilan du thème "Fractionnement des isotopes non traditionnels", LMTG, Toulouse, France, February 2009.

24- **F. Lacan**, A. **Radic**, C. Jeandel, G. Sarthou, F. Poitrasson. Iron isotopes, Development, first results, perspectives. Bonus/GoodHope postcruise meeting, Nice, France, January 2009.

23- **Lacan F.**, A. **Radic**, C. Jeandel, G. Sarthou, F. Poitrasson. Isotopes du fer: développement, premiers résultats, perspectives. Workshop GEOTRACES France, LSCE Gif / Yvette, France, 2 October 2008.

22- **Lacan F.**, A. **Radic**, F. Poitrasson, R. Freydier, F. Candaudap, G. Sarthou. Mesure de la composition isotopique du fer dans la phase dissoute de l'eau de mer. Séparation chimique et mesure sur MC-ICPMS. Workshop ISOTRACE 2008. ENS Lyon, France, 9-11 September 2008.

21- **Lacan F**. and **Radic** A. **Invited talk**. Cd and Fe isotopes in oceanography. Workshop "Heavy stable isotopes (Zn, Cu, Cd, Fe, Pb): tracers of source and biogeochemical processes in the environment". Université Libre de Bruxelles, Belgium, 20 May 2008.

20- Arsouze, T., J-C Dutay, C. Jeandel and **F. Lacan**. Modeling the Nd cycle with a global circulation model. GEOTRACES Data-Model Synergy Workshop. Delmenhorst, Germany. 10-13 September 2007.

19- **Lacan F.** Neodymium and iron isotopes as tracers of lithogenic matter sources in the Equatorial Pacific. EUCFe workshop. University of Washington, Seattle, USA. 4 September 2007.

18- Arsouze, T., J-C Dutay, C. Jeandel and **F. Lacan**. The Nd oceanic cycle modeling using a coupled dynamical/biogeochemical model. NEMO users meeting. Paris, France. 22 May 2007.

17- Zhang Y., **F. Lacan** and C. Jeandel Dissolved Rare Earth Elements data for the Keops project, Workshop KEOPS, 6-7 Juin 2006, Toulouse

16- **Lacan F** and C. Jeandel. Isotopes du fer et du néodyme comme traceurs des apports Amazoniens à l'Atlantique. Workshop ANR Amandes: First Scientific Meeting. LEGOS, Toulouse, France. 4 January 2006

15- **Lacan F.** Le fer isotopique dans BOA. Workshop programme ANR BOA. LEMAR, Brest, France. March 2006.

14- **Lacan, F.,** C. Jeandel, P. Brunet, T. Arsouze, J.C. Dutay, M. Souhaut, M. Roy-Barman, F. Candaudap, J.C. Gascard. Le programme SIGNATURE: Composition isotopique de néodyme de la NADW. National program for the study of the climate dynamic (PNEDC) meeting. May 2005. Meudon Observatory (France).

13- **Lacan F**., Jeandel C. and Francois R. Invited seminar. Contribution of diverse isotopic systems, neodymium, cadmium and iron, to the study of oceanic biogeochemical cycles. Centre d'Océanologie de Marseille (COM, France). April 2005

12- **Lacan F**., Jeandel C. and Francois R. Invited seminar. Contribution of diverse isotopic systems, neodymium, cadmium and iron, to the study of oceanic biogeochemical cycles. Institut des Sciences de la Terre, de l'Environnement et de l'Espace de Montpellier (ISTEEM, France). April 2005

11- **Lacan F**., Jeandel C. and Francois R. Invited seminar. Contribution of diverse isotopic systems, neodymium, cadmium and iron, to the study of oceanic biogeochemical cycles. Observatoire Midi Pyrenees (OMP, France). April 2005

10- **Lacan F.**, Jeandel C. and Francois R. Invited seminar. Neodymium, cadmium and iron isotopes in the ocean: constrains on margin fluxes, thoughts about metal speciation. Laboratoire des Sciences du climat et de l'Environnement (LSCE, France). November 2004.

9- Jeandel, C. and **F. Lacan**. Invited seminar. The neodymium paradox solved by the boundary exchange. Lamont Doherty Columbia University (LDEO, USA), July 2004.

8- Jeandel, C. and **F. Lacan**. Invited seminar. The boundary exchange and its influence on the Nd isotope oceanic cycle. Woods Hole Oceanographic Institution (WHOI, USA), July 2004.

7- Jeandel C. and **Lacan F**. Invited seminar. The neodymium paradox: myth or reality? Southampton Oceanographic Center (SOC, UK). May 2004.

6- **Lacan F.**, Jeandel C. and Francois R. Invited seminar. Neodymium, cadmium and iron isotopes: constrains on oceanic biogeochemical cycles. Laboratoire des Sciences de l'environnement marin (LEMAR, France). April 2004.

5- **Lacan F.** and Jeandel C. Neodymium isotopes in the water masses of the Nordic Seas and the Subarctic Atlantic. Woods hole Oceanographic Institution (WHOI, USA). December 2003

4- **Lacan** F. and Jeandel C. Invited seminar. Subpolar mode water traced by neodymium isotopes. Laboratoire de Physique de l'Océan (LPO, France). February 2003.

3- **Lacan F.**, Jeandel C. and Souhaut M. Circulation in Denmark Strait traced by neodymium isotopes. LEGOS evaluation committee, (LEGOS, France). May 2002.

2- Jeandel C., **Lacan F.** and Tachikawa K. Nd isotopic compositions: what proxy in oceanography?. Workshop PROXYCAL, Gif/Yvette, March 2001

1- Jeandel C., Roy-Barman M., Coppola L., **Lacan F.**, Athias V. and Mazzega P. What parameters need to be measured for quantifying fluxes in the water column? PROOF Modelization workshop, Arcachon (France). January 2001.

Vulgarisation

Lacan F. A Global Compilation of the Neodymium Isotopic Composition of Seawater for GEOTRACES. GEOTRACES Science Highlights. GEOTRACES web site

Lacan F. and **Radic** A. 2011. Suivre le fer océanique à l'aide de ses isotopes : une première. INSU web site, CNRS web site, Toulouse 3 University web site, Midi Pyrenees Observatory web site, LEGOS web site, Infocean, La lettre de l'océan, du littoral et des recherches appliquées N°491, 2 mai 2011 PDF.

Lacan F. Exposé dans le cadre La Novela, festival des savoirs à Toulouse, sur l'exploration scientifique, devant 200 élèves de CM1/CM2. October 2009. HTML

Lacan F. Interview sur le projet Bonus/Goodhope dans le cadre de l'année polaire internationale, pour un groupe d'étudiant de l'Univ. Toulouse III. April 2009. HTML

Lacan F., **Radic** A., Jeandel C., Poitrasson F., Sarthou G., Pradoux C. and Freydier R. 2008. Géochimie marine. Une première : la mesure des isotopes du fer dans l'océan. Toulouse III University Newsletter: PDF

Lacan F., **Radic** A., Jeandel C., Poitrasson F., Sarthou G., Pradoux C. and Freydier R. 2008. Géochimie marine - Les isotopes sur les traces du fer dans l'océan. LEGOS web site: HTML

Lacan F., **Radic** A., Jeandel C., Poitrasson F., Sarthou G., Pradoux C. and Freydier R. 2008. Géochimie marine - Les isotopes sur les traces du fer dans l'océan. Observatoire Midi Pyrénées web site: HTML

Lacan F., **Radic** A., Jeandel C., Poitrasson F., Sarthou G., Pradoux C. and Freydier R. 2008. Sur les traces des isotopes du fer dans l'océan. INSU web site: HTML

Lacan F. Interview à bord du Navire de recherche Marion Dufresne, campagne Bonus/Goodhope; réalisation V. Pasquero. March 2008. Movie. Diffusé notamment lors d'une exposition sur l'Année Polaire Internationale et l'Océan Austral à Brest (2008 Juillet), et à Toulouse.

Lacan F. and Jeandel C. 2005. Marges continentales : un piégé pour un rendu. Le Journal du CNRS N°189, octobre 2005. HTML

Lacan F. and Jeandel C. 2005. Entre continent et océan... La Lettre du CNRS en Midi Pyrénées. May 2005. n°98, p.3. PDF

Lacan F. and Jeandel C. 2005. Les marges continentales, des zones d'échange de matière entre continents et océans. INSU web site: HTML

II. Parcours scientifique, principaux résultats et perspectives

1. Introduction

Comme je l'ai dit ci-dessus, je m'intéresse aux **cycles de la matière au sein de l'océan**. Pourquoi ? Il y a une première raison fondamentale, dénuée de toute considération pratique (que l'on peut qualifier de "socio-économiques"). L'océan fait partie de notre vie, au même titre que les étoiles ou les arbres, il est intéressant d'essayer de le connaître, de comprendre comment il fonctionne. Il s'agit d'une soif de savoir, de curiosité, instinctive. L'enfant à envie de savoir pourquoi la mer est salée, pas parce qu'il y entrevoit des perspectives de développements socio-économiques, mais parce que c'est quand même surprenant qu'elle soit salée alors que les rivières ne le sont pas! Serge Haroche, prix Nobel de physique 2012, dit de la recherche fondamentale qu'elle "doit être motivée par la **curiosité intellectuelle pure**" (Le Monde.fr, jeudi 11 octobre 2012).

A coté de cette motivation fondamentale, il existe aussi des raisons pratiques, socio-économiques, de s'intéresser aux cycles des éléments dans l'océan. Via **l'interface air-mer**, les cycles des éléments dans l'océan sont liés aux cycles des éléments dans l'atmosphère, qui sont eux-mêmes liés, pour certains, au **climat**. On citera notamment le dioxyde de carbone qui participe à l'effet de serre, ou le sulfure de diméthyle qui participe à la formation des nuages. La composition chimique de l'eau de mer conditionne aussi en partie la production biologique primaire marine et par suite la chaîne alimentaire marine et les **ressources halieutiques** (pêches). Comprendre les cycles biogéochimiques marins permet aussi de mieux appréhender les questions de qualité de l'eau et de **pollution** du littoral. Enfin, les cycles de certains éléments peuvent nous renseigner, indirectement, sur des processus auxquels ces éléments prennent part. Ces éléments sont alors utilisés comme **traceurs**. Outre les applications citées ci-dessus (composition chimique de l'atmosphère, biologie marine et qualité de l'eau), ces éléments permettent de quantifier la **circulation océanique** et donc nous renseignent sur les flux de chaleur, qui, via l'interface air-mer, ont un impact sur le climat.

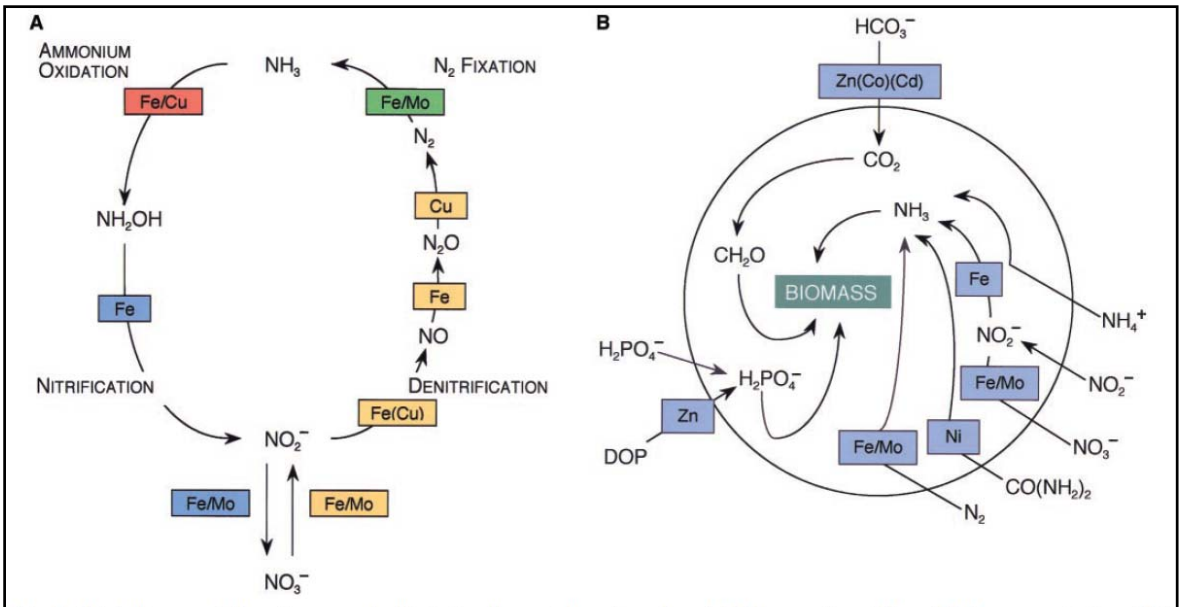

Fig. 3. (**A**) A diagram of the nitrogen cycle, illustrating the metal cofactors in each enzymatically catalyzed step. Color coding identifies the sets of reactions involved in nitrogen fixation (green), denitrification (gold), nitrification (blue), and ammonium oxidation (red). All the metals shown here (with the exception of Mo, which has a concentration of 0.1 μM) are depleted in surface seawater. (**B**) Primary metal requirements for carbon, nitrogen, and phosphorus acquisition and assimilation by marine phytoplankton.

Figure 2: Rôles joués par ces micro-nutritifs lors de l'acquisition et l'assimilation du carbone de l'azote et du phosphore [*Morel et Price*, 2003].

Le cycle océanique du fer a reçu une attention particulière ces dernières décennies. Pour croître le phytoplancton a notamment besoin d'éléments nutritifs. Parmi eux, on distingue les éléments dont les abondances dans l'eau de mer sont tellement grandes, qu'il y en a toujours suffisamment pour satisfaire les besoins des producteurs primaires, il s'agit notamment du carbone, de l'hydrogène et de l'oxygène, du souffre, du potassium, du calcium, etc. En pratique, lorsqu'on parle d'éléments nutritifs en océanographie, on ne pense pas à ces derniers mais aux trois éléments nutritifs, dits majeurs ou macronutriments, azote, phosphore et silicium, dont les concentrations océaniques sont assez importantes (de l'ordre de 1 à 100 µmol/kg) mais qui peuvent être totalement consommés en surface par les producteurs primaires et ainsi limiter cette production. Si ces nutritifs majeurs sont indispensables, il existe aussi un ensemble d'éléments, des métaux, dits micro-nutritifs ou micronutriments, moins abondants (de l'ordre de 1 nmol/kg, voire pmol/kg pour le Co), mais aussi nécessaires aux producteurs primaires: fer, cobalt, nickel, cuivre, zinc et cadmium. Les rôles joués par ces micro-nutritifs lors de l'acquisition et de l'assimilation du carbone, de l'azote et du phosphore sont illustrés sur la Figure 2. On y voit notamment la forte implication du fer en tant que co-facteur d'enzyme dans les différentes étapes du cycle de l'azote. Le fer joue aussi le rôle de transporteur d'électrons lors des processus de photosynthèse et de respiration.

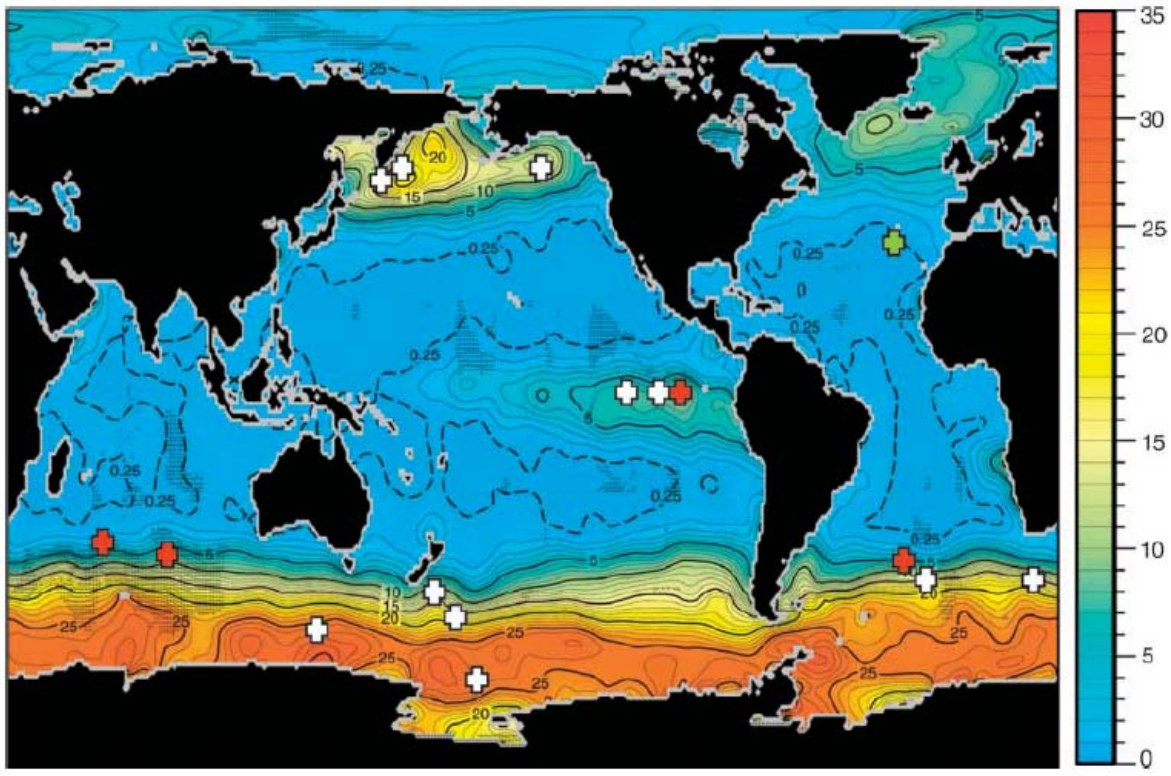

Figure 3: Concentrations de nitrates (µmol/L) dans la couche mélangée de surface, en moyenne annuelle, mettant en évidence les régions HNLC.
Sont indiquées les positions des sites d'expériences de fertilisation en fer artificielles (croix blanches) et naturelles (croix rouges), ainsi que de fertilisation en Fe et P (croix verte) [Boyd et al., 2007].

A la fin des années 1980, Martin et ses collègues suggèrent que si la production primaire ne consomme pas l'intégralité des macronutriments dans certaines régions, c'est parce que le phytoplancton y est carencé en fer [*Martin et Fitzwater*, 1988; *Martin et Gordon*, 1988]. Ces régions sont couramment nommées *High Nutrient Low Chlorophyll* (HNLC). Elles sont visibles sur la Figure 3 Ces auteurs proposèrent en outre que des apports de fer atmosphériques 50 fois plus importants pendant le dernier maximum glaciaire (LGM, comparés à l'holocène) pourraient expliquer un accroissement de la production primaire marine et ainsi un pompage accru de CO_2 atmosphérique

(ce qu'on appelle la pompe biologique de carbone), ce qui permettrait d'expliquer les faibles teneurs en CO_2 de l'atmosphère enregistrées pour cette période [*Martin*, 1990]: la fameuse "*Iron Hypothesis*", et la fameuse phrase de John Martin "*Give me half a tanker of iron and I'll give you an Ice Age*". D'où un rôle potentiellement majeur du cycle océanique du fer sur le contrôle du climat. Ces travaux ont motivé un effort de recherche très important depuis lors pour mieux comprendre le cycle du fer dans l'océan et son impact sur la production primaire. Voir notamment Boyd et al. [2007] pour une synthèse de 12 expériences de fertilisation artificielle en fer de l'océan. Cet effort de recherche a conduit à modérer de manière substantielle les propos de Martin et al. ([*Watson et al.*, 2000] suggèrent par exemple qu'une augmentation d'apport de fer dans l'océan Austral ne pourrait expliquer que la moitié de la baisse de 80 ppm du CO_2 atmosphérique au LMG). Il a néanmoins confirmé l'importance des cycles des micro-nutritifs, et en particulier du fer, sur la dynamique de la production primaire. Différents travaux de modélisation suggèrent notamment que la production primaire est limitée par le fer dans 30 à 50% de l'océan mondial [*Moore et Braucher*, 2008 et références incluses]. La Figure 4 donne une estimation des rôles limitants des macronutriments et du fer.

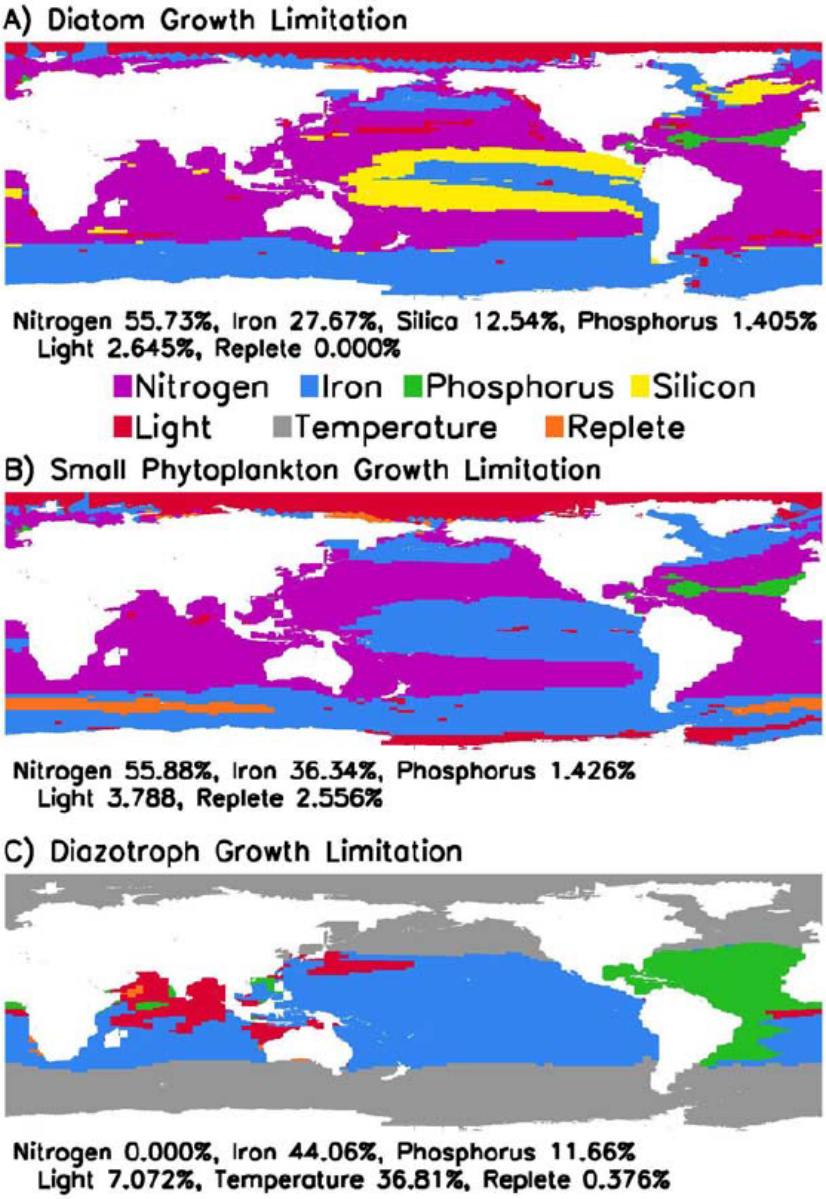

Figure 4: Facteur limitant le plus les taux de croissance pour chaque groupe de phytoplancton pour les mois d'été de chaque hémisphère [*Moore et al.*, 2004].

Mes travaux de recherche ont donc été largement – mais pas seulement – motivés par l'objectif suivant:

> Progresser dans notre compréhension du cycle océanique des éléments, notamment du fer, dans l'optique de mieux contraindre **la pompe biologique de carbone**

Comprendre le cycle d'un élément dans l'océan c'est comprendre ce que j'appelle son **cycle interne**, c'est-à-dire les processus qui contrôlent ce qui lui arrive au sein de l'océan, mais c'est aussi comprendre **ses sources et ses puits**, autrement dit, comment il entre dans le réservoir océanique et comment il en sort, ou encore ce qu'il se passe aux **interfaces de l'océan**. Pour la quasi-totalité des éléments, le puits consiste en un flux particulaire vers les sédiments. La connaissance des flux de particules (qui dépasse le cadre de l'étude du cycle d'un élément en particulier) et la connaissance du cycle interne de l'élément considéré, qui permet d'inférer les concentrations de l'élément sur les particules, permettent de contraindre ce puits. En supposant donc que les flux de particules sont connus, comprendre le cycle d'un élément se résume (dans la grande majorité des cas) à comprendre **son cycle interne et ses sources.**

Lorsque j'ai commencé la recherche, à la fin des années 1990, les sources de nombreux éléments étaient mal connues. C'est encore largement le cas aujourd'hui. Etaient considérés les apports d'éléments dissous par les rivières, les apports atmosphériques (secs et humides) et les apports hydrothermaux. Pour un grand nombre d'éléments (notamment le fer) ces derniers étaient considérés n'avoir qu'un impact local, ou du moins restreint à l'océan profond. Les sources d'origines sédimentaires, qu'il s'agisse de sédiments authigènes ou de particules lithogènes (apportées par l'érosion des continents), étaient de même considérées n'avoir qu'un impact local. Cette vision des choses est bien résumée par la citation suivante concernant le cycle du fer extraite d'un article publié à *Nature* en 2005: "*Iron supply reaches the oceans mainly from rivers as suspended sediment in a vast global transport system (Table 1). However, fluvial and glacial particulate iron is efficiently trapped in near-coastal areas (4), except where rivers discharge directly beyond the shelf. Hydrothermal inputs are rapidly precipitated at depth in the oceans. Hence, the dominant external input of iron to the surface of the open ocean is aeolian dust transport, mainly from the great deserts of the world*" [*Jickells et al.*, 2005]. Cette vision des choses était largement partagée.

Mon premier travail en géochimie marine portait sur une hypothèse contredisant cette vision des choses. Il s'agissait en effet d'étudier si des apports sédimentaires le long de la marge Ouest du Pacific pouvaient dominer les apports de fer au centre de cet océan (à environ 4000 km de là). Ce premier travail m'a fait prendre conscience de l'importance potentiellement sous-estimée de ces sources sédimentaires à l'interface continent/océan pour l'océan ouvert. Par la suite de nombreux autres travaux ont confirmé le rôle important de cette source pour certains éléments. Un second fil conducteur de mes activités de recherche a donc été le suivant :

> Progresser dans notre compréhension des **sources sédimentaires le long des marges continentales** et de leurs impacts sur les cycles des éléments dans l'océan.

Enfin, mes travaux m'ont progressivement, doucement mais sûrement, montré l'importance cruciale du cycle des particules dans l'océan. En effet, bien que ma directrice de thèse ait depuis longtemps porté son attention sur le cycle des particules, la formation initiale qu'elle m'a donnée, concernait uniquement les phases dissoutes dans l'eau de mer. J'ai donc ignoré assez longtemps cet aspect des choses, qui s'est révélé à moi petit à petit. Ces particules sont à la fois très complexes, car

très diverses, biogéniques, lithogéniques ou encore chimiogéniques (je ne crois pas que ce terme existe, mais il me semble explicite et nécessaire), et particulièrement peu étudiées (car souvent difficiles à échantillonner dans l'océan ouvert). Nos connaissances sur le cycle particulaire de certains éléments sont extrêmement sommaires. Il en est donc nécessairement de même pour les interactions entre phases dissoutes et particulaires.

Je me suis donc attaché à échantillonner systématiquement ces particules afin de compléter les phases dissoutes plus couramment échantillonnées. Une autre ligne directrice de mes activités a donc été la suivante.

> Progresser dans notre compréhension des **interactions dissous/particules** qui régissent en partie les cycles océaniques internes de certains éléments.

Nous verrons par la suite que mes activités de recherches ont aussi concerné d'autres thématiques, mais je dirais que les trois thèmes encadrés ci-dessus 1) les cycles des éléments pour leurs impacts sur la pompe biologique de carbone, 2) les sources sédimentaires et 3) les interactions dissous/particules, constituent la colonne vertébrale de mon parcours scientifique jusqu'à présent.

Mes travaux m'ont conduit à aborder ces questions par l'usage d'éléments en trace et de leurs compositions isotopiques, *Trace Elements and Isotopes* (TEIs), qui constituent le cœur du programme international GEOTRACES.

2. Les isotopes du néodyme et les concentrations de terres rares: traceurs des interactions dissous/particules et de la circulation océanique.

J'ai donc fait mes premiers pas en géochimie marine sur la thématique des isotopes du néodyme (Nd) et des concentrations de terres rares (REE).

Les REE constituent un groupe d'éléments, dont le Nd fait partie, aux propriétés physico-chimiques proches. Les processus naturels fractionnent ces éléments, de sorte que l'étude de l'abondance relative des différentes REE nous renseigne sur ces processus. Afin d'étudier ces fractionnements dans l'océan, on normalise les concentrations de REE par rapport à une référence lithogénique (ou terrigène), représentant la source de REE pour l'océan. Les spectres de REE ainsi obtenus mettent en évidence les anomalies par rapport à la référence. Un spectre typiquement océanique de REE dissoutes[1] est représenté sur la figure Figure 5.

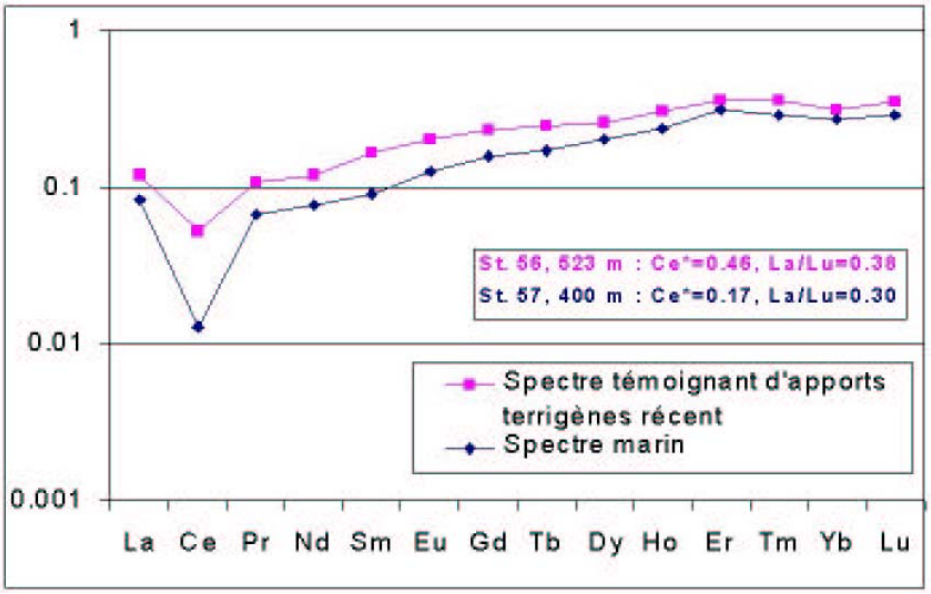

Figure 5: Spectres de REE.
Concentrations de REE normalisées au PAAS (Post Archean Sedimentary Shale) et multipliées par 10^6. Le spectre bleu présente une forte anomalie négative de Ce, ainsi qu'un appauvrissement en REE légère (La, Pr, Nd) par rapport aux REE lourdes (Tm, Yb, Lu) marqué. Au contraire le spectre rose, est plus "plat", il présente moins d'anomalie, il est plus proche de la référence terrigène. Pour information ces données proviennent de l'Atlantique Nord [*Lacan*, 2002].

L'anomalie de Ce est attribuée à l'oxydation du Ce. L'oxyde de Ce formé est insoluble, il est donc soustrait à la colonne d'eau, ce qui explique cette anomalie négative (par rapport à la source) dans la phase dissoute. L'appauvrissement des REE légères (LREE) par rapport aux REE lourdes (HREE) est quant à lui attribué à l'effet du scavenging[2] qui affecte d'avantage les LREE que les HREE [*Goldstein et Hemming*, 2003]. Ainsi, lorsqu'on s'éloigne des sources externes de REE, plus une masse d'eau est soumise à des environnements oxydants et plus elle est soumise au scavenging, plus ces anomalies

[1] Par abus de langage, le terme "dissous" est couramment utilisé au sein de la communauté des géochimistes marins pour désigner ce qui est en réalité la fraction passant au travers d'un filtre, dont la porosité varie selon les travaux, mais se trouve généralement autour de 0.2 à 0.4µm. A une telle porosité, de nombreuses petites particules, ou colloïdes, se retrouvent dans le filtrat, de sorte que cette fraction dissoute recouvre en réalité de nombreuses phases (non dissoutes au sens strict). Je me conformerai à cet usage.

[2] Le scavenging (qui n'a pas d'équivalent en français) traduit la soustraction d'espèces dissoutes par adsorption sur les particules chutant dans la colonne d'eau.

seront marquées. Des anomalies marquées suggèrent donc que les REE présentes dans la masse d'eau y ont été apportées il y a longtemps et que les effets des processus océaniques ont pu s'y exprimer. Au contraire un spectre plus plat suggère que ces processus océaniques n'ont pas pu fractionner les REE, indiquant un apport de REE lithogénique plus récent. Il existe d'autres anomalies de REE que celles mentionnées ci-dessus, notamment des anomalies de Eu, mais ceci sort du cadre de cette thèse.

Parmi les REE, le Nd est particulièrement intéressant. Il possède 7 isotopes naturels qui sont tous stables ou radioactifs mais avec des demi-vies extrêmement longues (>10^{15} ans) de sorte qu'on peut les considérer stables en sciences de la Terre. Le ^{143}Nd est radiogénique, issu de la désintégration du ^{147}Sm avec une demi-vie de 100 milliards d'années. L'hétérogénéité des compositions chimiques (rapports Nd/Sm) et des âges des roches induisent des hétérogénéités de leurs CI de Nd. Cette CI est exprimée par la variable ε_{Nd} définie comme suit:

$$\varepsilon_{Nd} = \left[\frac{\left(^{143}Nd/_{144}Nd\right)_{échantillon}}{\left(^{143}Nd/_{144}Nd\right)_{CHUR}} - 1\right] \times 10^4$$

Équation 1

Où CHUR signifie Chondritic Uniform Reservoir, avec (^{143}Nd/$_{144}$Nd)$_{CHUR}$=0.512638 [*Jacobsen et Wasserburg*, 1980]

Les compositions isotopiques de Nd des marges entourant les bassins sont représentées sur la Figure 6. Elles peuvent être considérées comme constantes aux échelles de temps qui nous intéressent ici (celles de l'océan moderne, voire celles couvrant les dernières variations climatiques, quelques dizaines à centaines de milliers d'années).

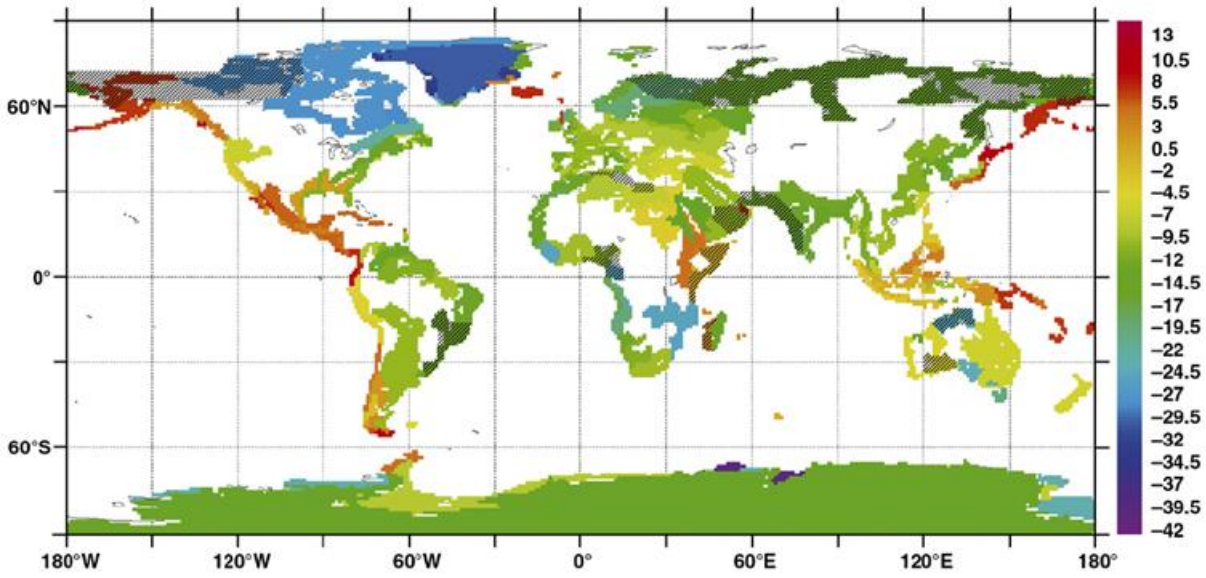

Figure 6: Composition isotopique de néodyme des marges entourant les océans [*Jeandel et al.*, 2007].

Au sein de l'océan, le Nd est d'origine lithogénique. Ses concentrations sont de l'ordre de 10^{-12} g/g (10 pmol/kg). Il se trouve, dans l'océan ouvert, principalement sous forme dissoute (90 à 95%) [*Alibo et Nozaki*, 1999; *Jeandel et al.*, 1995; *Sholkovitz et al.*, 1994]. Son temps de résidence est de l'ordre de 300 à 1000 ans [*Arsouze et al.*, 2009; *Tachikawa et al.*, 2003]. Aucun processus ne fractionne les isotopes du Nd dans l'environnement, de sorte qu'en l'absence de source externe ε_{Nd} se comporte de manière quasi-conservative. Enfin la CI de Nd de l'eau de mer est enregistrée dans diverses archives

sédimentaires. L'ensemble de ces propriétés a conduit à utiliser la CI de Nd en tant que traceur 1) de la circulation océanique (aux échelles intra- et inter-bassins) moderne et passée, 2) des interactions dissous/particules et 3) des apports de matière lithogéniques à l'océan. La Figure 7 illustre la manière dont les signatures isotopiques des continents s'impriment sur les masses d'eau et sont redistribuées par la circulation océanique.

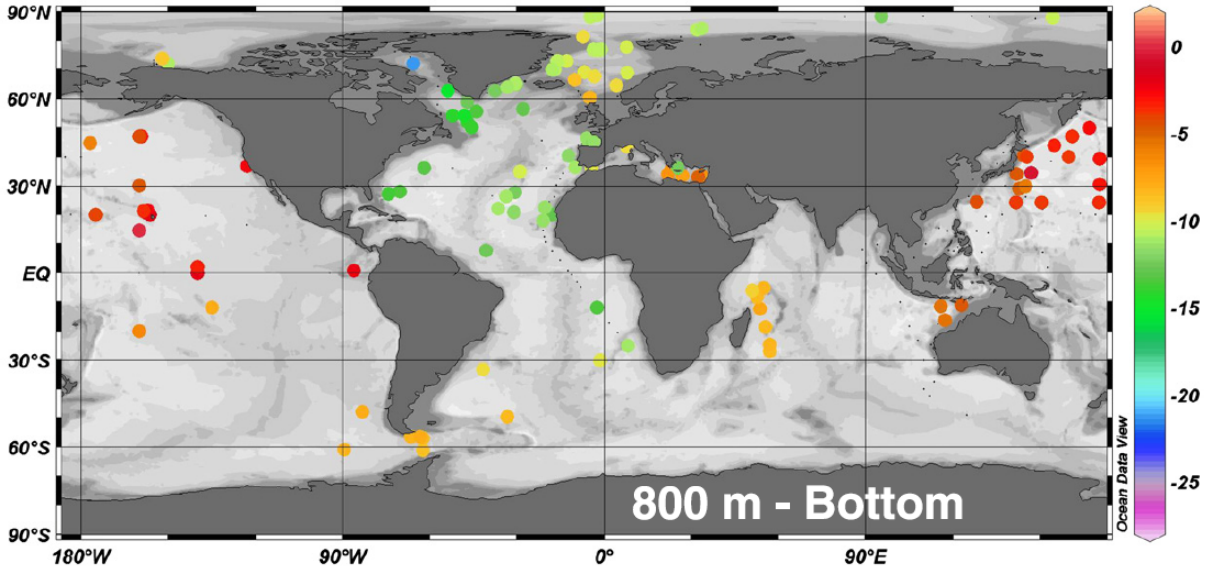

Figure 7: Composition isotopique de néodyme de l'eau de mer (filtrée ou non filtrée) moyennée entre 800m de profondeur et le fond [*Lacan et al.*, 2012].

a. Apports lithogéniques dans le Pacifique Equatorial

Le Pacifique Equatorial Est est une région HNLC (cf. Figure 3). Le sous-courant équatorial (EUC) coule vers 200m de profondeur le long de l'Equateur depuis la frontière Ouest du bassin, la région de la Papouasie Nouvelle Guinée, en remontant progressivement jusque dans la partie Est du bassin, et étant de ce fait progressivement soumis à l'influence de l'upwelling équatorial. L'EUC est enrichi en fer. Coale et al. [1996] suggèrent que la production primaire de cette région est contrôlée par le fer apporté en surface par l'upwelling depuis l'EUC. Wells et al. [1999] suggèrent ensuite que les apports de fer dans la région de Papouasie Nouvelle Guinée (PNG) contrôlent les concentrations de fer dans l'EUC, et donc par suite la production primaire du Pacifique Equatorial Est. L'objectif de mon stage de DEA était d'utiliser les REE et les isotopes du Nd pour vérifier si le fer observé dans l'EUC au centre du Pacifique provenait effectivement de la région de Papouasie Nouvelle Guinée. Les mesures d'ε_{Nd} réalisées dans les eaux sources de l'EUC, dans le Pacifique Tropical Sud, et à l'équateur, aux densités caractéristiques de l'EUC sont représentées sur la Figure 8 [*Lacan et Jeandel*, 2001]. Elles montrent une augmentation d'ε_{Nd} au cours du trajet de ces eaux, qui ne peut s'expliquer que par un apport de Nd radiogénique (ε_{Nd} élevé). Les formations géologiques du bord Ouest du bassin, notamment la PNG, ont des signatures isotopiques suffisamment radiogéniques (Figure 6) pour que des apports lithogéniques provenant de ces formations puissent expliquer les variations de signature isotopique mesurées dans la masse d'eau. Nos mesures d'ε_{Nd} confirment donc l'hypothèse selon laquelle **les apports lithogéniques enrichissant le sous-courant équatorial pacifique proviennent de la région de PNG.** Elles rejettent en particulier les hypothèses alternatives de sources provenant d'aérosols asiatiques ou australiens, dont les CI de Nd ne permettraient pas d'expliquer les variations mesurées dans l'eau de mer**. Elles s'opposent aussi à la vision selon laquelle les apports aux marges n'auraient qu'un impact local et n'atteindraient pas l'océan ouvert.** Ici les apports sont transportés sur au moins 4000 km.

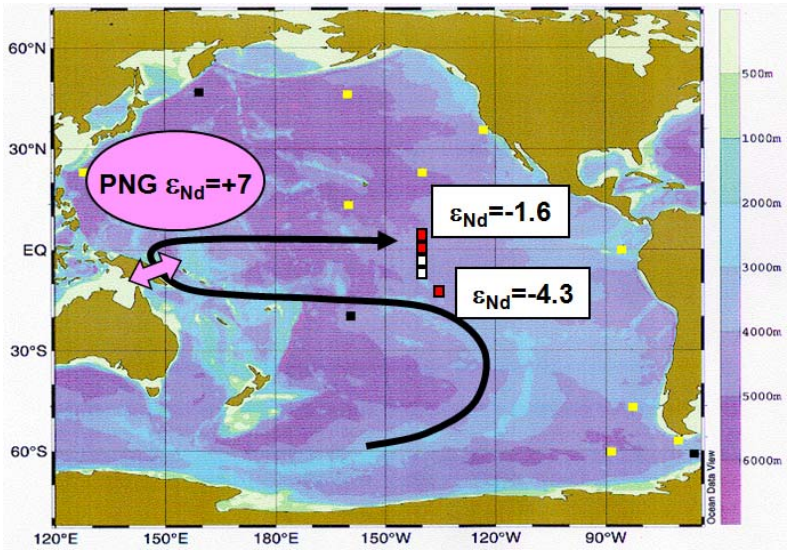

Figure 8: CI de Nd aux densités du sous-courant équatorial (EUC).

Mes données, dans les eaux de l'EUC, mais aussi dans d'autres masses d'eau (Eau Antarctique Intermédiaire notamment), combinées aux données de flux des masses d'eau, m'ont permis d'estimer les **flux de Nd lithogéniques nécessaires** pour expliquer les variations observées dans les masses d'eau. Cela génère des contraintes sur la nature des sources externes impliquées. Dans cette région, les estimations des apports de Nd dissous par les rivières et des apports atmosphériques sont très inférieures aux flux nécessaires pour modifier les signatures des masses d'eau. Les flux hydrothermaux étant considérés ne pas constituer une source pour l'océan (du fait de processus de scavenging liés à la formation d'oxy-hydroxydes de Fe), la seule source externe possiblement responsable des variations observées était les apports de particules par les rivières. Les décharges sédimentaires dans cette région sont considérables. Ces particules se déposent sur le plateau mais aussi la pente continentale et peuvent atteindre l'océan profond [*Milliman*, 1995]. La dissolution de quelques pourcent de ces particules permet d'expliquer les variations observées dans les masses d'eau. Ce travail nous a donc aussi permis de suggérer que **la source des apports externes dans la région de PNG était très largement dominée par la dissolution de particules apportées par l'érosion des continents (principalement fluviale) et déposées sur le plateau et la pente.** Cela a été confirmé par d'autres travaux indépendants [*Mackey et al.*, 2002; *Slemons et al.*, 2010].

Enfin ces données suggèrent l'existence de **processus d'échange de Nd entre les marges et les masses d'eau**. Dans l'Eau Antarctique Intermédiaire (AAIW), les variations de compositions isotopiques sont observées sans variation de la concentration de Nd. Pour modifier la CI de Nd d'une masse d'eau il est nécessaire de lui apporter du Nd de CI différente. Pour modifier la CI d'une masse d'eau sans modifier sa concentration, il est donc nécessaire de lui apporter du Nd de CI différente et de lui soustraire du Nd. Ainsi lorsqu'une masse d'eau longe une marge, des flux de matières peuvent exister entre sédiments et masses d'eau sans que ceux-ci soient visibles si l'on ne mesure que les concentrations. L'outil isotopique permet donc de voir des processus difficilement visibles autrement. Nous reviendrons abondamment sur ce sujet ultérieurement, dans un cadre plus global, je n'en dis donc pas plus dans cette partie sur le Pacifique Equatorial.

Ce travail a été important pour moi. Il concernait déjà le fer, qui constituera ensuite mon projet de recherche pour le CNRS. Il a conduit à un certain nombre d'autres travaux que je vais décrire ci-dessous. L'article publié sur ce travail [*Lacan et Jeandel*, 2001] fait partie des articles ayant eu le plus d'impact parmi ceux auxquels j'ai participé (en moyenne près de 7 citations par an). En écrivant ces

lignes, je mesure l'impact structurant que peut avoir le premier travail d'un étudiant sur sa future carrière de chercheur.

Les échantillons utilisés dans cette 1ère étude étaient néanmoins très distants de la zone de PNG. La résolution spatiale des données était très faible. Afin de confirmer ou d'infirmer nos conclusions j'ai monté le projet ISOFERIX (LEFE-INSU) qui a permis un échantillonnage beaucoup plus important tout le long de l'équateur de 140°W jusque dans la région de PNG. Avec non seulement de l'eau de mer filtrée mais aussi des échantillons de particules (prélevées par pompes in situ). La campagne en mer, EUC-Fe, était organisée en 2006 par J. Murray de l'Univ. de Washington à Seattle. J'ai de plus obtenu, via une collaboration au sein du LEGOS avec C. Maes et G. Eldin, des échantillons en amont de la PNG, en mer de Corail, dans le cadre de la campagne FLUSEC. Entre temps, C. Jeandel avait obtenu des échantillons provenant de la campagne BIOSOPE organisée par H. Claustre (LOV) dans le Pacifique Sud Est. Dans le cadre de la campagne INDOMIX (organisée par A. Koch Larrouy, LEGOS) dans le Throughflow indonésien, j'ai collecté des échantillons au Nord et à l'Ouest de la Nouvelle Guinée. Finalement nous venons de réaliser un échantillonnage intensif en Mer des Salomon et de Corail, dans le cadre de la campagne PANDORA (projet SOLWARA), projet structurant pour le LEGOS, fédérant physiciens et géochimistes. L'ensemble des échantillons ainsi collectés pour des mesures de CI de Nd et de concentration de REE (notamment) est représenté sur la Figure 9.

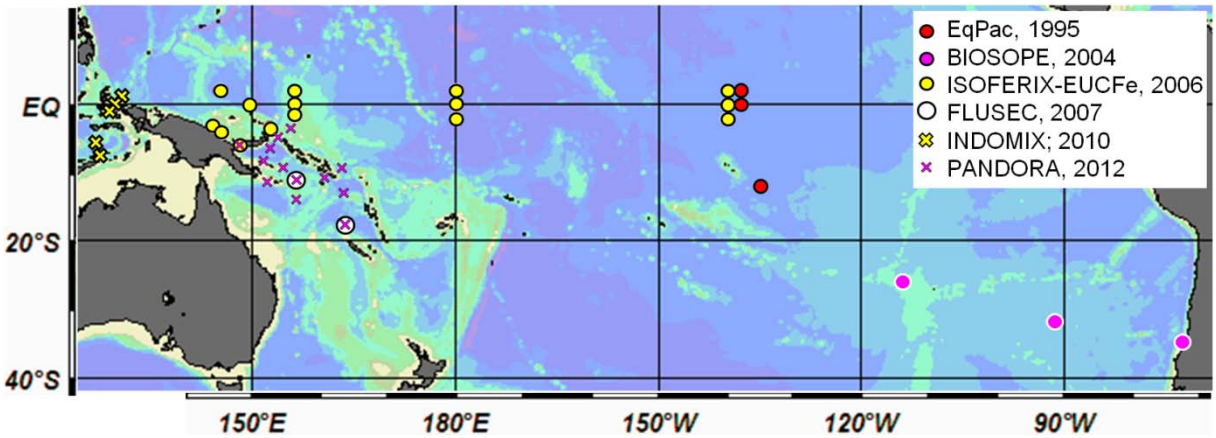

Figure 9: Stations où la CI de Nd et les [REE] ont été, ou seront, mesurées au LEGOS.

Les analyses des échantillons EUCFe-ISOFERIX et FLUSEC ont déjà eu lieu, dans le cadre du Master 2 et du doctorat de M. Grenier et du Master 2 d'A. Cros. Elles permettent de préciser les choses. Si elles confirment l'existence d'apports externes dans la région de PNG, elles suggèrent également des apports lithogéniques en amont, aux masses d'eau coulant depuis les Samoa vers la mer des Salomon. Elles suggèrent également des apports provenant des côtes sud-américaines ou des îles Galapagos aux eaux s'écoulant le long de l'Equateur d'Est en Ouest entre 200 et 550m de profondeur. Dans les deux cas **la dissolution de particules déposées sur les pentes de ces formations est proposée comme le processus dominant ces sources** [*Grenier et al.*, 2012].

Les analyses des échantillons BIOSOPE ont été réalisées dans le cadre du Master 2 de H. Delattre. Ces mesures confirment aussi l'existence **d'interaction sédiments/eau de mer** le long des cotes sud américaines. Par ailleurs, elles suggèrent, à l'encontre des travaux précédents sur le sujet, un **impact possible des sources hydrothermales sur le cycle des isotopes du néodyme** [*Jeandel et al.*, 2013]. Cette hypothèse corrobore d'autres travaux récents, sur le cycle du fer, suggérant un impact non négligeable des sources hydrothermales à des distances de plusieurs milliers de km des sources, y compris à la surface de l'océan [*Fitzsimmons et al.*, 2012; *Tagliabue et al.*, 2010].

L'encadrement d'A. Cros, de M. Grenier et de H. Delattre a été principalement assuré par C. Jeandel. Je les ai néanmoins encadrés (parfois officiellement, parfois officieusement, cf. chapitre I) en ce qui concerne leurs mesures de concentrations de REE et j'ai activement collaboré à ces travaux.

b. Signature isotopique de Nd de l'Eau Profonde Nord Atlantique

Mon doctorat a porté sur l'étude des CI de Nd et des [REE] dans le gyre subpolaire Nord Atlantique et les mers Nordiques [*Lacan*, 2002]. J'ai exploité des échantillons prélevés dans le cadre du Projet SIGNATURE aux stations représentées sur la Figure 10.

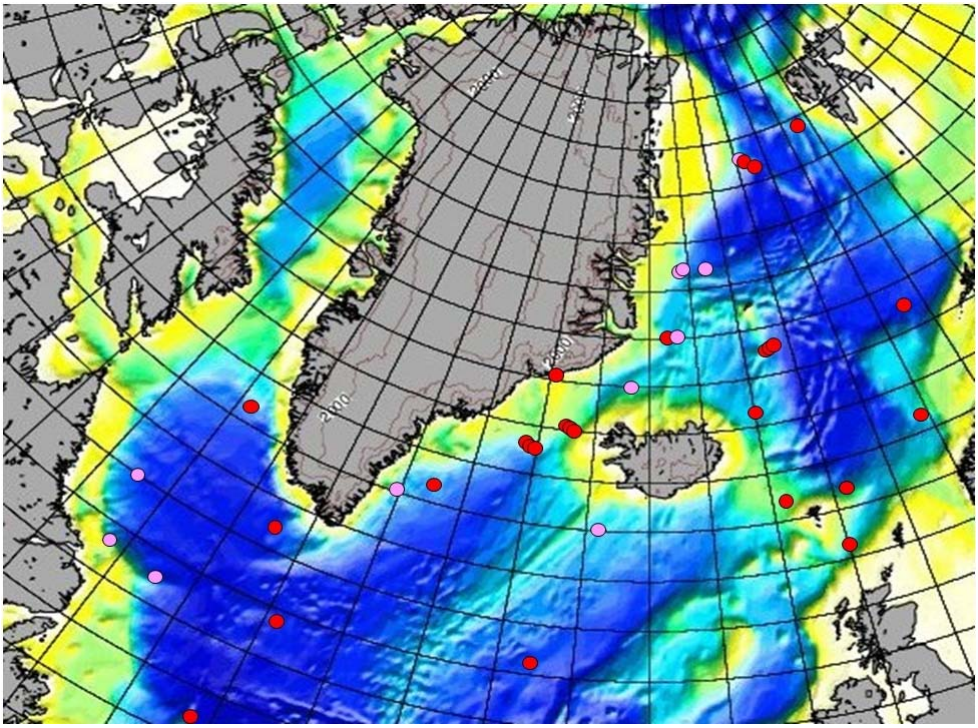

Figure 10: Carte d'échantillonnage du projet Signature.
En rouge profils complet de CI de Nd, en rose quelques mesures seulement.

Comme on le voit sur la Figure 6, les continents bordant l'Atlantique Nord sont globalement caractérisés par des CI de Nd très peu radiogéniques. Le Pacifique est au contraire entouré de formations très radiogéniques. Les formations entourant l'Atlantique Sud, l'Indien et l'Océan Austral ont des signatures intermédiaires. En première approximation, la CI de Nd des formations bordant les océans, augmentent de manière monotone lorsqu'on suit un parcours partant dans l'Atlantique Nord, passant par l'Atlantique Sud, l'Océan Austral et l'Indien pour finir dans le Pacifique. Cette évolution se retrouve dans les masses d'eau, comme illustré sur la Figure 7. De ce fait la CI de Nd est abondamment utilisée en paléocéanographie pour reconstruire les **variations de la circulation thermohaline globale** [e.g. *Piotrowski et al.*, 2008]. L'objectif principal de mon doctorat était de mieux comprendre la manière dont l'Eau Profonde Nord Atlantique (NADW) acquiert sa signature isotopique de Nd.

J'ai mesuré la CI de Nd (et les [REE]) de plus de 200 échantillons d'eau de mer, ce qui faisait plus que doubler le nombre de données disponibles à cette époque. Parallèlement j'ai conduit une étude approfondie de l'hydrodynamique de la région (masses d'eau et courants), ce qui m'a permis d'enregistrer ma thèse de doctorat à l'Univ. Toulouse III sur une double thématique: géochimie et hydrographie.

L'interprétation de ces données en relation à l'hydrologie (mélanges des masses d'eau) et à la géologie (apports externes) de la zone d'étude a permis d'améliorer notre connaissance de la circulation et du traceur ε_{Nd} [*Lacan et Jeandel*, 2004a, 2004b, 2004c]. L'étude des signatures isotopiques de l'Eau Subarctique Intermédiaire (SAIW), de l'Eau Profonde de la Mer de Norvège et de l'Eau Modale Subpolaire (SPMW) nous a permis de préciser leur histoire (trajectoires, mélanges). En particulier, nous confirmons que l'origine de la SAIW se trouve dans le courant du Labrador et nous suggérons que la SPMW résulte d'un mélange à deux pôles : l'Eau Centrale Nord Atlantique (NACW) et des eaux provenant du courant du Labrador (LCW). La Figure 11 illustre notamment la manière dont ε_{Nd} permet d'exclure la participation des eaux du *Denmark Strait* à ce mélange [*Lacan et Jeandel*, 2004c]. Ce dernier résultat a été confirmé par des études de modélisation à haute résolution (20km de résolution horizontale) de la circulation de la zone [*Deshayes et al.*, 2007]. Il est particulièrement important du fait que l'Eau de la Mer du Labrador (Laborador Sea Water, LSW, une des composante majeure de la NADW) est formée par convection profonde directement à partir de la SPMW. Ce résultat illustre aussi le caractère conservatif d'ε_{Nd}.

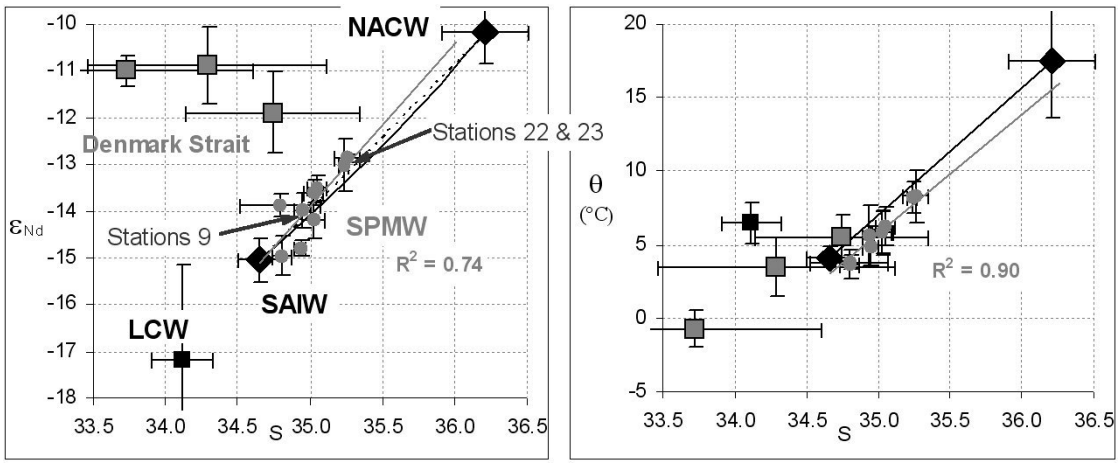

Figure 11: Propriétés moyennes de la SPMW [*Lacan et Jeandel*, 2004c].
Les courbes théoriques de mélange conservatif sont représentées en traits pleins noirs (il s'agit d'une hyperbole dans le diagramme ε_{Nd} vs. S (peu distinguable de la ligne droite en pointillée). Les régressions linéaires pour la SPMW sont représentées par des segments gris.

La NADW est en réalité composée de 3 couches (supérieure, centrale et inférieure), *upper*, *middle* et *lower* NADW (uNADW, mNADW et uNADW). Ces dernières sont elles même formées en grande partie à partir de masses d'eau de notre région d'étude, respectivement Labrador Sea Water (LSW), North East Atlantic Deep Water (NEADW) et North West Atlantic Bottom Water (NWABW). Ces 3 masses d'eau constituent ce qu'on appelle la proto-NADW. Les C.I. de Nd de ces masses d'eau sont représentées sur la Figure 12.

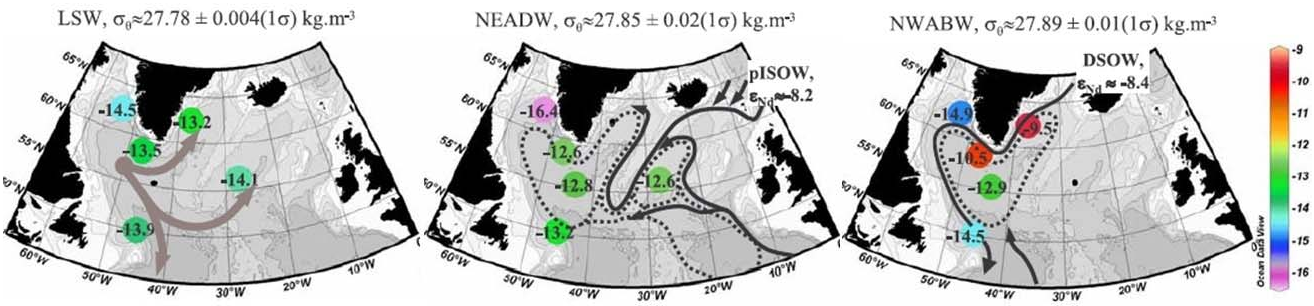

Figure 12: CI de Nd des trois couches de la proto-NADW [*Lacan et Jeandel*, 2005a].
Les valeurs moyennes des densités potentielles des échantillons sont indiquées.

L'étude de l'évolution des CI de Nd au cours des trajets de ces masses d'eau a permis de proposer un schéma expliquant les mécanismes d'acquisition des signatures isotopiques de ces masses d'eau. Ce schéma est représenté sur la Figure 13. Ces mécanismes sont d'une part les mélanges de masses d'eau et d'autre part les apports externes. Concernant les mélanges de masses d'eau, les données de CI de Nd sont compatibles avec les schémas admis pour la formation des couches supérieure et inférieure de l'Eau Profonde Nord Atlantique. En revanche, elles suggèrent une composition de la NEADW significativement différente de celle de la mNADW. Ces résultats soulignent notre méconnaissance des mécanismes de formation de cette masse d'eau, pourtant très importante puisqu'elle constituera le cœur de la NADW [*Lacan et Jeandel*, 2005a].

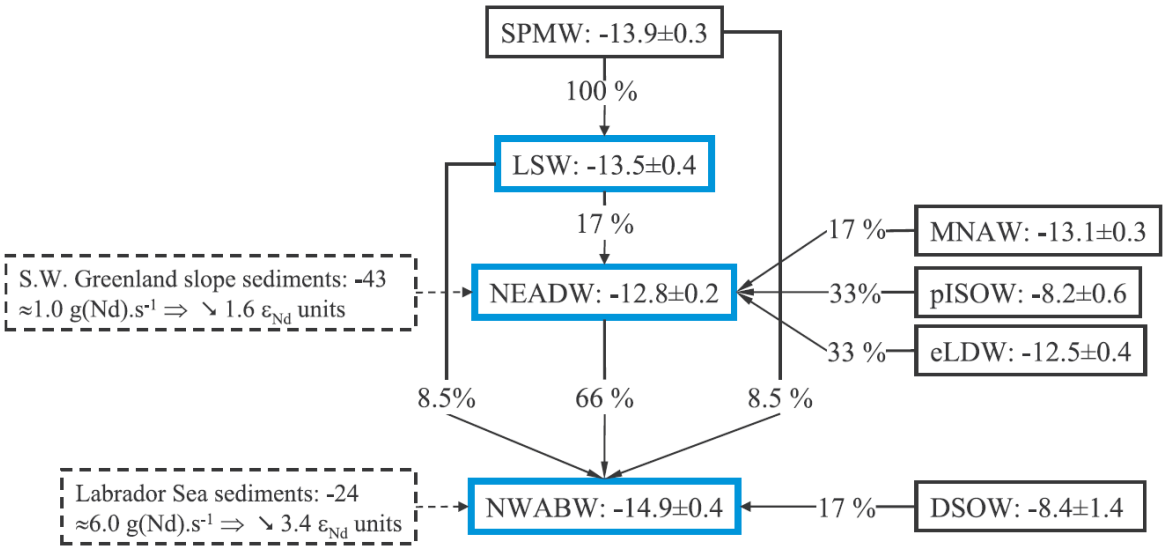

Figure 13: Schéma de l'acquisition de la CI de Nd des 3 couches de la proto-NADW
Les contributions relatives des différentes masses d'eau sources sont indiquées. Les apports lithogéniques sont décrits dans les cadres pointillés, incluant leur CI de Nd, les flux de Nd estimés, et les conséquences de ces apports sur les CI de Nd des masses d'eau ("↘" indique une diminution). MNAW: Modified North Atlantic Water; pISOW: pure Iceland Scotland Overflow Water, eLDW: Eastern Lower Deep Water, DSOW: Denmark Strait Overflow Water **[*Lacan et Jeandel*, 2005a].**

Les apports lithogéniques jouent un rôle important dans l'acquisition de la CI de Nd de la NADW. Jusqu'à ce travail les apports non-radiogéniques provenant des régions canadiennes et groenlandaises avaient été mis en avant pour expliquer la signature non-radiogénique de la NADW (d'environ -13.5) [*Von Blanckenburg et Nagler*, 2001; *Piepgras et Wasserburg*, 1987]. Notre jeu de données, offrant une résolution spatiale bien supérieure aux études précédentes, suggère que les apports lithogéniques affectant la NEADW et la NWABW proviennent de la marge groenlandaise mais ne suggère pas de contribution de la marge canadienne. A l'inverse, la LSW semble recevoir des apports externes provenant de la Baie de Baffin et de la marge du Labrador via les contributions de l'Eau du Courant du Labrador et de la SAIW à la formation de la LSW.

De plus, nos données suggèrent que, même si les sources non-radiogéniques dominent les apports externes à la proto-NADW, les apports radiogéniques, le long de la ride Groenland-Ecosse (formations basaltiques d'Islande et des Iles Féroé), ont aussi un impact très important (ils augmentent les signatures de la Denmark Strait Overflow Water et de l'Iceland Scotland Overflow Water de 2.5 et 1.8 unités ε_{Nd}). Les apports lithogéniques affectant la CI de Nd de la NADW dans sa zone de formation doivent donc être considérés comme la somme d'apports radiogéniques et non-radiogéniques.

Les processus responsables de ces apports externes ont été attribués, de même que dans le Pacifique à **des interactions sédiments/masses d'eau**, en suivant un raisonnement similaire, basé sur les calculs de flux de Nd nécessaires pour expliquer les variations observées dans les masses d'eau. Ici aussi, seuls les apports de particules déposées par l'érosion continentale sur les marges constituent

des flux suffisants, les autres sources sont très largement trop faibles. Ici aussi, des variations de CI sans variation de concentration de Nd ont été observées, suggérant des processus d'échange. Nous y reviendrons.

Globalement ce travail a apporté de nouvelles contraintes sur la circulation des masses d'eau et les apports terrigènes participant à la formation de la NADW et à l'acquisition de sa signature isotopique de Nd.

Il a aussi permis de progresser sur notre compréhension du traceur ε_{Nd} lui-même. Il a confirmé la conservativité d'ε_{Nd} à l'abri d'influence terrigène. Il a mis en évidence **l'influence de sédiments d'origine cristalline sur la C.I. de Nd des masses d'eau** et confirmé celle de sédiments d'origine basaltique. Ces résultats permettent notamment une meilleure exploitation de ce traceur en paléocéanographie.

c. *Boundary Exchange.*

Observations in situ

Plusieurs études régionales in situ ont mis en évidence les processus d'échange de Nd aux marges continentales. Mes propres travaux, le long des marges de Papouasie Nouvelle Guinée et du Groenland, mais aussi précédemment des travaux dans l'océan Indien [*Jeandel et al.*, 1998]. Des données dans le Pacifique Nord-Ouest de nos collègues Japonais suggéraient de même. Ces observations sont résumées sur la Figure 14. La connaissance des concentrations et CI de Nd en amont et en aval de la zone de contact ainsi que du flux de la masse d'eau permet, par l'application du modèle représenté sur la Figure 15 et des hypothèses de l'état stationnaire et de la conservation de la masse (pour la concentration et ε_{Nd}), d'estimer les flux externes de Nd apportés à la masse d'eau et les flux de Nd soustraits de la masse d'eau, par les équations :

$$F_{Nd}^{Addition} = F_W \times [Nd]^{Initial} \times \frac{\varepsilon_{Nd}^{Final} - \varepsilon_{Nd}^{Initial}}{\varepsilon_{Nd}^{Addition} - \varepsilon_{Nd}^{Final}} \qquad \text{Équation 2}$$

$$F_{Nd}^{Removal} = F_W \times \frac{[Nd]^{Final} \times \left(\varepsilon_{Nd}^{Final} - \varepsilon_{Nd}^{Addition}\right) - [Nd]^{initial} \times \left(\varepsilon_{Nd}^{Initial} - \varepsilon_{Nd}^{Addition}\right)}{\varepsilon_{Nd}^{Addition} - \varepsilon_{Nd}^{Final}} \qquad \text{Équation 3}$$

Ce modèle a permis d'estimer que pour les 4 masses d'eau de la Figure 14 les flux de soustraction équivalaient à 60 à 100% des flux apportés. Ces processus d'échanges ayant été observés dans des régions très contrastées, d'un point de vue hydrodynamique, biologique et géochimique, **nous avons proposé que ce concept d'échange aux marges, que nous avons nommé *Boundary Exchange,* pouvait être important à l'échelle globale** pour notre compréhension du cycle des isotopes du Nd. Un tel processus permettait de résoudre le "paradoxe du néodyme": les variations de compositions isotopiques dans l'océan sont beaucoup plus fortes que celles qui résulteraient des apports déduits des variations de concentrations. En d'autre termes, ne considérer que les apports nets (apports – soustractions) de Nd était une simplification qui ne permettait pas de rendre compte de l'ensemble des processus nécessaires pour expliquer le cycle des isotopes du Nd. Nous rejoignions en cela une étude de modélisation globale à 10 boîtes du cycle des isotopes du Nd [*Tachikawa et al.*, 2003]. Nous suggérions aussi qu'il était important de comprendre de tels processus en ce qu'ils pouvaient avoir un impact, au-delà du Nd, sur la chimie de l'océan et sur le transfert d'éléments réactifs (y compris des polluants) à l'interface continent/océan.

L'article résumant ce travail, [*Lacan et Jeandel*, 2005b], est, parmi ceux auxquels j'ai participé, celui ayant eu le plus d'impact avec en moyenne plus de 12 citations par an.

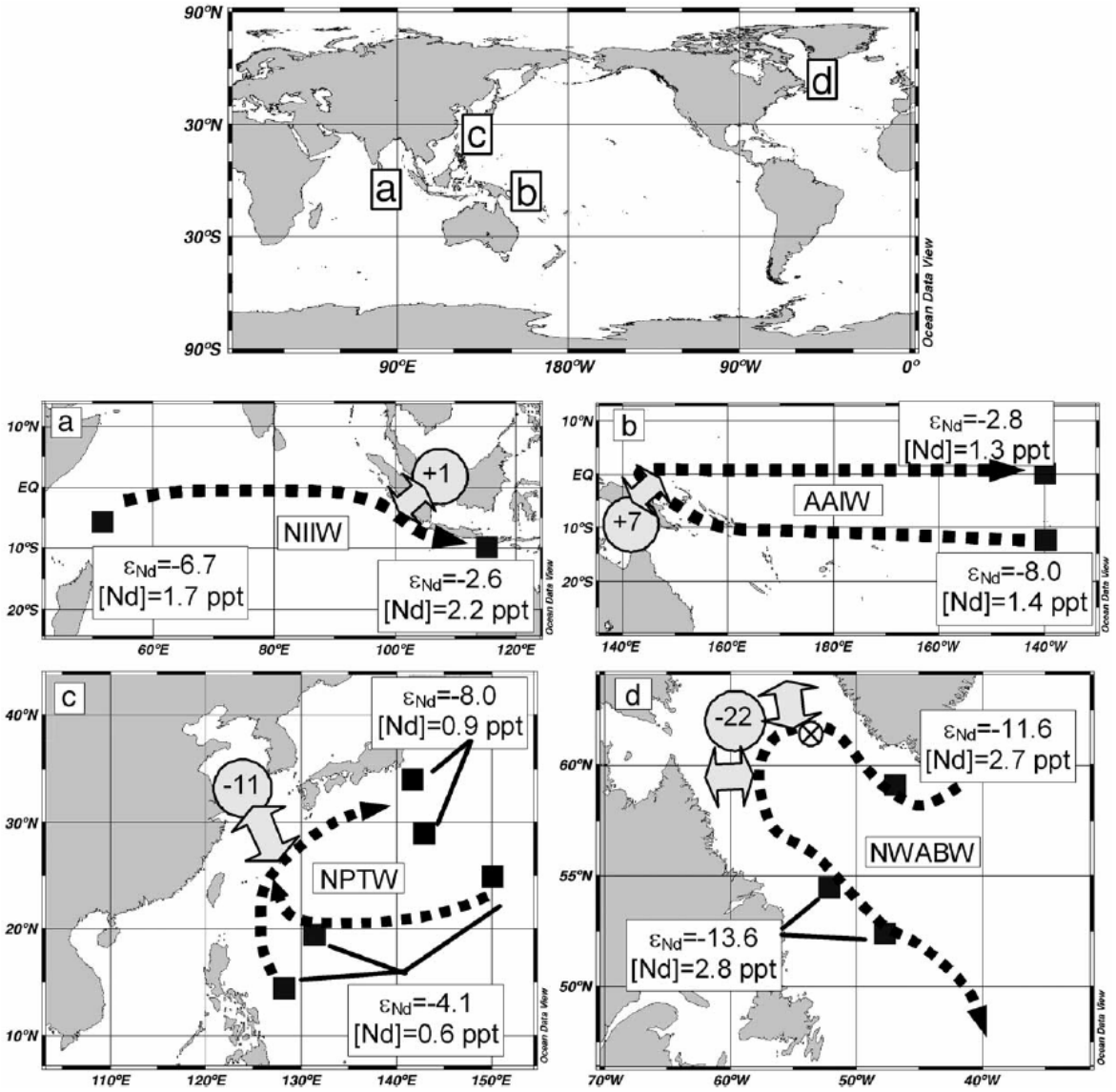

Figure 14: Observation in situ du Boundary Exchange.
NIIW: North Indian Intermediate Water, AAIW: Antarctic Intermediate Water, NPTW: North Pacific Tropical Water and NWABW: North West Atlantic Bottom Water. **[*Lacan et Jeandel*, 2005b].**

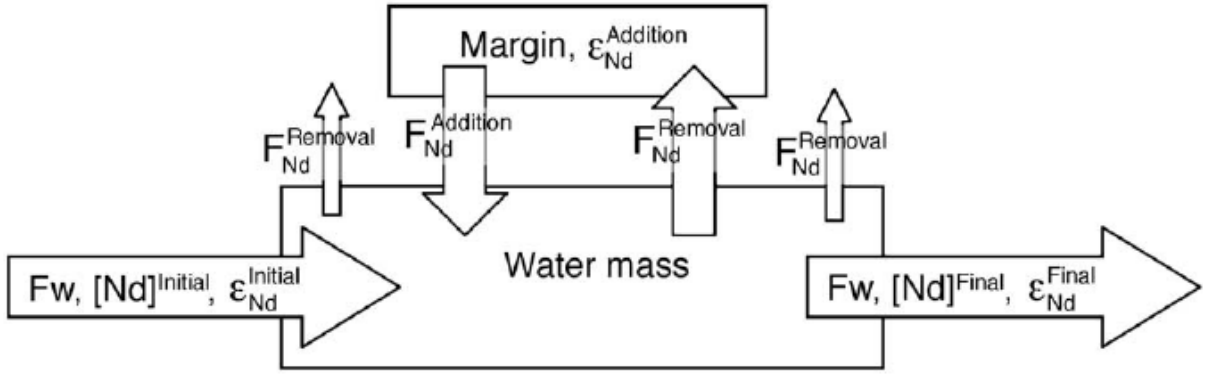

Figure 15: Modèle en boite du Boundary Exchange.
Initial et Final se réfèrent aux mesures dans la masse d'eau respectivement en amont et en aval de la zone de contact. Addition et Removal se réfèrent respectivement à l'apport externe de Nd de la marge vers la masse d'eau et à la soustraction de Nd de la masse d'eau vers la marge. Fw est le flux d'eau de la masse d'eau **[*Lacan et Jeandel*, 2005b]**.

Modélisation

Afin de tester l'importance globale du *Boundary Exchange*, il était nécessaire de mettre en ouvre une simulation globale du cycle des isotopes du Nd. Ce travail a été réalisé dans le cadre de la thèse de T. Arsouze (encadrée par C. Jeandel et J.C. Dutay, LSCE), à laquelle j'ai activement collaboré. Différentes approches de modélisation ont été utilisées. Elles étaient toutes les premières du genre, et ont été suivies par d'autres travaux menés par nos collègues.

Dans un premier temps un modèle de circulation océanique pure, sans modèle biogéochimique, donc sans particules. Le puits de Nd ne pouvant être correctement modélisé (sans particules), ce premier modèle supposait une concentration de Nd constante dans tout l'océan, seule la variable ε_{Nd} était modélisée, en tant que traceur passif. La simulation était réalisée "offline". Le modèle négligeait volontairement toutes les sources de Nd, sauf le *Boundary Exchange* paramétrisé comme un terme de rappel à la marge. Les marges sont définies ici comme les fonds compris entre 0 et 3000m. Le fait qu'une telle simulation soit en mesure de reproduire les grandes lignes de la distribution d'ε_{Nd} à l'échelle globale, nous a permis de conclure que le processus de *Boundary Exchange* constituait probablement la source et le puits majeurs du Nd dans l'océan [*Arsouze et al.*, 2007].

Cette modélisation, extrêmement simplifiée, présentait des limitations très fortes. Une seconde approche, beaucoup plus complète a été mise en œuvre. Le modèle de circulation (NEMO) a été couplé à un modèle de biogéochimie (PISCES), ce qui fournissait des champs de particules [*Arsouze et al.*, 2009]. Dès lors les puits pouvaient être modélisés (export du Nd particulaire vers le sédiment). A l'exception des sources hydrothermales (dont on pensait alors qu'elles n'avaient pas d'impact significatif sur ε_{Nd}), les autres sources ont été prises en compte (aérosols, apport dissous par les rivières et apports sédimentaires). Les interactions dissous/particules étaient représentées par un processus de scavenging réversible à l'équilibre. La Figure 16 résume ces processus et présente des résultats de ce travail.

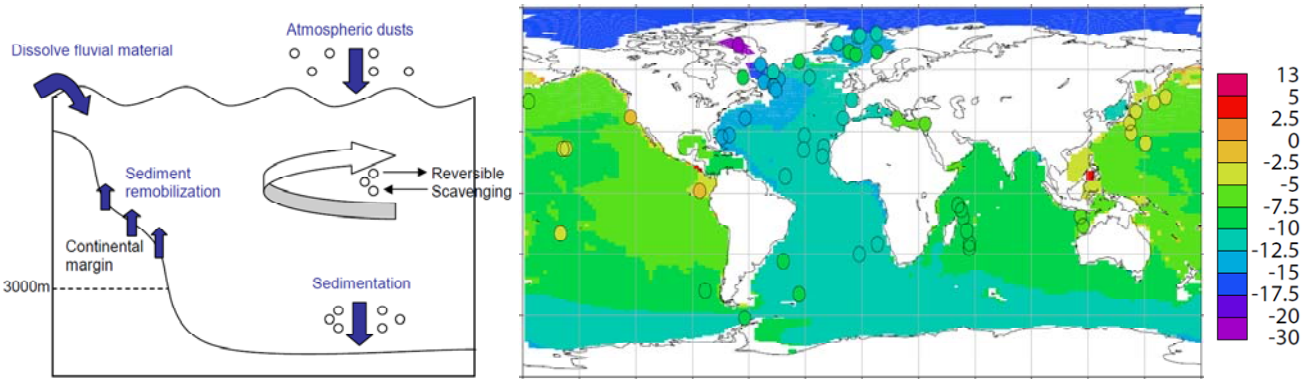

Figure 16: Modélisation couplée physique/biogéochimie du cycle d'ε_{Nd} [*Arsouze et al.*, 2009].

La recherche de la meilleure correspondance modèle/données a permis d'estimer l'intensité de la source sédimentaire (les 2 autres étant prescrites). Les résultats suggèrent que la **source sédimentaire aux marges représente en moyenne globale 95% des apports de Nd à l'océan. La soustraction du Nd par les flux particulaires aurait lieu à 64% au dessus des marges. Ces 2 résultats confirment l'importance à l'échelle globale du processus de *Boundary Exchange* et de la source sédimentaire sur le cycle d'ε_{Nd}.** Ils suggèrent en outre que ces apports sédimentaires nécessiteraient de **dissoudre de 3 à 5 % des particules apportées à l'océan par les rivières**, ce qui est en très bon accord avec les estimations proposées sur la bases des études régionales in situ [*Lacan et Jeandel*, 2005b et références incluses]. La prise en compte de ces processus d'échanges aux marges conduit à une estimation réduite du temps de résidence du Nd océanique à 360 ans [*Arsouze et al.*, 2009].

Deux études de modélisation supplémentaires ont été réalisées par T. Arsouze. L'une consistait en une adaptation de la première simulation (modèle de circulation océanique pure) aux conditions du

dernier maximum glaciaire [*Arsouze et al.*, 2008]. Ce travail suggérait que l'Atlantique Ouest était plus sensible, en termes de CI de Nd, à ces variations climatiques et soulignait le besoin d'acquérir d'avantage de données d'archives de CI de Nd dans ces régions.

La seconde consistait (de même avec le modèle de circulation seulement) en une étude régionale, à haute résolution dans l'Atlantique Nord [*Arsouze et al.*, 2010]. Les modélisations à l'échelle globale avaient une résolution horizontale de 2°x2°. Ici, la résolution était de 1/4°, "eddy-permitting". Les simulations pouvaient être comparées aux données relativement abondantes dans la région, en grande partie issues de mon doctorat. Ces travaux ont confirmé ce qui avait été obtenu précédemment à l'échelle globale, à savoir que le *Boundary Exchange* jouait un rôle dominant sur le cycle des isotopes du Nd. La paramétrisation de ce processus par un terme de rappel, fait apparaitre la notion de temps de relaxation, qui traduit l'échelle de temps caractéristique du processus. Ce travail à haute résolution a nécessité d'utiliser des temps de relaxation de quelques jours à quelques mois, alors que dans le travail à plus faible résolution (2°x2°), les temps utilisés étaient de l'ordre de 6 mois à 10 ans. L'interprétation de cette dépendance au modèle est restée à mon sens insuffisante. Cela étant, il me semble que les progrès sur la question du *boundary exchange* et plus spécifiquement sur les sources sédimentaires passent aujourd'hui d'avantage par des approches i*n situ* et expérimentales que par ce type de modélisation.

Impacts plus larges

Pour résumer, nous disons que quelques pourcents (disons entre 3 et 5%) des particules apportés par les rivières sur les marges semblent être ensuite dissous par l'eau de mer, et ceci y compris aux profondeurs intermédiaires et profondes. Ce message a été très difficile à faire accepter à la communauté. Beaucoup sont encore très sceptiques à ce sujet, mais petit à petit notre hypothèse fait son chemin. Nous n'avons d'ailleurs jamais compris ce scepticisme sachant que la plupart de la communauté admet sans aucune difficulté que quelques pourcent des aérosols se dissolvent dans les eaux de surface de l'océan. En fait je pense que ce scepticisme est de l'immobilisme, et je me réjouis d'être suffisamment mauvais en chimie pour n'avoir aucun a priori sur ce genre de question.

Le Nd des particules lithogéniques ne se dissout pas tout seul. La dissolution concerne aussi vraisemblablement d'autres éléments. Une importante fraction du Nd particulaire est contenue dans un manteau d'oxydes et d'hydroxydes de fer et de manganèse qui enrobe les particules (Fe Mn coatings). Une hypothèse serait donc que cette dissolution ne concerne que cette enveloppe. Cette hypothèse ne tient pas. Ces enrobages contiennent du Nd adsorbé depuis la phase dissoute. Or les CI du Nd dissous dans les rivières ne permettent pas d'expliquer les variations observées à l'échelle globale dans l'océan. Nous suggérons donc qu'une partie du cœur lithogénique des particules est dissoute par l'eau de mer et participe aux sources sédimentaires observées. Dans ce cas, une dissolution de ces phases devrait libérer dans l'océan un grand nombre d'éléments constituant la matière lithogénique, notamment Si, Fe, Ca, Mg et Sr. Des expériences *in vitro* confirment que lorsque des particules de sédiments provenant de rivières ou d'estuaires sont mises en contact avec l'eau de mer, on assiste à une dissolution d'un grand nombre d'éléments, notamment Si, Ca, Mg [*Jones et al.*, 2012a]

Afin d'évaluer cet effet, nous avons, en première approximation, fait l'hypothèse (critiquable) que tous les éléments subissaient une dissolution comparable à celle du Nd, de 1 à 3 % (hypothèse de dissolution congruente). Il en résulte des apports non négligeables. Pour le Si le flux de dissolution sédimentaire équivaudrait à 12 à 96% des apports dissous par les rivières. Pour le Ca et le Mg, ces pourcentages seraient respectivement de 1-8% et 2-18%. Et pour le Fe, cette source sédimentaire représenterait plus de 23 fois les flux de Fe dissous apportés par les rivières. Bien que ces quantifications soient incertaines, et que les processus sous-jacents soient inconnus, ce travail suggère que les sédiments déposés sur les marges par le jeu des érosions successives sont une source significative d'éléments et de nutriments pour l'océan et souligne le besoin de quantifier et de comprendre les processus menant à ces flux, jusque là ignorés, à l'interface continent/océan. Par

exemple si les flux de Si apportés à l'océan sont plus grands que supposé jusqu'à présent, cela réduirait sont temps de résidence, ce qui accroîtrait l'efficacité calculée de la pompe biologique de CO_2. En outre l'altération des silicates constitue un puits de CO_2 atmosphérique.

La prise en compte de l'altération sous-marine des silicates (la dissolution des sédiments d'origine lithogénique sur les marges) jusque-là négligée, en plus de la prise en compte de l'altération à la surface des continents, devrait apporter d'importantes nouvelles contraintes sur la régulation du CO_2 atmosphérique et donc du climat aux échelles de temps géologiques.

Ce travail a été récemment publié dans EOS [*Jeandel et al.*, 2011a]. Il constitue clairement le chaînon qui manquait jusqu'alors entre nos travaux de spécialistes sur le cycle des isotopes du néodyme et les questions scientifiques sur les grands cycles des éléments à la surface du globe et le climat. Ce chaînon manquant représente néanmoins à lui seul un effort de recherche important, que nous n'avons qu'effleuré. Les processus précis restent à être compris. L'impact des ces processus sur les différents éléments reste à être quantifié. L'approche expérimentale semble nécessaire à ce stade. Elle a été abordée avec des résultats prometteurs [*Jones et al.*, 2012b].

d. Base de données et compilations

L'implication du groupe GEOMAR du LEGOS sur la thématique des isotopes du néodyme a été tellement importante qu'elle nous a conduit à réaliser des compilations de données. Depuis 1999, reprenant la compilation globale des données d'ε_{Nd} dans l'eau de mer assemblée par K. Tachikawa, j'ai maintenu cette compilation jusqu'en septembre 2011. Depuis 2006 cette compilation a été mise à disposition de la communauté, librement, sur le site web de l'équipe de géochimie marine du LEGOS (http://www.legos.obs-mip.fr/recherches/equipes/geomar/Nd_DataBase). Elle a été particulièrement utile dans le cadre des travaux de modélisation décrits ci-dessus, y compris ceux de nos collègues. Fin 2011, avec l'émergence des données GEOTRACES, d'une part je n'étais plus en mesure de faire face au grand nombre de nouvelles données produites et d'autre part le programme GEOTRACES avec son centre de données allait prendre la relève. Il n'était plus utile que je continue. J'ai donc cessé d'alimenter cette compilation et nous avons publié un article décrivant cette base de données "pré-GEOTRACES" [*Lacan et al.*, 2012]. La Figure 7 en est un extrait.

Dans le cadre des travaux de modélisation, nous avions besoin de connaître les CI de Nd des marges à l'échelle globale. De même un gros travail de compilation a été entrepris pour aboutir à une base de données globale. Ce travail a été publié en 2007 [*Jeandel et al.*, 2007]. La Figure 6 en est tirée.

Ces deux travaux de compilation globale n'apportent pas à mon sens de conclusions radicalement nouvelles, ils permettent cependant de confirmer et/ou de préciser certaines affirmations, telle que par exemple l'augmentation progressive de la CI de Nd des marges et des masses d'eau, le long du trajet Atlantique Nord-Austral/Indien-Pacifique Nord (cf. Figure 6 et Figure 7). Ils sont de plus visiblement très utiles à la communauté, comme en témoigne le fort impact de la compilation des CI de Nd des marges (plus de 8 citations par an en moyenne); en ce qui concerne l'eau de mer, il est aujourd'hui trop tôt pour juger.

****

Ce qui précède ne constitue pas une liste exhaustive des travaux auxquels j'ai participé sur la thématique des isotopes du néodyme. J'ai aussi participé à des travaux dans l'océan Austral, dans la

région des îles Kerguelen ou au Sud de l'Afrique du Sud (projets KEOPS et Bonus/Goodhope) [*Garcia-Solsona et al.*, Submitted; *Zhang et al.*, 2008].

Globalement, ces travaux nous ont apporté des contraintes sur les trajectoires et les mélanges de masses d'eau, sur les interactions dissous/particules. **Le résultat majeur de ce travail, me semble-t-il, consiste en la proposition de l'existence (et de l'impact non négligeable) d'altération sous-marine des particules lithogéniques déposées sur les marges continentales par l'érosion physique des continents.**

Bien que ces sujets me semblent passionnants, je ne participe plus que marginalement à cette thématique de recherche, conduite de longue date par C. Jeandel. Elle reste néanmoins liée à mes travaux actuels sur le cycle du fer. Compte tenu de mon histoire et du fait que C. Jeandel et moi sommes dans la même équipe, des collaborations sur ce sujet ont toujours cours.

Et puisqu'il est l'heure de réfléchir à sa carrière passée et future, il a toujours flotté dans mon esprit l'idée, qu'à l'heure ou C. Jeandel cessera son activité (si ça arrive un jour !), j'aurai le devoir moral de poursuivre (sans nécessairement abandonner le reste) ses travaux sur les isotopes du Nd. Il m'apparaît aujourd'hui que cela ne sera très vraisemblablement pas nécessaire, car la relève pourra aussi bien être assurée par d'autres. Mais qui sait ? Nous verrons…

3. Quelques travaux pour s'ouvrir l'esprit

a. Isotopes du cadmium

La fin de mon doctorat (2002) a correspondu à l'émergence de nouveaux spectromètres de masses à multi-collection, dont la source d'ionisation est constituée d'un plasma d'argon (*Multi Collection Inductively Coupled Plasma Mass Spectrometer*, MC-ICPMS), contrairement aux spectromètres de masse disponibles jusqu'alors à thermo-ionisation (*Thermal Ionisation Mass Spectrometer*, TIMS) dont la source est constituée d'un filament chauffé par un courant électrique (j'avais utilisé un TIMS en doctorat pour le Nd). Ces nouvelles sources plasma offrent des capacités d'ionisation très supérieures aux sources des TIMS pour de nombreux éléments. L'étude des isotopes de ces éléments est donc devenue beaucoup plus facile qu'auparavant et de nombreux investigateurs se sont rués sur ces thématiques. C'est ce qu'on a appelé les "nouveaux isotopes" ou les "isotopes non traditionnels". Je trouve ces appellations assez malheureuses, ces isotopes ont toujours existé ! Je ne fais par leur promotion (de ces appellations). D'ailleurs le temps passe, ce qui était nouveau il y a 10 ans l'est un peu moins aujourd'hui. La Figure 17 illustre ce phénomène (en prenant l'exemple du Fe), qui me semble important car il démontre la dépendance des recherches fondamentales aux développements technologiques. On y voit l'augmentation considérable du nombre de publications sur les isotopes du fer à partir de 2001. Les MC-ICPMS ont notamment permis d'explorer les isotopes du Fe, Si, Cu, Zn, Mg, Hg, Sn et Ni dans l'environnement, ce qui était plus difficile auparavant.

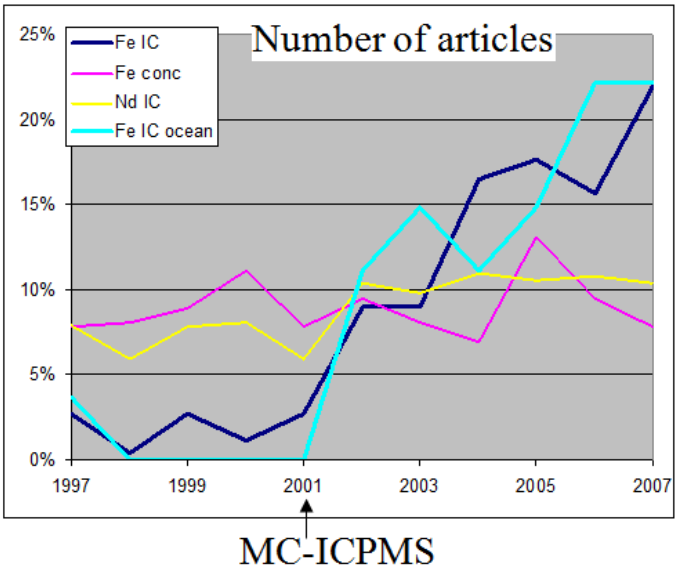

Figure 17: Avènement des MC-ICPMS et "isotopes non traditionnels".
Les différentes courbes indiquent sur une période de 10 ans la répartition des publications (source Web of Science). Alors que la production est à peu près stable pour les isotopes du Nd ou les concentrations de Fe (à titre de comparaison) le nombre de publications concernant les isotopes du fer ou les isotopes du fer dans le milieu marin augmente de manière brutale à partir de 2001, qui correspond à peu près à l'époque à laquelle les MC-ICPMS sont devenus disponibles commercialement.

Dans ce contexte je suis parti à la *Woods Hole Oceanographic Institution* pour développer la mesure des isotopes du Cd dans l'eau de mer sur une bourse Lavoisier (Ministère des Affaires Etrangères). Comme indiqué en introduction, le cadmium est un micro-nutritif. Il peut se substituer au Zn en tant que co-facteur d'une enzyme d'anhydraze carbonique ou même être utilisé directement par certaines formes de ces enzymes utilisant spécifiquement le Cd [*Cullen et al.*, 1999;

Morel et al., 1994]. Son cycle suit étroitement celui des phosphates dans l'océan actuel, de sorte qu'il est utilisé en paléocéanographie (via les enregistrements des rapports Cd/Ca dans les tests de foraminifères) pour reconstruire les distributions de phosphates et en déduire la circulation océanique et les cycles biogéochimiques passés [*Boyle*, 1988; *Elderfield et Rickaby*, 2000]. Naturellement de nombreuses questions demeurent et l'étude de son cycle isotopique pouvait apporter des éléments de réponses.

A cours de ces 18 mois de postdoc, j'ai développé le protocole de séparation chimique du Cd dissous de l'eau de mer et le protocole de mesure sur MC-ICPMS (Neptune), et je l'ai appliqué sur des échantillons du Pacifique Nord Ouest et de Méditerranée, ainsi que sur des expériences d'incubation de phytoplancton. **J'ai ainsi publié en 2006 i) le 1er protocole permettant les mesures des CI de Cd dans l'eau de mer et dans les cellules de phytoplancton, ii) les 1ères mesures de CI de cadmium dans l'océan, et iii) les 1ères mesures de fractionnement isotopique de cadmium lors de l'assimilation du Cd par le phytoplancton** [*Lacan et al.*, 2006].

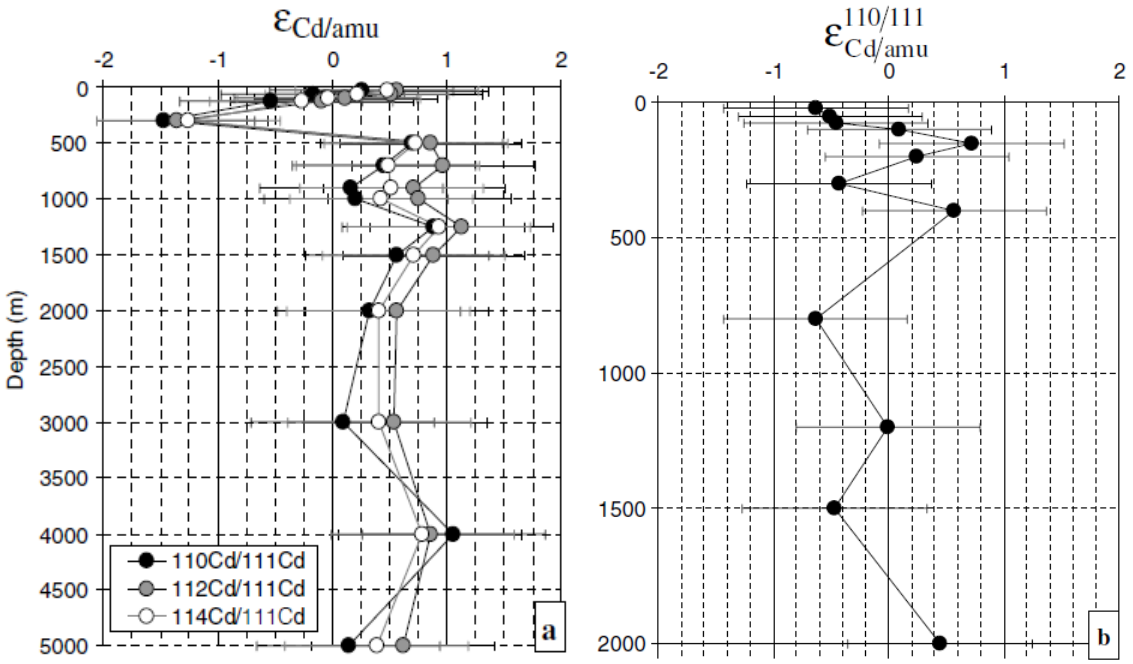

Figure 18: CI de Cd dans le NO Pacifique (a) et en Méditerranée (b).
Les barres d'erreurs correspondent à la moyenne des différences des réplicats, 0.8 unité $\varepsilon_{Cd/amu}$. Compte tenu de la notation "/amu" (par unité de masse atomique), les valeurs croissantes d'$\varepsilon_{Cd/amu}$ indiquent un enrichissement en isotopes lourds [*Lacan et al.*, 2006].

Compte tenu du timing relativement serré et de mon statut de postdoc, les échantillons ont été choisis plus en fonction d'opportunités qu'en résultat d'une réflexion. Ils étaient en outre trop peu volumineux (500mL) pour obtenir les meilleures précisions possibles. Mais c'est ce que j'avais, c'était déjà pas mal ! Compte tenu des barres d'erreurs (que je pense avoir légèrement surestimées par excès de prudence), les variations observées en Méditerranée ne sont pas significatives tandis que celles observées dans le Pacifique mettent en évidence des différences significatives entre les eaux de subsurface (à 300m) et les eaux de surface et profondes (voir Figure 18). Ces résultats ont suggéré que **1) différentes masses d'eau pouvaient avoir des signatures isotopiques distinctes, 2) le phytoplancton consommait préférentiellement le Cd léger, 3) les eaux profondes avaient une signature plutôt constante.** La préférence du phytoplancton pour le Cd léger a été confirmée par les mesures d'expériences *in vitro*, dont les résultats sont présentés sur la Figure 19. Ces résultats étaient très encourageants et promettaient que les isotopes du Cd nous apporteraient de nouvelles contraintes sur son cycle dans l'océan moderne et pouvaient conduire à de potentielles applications paléocéanographiques. Il ne m'a malheureusement pas été possible de continuer. A ma

connaissance, depuis ces premières mesures il y a aujourd'hui 10 ans, seuls 2 groupes (Imperial College London, M. Reckhamper et Max Planck Insitute, W. Abouchami) ont publié sur cette thématique [*Abouchami et al.*, 2011; *Ripperger et al.*, 2007]. Leurs travaux confirment et précisent (grâce à une meilleure précision analytique, à de meilleures résolution spatiales et à des sites mieux choisis) l'ensemble de nos résultats: les 3 points listés ci-dessus.

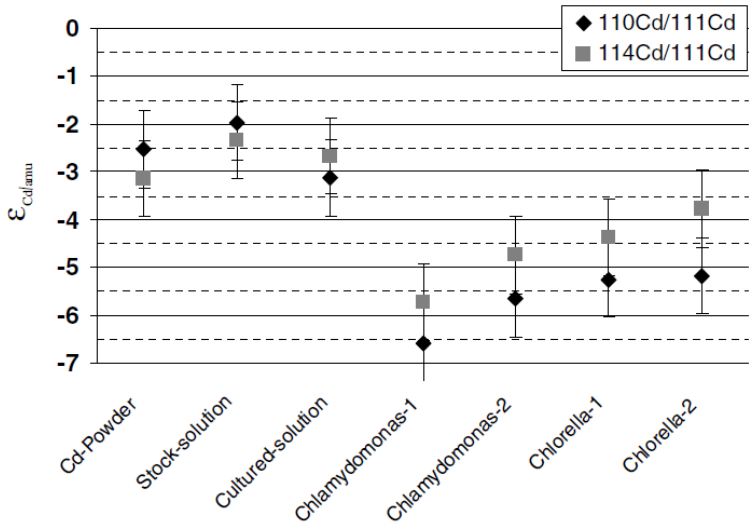

Figure 19: Fractionnement isotopique du Cd lors d'expériences de cultures in vitro.
Cd Powder: poudre utilisée pour fabriquer la "Stock-solution"; Stock-solution: solution initiale utilisée pour les cultures; Cultured-solution: solution de culture après la culture des cellules de Chlamydomonas (qui n'ont consommé qu'une infime partie du stock), pour chaque espèce, les échantillons de cellules ont été séparés en duplicats (1 et 2). Compte tenu de la notation "/amu" (par unité de masse atomique), les valeurs croissantes d'$\varepsilon_{Cd/amu}$ indiquent un enrichissement en isotopes lourds [*Lacan et al.*, 2006].

Ce premier postdoc a été très important pour moi. Pour 3 raisons: il m'a introduit au monde des isotopes stables, il m'a familiarisé avec le monde du phytoplancton, il m'a prouvé que je pouvais réaliser des développements analytiques des plus délicats. Ces 3 points ont été déterminants dans la construction de mon projet de recherche sur les isotopes du fer. Ce postdoc m'a aussi fait découvrir le monde de la recherche à l'américaine, avec ses avantages et ses inconvénients.

b. Modélisation du $^{231}Pa/^{230}Th$

Le couple $^{231}Pa/^{230}Th$ constitue un traceur des flux de particules et de la dynamique des masses d'eau profondes [*Yu et al.*, 1996]. Bien qu'il ait été considéré comme un proxy fiable et puissant de l'activité de la circulation de retournement méridienne (MOC) atlantique passée [*Gherardi et al.*, 2009; *McManus et al.*, 2004], le cycle de ces éléments et en particulier leur comportement vis-à-vis des différents types de particule était mal connu [*Chase et al.*, 2002], et c'est toujours le cas aujourd'hui. Résultat, ne maîtrisant pas suffisamment le traceur, lorsque la résolution des données augmente, des résultats totalement inattendus apparaissent et des conclusions opposées aux précédentes sont tirées. Cette situation de controverse est très bien illustrée par 2 papiers publiés dans Nature, en 2004 et 2010, le dernier concluant à une circulation inversée (donc avec une dominante du Sud vers le Nord) au LGM alors que le précédent concluait à une situation proche de l'actuelle (donc avec une dominante du Nord vers le Sud) [*McManus et al.*, 2004; *Negre et al.*, 2010]. La modélisation fait partie de la palette d'outils à notre disposition pour progresser dans notre compréhension des cycles des éléments. De retour en France, au LSCE, en collaboration avec J.C. Dutay, nous avons donc entrepris la modélisation du cycle de ce couple de traceur, à l'échelle globale

en couplant le modèle de circulation NEMO (en configuration ORCA2, 2°x2°) avec le modèle de biogéochimie PISCES [*Dutay et al.*, 2009].

Le modèle PISCES a été écrit pour simuler les flux de carbones à travers l'océan, pas les flux de Th ou de Pa. Cet exercice de modélisation nous a permis de constater que **les concentrations en petites particules simulées par PISCES dans les couches de fond étaient beaucoup trop petites** comparées aux contraintes amenées par les distributions de $^{231}Pa/^{230}Th$ mais aussi aux observations directes des concentrations en particules. En effet, les coefficients de partition dissous/particules qu'il nous a fallu utiliser pour obtenir des résultats compatibles avec les données (comme par exemple ceux représentés sur la Figure 20) étaient irréalistes, comparés aux valeurs mesurées de ces coefficients de partition [e.g. *Chase et al.*, 2002].

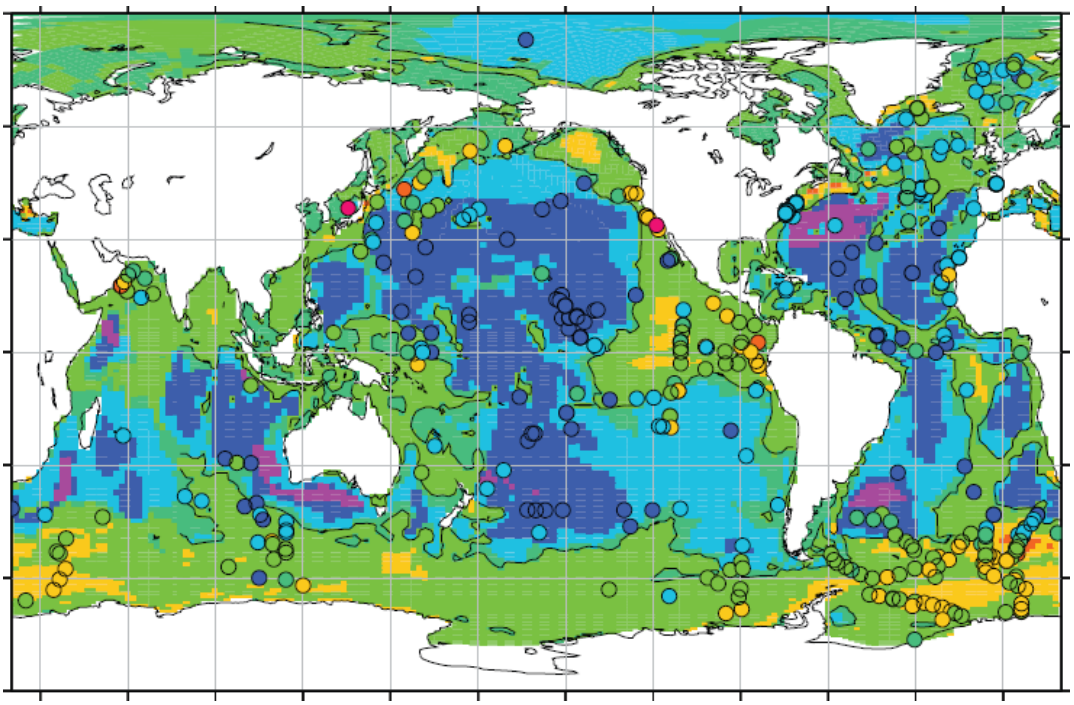

Figure 20: Simulation de $^{231}Pa/^{230}Th$ dans NEMO/PISCES.
Simulation du rapport $^{231}Pa/^{230}Th$ dans le flux vers le sédiment. Les observations sont indiquées par les disques. **[*Dutay et al.*, 2009]**

Ayant été recruté au CNRS au LEGOS, 6 mois après le début de ce postdoc, le travail a été terminé et publié par J.C. Dutay (je ne suis que 2ème auteur). Il m'a néanmoins permis d'acquérir une expérience en modélisation (physique et biogéochimique), ce qui m'a beaucoup apporté dans ma participation aux travaux de T. Arsouze de modélisation du cycle du Nd (cf. ci-dessus), et qui me permet d'envisager sereinement de tels travaux dans le futur.

Je dirais que le modèle **PISCES était à l'époque trop tourné vers le cycle du carbone** pour nous faire sensiblement avancer dans notre compréhension du cycle du couple $^{231}Pa/^{230}Th$. En revanche cette étude nous a permis de prendre conscience de ce défaut et de suggérer aux développeurs de PISCES des améliorations pour **rendre ce modèle plus adapté aux éléments plus réactifs**, de type de ceux retenus comme "*core parameters*" par le programme GEOTRACES. Outre le $^{231}Pa/^{230}Th$ et le Nd, le couple NEMO PISCES a été utilisé pour des simulations globales du cycle du fer et de l'aluminium [*Aumont et Bopp*, 2006; *Aumont et al.*, 2003; *van Hulten et al.*, 2012; *Tagliabue et al.*, 2010].

4. Les isotopes du fer

Tracer les apports lithogéniques, et notamment ceux de fer, à l'océan avec les isotopes du néodyme c'est bien. Avec les isotopes du fer, cela pourrait être mieux !

a. Introduction

Le cycle interne océanique de fer est très complexe (Figure 21). Il est nécessaire de considérer ses spéciations physiques, biologiques et redox, et les processus biologiques, physiques et chimiques. La plupart des études se sont focalisées jusqu'à présent sur la phase dissoute de Fe (DFe, habituellement définie comme < 0.2µm). Cependant, le réservoir total de fer est souvent dominé par les particules Fe [PFe, *De Barr et de Jong*, 2001]. Le réservoir dissous se divise en une fraction soluble et une fraction colloïdale. Une grande partie de la fraction dissoute, jusqu'à 90 % dans les eaux de surface, peut être colloïdal [*Wu et al.*, 2001]. Alors que la phase soluble est supposée être la plus biodisponible, certaines espèces peuvent aussi consommer du Fe colloïdal [*Chen et al.*, 2003] ou des nano-particules [*Raiswell et al.*, 2008]. Bien sûr, cela soulève la question des flux entre ces différents réservoirs. Une conclusion majeure des 2 dernières décennies est le fait que presque tous le DFe (plus de 99 %) est complexé par des ligands organiques, sur toute la colonne d'eau [e.g. *Croot et Johansson*, 2000]. Les origines de ces ligands restent mal connues. Ils réduisent les pertes de DFe par scavenging et précipitation et peuvent aider à son assimilation par certaines espèces de phytoplancton. Enfin, il faut considérer sa spéciation redox. Le Fe^{II} est la phase la plus soluble, mais il est rapidement oxydé dans l'océan oxique. Le Fe^{III} est thermodynamiquement le plus stable, mais le Fe^{III} inorganique a une très faible solubilité et précipite en hydroxydes et oxydes de fer. Le Fe^{III} reste cependant la phase plus abondante en eau de mer, car sa complexation avec les ligands organiques empêche sa précipitation [*Sarthou et al.*, 2011].

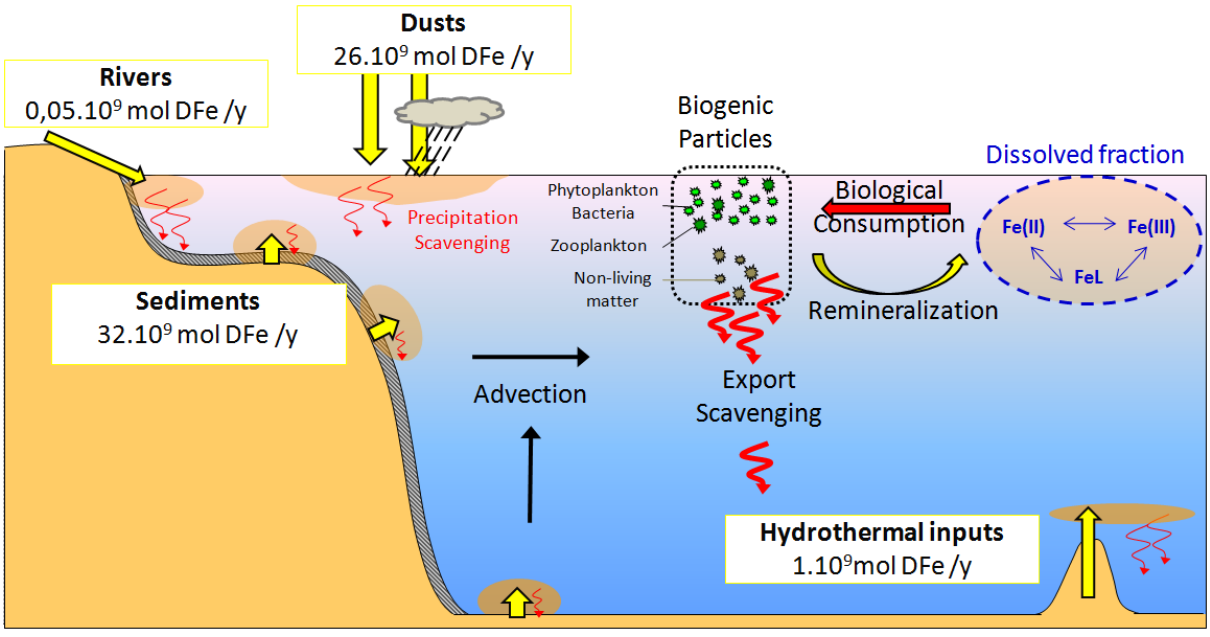

Figure 21: Schéma du cycle océanique du Fe.
Flux provenant de **[*De Barr et De Jong*, 2001; *Bennett et al.*, 2008; *Moore et Braucher*, 2008]**.

L'implication du Fe dans la production primaire exerce un contrôle fort sur son cycle interne, comme le montre son profil vertical de type "nutritif": appauvrissement en surface (due à l'absorption par le phytoplancton) et des enrichissements intermédiaires et profonds (dus à la reminéralisation; voir Figure 22). À la différence des principaux éléments nutritifs, le Fe ne présente

pas des concentrations croissantes en profondeur au cours du vieillissement des masses d'eau. Les concentrations des eaux profondes de l'Atlantique sont légèrement supérieures à celles de l'Océan Austral et du Pacifique. Ceci est attribué à l'effet du scavenging (le Fe est plus réactif vis-à-vis des particules que les macro-nutritifs) [*Boyd et Ellwood*, 2010]. Les profils de Fe révèlent donc les forts contrôles exercés par le cycle de la matière organique et le cycle des particules sur le cycle du Fe. L'ensemble de ces processus conduit à des profils typiques de DFe dans l'océan ouvert présentant des concentrations allant de 0,02 à 0.4nM à la surface et de 0,4 à 1nM en profondeur [*Johnson et al.*, 1997].

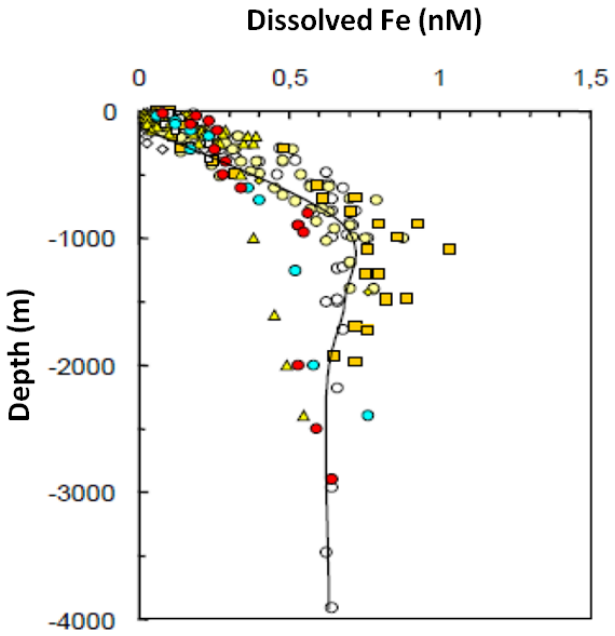

Figure 22: Profil vertical de Fe typique dans l'océan ouvert [*Johnson et al.*, 1997].

Jusqu'à très récemment toutes les études du cycle océanique du fer étaient basées sur la mesure des concentrations de fer dans l'eau de mer (y compris ses spéciations). Aujourd'hui, la mesure de sa composition isotopique est devenue possible. Comme cela a été le cas pour le carbone, d'oxygène ou d'azote (avec l'étude de leurs isotopes), l'étude des isotopes du Fe devrait permettre des avancées majeures dans notre compréhension du cycle du Fe.

Dans tout ce qui suit les compositions isotopiques de Fe seront exprimées par la variable:

$$\delta^{56}Fe=[(^{56}Fe/^{54}Fe)_{sample}/(^{56}Fe/^{54}Fe)_{IRMM\text{-}14}\ -1]x10^{3} \qquad \text{Équation 4}$$

où IRMM-14 est un standard tel que les roches ignées terrestres sont caractérisées par une signature (très précisément définie) de 0.07‰ [*Poitrasson*, 2006].

Depuis l'avènement des MC-ICPMS, dans les années 2000, la communauté internationale s'est précipitée pour étudier les isotopes de fer dans l'environnement (cf. Figure 17). Toutefois, cette mesure dans l'eau de mer est extrêmement difficile (à cause de sa très faible teneur en Fe et la matrice salée). Dans un premier temps, la plupart des études ont été menées dans d'autres environnements (roches, sols, eaux douces, in vitro...). Une des principales conclusions de ces travaux est que les processus d'oxydoréduction exercent un contrôle important sur les isotopes de Fe dans l'environnement, le fer réduit étant beaucoup plus léger que le fer oxydé, avec les différences isotopiques entre les deux phases variant de 1 à 3,5 [*Johnson et al.*, 2008; *Wu et al.*, 2011 et références incluses]. Cela est schématisé sur la Figure 23.

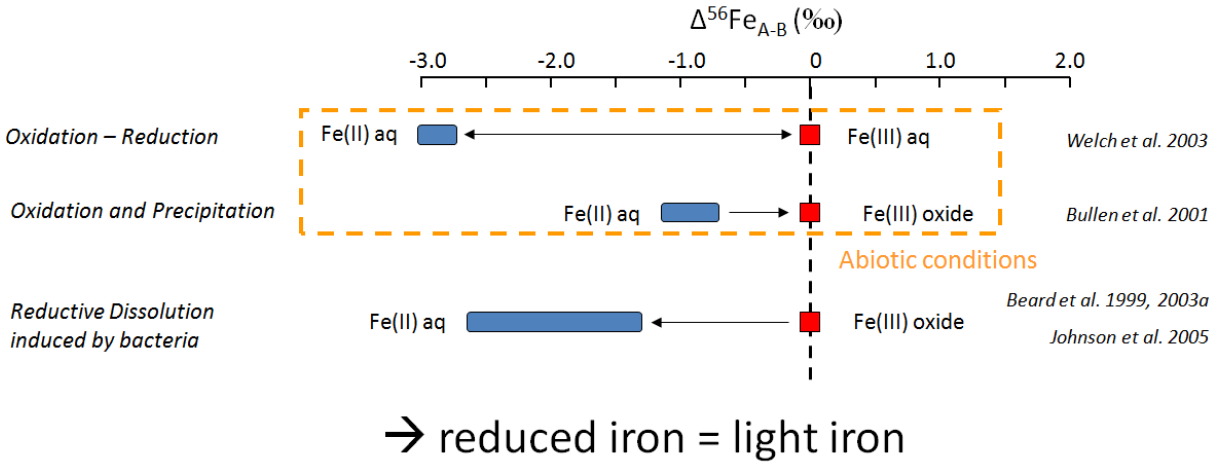

Figure 23: Fractionnement isotopique du Fe lors de processus d'oxydoréduction.
Données de **[*Beard et al.*, 2003a, 1999; *Bullen et al.*, 2001; *Johnson et al.*, 2005; *Welch et al.*, 2003]**.

En raison notamment du rôle essentiel de Fe dans l'océan, plusieurs études se sont intéressées indirectement au cycle océanique des isotopes du Fe, par l'intermédiaire de proxy, tels que les dépôts d'hydroxydes de ferromanganèse marins [Levasseur et al., 2004], ou en étudiant les frontières de l'océan, estuaires [e.g. *Escoube et al.*, 2009], aérosols [e.g. *Waeles et al.*, 2007], sédiments [e.g. *Severmann et al.*, 2010] ou hydrothermalisme [e.g. *Rouxel et al.*, 2008]. Cela a permis d'avoir une vision des signatures isotopiques de Fe des diverses sources à l'océan. Elles sont représentées sur la Figure 24.

La mesure étant plus facile dans les eaux côtières concentrées en Fe (comparées à l'océan ouvert), quelques études ont aussi porté sur les isotopes de Fe dans de tels environnements [*De Jong et al.*, 2007; *Rouxel et Auro*, 2010]. Bien qu'intéressantes en soi pour l'étude de ces environnements et pour caractériser les sources de fer à l'océan, aucune des mesures décrites ci-dessus ne pouvait remplacer la mesure des isotopes du fer au sein de la colonne d'eau océanique, si l'objectif est d'étudier le cycle du fer dans l'océan.

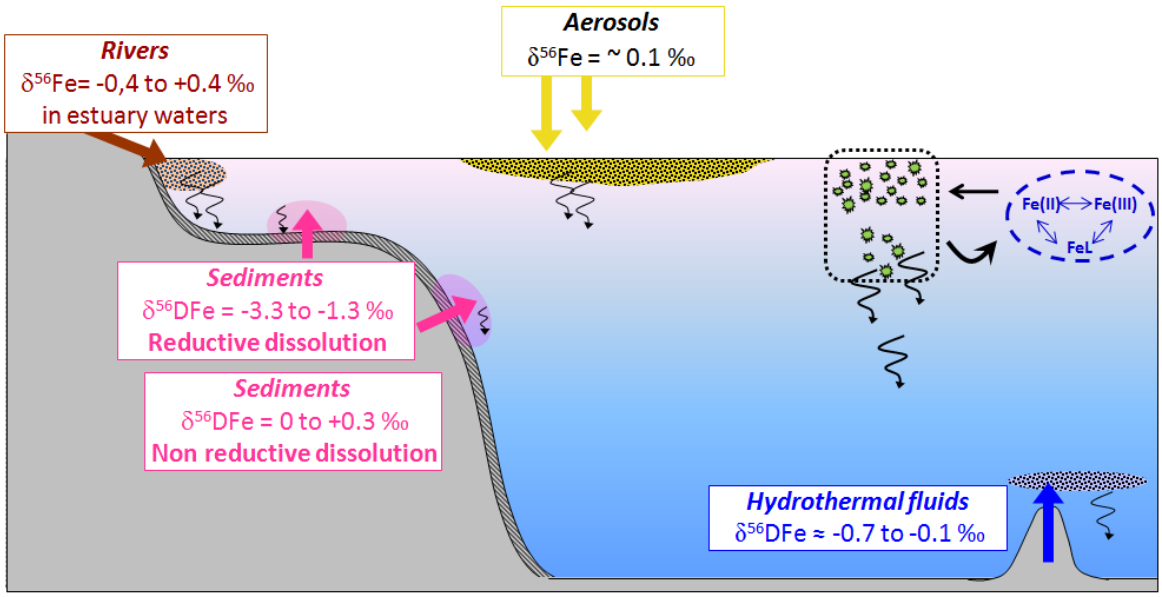

Figure 24: CI de Fe des sources de Fe à l'océan.
[*Beard et al.*, 2003b; *Bergquist et Boyle*, 2006; *Escoube et al.*, 2009; *Homoky et al.*, 2009; *Ingri et al.*, 2006; *de Jong et al.*, 2007; *Radic et al.*, 2011; *Rouxel et al.*, 2008; *Severmann et al.*, 2006, 2010; *Sharma et al.*, 2001; *Waeles et al.*, 2007].

Cela étant cette mesure présente un défi analytique très important. En 2005, aucune mesure n'avait encore été produite dans l'océan, ce qui m'a permis de proposer mon projet de recherche au CNRS sur cette thématique encore vierge. Ce projet était basé sur une hypothèse de travail. A cette époque, comme indiqué en introduction, le débat sur l'importance de la source sédimentaire de fer (relativement aux aérosols) pour l'océan ouvert de surface était posé et actif. Les poussières avaient été caractérisées avec une signature similaire à celle de la croûte continentale, c'est-à-dire δ^{56}Fe≈0.1‰ [*Beard et al.*, 2003b; *Waeles et al.*, 2007]. Des expérience in vitro suggéraient que la réduction bactérienne du fer survenant dans les sédiments et libérant le fer dissous dans l'eau de mer était caractérisée par des signatures isotopiques légères, δ^{56}Fe autour de 1.2‰ à 1,3 % plus léger que la source de fer solide [*Beard et al.*, 2003a]. Ceci a été confirmé plus tard par des mesures in situ des eaux interstitielles sédimentaires le long de la marge californienne, caractérisées par des signatures très légères à l'interface eau de mer / sédiment, de -3,3 à - 1, 3‰ [*Severmann et al.*, 2006, 2008, 2010]. L'idée était donc simple : si nous pouvons mesurer la composition isotopique du DFe dans l'océan, et si les signatures de source sont conservées dans la colonne d'eau, **les isotopes du fer devraient permettre de retracer les sources de fer dans l'océan et de quantifier l'importance relative des poussières par rapport aux sédiments des marges**.

b. Développement analytique

Dans un premier temps, j'ai donc travaillé au développement d'un protocole permettant de mesurer la CI du Fe dissous dans l'eau de mer, y compris dans les eaux de surface des régions HNLC où le fer se trouve en très faibles concentrations. J'ai d'abord travaillé seul à ce développement (2005-2007) puis avec ma 1ère doctorante, Amandine Radic, à partir de sept. 2007. Nous avons abouti à un 1er protocole adapté à des concentrations de Fe supérieures ou égales à 0.14nM. Il s'agissait du 1er protocole jamais publié permettant la mesure des CI de Fe dans l'océan ouvert. En effet, le seul autre travail publié à cette époque ne permettait des mesures que sur des eaux dont les concentrations en fer étaient supérieures à 2nM, ce qui n'était pas adapté aux concentrations océaniques (mais aux eaux côtières)[*De Jong et al.*, 2007]. Nous avons publié ce protocole en 2008 avec les 1ères mesures d'échantillons océaniques provenant de l'Atlantique Sud (campagne Bonus/GoodHope) [*Lacan et al.*, 2008]. Nous avons progressivement amélioré ce protocole (en réduisant les blancs) ce qui le rendait adapté aux eaux dont les concentrations de DFe étaient supérieures ou égales à 0.013nM (13pM), autrement dit toutes les eaux océaniques puisqu'à l'heure actuelle les plus faibles concentrations de fer mesurées sont de 0.02nM [*Sarthou et al.*, 2003]. Nous avons publié ce travail en 2010 [*Lacan et al.*, 2010]. Ayant commencé ce travail 2 ans avant le début de la thèse d'A. Radic, cette dernière n'avait pas une vision complète de ce développement analytique, en particulier ce qui concernait les mesures spectrométriques (corrections des fractionnements de masse instrumentaux). J'ai donc rédigé moi-même ces 2 publications, A. Radic en étant la 2ème auteure. Nous prenions à cette époque une avance importante au sein de la communauté internationale, car malgré les efforts des équipes les plus renommées dont certaines avaient commencé à travailler sur ce développement dès 2003 (MIT, WHOI, Univ. of Miami, CALTECH (USA), NIOZ (NL), NOC (UK), Otago Univ. (NZ), et probablement d'autres), **nous avons été les 1ers à publier un protocole adapté à l'océan ouvert, les 1ers à publier des données dans l'océan ouvert**, et finalement les 1ers à publier un protocole adapté à l'ensemble des eaux océaniques (y compris HNCL). A ce jour, une seule autre équipe, celle de Seth John (Univ. of South Carolina, USC, précédemment à Caltech), a publié un protocole et des données dans l'océan ouvert, mais leur protocole avec un blanc de 0.02nM n'est adapté qu'aux eaux de mer avec des concentrations supérieures à 0.2nM (en considérant une contribution de blanc tolérable de 10%), ce qui reste relativement important et inadapté aux eaux de surface des régions HNLC [*John et Adkins*, 2010]. **Nous restons donc les seuls aujourd'hui à être capable de réaliser les mesures de CI de DFe dans tout l'océan**. Les mesures dans les particules en suspension sont beaucoup plus faciles, car il n'est pas nécessaire de préconcentrer le fer (déjà préconcentré sur la membrane filtrante). Ce développement n'a pas fait l'objet d'une publication. Ces développements analytiques seront brièvement repris dans la partie II.5.

Les résultats d'Amandine Radic sont présentés sur la Figure 25.

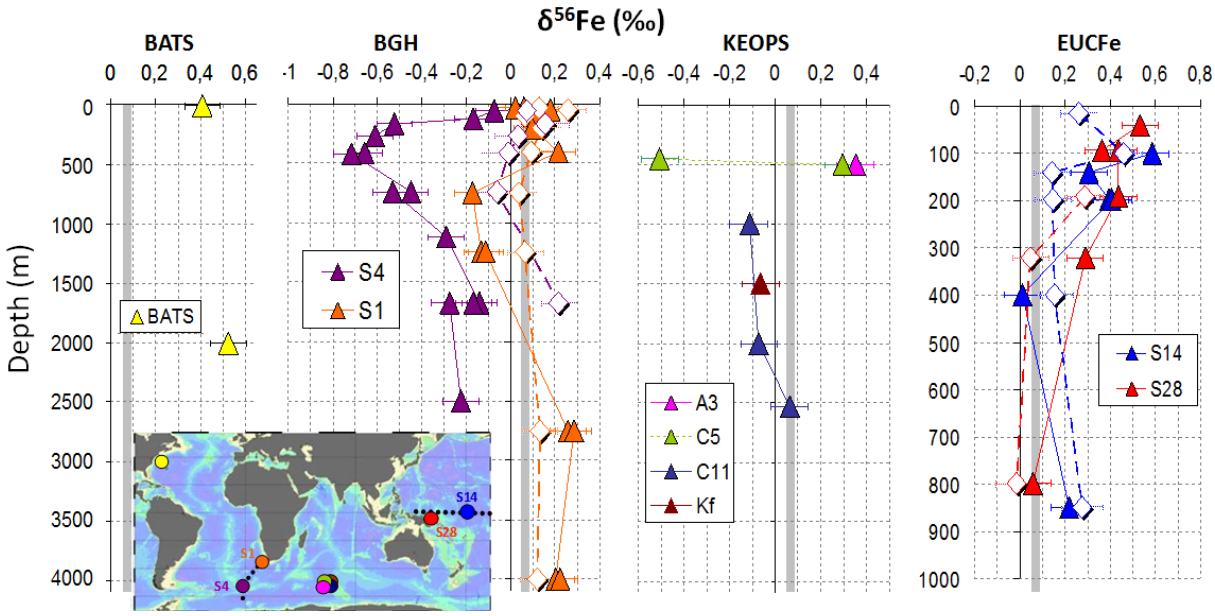

Figure 25: Données de la thèse d'Amandine Radic.
Les symboles pleins correspondent au DFe (<0.4µm), les symboles creux au PFe (>0.4µm, le protocole dissout entièrement les particules). La bande grise indique la signature de la croute continentale.

a. Suivi des masses d'eau

La Figure 26 met en évidence les masses d'eau que l'on a mesurées plusieurs fois le long de leur trajet. La station S4 (Super 4) de la campagne Bonus/GoodHope (2008), située au Sud du front polaire, a permis d'échantillonner des masses d'eau que l'on retrouve sur le plateau des îles

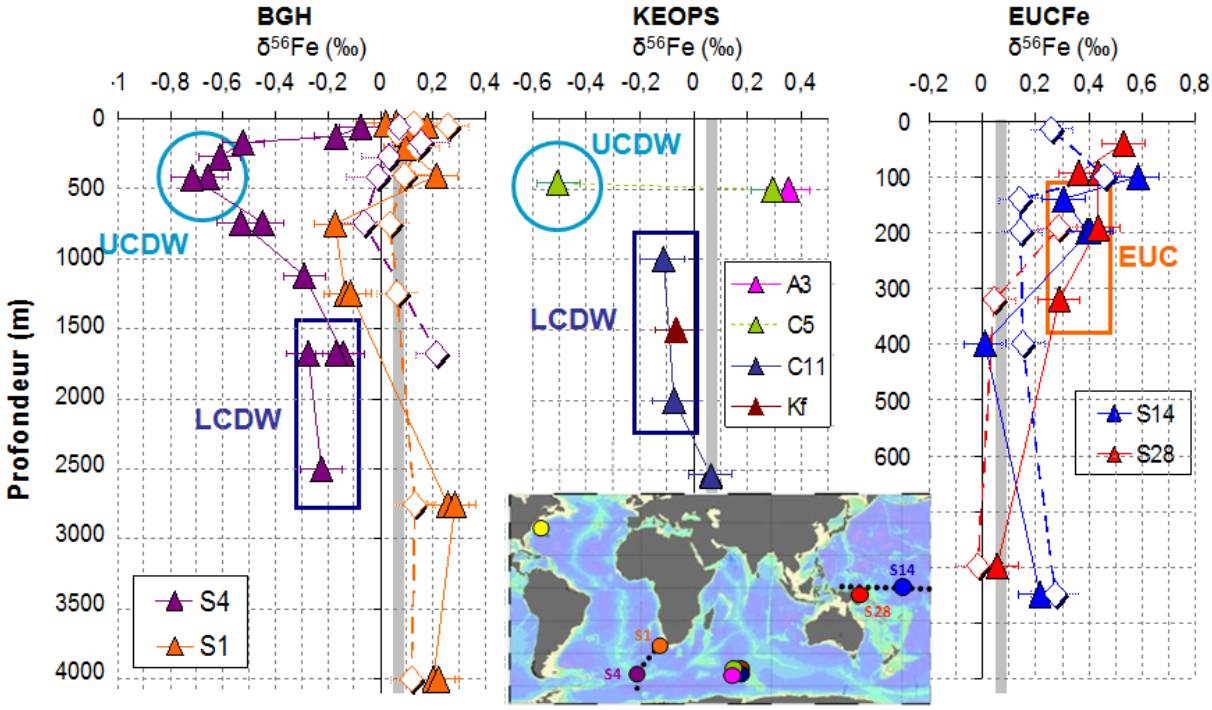

Figure 26: Préservation des CI de Fe au sein des masses d'eau.
Les symboles pleins correspondent au DFe (<0.4µm), les symboles creux au PFe (>0.4µm, le protocole dissout entièrement les particules). La bande grise indique la signature de la croute continentale.

Kerguelen, de même au Sud du front polaire, et qui ont été échantillonnées au cours de la campagne KEOPS (2005): l'Upper Circumpolar Deep Water (UCDW) et la Lower Circumpolar Deep Water (LCDW). L'étude des propriétés hydrographiques des échantillons permet de conclure que le cœur de ces masses d'eau (où ont été prélevés les échantillons) est bien préservé au cours de ce trajet d'environ 4000km, c'est-à-dire que l'effet du mélange y est négligeable. On remarque que les signatures isotopiques de fer de ces masses d'eau profondes sont assez semblables aux deux endroits, respectivement environ -0.6‰ et -0.15‰, pour l'UCDW et la LCDW. De même, les masses d'eau du sous-courant équatorial pacifique, échantillonnées dans la région de Papouasie Nouvelle Guinée (PNG) et à la ligne de changement de date, encore une fois à environ 4000km de distance, ont une CI de Fe qui ne change pour ainsi dire pas d'environ +0.35‰. Ces observations suggèrent une première conclusion: **les signatures isotopiques des masses d'eau profondes et de subsurface semblent se préserver sur de longues distances en l'absence d'apport externe de fer**. Cette conclusion devra être confirmée par davantage d'observations, mais elle est de très bon augure pour utiliser la CI de fer pour tracer l'origine du fer au sein de l'océan. Ce résultat n'est que partiellement publié. Il l'est en ce qui concerne le Pacifique Equatorial [*Radic et al.*, 2011].

b. Apports sédimentaires

Amandine Radic a aussi obtenu des mesures dans régions où des apports de fer d'origine sédimentaire étaient suspectés: le long de la marge de Papouasie Nouvelle-Guinée (connue pour être une source importante de fer dissous dans le Pacifique équatorial [*Mackey et al.*, 2002; *Slemons et al.*, 2010]), au large de la marge d'Afrique du Sud et au-dessus des sédiments du Plateau de Kerguelen, où de même des sources de fer d'origine sédimentaire ont été mises en évidence [*Blain et al.*, 2008]. Alors que nous nous attendions à trouver la signature isotopique légère qui était sensée caractériser les sources sédimentaires du fait des processus de dissolution réductrice du fer [*Severmann et al.*, 2010] nous avons mesuré dans les 3 cas **une signature légèrement lourde, d'environ +0.3‰ : le DFe étant systématiquement ~0.2‰ plus lourd que le PFe**. Les processus de réduction du fer produisant du fer léger, nos observations suggérèrent donc l'existence d'une "**libération non réductrice de fer dissous provenant des sédiments**". Ces résultats ont été confirmés par des données supplémentaires de ma seconde doctorante, Marie Labatut, qui a poursuivi le travail dans le Pacifique et dans la région de PNG. En fin de compte, nos résultats ne permettaient pas de suivre notre hypothèse de travail initiale (les isotopes du Fe comme un outil permettant de distinguer les poussières par rapport aux apports sédimentaires), mais **ils permettaient de mettre en évidence un processus jusqu'à présent ignoré**.

Ce résultat n'était à la réflexion pas si surprenants puisque les travaux d'Elrod et al. [2004] et de Servermann et al. [*Severmann et al.*, 2004, 2006, 2008, 2010] qui mettaient en avant la dissolution réductrice du fer avaient été conduits dans des environnements particulièrement réducteurs, dans la **zone de minimum d'oxygène** (OMZ) du Nord Est Pacifique (marge de Californie). Des mesures de CI de DFe dans le bassin de San Pedro et de Santa Barbara avaient d'ailleurs confirmé la transmission du signal négatif de ces sédiments très réducteurs dans les colonnes d'eau anoxiques à suboxiques de cette région [*John et al.*, 2012], avec des valeurs aussi basses que -3.4‰ dans les eaux de fond du bassin de Santa Barbara (où la concentration de DFe de près de 30nM témoigne d'apports sédimentaires très importants). Ces données sont reportées sur la Figure 27.

Au contraire, nos études ont été conduites **dans des colonnes d'eau oxygénées** à l'écart de toute OMZ. Compte tenu du fait que nous avons observé cette libération non réductrice de Fe depuis les sédiments le long de toutes les marges que nous avons étudiées, nous suggérons que ce processus pourrait être globalement significatif. Compte tenu du fait que les eaux de mer oxygénées sont largement plus répandues que les OMZ (cf. Figure 28), nous suggérons même que ce processus pourrait être plus important à l'échelle globale que la dissolution réductrice, seul processus considéré jusqu'à présent dans les modèles globaux du cycle du fer océanique. Ces conclusions rejoignent celles tirées de nos travaux sur les isotopes du néodyme sur l'altération sous-marine des particules lithogéniques (présentés précédemment) [*Arsouze et al.*, 2009; *Jeandel et al.*, 2011a; *Lacan et*

Jeandel, 2005b]. En supposant (ce qui reste encore très spéculatif) que le processus lié à la libération de Nd dissous le long des marges est le même que le processus de libération non réductrice de DFe depuis les sédiments mis en évidence ici par les isotopes du Fe, alors l'estimation des flux de fer associé à l'altération sous-marine des particules lithogéniques [*Jeandel et al.*, 2011a] peut être attribué au processus de libération non réductrice de DFe. Il en découlerait que ce processus induit un flux de DFe supérieur à celui (considéré jusqu'à présent) de la dissolution réductrice du Fe. Ceci est résumé sur la Figure 28. Ceci reste cependant très spéculatif et nécessite d'être d'avantage étudié, notamment par des expériences in vitro.

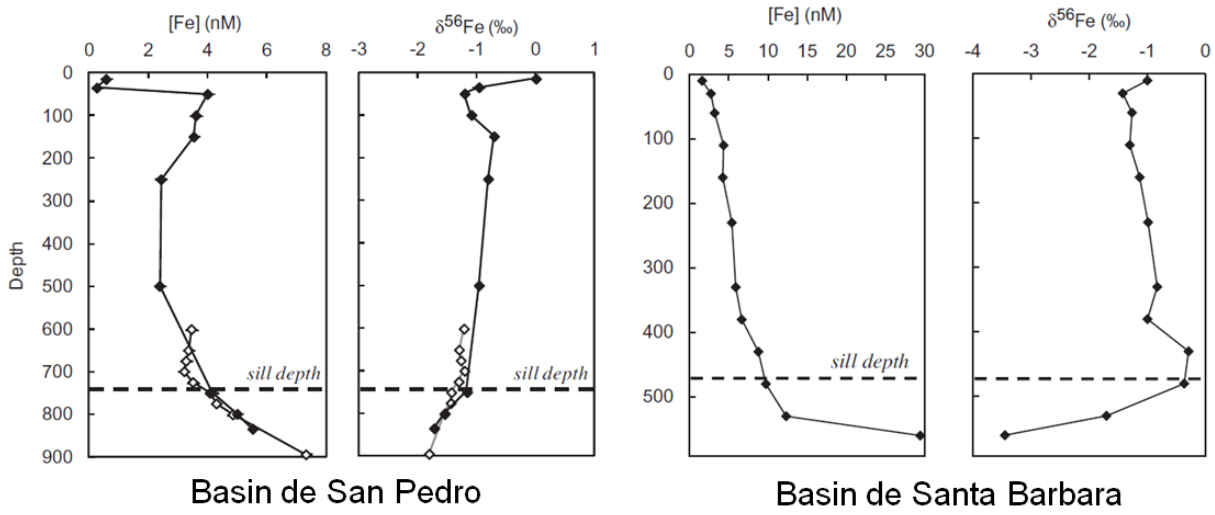

Figure 27: [DFe] et CI de DFe le long de la marge californienne.
Les concentrations d'O2 au fond du bassin de San Pedro sont typiquement de 2 à 5 µM, tandis qu'elles varient 0 à 16 µM au fond du bassin de Santa Barbara **[*John et al.*, 2012]**.

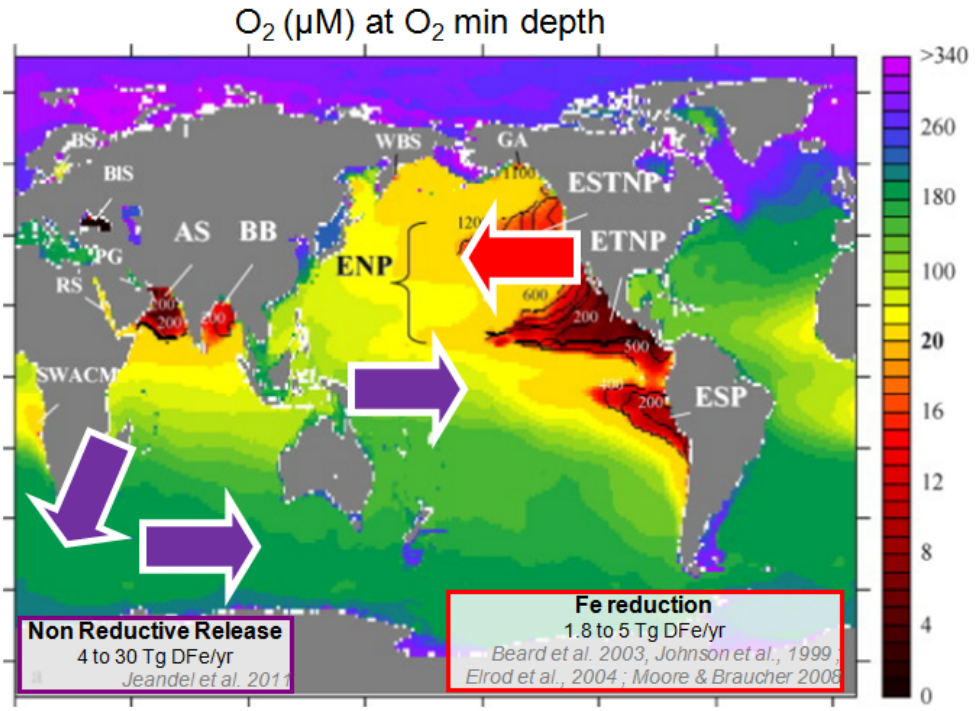

Figure 28: Sources sédimentaire de Fe et OMZ.
La carte présentant les zone de minimum d'oxygène est issue de [*Paulmier et Ruiz-Pino*, 2009]. Les flèches violettes et rouge indiquent les lieux où des apports sédimentaires de DFe ont été attribués, sur la base des isotopes du Fe respectivement à une libération non réductrice et à une dissolution réductrice. Les flux indiqués pour la libération non réductrice sont encore très spéculatifs et nécessitent d'être d'avantage contraints.

Une petite remarque sur la démarche scientifique. Comme je l'ai écrit ci-dessus, nos résultats ne nous ont pas permis de suivre notre hypothèse de travail initiale. Sur une thématique aussi vierge que celle des isotopes du fer dans l'océan, une bonne hypothèse de travail est nécessaire, mais les résultats que l'on peut obtenir peuvent s'avérer totalement différents de ce que l'on avait prévu tout en apportant des information très intéressantes. D'une certaine manière, il s'agit d'exploration, nous découvrons le cycle des isotopes du fer dans l'océan, qui sait ce que nous trouverons…

c. Impact de l'oxygène

Le profil de CI de DFe obtenu à la station S4 (au dessus de la ride médio-atlantique) de la campagne Bonus/GoodHope, par A. Radic, au Sud du front polaire dans le secteur Atlantique de l'océan Austral, présente une allure très intéressante. Il est visible sur la Figure 25, mais est aussi représenté de manière plus visible et avec des données complémentaires sur la Figure 29. On y voit très clairement **un minimum de CI de DFe à 450m, en plein cœur de l'Upper Circumpolar Deep Water (UCDW), caractérisée par un minimum de concentration en oxygène dissous**. La variation monotone de la concentration de DFe avec la profondeur exclut l'hypothèse d'un processus local qui libérerait du fer dissous léger à l'endroit de la station S4. En effet si tel était le cas un extremum de CI de DFe devrait correspondre à un extremum de concentration de DFe. Par ailleurs si du DFe léger était libéré localement à partir du PFe, un profil de CI de PFe "miroir" de celui de DFe serait observé (puisque les concentrations de ces 2 phases sont quasi identiques, cf. Figure 29). Ce n'est pas le cas. Ces 2 arguments suggèrent donc que cette signature légère ne peut pas être interprétée en une dimension (modèle 1D vertical), mais est transportée avec la masse d'eau. N'ayant pas de donnée en amont, nous ne pouvons qu'émettre des hypothèses. Nous savons que le minimum d'O_2 de l'UCDW résulte de la respiration des bactéries qui dégrade la matière organique. En d'autres termes ce minimum est dû à la reminéralisation de la matière organique (MO). Cela suggère déjà 2 possibilités: 1) cette signature isotopique est liée aux processus de reminéralisation de la MO, ou 2) elle est liée à la concentration en oxygène de l'UCDW mais pas directement à la reminéralisation de la MO. Dans le cas n°1, nous avons encore plusieurs possibilités: 1a: la MO a une CI de Fe pas particulièrement légère, mais la libération de DFe à partir de la MO fractionne les isotopes du Fe en favorisant les isotopes légers; 1b: la MO est isotopiquement légère. Enfin, hypothèse n°3, nous ne pouvons exclure que l'UCDW a été enrichie en Fe léger par une source externe au cours de son histoire (par exemple du fer libéré par dissolution réductrice le long d'une marge). Je ne pense pas que nos données nous permettent de trancher entre ces différentes possibilités.

Les données obtenues à la station S1 de la campagne Bonus/GoodHope, plus près de la marge Sud Africaine, confirment les observations de la station S4 (au Sud du front polaire). Ce profil est représenté sur la Figure 30. Les variations sont nettement moins marquées, mais on observe tout de même le minimum de CI de DFe dans le cœur de l'UCDW, qui se trouve beaucoup plus profond à cette latitude (vers 1200m de profondeur), toujours caractérisé par un minimum de [O_2]. J'interprète la moindre amplitude de ces variations par le fait que cette station est soumise à des apports continentaux (dont témoignent les concentrations de PFe assez importantes, mais aussi les données de CI de Nd, les spectres de REE [*Garcia-Solsona et al.*, Submitted] ou les données de PAl non publiées) caractérisés par des signatures isotopiques de Fe proches de la valeur crustale. En d'autres termes, les CI de Fe sont ici **tamponnées par les apports lithogéniques qui ramènent les CI de DFe des eaux vers la valeur crustale**.

L'ensemble de ce travail sur la campagne Bonus/GoodHope n'est pas encore publié. Cela s'explique en partie par le fait qu'A. Radic, qui a produit ces données, n'a pas poursuivi la recherche après son doctorat, mais aussi par le fait que le jeu de données de cette campagne est encore incomplet. Il sera complété par les données de 3 autres stations, qui sont en cours de mesure par C. Abadie, mon 3ème doctorant (les particules sont déjà mesurées, il reste le dissous).

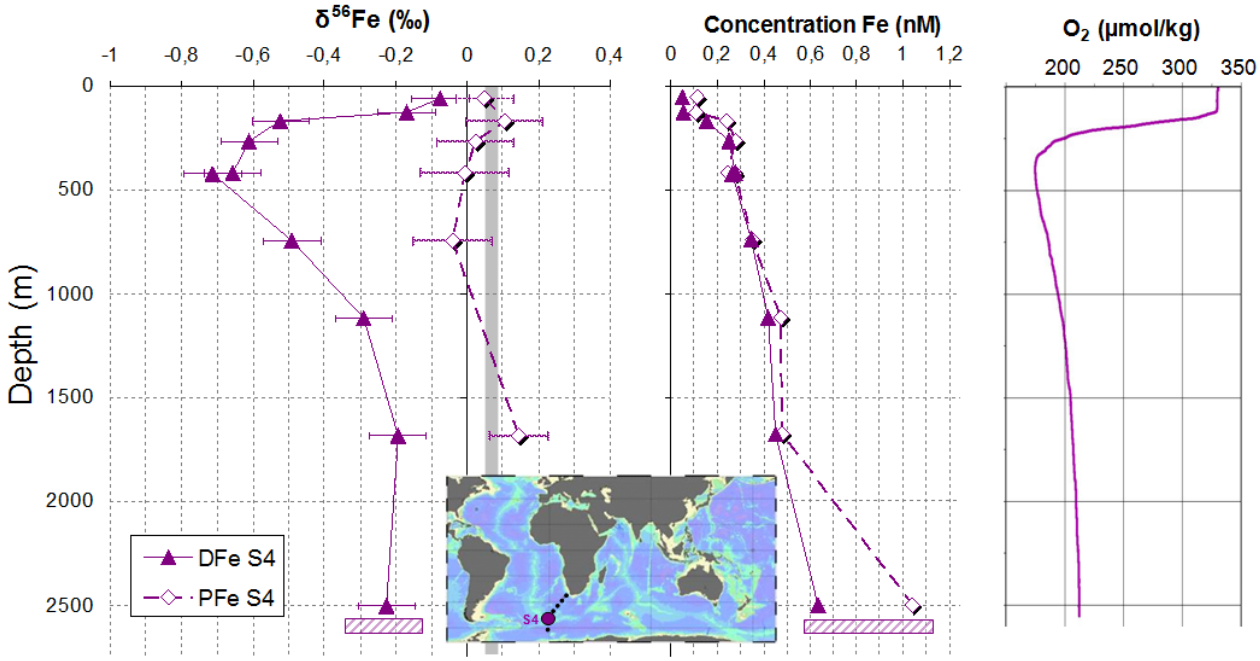

Figure 29: CI de Fe et concentration de Fe et d'O2 à S4 Bonus/GoodHope.
Les symboles pleins correspondent au DFe (<0.4µm), les symboles creux au PFe (>0.4µm, le protocole dissout entièrement les particules). La bande grise indique la signature de la croute continentale.

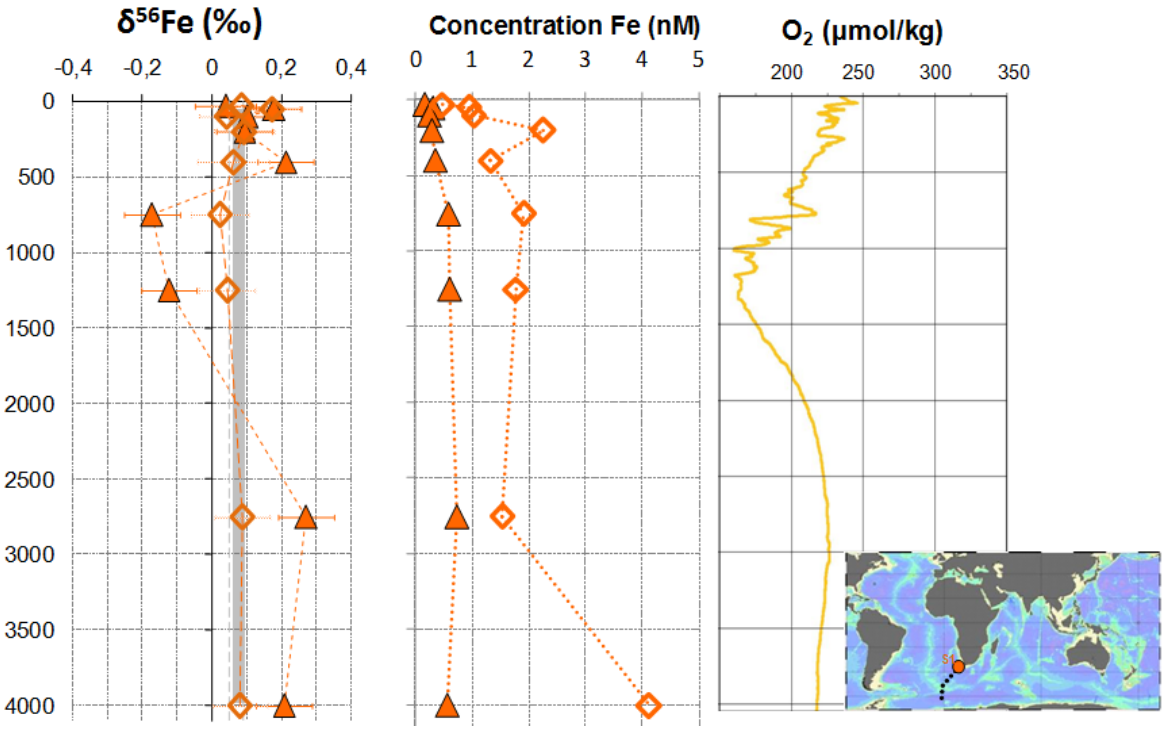

Figure 30: CI de Fe et concentration de Fe et d'O2 à S1 Bonus/GoodHope.
Les symboles pleins correspondent au DFe (<0.4µm), les symboles creux au PFe (>0.4µm, le protocole dissout entièrement les particules). La bande grise indique la signature de la croute continentale.

d. Consommation par le phytoplancton

Enfin, les données obtenues jusqu'à présent nous permettent d'évaluer l'éventuel fractionnement isotopique associé à la consommation du DFe par le phytoplancton. Avant tout il est nécessaire de préciser quelques notations. Supposons un processus ou une réaction qui produit la substance B à partir de la substance A.

Le facteur de fractionnement de l'élément E entre les substances A et B est défini par:

$$\alpha^{i/k}E_{B-A} = \frac{R^{i/k}E_B}{R^{i/k}E_A} \qquad \text{Équation 5}$$

Où $R^{i/k}E$ est le rapport le l'isotope i sur l'isotope k de l'élément E, par exemple $^{56}Fe/^{54}Fe$.

L'équation 5 est équivalente en notation δ à :

$$\alpha^{i/k}E_{B-A} = \frac{1+\frac{\delta^{i/k}E_B}{1000}}{1+\frac{\delta^{i/k}E_A}{1000}} \qquad \text{Équation 6}$$

$\delta/1000$ étant très inférieur à 1, on simplifie cette équation en :

$$10^3 \ln\alpha^{i/k}E_{B-A} \approx 10^3\left(\alpha^{i/k}E_{B-A}-1\right) \approx \delta^{i/k}E_B - \delta^{i/k}E_A \equiv \Delta^{i/k}E_{B-A} \qquad \text{Équation 7}$$

$\Delta^{i/k}E_{B-A}$ est appelé différence isotopique (*isotopic difference*) ou encore fractionnement isotopique (*isotope fractionation*).

Le modèle de distillation de Rayleigh est un modèle qui suppose que le produit de la réaction est isolé du système (en termes d'échange isotopique) immédiatement après sa formation; par exemple précipitation d'un minéral depuis une solution. Le fractionnement isotopique peut être un fractionnement à l'équilibre (si la réaction est lente) ou cinétique (réaction rapide), mais, quoi qu'il en soit, après la réaction le produit est isolé.

Sans entrer dans les détails (compliqués des calculs de la distillation de Rayleigh), les évolutions des CI du substrat (A) et du produit (B) sont données par:

$$\left(\delta^{i/k}E_A\right)_f \approx \left(\delta^{i/k}E_A\right)_{f=1} + \Delta^{i/k}E_{B-A}\ln(f) \qquad \text{Équ. 8, évolution du substrat en distillation de Rayleigh}$$

$$\left(\overline{\delta^{i/k}E_B}\right)_f \approx \left(\delta^{i/k}E_A\right)_{f=1} - \Delta^{i/k}E_{B-A}\frac{f\ln(f)}{1-f} \qquad \text{Équ. 9, évolution du produit accumulé en distillation de Rayleigh}$$

$$\left(\delta^{i/k}E_{B-inst}\right)_f \approx \left(\delta^{i/k}E_A\right)_{f=1} + \Delta^{i/k}E_{B-A}\times(1+\ln f) \qquad \text{Éq. 10, évolution du produit instantané en distillation de Rayleigh}$$

Où f est la fraction de A restante.

Pour estimer le fractionnement isotopique associé à la consommation de DFe par le phytoplancton, nous avons utilisé plusieurs approches.

La première ne tire partie que des données de DFe. Nous l'avons appliquée dans l'Atlantique Sud (Bonus/GoodHope station S1) et dans le Pacifique Equatorial (EUCFe, équateur/ligne de changement de date). Dans les 2 cas nous avons estimé un état initial préfloraison. Dans l'Atlantique Sud nous avons supposé que la masse d'eau qui se trouve juste sous la couche mélangée d'été représentait la couche mélangée d'hiver, et donc l'état initial préfloraison. Dans le Pacifique Equatorial l'état initial a été caractérisé par les eaux du sous-courant situées en dessous de la zone de production primaire et qui alimentent cette dernière via l'upwelling équatorial. La CI du DFe mesurée dans le maximum de fluorescence (comme proxy du maximum de chlorophylle; ce n'est pas parfait mais lors de l'échantillonnage c'est la seule donnée instantanément disponible) est pour sa part considérée comme représentative de la couche où a eu lieu la consommation par le phytoplancton depuis l'état initial. La comparaison de l'état initial et de l'état final permet par le modèle de distillation Rayleigh de calculer le facteur de fractionnement suivant l'équation 8. Nous avons obtenu:

Dans l'Atlantique Sud: $\left|\Delta^{56/54}\mathrm{Fe}_{\mathrm{Phyto-SW}}\right| < 0.32‰$ [*Lacan et al.*, 2008]

Dans le Pacifique Equ. (Eq. 180°E): $\Delta^{56/54}\mathrm{Fe}_{\mathrm{Phyto-SW}} = -0.25 \pm 0.10‰\ (2\mathrm{SD})$ [*Radic et al.*, 2011]

La seconde approche consiste à comparer les CI des phases particulaires et dissoutes à l'endroit du maximum de fluorescence. On suppose que le fer présent dans la phase particulaire est intégralement contenu dans le phytoplancton. Il s'agit d'une approximation. Cette approche a été appliquée dans le Pacifique Equatorial, en supposant, soit que les particules prélevées représentaient la production instantanée (le plancton produit est rapidement exporté hors de la zone euphotique), soit qu'elles représentaient la production accumulée (pas d'export). Cette 2ème situation nous a semblé moins probable [*Radic et al.*, 2011]. Les équations 9 et 10 mènent à:

Pacifique Equ. (Eq. 180°E), production accumulée: $\Delta^{56/54}\mathrm{Fe}_{\mathrm{Phyto-SW}} = -0.08 \pm 0.07‰\ (2\mathrm{SD})$

Pacifique Equ. (Eq. 180°E), production instantanée: $\Delta^{56/54}\mathrm{Fe}_{\mathrm{Phyto-SW}} = -0.13 \pm 0.11‰\ (2\mathrm{SD})$

Très récemment, Marie Labatut a terminé les mesures de l'ensemble des échantillons du Pacifique Equatorial. Ces données nous ont permis de compléter ce dernier résultat, i.e. d'estimer le fractionnement associé à la consommation biologique par le phytoplancton en supposant un modèle de distillation de Rayleigh et que les particules représentent la production instantanée de phytoplancton. Trois estimations supplémentaires (en plus du point à EQ. 180°E) sont représentées sur la Figure 31.

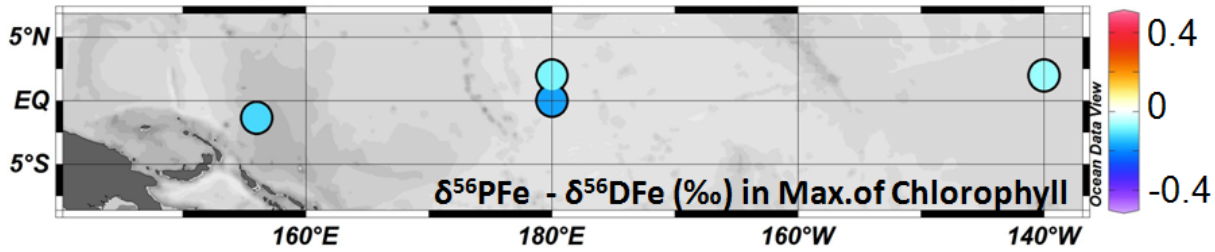

Figure 31: Fractionnement isotopique lors de la consommation de DFe par le phytoplancton.
Voir le texte pour les détails.

Globalement, l'ensemble de ces estimations, à partir de données in situ et basées sur des raisonnements différents, suggère que le **fractionnement isotopique associé à la consommation du DFe par le phytoplancton est faible, probablement inférieur à 0.2 ou 0.3‰. Il semblerait que le phytoplancton consomme préférentiellement les isotopes légers du fer.**

5. Développements analytiques

Les développements analytiques sont pour moi une activité quasi-incessante qui accompagne les travaux sur les échantillons réels. Il faut toujours améliorer les protocoles, les adapter aux nouveaux produits disponibles (nouvelles résines, nouveaux spectromètres…), cela permet d'améliorer la qualité des mesures, de minimiser la taille des échantillons (problématique lorsqu'elle est de l'ordre de 10L), et de mesurer de nouvelles choses.

En 2006 j'ai développé le 1er protocole permettant la mesure des isotopes du cadmium dans l'océan, je n'y reviens pas [*Lacan et al.*, 2006].

En 2008 et 2010 nous avons publié notre protocole pour la mesure des isotopes du fer. J'ajoute ici que ce protocole est toujours en développement. La nouvelle résine NOBIAS-CHELATE-1 semble plus performante que la résine Quiagen NTA Superflow que nous utilisons actuellement. Elle devrait permettre de meilleurs blancs, donc des échantillons plus petits et aussi la préconcentration simultanée de plusieurs métaux. Nous travaillons aussi parallèlement au développement de l'étape de purification en essayant de réduire la taille des colonnes pour encore réduire nos blancs. La validation des mesures d'isotopes du fer a donné lieu à une intercalibration internationale dans le cadre de GEOTRACES. Il s'agissait de mesures "en aveugle": nous ne connaissions pas les résultats des autres au moment de soumettre les nôtres. Les résultats sont présentés sur la Figure 32. Trois équipes ont participé à l'époque. Le travail a été publié récemment [*Boyle et al.*, 2012]. Cela étant cette intercalibration a été réalisée sur des échantillons assez concentrés en fer (>0.4nM). Elle ne présume donc en rien des capacités de chacun à mesurer des échantillons moins concentrés. Le "Lab A", qui n'avait pas de prétention de documenter l'océan ouvert (et qui ne le fait d'ailleurs pas), avait, même à ces concentrations relativement fortes, des difficultés à obtenir des mesures précises. Il me semblerait important de réitérer cet exercice d'intercalibration sur des eaux où [Fe]<0.1nM. Un 2nd exercice a été planifié en 2013 (nous y participerons), les concentrations minimums prévues sont de 0.1 à 0.3nM.

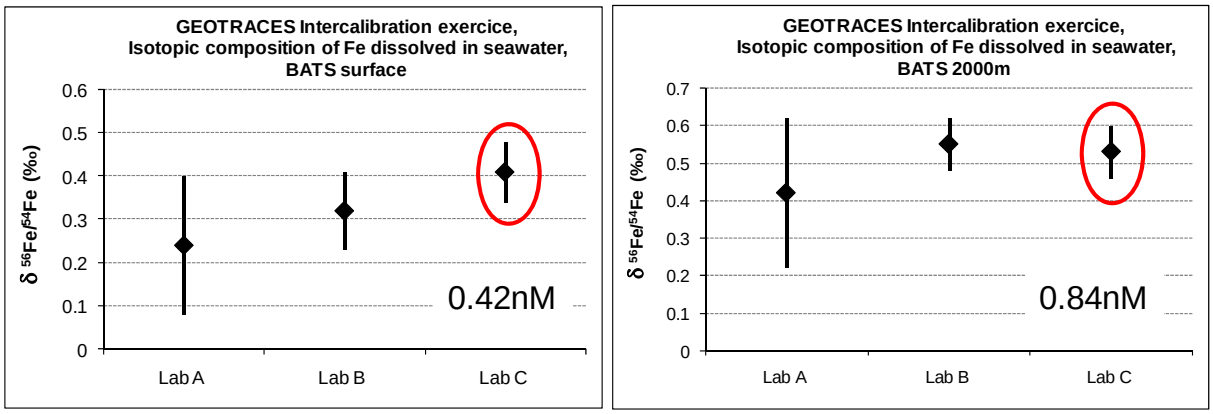

Figure 32: Intercalibration GEOTRACES pour les CI de Fe.
Nous sommes le "Lab C".

Très brièvement j'ai aussi participé à l'intercalibration internationale GEOTRACES pour les concentrations de REE [*Van de Flierdt et al.*, 2012], à un travail de développement d'une technique de mesure des concentrations de REE par dilution isotopique avec 10 spikes [*Rousseau et al.*, 2013] et à une technique de séparation de Ra, Nd, Th, Pa et U d'un même échantillon naturel [*Jeandel et al.*, 2011b].

J'ai participé à un exercice d'intercalibration national du géostandard SLRS-5 (eau de rivière du Canada) [*Yeghicheyan et al.*, 2013].

Enfin, dans le cadre de mon activité au sein du service ICPMS de l'Observatoire Midi Pyrénées, je développe actuellement un standard multi-élémentaire pour la détermination simultanée d'une cinquantaine d'éléments dans des échantillons naturels (eaux douces et eaux de mer, roches, sols, etc…).

6. Perspectives

La thématique des isotopes du fer dans l'océan en est encore à ses balbutiements. Les résultats obtenus jusqu'à présent sont, de mon point de vue, très encourageants, et les questions qui demeurent sur le cycle océanique du fer restent nombreuses. Il me semble important de poursuivre sur cette thématique et de continuer à documenter les CI de Fe dans l'océan. Par ailleurs je prévois des mesures de fractionnement par des expériences in vitro et des travaux de modélisation. Parallèlement, bien que marginalement, je souhaite poursuivre des travaux engagés sur les particules en suspensions. Enfin il me semble important de diversifier mes outils d'analyses.

a. Les campagnes

Je possède d'ores et déjà un certain nombre d'échantillons en stock. Les campagnes passées et futures sur lesquelles j'ai ou j'aurai des échantillons pour les isotopes du fer sont représentées sur la Figure 1 : EUCFe, KEOPS1, Bonus/GoodHope, KEOPS2, PANDORA pour les campagnes passées, et GEOVIDE et potentiellement la section GEOTRACES GI05 dans l'Océan Indien Sud. Les échantillons EUCFe (dissous et particules) sont mesurés, ceux de Bonus/GoodHope (dissous et particules) sont en passe de l'être, il me reste encore des échantillons KEOPS1 et l'ensemble des échantillons KEOPS2 et PANDORA à mesurer. Sans parler bien entendu de GEOVIDE et éventuellement de la section française de Geotraces dans l'Indien entre Durban-Kerguelen, prévue entre 2015 et 2020. Cela constitue des **perspectives assez importantes en termes de documentation de l'océan**. Les résultats d'EUCFe, obtenus dans le cadre du doctorat de Marie Labatut, sont représentés sur la Figure 33; ils restent à être interprétés.

En ce qui concerne le dissous, je ne pense pas changer grand-chose à court terme. Passer à de **l'ultra filtration pour séparer les fractions colloïdales du vraiment dissous est une perspective** (très intéressante) mais à long terme. En effet plus on multiplie les fractions, plus on augmente le blanc et plus on diminue la quantité de fer dans chacune des fractions. Il faudra soit de grands volumes, soit des techniques encore plus propres.

En ce qui concerne les particules en suspension, je pense m'orienter vers un protocole de **lessivage partiel** plutôt que de dissolution totale des particules tel que je le fais actuellement. En effet la partie réfractaire des particules qui n'est dissoute que dans des acides puissants n'interagit probablement jamais avec la phase dissoute dans l'eau de mer. On peut se poser la question de l'utilité de mesurer cette fraction. De plus cette fraction, la plupart du temps lithogénique, a tendance à tamponner le reste du signal, éventuellement contenu dans la fraction labile. La difficulté d'une telle approche est le risque de fractionnement isotopique lors du lessivage partiel. Un protocole qui semble ne pas fractionner les isotopes du fer vient d'être communiqué à l'AGU de décembre 2012 [*Revels et John*, 2012]. Il est aussi important de s'assurer de l'absence de ré-adsorption lors du lessivage. Un lessivage séquentiel peut aussi être envisagé pour accéder dans un 1^{er} temps à la partie labile et dans un 2^{nd} temps à la partie réfractaire. J'envisage de réaliser ces travaux dans le cadre de l'ANR BITMAP de H. Planquette (LEMAR) qui vient de commencer, et sur laquelle nous avons prévu d'étudier en détails les CI de Fe sur différentes **fractions de taille** de particules.

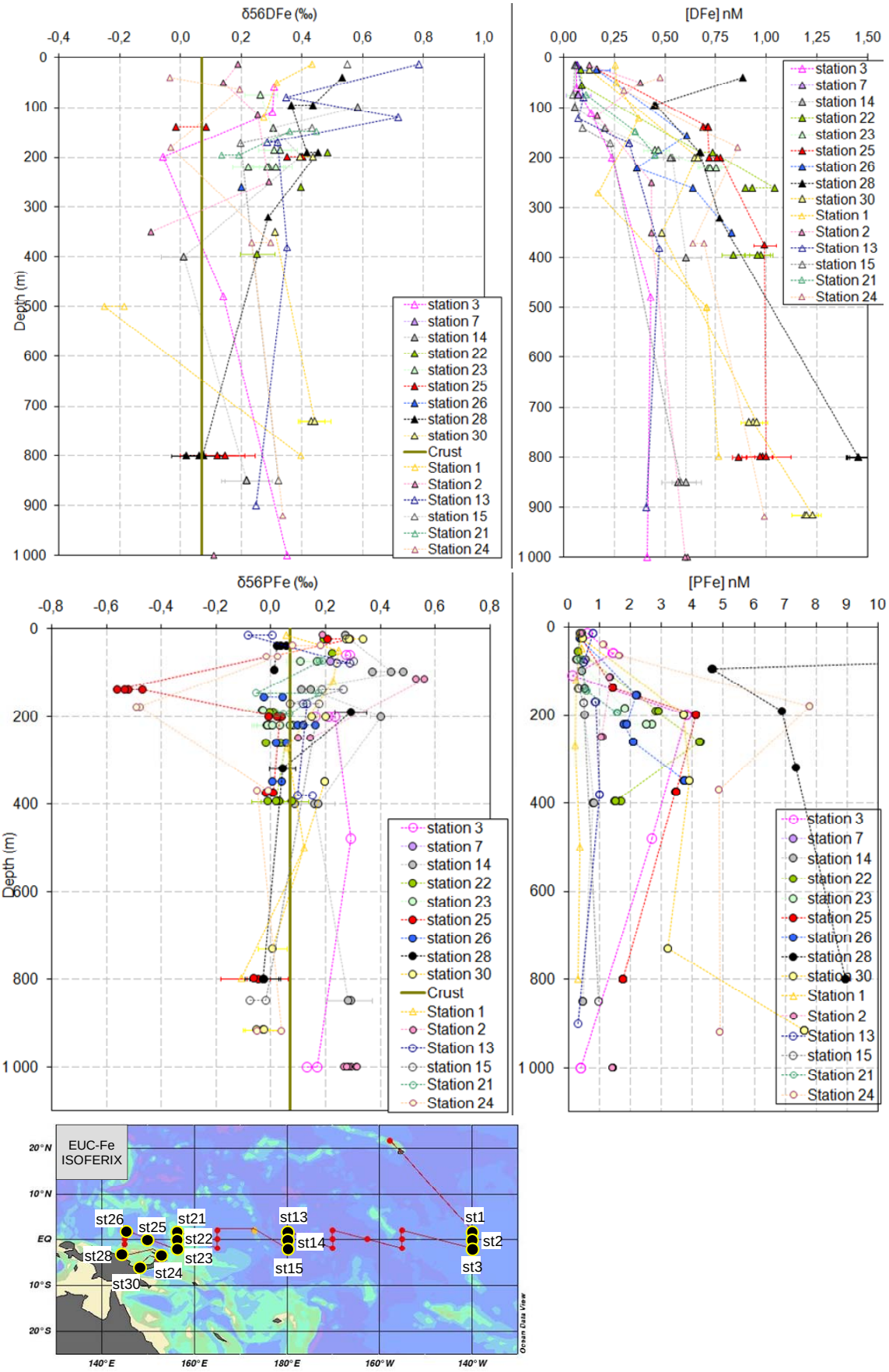

Figure 33: Données de la thèse de Marie Labatut.

b. Les études in vitro

Bien que la mesure des fractionnements isotopiques in situ soit de mon point de vue une stratégie puissante, il est aussi nécessaire, car complémentaire, de réaliser des mesures de ce type en milieu contrôlé. Cela permet notamment d'isoler les processus.

J'envisage de mesurer les facteurs de **fractionnement isotopique liés à l'absorption du DFe par le phytoplancton** par des expériences d'incubation de phytoplancton en collaboration avec G. Sarthou (CNRS, LEMAR, Brest, Fr.). L'approche sera double: 1) des cultures d'espèces modèles telles que Thalassiosira oceanica, dans des milieux artificiels et 2) des incubations d'échantillons naturels effectuées à bord. Pour ce 2ème point des incubations ont d'ores et déjà été réalisées au cours de la campagne KEOPS2 (il reste à faire les mesures). Différentes conditions d'incubation, notamment divers niveaux de stress de Fe seront testés, afin de voir si cela a un effet sur les fractionnements isotopiques de Fe. J'ai déjà une petite expérience de telles études, puisque que j'ai publié les premiers facteurs de fractionnement isotopique du cadmium liés à son absorption par le phytoplancton dans des expériences d'incubation [*Lacan et al.*, 2006]. À ce jour il n'existe aucune donnée publiée de ce genre pour l'absorption du DFe par le phytoplancton dans les conditions océaniques. Certains travaux sont néanmoins en cours.

J'envisage aussi d'étudier les facteurs de fractionnement isotopique associés aux processus 1) **d'adsorption/désorption et 2) de dissolution/précipitation**, dans des conditions contrôlées. Bien qu'il y ait déjà eu plusieurs études présentant des facteurs de fractionnement isotopique de Fe associés à ces processus, aucun d'entre eux ne visait à reproduire les conditions océaniques modernes [Wu et al., 2011 et références incluses]. Ceci sera réalisé en collaboration avec F. Poitrasson (chercheur au CNRS, GET, Toulouse, France), C. Jeandel et P. Behra (professeur, Univ. de Toulouse) [*Jones et al.*, 2012a, 2012b; *Saunier et al.*, 2011].

En règle générale, les expériences in vitro de fractionnement isotopique du Fe n'ont jamais été menées dans **des conditions réalistes d'océan ouvert** (salinité de 35 et à très faible concentration de Fe, de l'ordre de 0,1 à 1 nM). La raison en est simple, seuls 2 à 3 groupes sont capables de mesurer les isotopes de Fe dans de telles conditions. Nous utiliserons des équipements spécifiques pour le faire, notamment un conteneur de 1 m^3 en PEEK (collaboration C. Jeandel et P. Behra).

c. La modélisation

J'envisage aussi de travailler à la modélisation du cycle des isotopes du fer. Les données sont assez peu nombreuses pour l'instant, mais il va y en avoir de plus en plus dans les années à venir, et même avec des jeux de données restreints la modélisation peut aider à progresser.

L'ensemble de la palette des modèles me semble intéressant, modèles à 1 ou 2 dimensions, ou modèles plus réalistes couplant modèles de circulation (à l'échelle régionale ou globale) et modèle de biogéochimie. Cette perspective s'inspire de ce que nous avons fait avec NEMO-PISCES pour le Nd et le ^{231}Pa/^{230}Th [*Arsouze et al.*, 2009; *Dutay et al.*, 2009], ou encore de travaux récents d'inversion de données de la campagne KEOPS1 avec un modèle en boite [*De Brauwere et al.*, 2012]. Je souhaite réaliser ces travaux en collaboration avec J.C. Dutay, L. Bopp et O. Aumont, pour ce qui concerne NEMO-PISCES, et A. de Brauwere pour ce qui concerne les modèles en boite et les inversions.

Les objectifs seront notamment 1) de tester si les observations in situ et/ou in vitro peuvent être globalisées ou régionalisées, 2) d'estimer quels processus ont le plus fort impact sur le cycle des isotopes de Fe, 3) éventuellement de tester la sensibilité du cycle océanique des isotopes du fer à des conditions climatiques variables (par ex. dernier maximum glaciaire) afin de voir si et comment ce nouveau traceur peut être utilisé pour des applications en paléocéanographie, ou comme un indicateur des modifications futures de son cycle.

d. Les particules en suspension

Très brièvement je voudrais dire quelques mots sur les particules en suspension. Comme nous l'avons vu les particules jouent un rôle important sur le cycle du fer. Il n'est pas possible de ne pas en tenir compte. Notamment, lorsqu'il s'agit de modélisation, il est nécessaire d'avoir des données sur les distributions des traceurs dans les particules (par ex. PFe), mais aussi d'avoir des données sur les distributions des particules elles mêmes (MO, $CaCO_3$, silice biogène, particules lithogéniques, oxydes de fer et de manganèse…). Cela étant les données sont assez rares.

Y. Nozaki a produit un magnifique tableau périodique des profils des éléments dissous (cf. Figure 34). Lorsque nous prélevons pour les isotopes du fer particulaire, nous obtenons des échantillons sur lesquels il est relativement aisé de mesurer par ICPMS les concentrations en un nombre assez important d'éléments. Dans le cadre du Master 1 de M. Labatut nous avons donc produit un tableau similaire pour les particules en suspension dans l'Océan Austral. Ces données sont encore préliminaires, il reste du travail pour les valider. Je les ai tout de même représentées sur la Figure 35. Je pense que ce type de données peut être très utile pour l'étude du cycle de certains éléments. Ces données issue de la campagne Bonus/GoodHope ont par exemple été utilisées en ce qui concerne le cobalt en collaboration avec le LEMAR [*Bown et al.*, 2011] ou en ce qui concerne les REE avec E. Garcia-Solsona au LEGOS [*Garcia-Solsona et al.*, Submitted].

Par ailleurs elles peuvent être très utiles pour estimer les "masses composites" des particules. Il est très difficile, voire impossible, de mesurer directement les masses des particules dans l'océan ouvert avec précision. Cette conclusion me vient notamment de discussions avec des chercheurs ayant passé leur carrière sur ces particules, notamment J. Bishop et Nick Mc Cave. Les quantités de sels présentes sur les membranes posent en effet des difficultés, et rincer les membranes avec de l'eau douce pose aussi des problèmes. Pour contourner ces difficultés il est possible de calculer une masse composite. On suppose que la particule est constituée de MO + silice biogène + calcite + particules lithogénique + hydroxyde de fer + hydroxyde de Mn. On utilise un proxy pour chacune de ces phases (par exemple le Ca permet d'estimer les quantités de $CaCO_3$) et on estime ainsi la masse totale de particule. Comme je l'ai dit plus haut, ces quantités sont indispensables dès qu'il s'agit de modélisation. Les mesures ICPMS peuvent donc être très utiles dans ce cadre puisqu'elles permettent de déterminer Ca, Al, ^{232}Th, Fe et Mn, ce qui permet d'estimer 4 des 6 phases listées ci-dessus. Associées aux mesures de MO et de silice biogène, elles permettent la quantification des masses composites des particules.

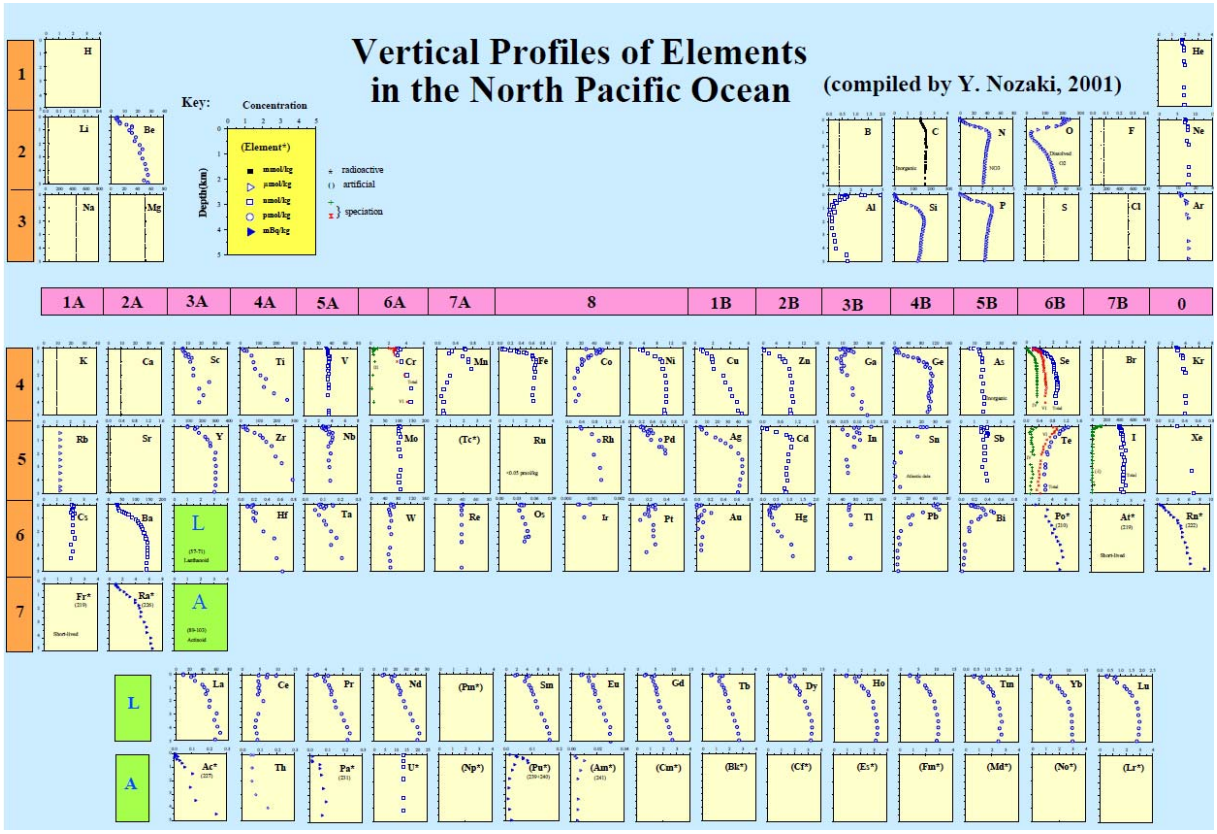

Figure 34: Tableau périodiques des éléments dissous dans le Nord Pacifique. [*Nozaki*, 1997]

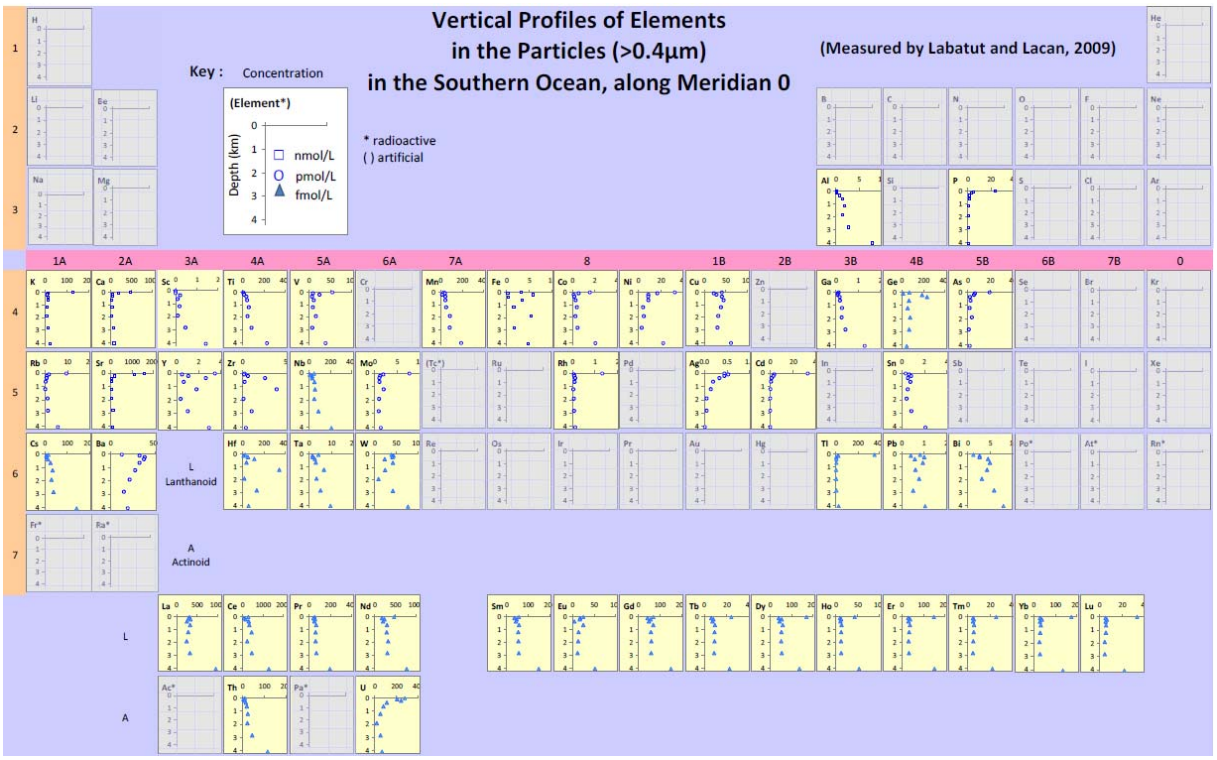

Figure 35: Tableau périodique des éléments dans les particules en suspensions dans l'océan Austral.
ATTENTION, il s'agit de données préliminaires, qui ne sont pas toutes validées.

e. Sortir de l'ICPMS

Cette partie prend le contre pied de la précédente. Les contradictions sont parfois difficiles à résoudre.

Depuis mes débuts, j'ai réalisé mes mesures quasi exclusivement à l'aide de spectromètres de masse, notamment d'ICPMS. Je me suis en quelque sorte enfermé dans cet outil. L'outil est puissant, mais a ses spécificités, il ne peut pas tout faire, loin de là. L'usage d'ICP-OES me permettrait déjà de meilleures mesures des éléments majeurs. Mais les ICP nécessitent de détruire l'échantillon. Je réalise qu'il est important que je diversifie ces outils (tout en conservant naturellement l'ICPMS comme outil majeur si ce n'est central). En 2011, nous avons réalisé avec Cyril Abadie, mon 3ème doctorant, des mesures au microscope électronique à balayage couplé à un système d'analyse EDS (*energy dispersive X-ray spectrometry*) sur les particules en suspension de Bonus/GoodHope. J'ai découvert qu'on pouvait mesurer autre chose que des concentrations ou des compositions isotopiques ! Quelques images prises aux MEB sont représentées sur la Figure 36. Pour aller plus loin dans cette direction, il me semble que l'usage de techniques de cartographie des particules, telle que par exemple le Nano-SIMS ou le XANES, sont très intéressantes [*Tachikawa et al.*, 2013].

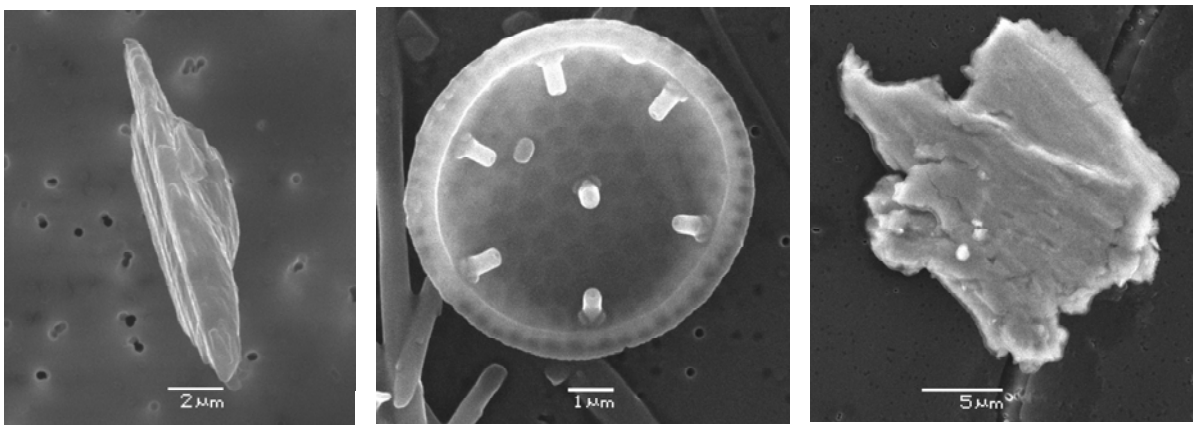

Oxyde de fer en S3 Diatomée en S1 Cu et Zn en S1

Figure 36: Images prises aux MEB des particules de Bonus/GoodHope.

III. Cinq publications choisies

1. Radic, Lacan and Murray. 2011. EPSL. Une source de fer jusque là ignorée

Earth and Planetary Science Letters 306 (2011) 1–10

Contents lists available at ScienceDirect

Earth and Planetary Science Letters

journal homepage: www.elsevier.com/locate/epsl

Iron isotopes in the seawater of the equatorial Pacific Ocean: New constraints for the oceanic iron cycle

Amandine Radic [a], Francois Lacan [a,*], James W. Murray [b]

[a] Laboratoire d'Etudes en Géophysique et Océanographie Spatiale, CNRS / CNES / IRD / Universite Toulouse III, Observatoire Midi Pyrénées, F-31400 Toulouse, France
[b] School of Oceanography, University of Washington, Seattle, WA, USA

ARTICLE INFO

Article history:
Received 4 August 2010
Received in revised form 25 February 2011
Accepted 11 March 2011
Available online 20 April 2011

Keywords:
Iron isotopes
Equatorial Undercurrent
Papua New Guinea
equatorial Pacific
dissolved and particulate iron
biogeochemical cycle

ABSTRACT

This study presents the isotopic compositions and concentrations of dissolved and particulate iron from two seawater profiles of the western and central equatorial Pacific Ocean, sampled during the EUCFe cruise. Most of the δ^{56}Fe values are positive (relative to IRMM-14), from +0.01 to +0.58‰ in the dissolved fraction (DFe) and from −0.02 to +0.46‰ in the particulate fraction (PFe). The mean measurement uncertainty of ±0.08‰ (2SD) allows the observation of significant variations. Most of the isotope variations occur in the vertical and not in the horizontal direction, implying that each isotope signature is preserved over long distances within a water mass.

The thermocline waters of the Papua New Guinea (PNG) area, mostly influenced by sedimentary inputs, display a mean δ^{56}DFe value of +0.37‰ (±0.15‰, 2SD). This isotopic signature suggests that the process releasing dissolved iron into the seawater in this area is a non reductive dissolution of sediments (discharged by local rivers and likely re-suspended by strong boundary currents), rather than Dissimilatory Iron Reduction (DIR) within the sediment (characterized by negative δ^{56}DFe). These positive δ^{56}DFe values seem to be the result of a mean isotopic fractionation of $\Delta^{56}Fe_{DFe\text{-}PFe} = +0.20$‰ (±0.11‰, 2SD) produced by the non reductive dissolution. At 0°N, 180°E, the Fe isotope signature of the Equatorial Undercurrent (EUC) waters is identical to that of the PNG station within the range of the uncertainty. This suggests that the dissolved iron feeding the EUC, and ultimately the eastern Pacific high nutrient low chlorophyll area, is of PNG origin, likely released by a non reductive dissolution of terrigenous sediments.

Significant Fe removals are observed within the thermocline and the intermediate waters between the PNG and the open ocean stations. The corresponding isotopic fractionations appear to be small, with $\Delta^{56}Fe_{removed\text{-}SW\ Fe}$ values of −0.30±0.31‰ to −0.18±0.12‰ (2SD) for DFe removal and of −0.10±0.04‰ to −0.05±0.31‰ (2SD) for PFe removal. In the chlorophyll maximum of the open ocean station, the isotopic fractionation associated with biological uptake is estimated at $\Delta^{56}Fe_{phyto\text{-}DFe} = -0.25 \pm 0.10$‰ to -0.13±0.11‰ (2SD). Although these fractionations are based on a limited dataset and need to be further constrained, they appear to be small and to limit the transformations of the iron source signatures within the ocean.

1. Introduction

In wide regions of the ocean, phytoplankton growth does not use all of the available macronutrients. Such regions are called High Nutrient Low Chlorophyll (HNLC) areas (Southern Ocean, subartic and equatorial Pacific Oceans). Martin (1990) hypothesized that fertilization of the Southern Ocean with iron could have increased primary production and contributed to the CO_2 drawdown observed in the last glacial maximum. This hypothesis motivated numerous studies focused on iron during the last 2 decades. Although these studies revealed that Martin's "iron hypothesis" could only explain a fraction of the last glacial maximum CO_2 drawdown (Kohfeld et al., 2005), they confirmed the key role played by iron in the biological and chemical oceanic cycles (e.g., Boyd et al., 2007).

In seawater, iron occurs in two oxidation states, Fe(II) and Fe(III), and in a wide range of chemical species. Although Fe(III) is the least soluble form, it is the thermodynamically favored form in oxic seawaters and the most abundant. Organic ligands complex to more than 90% of the dissolved iron (DFe) and control the solubility of the dissolved pool (Johnson et al., 1997; Kuma et al., 1996; Rue and Bruland, 1995). The particulate iron pool (PFe) encompasses biogenic forms (phyto/zooplankton and non-living organic matter) and inorganic forms. All these forms interact through numerous processes like biological uptake/degradation, adsorption/desorption, and precipitation/dissolution (e.g., de Baar and de Jong, 2001; Ussher et al., 2004). Uncertainties remain about these processes, such as the effect of organic complexation on the kinetics of the phase transitions, biological uptake, scavenging and on Fe bioavailability (Ussher et al.,

* Corresponding author. Tel.: +33 561333043; fax: +33 561253205.
E-mail address: Francois.Lacan@legos.obs-mip.fr (F. Lacan).

0012-821X/$ – see front matter © 2011 Elsevier B.V. All rights reserved.
doi:10.1016/j.epsl.2011.03.015

2004). The Fe distribution in the ocean results from the balance between its sources and sinks. The only sink is the removal by settling particles whereas there are numerous potential iron sources. In the open ocean, the main DFe source was traditionally considered to be atmospheric deposition (Jickells et al., 2005). During the last decade, numerous studies suggested that sedimentary inputs also have a significant impact on the global oceanic iron budget. These include shelf iron flux measurements in benthic chambers, water column Fe concentrations measurements and modeling (e.g., Coale et al., 1996; Elrod et al., 2004; Lam and Bishop, 2008; Lam et al., 2006; Moore and Braucher, 2008; Severmann et al., 2010; Slemons et al., 2009; Tagliabue et al., 2009). Recently, hydrothermal contribution to surface DFe has been suggested to be significant, especially in the Southern Ocean (Tagliabue et al., 2010). However the relative importance of these different iron sources still remains to be quantified, in particular in HNLC areas.

Recent studies have suggested using the DFe isotope composition in the water column as a tracer of iron sources (John and Adkins, 2010; Lacan et al., 2008). The iron isotope composition is expressed by δ^{56}Fe defined as: $\delta^{56}Fe = \left[\frac{\left(^{56}Fe/^{54}Fe\right)_{sample}}{\left(^{56}Fe/^{54}Fe\right)_{IRMM-14}} - 1\right] \times 10^3$. In the following, the values of δ^{56}Fe are reported relative to the IRMM-14 reference material (the δ^{56}Fe of igneous rocks relative to IRMM is of $+0.09 \pm 0.1$‰, 2SD; Beard et al., 2003a). The potential of this emerging tracer is notably related to the two distinct isotopic imprints of its main sources to the open ocean. δ^{56}Fe values ranging from $-3.31‰ \pm 0.07‰$ to -1.73 ± 0.04‰ (2SD) in coastal sediment pore waters just below the seawater interface were interpreted as reflecting bacterial iron reduction (Homoky et al., 2009; Severmann et al., 2006). In addition, benthic chamber measurements from the Oregon–Californian continental shelf display an average δ^{56}DFe value of -2.6 ± 1.1‰ 2SD (Severmann et al., 2010). These studies imply that the diagenetic sedimentary source in reducing environments is likely characterized by a very negative δ^{56}Fe signature. In contrast, aerosol δ^{56}Fe values measured so far range from -0.03‰ to 0.24 ± 0.08‰ (2SD; Beard et al., 2003b; Waeles et al., 2007) which is close to the crustal value: 0.07 ± 0.02‰ (2SD; Poitrasson, 2006). Some studies have characterized δ^{56}Fe of other iron sources which may locally contribute to a significant flux. A few hydrothermal fluids have been measured; they display δ^{56}Fe values between -0.65 and -0.12 ± 0.06‰ (2SD) in the initial fluids (Beard et al., 2003b; Rouxel et al., 2008; Sharma et al., 2001). Concerning river inputs, a range of -0.60 ± 0.14‰ to $+0.36 \pm 0.06$‰ was measured in the DFe content of various fresh river waters, whereas a range of -0.90 ± 0.04‰ to 0.31 ± 0.09‰ (2SD) was measured in the PFe (Bergquist and Boyle, 2006; de Jong et al., 2007; Escoube et al., 2009; Ingri et al., 2006). In estuarine environments, a decreasing of the δ^{56}Fe (down to -1.2‰) in the DFe pool was measured during the flocculation in the Scheldt estuary (de Jong et al., 2007), whereas no significant change was observed in the North River estuary (USA), with an average value of $+0.43$‰ in the DFe pool (Escoube et al., 2009).

In addition to the diversity of these source signatures, the processes involved in the transformations between the different iron species could potentially fractionate iron isotopes and modify the δ^{56}Fe value of the DFe pool in seawater. Their influence on δ^{56}Fe still remains unclear. Although none of these processes has been directly investigated under oceanic conditions, redox conversions seem to generate the largest isotopic fractionations, leading to a Fe(II) pool enriched in light isotopes and a Fe(III) pool enriched in heavy isotopes (e.g., Johnson et al., 2008). Among the numerous studies which have estimated isotopic fractionations (corresponding to *in vitro* experiments mostly), some of them are reported below. Oxidation of $Fe(II)_{aq}$ to $Fe(III)_{aq}$ followed by precipitation of $Fe(III)_{aq}$ as Fe oxides or hematite is suggested to lead to a fractionation such that $\Delta^{56}Fe_{Fe(III)solid-Fe(II)aq} \approx +0.9$ to $+3.0$‰, the dissolved $Fe(II)_{aq}$ remaining after these processes would then be lighter than the initial DFe (Beard and Johnson, 2004; Bullen et al., 2001). Reductive dissolution, in the presence of light and oxalate at pH = 3–5, has been shown to fractionate iron isotopes: $\Delta^{56}Fe_{Fe(II)aq\text{-}Goethite} = -1.7$ to 0‰ (dissolved Fe is lighter than the solid source; Wiederhold et al., 2006) whereas proton promoted dissolution did not show any significant isotopic fractionation (Waeles et al., 2007; Wiederhold et al., 2006). Sorption mechanisms seem to fractionate Fe isotopes such that adsorbed Fe is heavier than the initial $Fe(II)_{aq}$, with a $\Delta^{56}Fe_{Fe(II)adsorb\text{-}Fe(II)aq}$ of $+0.3$ to $+0.9$‰ for hematite and goethite respectively (Crosby et al., 2007; Johnson et al., 2008). Complexation of iron with siderophores has been shown to fractionate iron isotopes at acidic pH, yielding $\Delta^{56}Fe_{Fe(III)siderophore\text{-}Fe(III)inorg} = +0.60 \pm 0.15$‰ (Dideriksen et al., 2008). Biological uptake performed by higher plants (especially vegetables) may induce a small isotopic fractionation, incorporated iron being 0.2‰ heavier than the iron from soils ($\Delta^{56}Fe_{plants\text{-}soil} \approx +0.2$‰; Guelke and Von Blanckenburg, 2007). Although these isotopic fractionations may complicate the use of the iron isotopes as a source tracer, they may help understand the iron speciation in seawater.

While numerous studies report iron isotope data in the marine environment, such as plankton tows, pore waters, aerosols, seafloor or estuaries (e.g., Bergquist and Boyle, 2006; de Jong et al., 2007; Rouxel and Auro 2010; Severmann et al., 2006), very few studies have provided δ^{56}Fe of the seawater. Coastal seawater samples with relatively high DFe concentrations display δ^{56}DFe values from -0.3‰ to $+0.2 \pm 0.14$‰ (2SD) in the North Sea (de Jong et al., 2007) and from -1.82 ± 0.03‰ to 0.00 ± 0.09‰ (2SD) in the San Pedro Basin off the Californian margin (John and Adkins, 2010). For typical open ocean iron concentrations, very few DFe isotope data have been published so far. For DFe concentrations lower than 0.9 nM, ranges of values have been reported, from $+0.3$ to $+0.7 \pm 0.07$‰ (2SD) in the western Subtropical North Atlantic, (John and Adkins, 2010; Lacan et al., 2010), from -0.13 to $+0.21 \pm 0.08$‰ (2SD) in the south-eastern Atlantic (Cape Basin; Lacan et al., 2008) and from -0.49 to -0.19 ± 0.08‰ (2SD) in the Atlantic sector of the Antarctic zone (Lacan et al., 2010), but only 8 actual data points have been published so far to our knowledge. Only one study reports δ^{56}Fe data in the particulate fraction of the seawater and displays δ^{56}PFe from -0.3 to $+0.4 \pm 0.14$‰ (2SD) in the North Sea (de Jong et al.; 2007). Thus seawater iron isotope data are very scarce and nearly inexistent in the open ocean. This study presents the first substantial dataset of Fe isotope compositions in the ocean, with 2 profiles of concentration and δ^{56}Fe in the dissolved and particulate fractions of seawater in the upper 900 m of the water column in the western and central equatorial Pacific.

The western equatorial Pacific is a crossroads of water masses, those involved in the complex zonal circulation of the equatorial Pacific and those of the western boundary currents (Fine et al., 1994). The Equatorial Undercurrent (EUC, see Fig. 1) carries thermocline waters along the equator (Lukas and Firing, 1984) from the western boundary to the eastern equatorial Pacific HNCL area (Behrenfeld et al., 1996). Numerous studies have suggested that the EUC, which is enriched in Fe from the western part of the basin and mainly from the Papua New Guinea (PNG) area, is the main source of iron to the open equatorial Pacific Ocean (e.g., Coale et al., 1996; Mackey et al., 2002; Slemons et al., 2009). Using samples from the same cruise as this study, Slemons et al (2010) showed that there was a maximum of total dissolvable Fe associated with the EUC (consistently 50–100 m deeper than the maximum eastward velocity), and that this maximum was mainly composed of particulate Fe. The total Fe concentrations increased toward the west, also consistent with a western source. These studies therefore suggest that the EUC dynamic and its iron sources could control primary production in the eastern equatorial Pacific. However, there remains little under standing of the process releasing iron to seawater in the western Pacific.

This study intends to answer to the following questions: Do the iron isotopes confirm that the Fe exported into the EUC is from the PNG area? Can they help to identify the Fe sources to the PNG waters

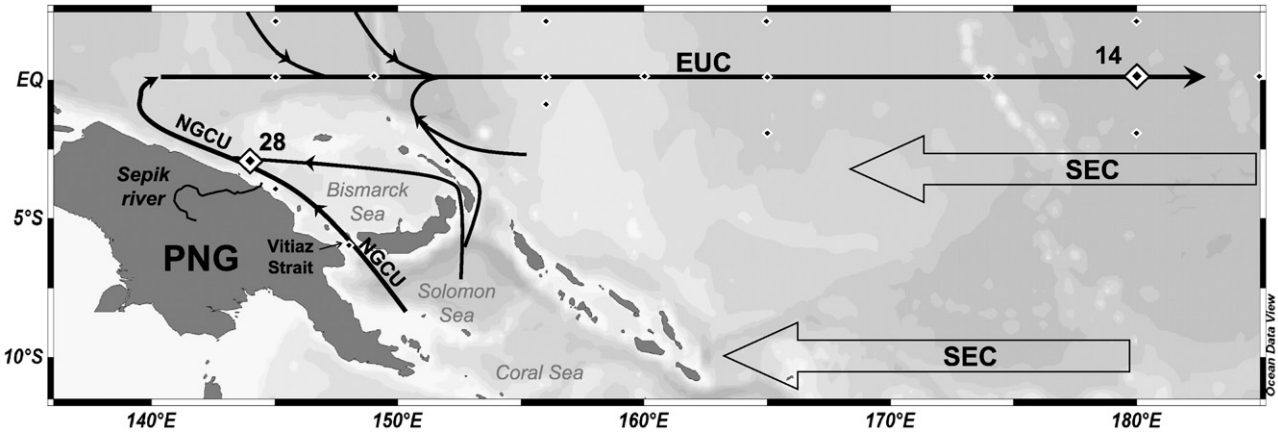

Fig. 1. Locations of stations 14 and 28 (EUCFe cruise, 2006) and main currents between 0 and 1000 m depth (adapted from Butt and Lindstrom, 1994): the South Equatorial Current (SEC), the Equatorial Undercurrent (EUC), the New Guinea Coastal Undercurrent (NGCU).

and the involved release processes? What does this new tracer teach us about the exchange processes between the different iron forms in the water column? Do these processes fractionate iron isotopes?

2. Sample location and water mass identification

The samples presented in this study were collected at two stations in the equatorial Pacific Ocean during the EUCFe cruise (R/V Kilo Moana cruise 0625; http://www.ocean.washington.edu/cruises/Kilo-Moana2006) in August–September 2006. The samples presented in this study were collected over a depth range of 0–900 m, at 0.0°N 180.0°E in the open ocean (station 14), and at 3.4°S 143.9°E near the PNG coast (station 28), as shown in Fig. 1. The regional circulation, simplified in Fig. 1, indicates a continuity of the intermediate and thermocline waters between both stations, from the PNG area towards the central equatorial Pacific (Butt and Lindstrom, 1994; Fiedler and Talley, 2006; Maes et al., 2007; Tsuchiya, 1991; Tsuchiya and Talley, 1996; Tsuchiya et al., 1989). Fig. 2A shows the potential temperature (θ), salinity, and potential density (σ_θ) of the water column down to 1000 m at both stations (also reported in Table 1). These hydrographic parameters allow us to identify the water masses sampled in this study, and to point out the correspondences between both stations. Two types of thermocline water masses were found in our profiles: the South Pacific Equatorial Water (SPEW), which is characterized by a high salinity maximum at temperatures above 20 °C (e.g., Tomczak and Godfrey, 2003), was sampled at 191 m St. 28 and at 140 m St. 14, and the 13 °C water (13°CW; Tsuchiya, 1981), underneath the SPEW, was sampled at 321 m St. 28 and at 198 m St. 14. The Antarctic Intermediate Water (AAIW), characterized by a salinity minimum, was sampled at 799 m St.28 and 849 m St.14. In the following, as a first order approximation, we will assume that the AAIW, 13°CW and SPEW sampled at station 14 come from the PNG area.

3. Sampling and methods

The samples were collected with 10 L acid-cleaned Go-Flo bottles attached on a trace-metal rosette (lent by Canadian GEOTRACES, University of Victoria, Canada and assembled at the University of Washington, USA; Slemons et al., 2010). The filtration was performed within a home made plastic room pressurized with filtered air, within 4 h of collection, with 0.4 µm pore size, 90 mm diameter Nuclepore membranes, fitted in Savillex PTFE filter holders, connected with PTFE tubing to the Go-Flo bottles pressurized with filtered air. All acids mentioned in the following were double-distilled, and their Fe concentrations were measured.

The filtered seawater was acidified to pH 1.80 two years after collection, and 3 to 9 months before the beginning of the analytical

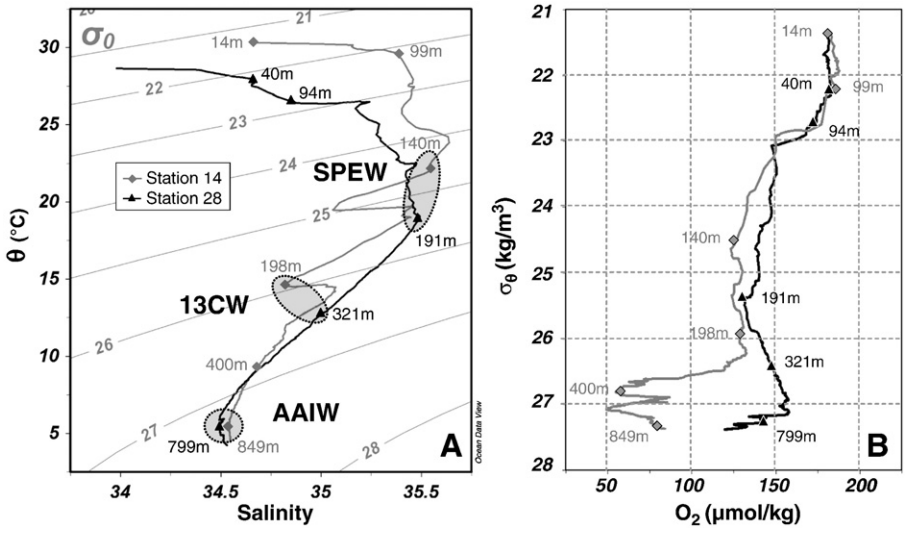

Fig. 2. A) Potential temperature (θ) — salinity diagram. Potential density (σ_θ) is shown (in kg m^{-3}). B) dissolved oxygen concentration profiles for station 14 (in grey) and station 28 (in black). The samples presented in this study are indicated by symbols and their depths are reported (in meters).

Table 1
Isotopic compositions and concentrations of dissolved and particulate Fe (from this study) and their corresponding sampling information and hydrographic parameters (from the EUCFe website, http://www.ocean.washington.edu/cruises/KiloMoana2006/) at stations 14 and 28 of the EUCFe cruise (2006). The 2SE is the internal precision of each isotopic composition measurement (at the 95% confidence level). The measurement uncertainty is ±0.08‰ (2SD, at the 95% confidence level) or the 2SE when the 2SE is larger than 0.08‰.

GoFlo bottle	Depth (m)	θ (°C)	Salinity	$[O_2]$ (μmol/kg)	θ_σ (kg/m^3)	Water mass	Dissolved fraction				Particulate fraction		
							Replicates	[DFe] (nM)	δ^{56}DFe (‰)	2SE (‰)	[PFe] (nM)	δ^{56}PFe (‰)	2SE (‰)
Station 28, cast TM56, 09/28/2006, bottom = 2256 m													
10	40	27.77	34.67	181.32	22.22		–	0.89	0.53	0.06	32.19	–	–
8	94	26.51	34.87	170.82	22.77		a	0.45	0.36	0.06	4.64	–	–
							a	0.45	0.44	0.08			
							Mean	*0.45*	*0.40*				
7	191	18.9	35.49	131.45	25.42	SPEW	b	0.67	0.45	0.08	6.97	0.29	0.06
							b	0.67	0.42	0.08			
							Mean	*0.67*	*0.43*				
5	321	12.88	35.02	147.61	26.43	13°CW	–	0.77	0.29	0.06	7.78	0.05	0.07
2	799	5.48	34.50	143.18	27.22	AAIW	b	1.46	0.07	0.08	9.63	–0.02	0.09
							b	1.46	0.08	0.08			
							b	1.46	0.02	0.07			
							b	1.46	0.06	0.07			
							Mean	*1.46*	*0.06*				
Station 14, cast TM28, 09/10/2006, bottom = 5260 m													
12	14	30.35	34.66	183.30	21.35		–	0.06	–	–	0.41	0.26	0.07
10	99	29.41	35.39	182.62	22.22		–	0.06	0.58	0.07	0.47	0.46	0.07
8	140	22.27	35.54	125.99	24.55	SPEW	–	0.20	0.31	0.08	0.58	0.14	0.08
6	198	14.75	34.83	129.79	25.90	13°CW	a	0.54	0.39	0.10	1.39	0.14	0.07
							a	0.53	0.40	0.06			
							Mean	*0.53*	*0.40*				
4	400	9.24	34.68	57.64	26.83	AAIW	–	0.61	0.01	0.06	0.87	0.15	0.08
2	849	5.34	34.54	75.58	27.27	AAIW	a	0.57	0.22	0.04	0.51	0.27	0.09
							a	0.61	0.22	0.05			
							Mean	*0.59*	*0.22*				

a indicates that the separation into several replicates has been performed before the chemical processing whereas *b* indicates that the separation has been performed just before the analysis at the Neptune (MC-ICPMS).

chemical treatments. The dissolved fraction was processed according to the procedure briefly described by Lacan et al. (2008) and detailed by Lacan et al. (2010). Briefly this procedure consists in a preconcentration with a NTA Superflow resin and purification with an AG1X4 anionic resin (200–400 mesh). For the entire DFe treatments, the average recovery was 91±25% (2SD, n=55), the blank was 2.9±1.6 ng (2SD, n=8).

For the particulate fraction, the filters were leached during 2 steps of 90 min at 130 °C in i) an aqua regia solution composed of 15 ml of 6 M HCl and 2.5 ml of 14 M HNO_3 and ii) the same solution with an addition of 0.5 ml of 23 M HF, as describe by Lacan et al. (in preparation). Then the solution was purified using the same procedure used for the DFe samples (Lacan et al., 2010). The total analytic blank for the PFe contributed less than 10% of the natural PFe content.

The iron isotope composition was measured with a Neptune Multi-Collector Inductively Coupled Plasma Mass Spectrometer (MC-ICPMS) at the Observatoire Midi Pyrénées (Toulouse, France). A ^{57}Fe–^{58}Fe double spike was used to correct the isotopic ratios from the artificial isotopic fractionations. The δ^{56}Fe values were calculated relative to the average of IRMM-14 measurements bracketing each sample. The internal precision of each measurement is given by the 2SE (2SE=2SD/√n; Table 1). The external precision was ±0.08‰ (2SD) and the δ^{56}Fe measurements were unbiased. The general performances of this method including the validation steps and the precision calculations are detailed by Lacan et al. (2010).

For this study, we performed several replicates of DFe samples at different steps of the processing (detailed in Table 1). Three samples were split into duplicates before the chemical processing and they reproduced to within ±0.04‰ (2SD) on average. Also two samples were split into replicates after the chemical processing, just before the mass spectrometric analysis, and they reproduced to within ±0.05‰ (2SD) on average. We consider that the external precision of the MC-ICPMS measurement (±0.08‰, 2SD) best characterizes the measurement uncertainty, excepted two analyses showing 2SE greater than the external precision (2SE=±0.09‰) for which the uncertainty is the 2SE (see Table 1).

The double spike method provides a precise and accurate determination of the iron concentration in the sample. The mean discrepancy between replicates was 1.9% (maximum discrepancy of 6.6%).

4. Results of iron concentrations and δ^{56}Fe

The dissolved iron concentrations range from 0.06 to 1.46 nM whereas the particulate iron concentrations range from 0.41 to 32.19 nM (see Fig. 3B and C and Table 1). Samples from the coastal station (28) display higher concentrations than samples from the open ocean station (14). At both stations, the PFe dominates the iron content.

At station 28, the DFe concentrations range from 0.45 (at 94 m) to 1.46 nM (at 800 m). These values are lower than the DFe concentrations reported by Mackey et al. (2002), closer to the PNG coast in the upper 150 m layer (between 1.3 and 2.6 nM). The surface sample shows a local maximum of 0.89 nM at the surface (40 m depth, in the vicinity of the chlorophyll maximum), also observed in the total acid soluble iron data by Mackey et al. (2002) and Slemons et al. (2010). At station 14 (open ocean), the DFe concentrations are very low in the upper 100 m layer (0.06 nM), then increase sharply up to 0.5 nM at 200 m depth and remain almost constant down to 800 m depth between 0.5 and 0.6 nM. This range is commonly observed in the open ocean (e.g., de Baar and de Jong, 2001; Johnson et al., 1997) and is in very good agreement with the few historical data available in the equatorial Pacific for depths shallower than 350 m, i.e., at 140°W (Coale et al., 1996) and at 90°W (Gordon et al., 1998). The PFe concentration profile displays a vertical maximum at 198 m in the lower part of the EUC, also observed by Slemons et al. (2010). Both

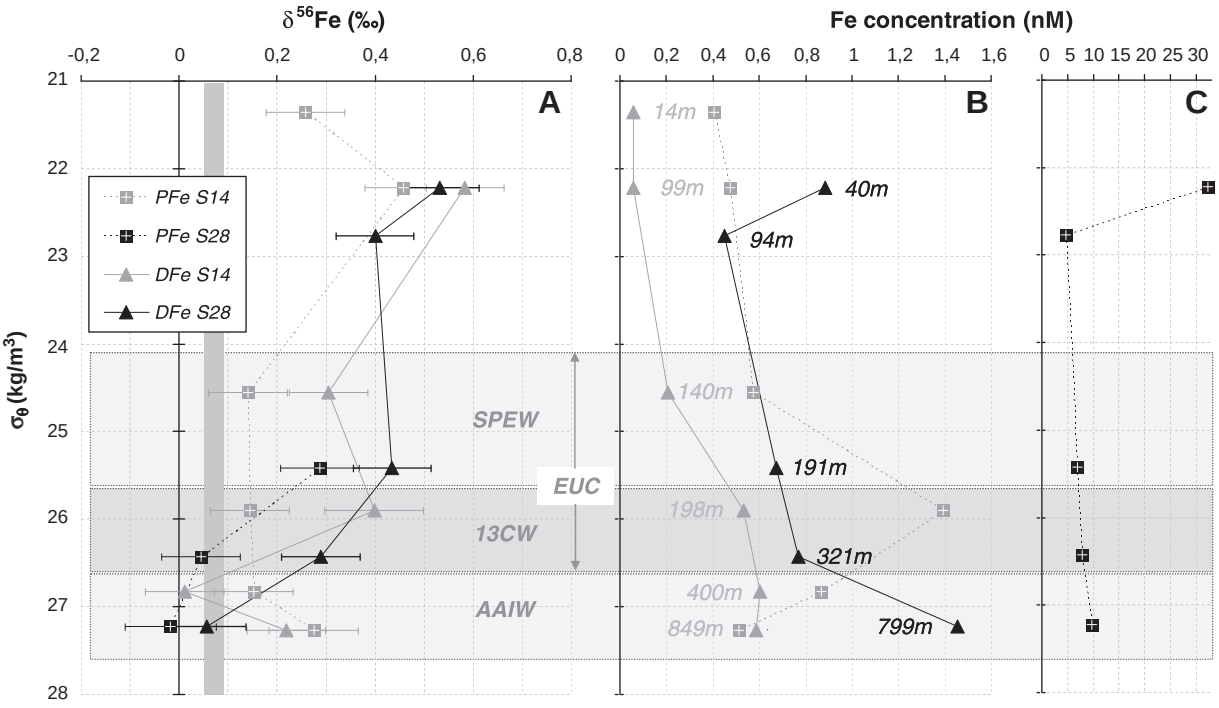

Fig. 3. δ^{56}Fe (A) and Fe concentration (B and C) in dissolved and particulate fractions of seawater from stations 14 and 28, versus potential density. In A, the vertical grey bar indicates the crustal value (0.07 ± 0.02‰, 2SD; Poitrasson, 2006). In B and C, the error bar is smaller than the symbols. Depths are indicated in B next to the data points. The large grey areas locate roughly the density of the water masses (SPEW, 13CW, AAIW; see text for details) and the Equatorial Undercurrent (EUC).

present profiles have lower DFe concentrations than those of Slemons et al. (2010). The latter range from 0.3 to 1.3 nM and 0.3 to 4.2 nM at Station 14 and 28 respectively. They were obtained by Flow Injection Analysis in similar samples (from the same cruise and the same location but collected from different casts and acidified immediately).

Fe isotope compositions are displayed as a function of potential density (σ_θ) in Fig. 3A. Both fractions show positive values of δ^{56}Fe (except one sample). They range from 0.01 to 0.58‰ in the dissolved fraction and from −0.02 to 0.46‰ in the particulate fraction. Most of the δ^{56}Fe variations occur in the vertical and not in the horizontal direction.

5. Discussion

Almost all the δ^{56}Fe values are positive. Since, there is no direct marine iron source with a clear positive signature, positive δ^{56}Fe in the seawater may be the result of fractionating processes. Considering that the largest isotopic fractionations occur during redox reactions (e.g., Johnson et al., 2008), the small δ^{56}Fe variations observed in this study suggest that redox conversions are only of minor importance in these waters.

5.1. Papua New Guinea area (station 28)

The coastal station (St. 28) is located about 30 km away from the PNG coast, in the currents from the southeast carrying south Pacific origin waters equatorwards, from 0 to 1000 m (Fine et al., 1994; Maes et al., 2007; Tsuchiya, 1991; Tsuchiya and Talley, 1996). Most of these waters have crossed the Vitiaz Strait within the New Guinea Coastal Undercurrent (NGCU; Butt and Lindstrom, 1994; Fiedler and Talley, 2006) as shown in Fig. 1.

High iron content of seawaters observed in all samples from station 28 (Fig. 3B and C) may reflect local inputs of iron since the stabilized concentrations found in the open ocean rarely reach 1 nM (e.g., de Baar and de Jong, 2001; Johnson et al. 1997). Indeed the northern PNG area is known to be subjected to significant local inputs of iron (e.g., Mackey et al., 2002). Isotopic compositions of dissolved Nd in seawater suggested that the dissolution of PNG shelf sediments could account for the lithogenic enrichment of the oceanic waters from the surface down to 800 m depth (Lacan and Jeandel, 2001). Total dissolvable Fe data in the Bismarck Sea show that the Fe concentrations within the NGCU increase along the northern coast of PNG and suggest that this Fe may be mainly supplied by slope sediments (Mackey et al., 2002; Slemons et al., 2010). The sediments being abundantly deposited on the shelf and slope by the local rivers (notably the Sepik river, located upstream of the station 28; see Fig. 1; Milliman and Syvitski, 1992), the sedimentary source must be linked to the riverine inputs. Although other kinds of sources could be invoked in this area, these studies emphasize the dominant role played by sediment remobilization.

The δ^{56}Fe data range from 0.06 to 0.53 ± 0.08‰ (2SD) in the DFe and from -0.02 ± 0.09‰ to 0.29 ± 0.08‰ in the PFe. The PFe accounts for ~90% of the iron content. In each sample, the DFe shows higher δ^{56}Fe than the PFe. Such DFe values are not consistent with the negative signature presupposed for the sedimentary source. As reported in the introduction, the sediments were found to release DFe with δ^{56}Fe from −3.3 to −1.7‰ (Homoky et al., 2009; Severmann et al., 2006). These values, measured in three locations characterized by high organic carbon accumulation rates, reflect the process of bacterial dissimilatory iron reduction (DIR) within the reductive sediment and the intense redox-recycling at the interface (Homoky et al., 2009; Severmann et al., 2006, 2010). Thus, the positive δ^{56}DFe values measured in the water column of station 28 do not suggest a significant DIR source contribution and may involve another kind of sedimentary iron release. Although the most studied sedimentary input of iron is the one associated with bacterial reduction, the release of dissolved elements in oxic seawater as been evidenced (Jeandel et al., in press; Jones et al., submitted for publication). Leaching experiments of sediments (in 0.5 M HCl) from the northern PNG slope, sampled between 0 and 1200 m depth,

display a mean δ^{56}Fe value of $+0.30\pm0.15$‰ 2SD (compared to a mean initial δ^{56}Fe of $+0.01\pm0.18$‰ 2SD; Murray et al., 2010). These values match very closely the dissolved values measured in the water column of station 28 ($+0.34\pm0.36$‰ 2SD, averaged over the whole water column). Taken together, these arguments suggest that the process supplying DFe to the seawater could be a non reductive release by the sediments rather than bacterial DIR. The local strong currents along the shelf may maintain oxic conditions in the surface layer of the sediments and limit the impact of DIR on the water column. Moreover, very large river sediment discharges and re-suspension of solid sediments occurring along the PNG coast (e.g., Kineke et al., 2000) would favor contact between the oxic seawater and the sediments. The transmissometry profile (see Fig. 5 by Slemons et al., 2010) shows turbid layers at station 28, especially between depths of 300 and 700 m, reflecting sediment re-suspension. This context, i.e., good oxygenation and resuspension of sediments, would favor a non reductive dissolution of sediment to the seawater rather than DIR. The word *dissolution* is used here and in the following in order to express a flux from the particulate to the dissolved phase, the dissolved phase being operationally defined as <0.40 µm for this study. The precise process involved in such dissolution is not known; it may be either dissolution (in the chemical sense) or desorption.

The vertical δ^{56}Fe heterogeneity at station 28 is difficult to interpret since the δ^{56}Fe of the upstream waters are unknown. Nevertheless, some hypotheses can be proposed. The surface sample (40 m) shows a vertical maximum, especially in the particle fraction (up to 32 nM). In addition to sediment remobilisation, iron inputs from aerosol and from rivers have to be considered for the surface layer. Based on Mn and Al data and modeling, dust deposition has been suggested to be possibly responsible for the high concentrations found above 100 m (Slemons et al., 2010). The δ^{56}DFe of $+0.53$‰ at 40 m depth is, among all the samples of station 28, the most different from the range characterizing solid aerosols (from -0.03‰ to 0.24 ± 0.08‰ 2SD observed in dusts, loess and continental aerosols; Beard et al., 2003b; Waeles et al., 2007). Assuming that the soluble iron derived from solid aerosols displays a similar signature (Waeles et al., 2007), the δ^{56}DFe at 40 m suggests that atmospheric iron inputs to the surface waters of this area are not significant. Based on Rare Earth Element patterns, river input of dissolved material from the northern PNG coast has been suggested to be responsible for about a fifth of the lithogenic inputs to the undercurrents of the Bismarck Archipelago (Sholkovitz et al., 1999). Station 28, being downstream of the Sepik River, the δ^{56}DFe in surface may also correspond to a riverine δ^{56}DFe signature (Bergquist and Boyle, 2006; De Jong et al., 2007).

At 800 m depth, in the core of the AAIW, the δ^{56}Fe is the lowest of the profile, with a value of $+0.06$‰ in DFe and -0.02‰ in PFe. These low δ^{56}Fe particles may be re-suspended from initially low δ^{56}Fe sediments (e.g. Yamaguchi et al., 2005) or may originate from hydrothermal activity (Rouxel et al. 2008). Actually there are numerous shallow ridges in the Bismarck Sea (e.g., Wells et al., 1999). Assuming that the bulk of the DFe is released by a non reductive dissolution of the suspended particles within the seawater, the low δ^{56}PFe could explain the low δ^{56}DFe observed. The DFe concentration of 1.46 nM at 800 m may suggest a direct input of DFe in this layer. Such low δ^{56}DFe source could be the hydrothermal activity (Beard et al., 2003b; Rouxel et al., 2008; Sharma et al., 2001).

Finally, the dominant source of iron to seawater in the PNG area is most likely a non reductive dissolution of iron from re-suspended sediments of the PNG margin. Because a contribution of other sources can not be completely rejected in surface and in the deep layer, we use the thermocline samples to characterize this new sedimentary signature. These samples display a DFe signature of $+0.37$‰ on average (±0.15‰, 2SD, n = 3). Assuming the steady state of the δ^{56}PFe in these samples (due to a large excess of PFe as a reactant) and that the whole DFe is released by the non reductive dissolution of the present suspended particles, the isotopic fractionation ($\Delta^{56}Fe_{DFe-PFe}$) is calculated as the difference between δ^{56}DFe and δ^{56}PFe Eq. (1).

$$\Delta^{56}Fe_{DFe-PFe} = \delta^{56}Fe_{DFe} - \delta^{56}Fe_{PFe} \quad (1)$$

This leads to $\Delta^{56}Fe_{DFe-PFe} = +0.20$‰ on average ($\pm0.11$‰, 2SD, n = 2). Such process may partly explain the positive δ^{56}DFe signature found in this study.

5.2. Thermocline waters in the EUC

The EUC is a strong eastward flowing current which crosses the whole Pacific Ocean along the equator. It is centered in the pycnocline (between 100 and 300 m depth, becoming shallower eastwards) with a maximum velocity around 1 m/s (Wyrtki and Kilonsky, 1984). The NGCU carries thermocline waters to the equator and constitutes the main source of waters to the EUC at its western end (see Fig. 1; Tsuchiya et al., 1989). As suggested by Goodman et al. (2005), over 2/3 of EUC waters at 140°W may be of southern origin.

As shown in Fig. 2A, the samples from 140 and 198 m at station 14 correspond to the same water masses as the samples from 191 and 321 m at station 28 respectively, the SPEW and the 13°CW respectively. Thus these water masses were sampled twice at two locations along their route between the PNG area and the central Pacific, being first carried by the NGCU and then by the EUC.

The δ^{56}DFe values of both water masses remain almost unchanged between stations 28 and 14 (Fig. 3A and Table 1): δ^{56}Fe = 0.29 and 0.40 ± 0.08‰ (2SD) for the 13°CW, and δ^{56}Fe = 0.43 and 0.31 ± 0.08‰ (2SD) for the SPEW, respectively. That is also the case for the δ^{56}PFe. The constancy of the δ^{56}Fe suggests that i) the Fe found in the EUC in the central Pacific is the same as the iron found in the PNG area, and thus the PNG is the source of iron to the EUC, as already suggested by earlier studies (Lacan and Jeandel, 2001; Mackey et al., 2002; Slemons et al., 2010), and ii) that the iron isotopic signature has been preserved in the EUC. Consequently, we suggest that the PFe in the EUC at 0°N, 180°E is a residue of sediments initially re-suspended near the PNG margin while the DFe content is the result of a non reductive dissolution of these sediments.

Along this flow, a removal of iron is observed between stations 28 and 14. While the upper part of the EUC (carrying the SPEW) has been abundantly renewed due to equatorial upwelling, the lower part of the EUC (carrying the 13°CW) is not significantly diluted along the route (Tsuchiya et al., 1989) and allows observing the effect of the removal process on the δ^{56}Fe. Assuming that the 13°CW sampled at station 28 is the source of the 13°CW in the lower EUC at station 14, the most likely process which removes 31% of DFe (from 0.77 to 0.54 nM) would be the adsorption of DFe on the settling particle surface (scavenging; Slemons et al., in press). Because the δ^{56}DFe difference between both locations is not significant, such removal seems not to fractionate iron isotopes. To further constrain this process, we estimated its isotopic fractionation. Assuming a Rayleigh fractionation, the isotopic fractionation associated with the DFe removal ($\Delta^{56}Fe_{rem\ DFe-SW\ DFe}$, assumed to be constant) is quantified with Eq. (2):

$$\Delta^{56}Fe_{rem\ DFe-SW\,DFe} \approx \left(\delta^{56}Fe^{f}_{SW\,DFe} - \delta^{56}Fe^{f=1}_{SW\,DFe}\right) / \ln(f) \quad (2)$$

where f is the fraction of DFe remaining in the water relative to the initial DFe concentration (69% in the present case); $\delta^{56}Fe^{f=1}_{SW\ DFe}$ is the initial δ^{56}DFe of the seawater and $\delta^{56}Fe^{f}_{SW\ DFe}$ is the δ^{56}DFe of the seawater at a given f. Eq. (2) leads to an isotopic fractionation of $\Delta^{56}Fe_{rem\ DFe\text{-}SW\ DFe} = -0.30\pm0.31$‰ (2SD). Although the large uncertainty does not allow a confident interpretation of the fractionation direction, this estimation shows that if there is an isotopic fractionation associated with scavenging of DFe from the water column, it is rather small.

In addition, 82% of the PFe is removed between stations 28 and 14, most likely by aggregation and settling of particles. As for the DFe removal, the resulting change of δ^{56}PFe is not significant. This corresponds to a potential isotopic fractionation such as $\Delta^{56}Fe_{rem\ PFe\text{-}SW\ PFe} = -0.05 \pm 0.07‰$ (2SD; as proceed for the DFe with Eq. (2)). This very small value is not surprising since one does not expect significant isotopic fractionation associated with such mechanisms.

5.3. Antarctic Intermediate Water (AAIW)

The AAIW reaches the equator from the South Pacific, carried by the intermediate NGCU via the PNG area (Tsuchiya, 1991; Tsuchiya and Talley, 1996). The isotopic composition of neodymium, that can be used to trace water mass pathways, also suggests that the AAIW found along the equator comes from the PNG area (Lacan and Jeandel, 2001). It will therefore be assumed in the following that the AAIW of station 28 is the source of the AAIW of station 14. The similarities of the potential temperatures and salinities of the AAIW from stations 28 and 14 support this assumption (Table 1 and Fig. 2).

The DFe concentration in the AAIW decreases significantly from 1.46 nM at station 28 to 0.60 nM at station 14 (Table 1). This corresponds to a 60% removal of the dissolved iron content. Despite this large iron removal, the δ^{56}DFe remains nearly constant, varying from $0.06 \pm 0.08‰$ (2SD) at station 28 to $0.22 \pm 0.08‰$ (2SD) at station 14. The difference of these 2 values is just significant and allows estimating the isotopic fractionation induced by the DFe removal. Eq. (2) leads to $\Delta^{56}Fe_{rem\ DFe\text{-}SW\ DFe} = -0.18 \pm 0.12‰$ (2SD). Such isotopic fractionation is very low and is consistent with the $\Delta^{56}Fe_{rem\ DFe\text{-}SW\ DFe}$ estimated in the 13°CW. This negative value means that the process would favor the removal of light iron isotopes. Assuming that such fractionation is induced by adsorption of DFe onto particles, this is not consistent with the $\Delta^{56}Fe_{fe(II)adsorb\text{-}Fe(II)aq}$ of +0,3 to +0,9‰ observed by Crosby et al. (2007) during in vitro experiments. This discrepancy is likely due to the very different iron speciation of the in vitro experiment compared to that of seawater. While the Crosby et al. experiments involves mainly the Fe(II) form, the Fe in seawater occurs predominantly in the Fe(III) form and interacts actively with organic ligands.

As for DFe, there is a major PFe removal (95%) between station 28 and station 14 in the AAIW. This removal, likely due to aggregation and settling of particles, accounts for an isotopic fractionation of $\Delta^{56}Fe_{rem\ PFe\text{-}SW\ PFe} = -0.10 \pm 0.04‰$ (2SD; with Eq. (2)). This value is consistent with the $\Delta^{56}Fe_{rem\ PFe\text{-}SW\ PFe}$ estimated in the 13°CW and, once again, underlines the minor influence of the PFe removal on the δ^{56}PFe signature.

The estimation of $\Delta^{56}Fe_{rem\ Fe\text{-}SW\ Fe}$ in the AAIW has to be considered cautiously, keeping in mind the scarcity of the data and the assumptions involved. First, it assumes that the removal is the only process undergone by the Fe between stations 28 and 14 in the AAIW, which is not obvious for the DFe. Actually the dissolved oxygen profiles (Fig. 2B) show that the oxygen content of the AAIW decreases significantly between these two locations, and suggests that significant bacterial remineralization occurred during the transit of the AAIW (mixing is neglected). The fractionation relative to the removal of DFe expressed here is valid only if the remineralization occurring in the water column does not significantly affect DFe isotopes during the transit of this water mass. Moreover the contribution from additional iron sources along the route of the EUC cannot be excluded and could possibly explain the increase of δ^{56}PFe between stations 28 and 14.

5.4. Biological uptake in the central equatorial Pacific (0°N, 180°E, station 14)

The surface waters at station 14 are fed by the equatorial upwelling and the westward flow of the South Equatorial Current (SEC; Wyrtki and Kilonsky, 1984). The surface waters at station 14 display low DFe concentrations (0.06 nM). The flux of total iron from aerosols to the surface ocean was quantified during the cruise and found to be extremely low in this area (Shank and Johansen, 2008). In addition the δ^{56}DFe of the subsurface water (0.58‰ at 99 m depth) is significantly different from the assumed atmospheric signature, ~0.1‰ (Beard et al., 2003b; Waeles et al., 2007).

The seawater at 99 m was sampled in the chlorophyll maximum as indicated by the fluorescence profile (Fig. 4). Such a sample therefore reflects the impact of the biological uptake on the δ^{56}Fe of the surrounding seawater. This sample displays a DFe concentration of 0.06 nM and a δ^{56}DFe of 0.58‰ (Table 1). The hydrographic parameters suggest that this seawater is the result of vertical mixing between the above and underlying waters. From the salinity data (we chose the salinity which is more conservative than the temperature in surface waters at the equator, see Table 1 and Fig. 2) we estimate that this seawater is a mixture of 83% of the underlying water (SPEW at 140 m, of which DFe concentration is 0.20 nM and δ^{56}DFe is 0.31‰), and 17% of the overlying water (of which DFe concentration is 0.06 nM and δ^{56}DFe is unknown). Assuming that the mixing conserves the DFe content, it would yield a DFe concentration of 0.18 nM at 99 m (before any biological consumption), of which 96% would come from the SPEW and 4% from the surface layer. Therefore we assume that the δ^{56}Fe resulting from the mixing is the same as that in the SPEW (0.31‰). Comparison of the DFe concentration resulting from the mixing (0.18 nM) with the DFe concentration observed in the 99 m sample (0.06 nM) suggests that there is a DFe removal of 0.12 nM (two third of the initial content). Because 99 m corresponds to the chlorophyll maximum location, we assume that the DFe removal is exclusively due to biological uptake. The difference between the δ^{56}DFe resulting from the mixing (0,31‰) and the measured value in the chlorophyll maximum (0,58‰) would then allow estimating the isotopic fractionation associated with the biological uptake. Assuming steady state and that this uptake follows a Rayleigh fractionation, Eq. (2) leads to an isotopic fractionation of $\Delta^{56}Fe_{phyto\text{-}SW\ DFe} = -0.25 \pm 0.10‰$ (2SD).

Assuming that all the particles at 99 m are phytoplankton organisms, the isotopic fractionation associated with the biological uptake can also be estimated using the PFe. According a Rayleigh distillation model, the PFe can be considered either as an instantaneous product or as a total product. Assuming that the phytoplankton

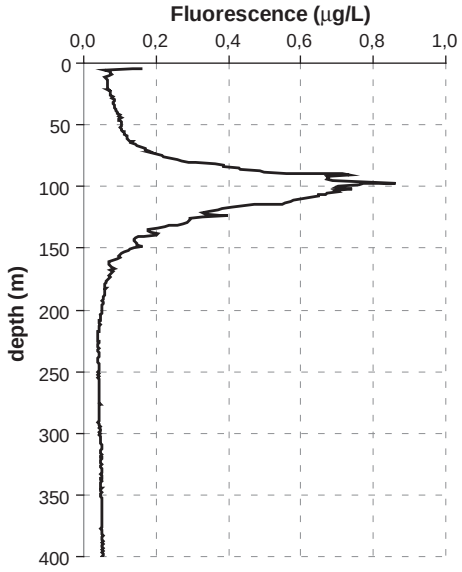

Fig. 4. Fluorescence profile measured at station 14 during EUCFe cruise (from the EUCFe website, http://www.ocean.washington.edu/cruises/KiloMoana2006/).

is not removed from the 99 m layer, PFe would correspond to the total product. Its isotopic composition ($\delta^{56}Fe^{f}_{phyto-tot}$) is defined in Eq. (3).

$$\Delta^{56}Fe_{phyto-SW\,DFe} \approx \left(\delta^{56}Fe^{f}_{SW\,DFe} - \delta^{56}Fe^{f}_{phyto-tot}\right)\frac{(1-f)}{ln(f)} \quad (3)$$

Eq. (3) leads to a $\Delta^{56}Fe_{phyto-SW\,DFe}$ of -0.08 ± 0.07‰ (2SD). Although the upwelling tends to decrease the flux of settling particles, it appears unrealistic to totally neglect this flux and to consider the PFe as the total product. Assuming that the phytoplankton is consistently removed from the 99 m layer, PFe would correspond to the instantaneous product (Fe that has been taken up by phytoplankton for an infinitely short time). In this case, the isotopic fractionation is the difference between the δ^{56}PFe and the δ^{56}DFe and corresponds to a $\Delta^{56}Fe_{phyto-SW\,DFe}$ of -0.13 ± 0.11‰ (2SD). This is consistent with the value deduced from the evolution of the DFe pool (-0.25 ± 0.10‰). These isotopic fractionations are small and reflect that phytoplankton would favor the uptake of light iron isotopes and that the surrounding waters would get heavier as they get depleted. These values are also in agreement with the range of $|\Delta^{56}Fe_{phyto\text{-}DFe}| < 0.32$‰, deduced from natural seawater samples in the southern Atlantic Ocean (Lacan et al., 2008), and with observations of isotope fractionation during Fe uptake by higher plants (Guelke and Von Blanckenburg, 2007). As better constrained isotopic fractionation induced by phytoplankton uptake in seawater will become available, the use of iron isotopes in Rayleigh distillation models could allow estimating the fraction of exported phytoplankton.

6. Conclusion

These δ^{56}Fe measurements constitute the first substantial dataset of this kind in the ocean. They come from two mid-depth profiles in the western and central equatorial Pacific Ocean. They range from +0.01 to +0.58‰ for DFe and from −0.02 to +0.46‰ for PFe. The average measurement uncertainty of ±0.08‰ (2SD) allows observing significant variations within these ranges. This uncertainty is only 3% of the whole range of variations observed in seawater so far (from −1.82 to +0.71‰; cf. introduction), which suggests that the isotopic composition of the Fe in seawater, both in the dissolved and particulate fractions, constitutes a new sensitive tracer of the oceanic iron cycle. In particular, these data provide new information about the iron sources and cycle in the equatorial Pacific Ocean. The small δ^{56}Fe variations observed in this study suggest that the redox conversion is only of minor importance for water column processes in this area. The largest δ^{56}Fe variations occur in the vertical and not in the horizontal direction. Each water mass appears to have its own isotope composition that is preserved over long distances.

Off Papua New Guinea (3°S, 144°E), where the dominant iron source is the margin sediments, the positive δ^{56}Fe of the dissolved fraction (from +0.06‰ to +0.53‰) indicates that iron is not produced by dissimilatory iron reduction and redox cycling (characterized by a very negative δ^{56}Fe) but might be released by the non reductive dissolution of sediment particles in seawater. The high sediment discharge from local rivers and the flow of strong western boundary currents along the northern coast of Papua New Guinea may remobilize the sediments and favor such dissolution. A distinct iron isotope signature is found to characterize this sedimentary source: a δ^{56}DFe of $+0.37 \pm 0.15$‰ (2SD, n = 3) and a $\Delta^{56}Fe_{DFe\text{-}PFe} = +0.20 \pm 0.11$‰ (2SD, n = 2) as estimated in the thermocline waters near PNG. The general positive values of the data set emphasize the role of the non-reductive dissolution of sediments in the marine iron isotope cycle. Because there is no evidence of atmospheric, hydrothermal and direct riverine Fe inputs in our samples, we did not add new constraint on their isotopic signatures. An overview of the marine iron isotope cycle, from elements of the literature and finding of this study, is proposed in Fig. 5.

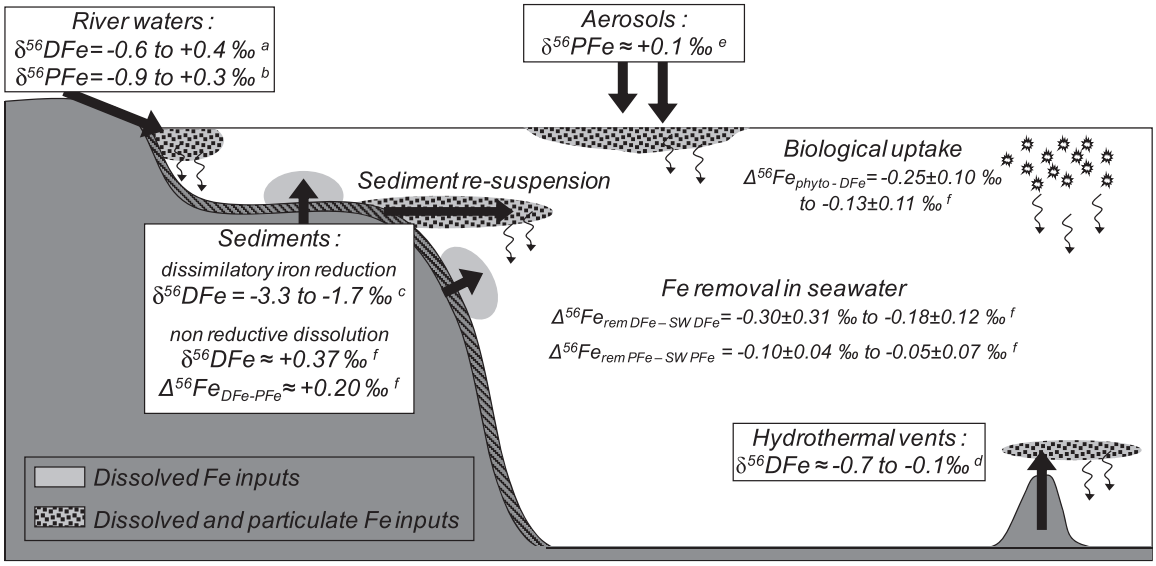

[a] Bergquist and Boyle, 2006 ; De Jong et al., 2007; Escoube et al., 2009

[b] Beard et al., 2003b ; Bergquist and Boyle, 2006; Ingri et al., 2006; Escoube et al., 2009

[c] Severmann et al., 2006 ; Homoky et al., 2009 ; Severmann et al., 2010. These δ^{56}Fe were observed in sediment pore waters and benthic chambers in reducing environments.

[d] Sharma et al., 2001 ; Beard et al., 2003b ; Rouxel et al., 2008

[e] Beard et al., 2003b ; Waeles et al,. 2007

[f] this study

Fig. 5. Schematic representation of the iron isotope cycle in the ocean inferred from the literature and from this study. The isotopic signatures of the main iron sources to seawater are represented. Estimates of the isotopic fractionations (in Δ^{56}Fe notation) associated with biological uptake and Fe removal in the water column are also shown but they have to be considered cautiously. See the Discussion for more details.

The hydrodynamic study of the region suggests that the station 28 (off PNG) might be considered as the main source of intermediate and thermocline waters to the station 14 (0°N, 180°E). Especially for the thermocline waters carried into the EUC, the δ^{56}Fe signatures remain unchanged between these two stations, which suggests the DFe found at 0°N, 180°E originates from the Papua New Guinea area and furthermore from the non reductive dissolution of the shelf sediments. This confirms that the iron feeding the eastern Pacific high nutrient low chlorophyll area would originate from PNG.

The dissolved and particulate Fe concentrations are found to decrease between the coastal PNG station and the dateline. Assuming that the former station is the source of the waters found at the latter station, isotopic fractionations associated with such Fe removal were assessed. They all display small values of $\Delta^{56}Fe_{\text{removed-SW Fe:}}$ -0.30 ± 0.31‰ to -0.18 ± 0.12‰ for scavenging of DFe (2SD) and of -0.10 ± 0.04‰ to -0.05 ± 0.31‰ (2SD) for aggregation/settling of particles. The isotopic fractionation associated with phytoplankton uptake, estimated at station 14 (0°N, 180°E) in the fluorescence maximum, is found to be characterized by $\Delta^{56}Fe_{\text{phyto-DFe}}=-0.25\pm0.10$‰ to -0.13 ± 0.11‰ (2SD). Phytoplankton would slightly favor the uptake of light iron, thereby making the DFe pool heavier. These estimations have to be considered cautiously and need to be further constrained. The limited extent of these fractionations within the water column may facilitate the use of iron isotopes as a tracer of DFe sources in the ocean.

This study illustrates the powerful potential of the Fe isotope composition in seawater as a new tracer of the oceanic Fe cycle, and more widely, of the oceanic biogeochemistry. In order to improve our understanding of this new tracer, we need to continue documenting the δ^{56}Fe in the ocean and in the iron sources, and to identify phase exchange processes which fractionate iron isotopes in the water column (from measurements of the dissolved and particulate phases in realistic oceanic condition). The multi-tracer approach should greatly help to clarify the complexity of the marine iron isotope cycle.

Acknowledgments

The CNRS (French National Center for Scientific Research) is thanked for supporting this study.

Comments of C. Jeandel, F. Poitrasson and an anonymous reviewer have greatly helped improve this manuscript. We greatly appreciate the efforts of the captain and crew of the Kilo Moana, and of marine technicians G. Foreman and D. Fitzgerald. C. Venchiarutti, O. Yigiterhan, J. Resing are thanked for their help with the sampling, and P. Dutrieux for his educational explanations about the local flows. We are grateful to L. Slemons, S. Severmann and J. McManus for having communicated unpublished data that helped to understand this dataset. We thank J. Chmeleff, for his efforts in fixing the numerous Neptune breakdowns, M. Grenier, for having supplied relevant retrotrajectories in the region, and also Kathy and Sarah for their everyday support during this study.

References

Beard, B., Johnson, C., 2004. Fe isotope variations in the modern and ancient earth and other planetary bodies. Rev. Mineral. Geochem. 55, 319–357.

Beard, B., Johnson, C., Skulan, J., Nealson, K., Cox, L., Sun, H., 2003a. Application of Fe isotopes to tracing the geochemical and biological cycling of Fe. Chem. Geol. 195, 87–117.

Beard, B., Johnson, C., Von Damm, K., Poulson, R., 2003b. Iron isotope constraints on Fe cycling and mass balance in oxygenated Earth oceans. Geology 31, 629–632.

Behrenfeld, M., Bale, A., Kolber, Z., Aiken, J., Falkowski, P., 1996. Confirmation of iron limitation of phytoplankton photosynthesis in the equatorial Pacific Ocean. Nature 383, 508–511.

Bergquist, B., Boyle, E., 2006. Iron isotopes in the Amazon River system: weathering and transport signatures. Earth Planet. Sci. Lett. 248, 54–68.

Boyd, P., Jickells, T., Law, C., Blain, S., Boyle, E., Buesseler, K., Coale, K., Cullen, J., de Baar, H., Follows, M., Harvey, M., Lancelot, C., Levasseur, M., Owens, N., Pollard, R., Rivkin, R., Sarmiento, J., Schoemann, V., Smetacek, V., Takeda, S., Tsuda, A., Turner, S., Watson, A., 2007. Mesoscale iron enrichment experiments 1993–2005: synthesis and future directions. Science 315, 612–617.

Bullen, T., White, A., Childs, C., Vivit, D., Schulz, M., 2001. Demonstration of significant abiotic iron isotope fractionation in nature. Geology 29, 699–702.

Butt, J., Lindstrom, E., 1994. Currents off the east-coast of New-Ireland, Papua-New-Guinea, and their relevance to regional undercurrents in the western equatorial Pacific-Ocean. J. Geophys. Res. Oceans 99, 12503–12514.

Coale, K., Fitzwater, S., Gordon, R., Johnson, K., Barber, R., 1996. Control of community growth and export production by upwelled iron in the equatorial Pacific Ocean. Nature 379, 621–624.

Crosby, H., Roden, E., Johnson, C., Beard, B., 2007. The mechanisms of iron isotope fractionation produced during dissimilatory Fe(III) reduction by Shewanella putrefaciens and Geobacter sulfurreducens. Geobiology 5, 169–189.

de Baar, H., de Jong, J., 2001. Distributions, sources and sinks of iron in seawater, dans: the biogeochemistry of iron in seawater. In: Turner, D., Hunter, K. (Eds.), IUPAC Series on Analytical and Physical Chemistry of Environmental Systems, vol. 7. John Wiley & Sons Ltd., Chichester, pp. 123–253.

de Jong, J., Schoemann, V., Tison, J., Becquevort, S., Masson, F., Lannuzel, D., Petit, J., Chou, L., Weis, D., Mattielli, N., 2007. Precise measurement of Fe isotopes in marine samples by multi-collector inductively coupled plasma mass spectrometry (MC-ICP-MS). Anal. Chim. Acta 589, 105–119.

Dideriksen, K., Baker, J., Stipp, S., 2008. Equilibrium Fe isotope fractionation between inorganic aqueous Fe(III) and the siderophore complex, Fe(III)-desferrioxamine B. Earth Planet. Sci. Lett. 269, 280–290.

Elrod, V., Berelson, W., Coale, K., Johnson, K., 2004. The flux of iron from continental shelf sediments: a missing source for global budgets. Geophys. Res. Lett. 31.

Escoube, R., Rouxel, O., Sholkovitz, E., Donard, O., 2009. Iron isotope systematics in estuaries: the case of North River, Massachusetts (USA). Geochim. Cosmochim. Acta 73, 4045–4059.

Fiedler, P., Talley, L., 2006. Hydrography of the eastern tropical Pacific: a review. Prog. Oceanogr. 69, 143–180.

Fine, R., Lukas, R., Bingham, F., Warner, M., Gammon, R., 1994. The western equatorial Pacific — a water mass crossroads. J. Geophys. Res. Oceans 99, 25063–25080.

Goodman, P., Hazeleger, W., De Vries, P., Cane, M., 2005. Pathways into the Pacific equatorial undercurrent: a trajectory analysis. J. Phys. Oceanogr. 35, 2134–2151.

Gordon, R., Johnson, K., Coale, K., 1998. The behaviour of iron and other trace elements during the IronEx-I and PlumEx experiments in the equatorial Pacific. Deep Sea Res. II 45, 995–1041.

Guelke, M., Von Blanckenburg, F., 2007. Fractionation of stable iron isotopes in higher plants. Environ. Sci. Technol. 41, 1896–1901.

Homoky, W., Severmann, S., Mills, R., Statham, P., Fones, G., 2009. Pore-fluid Fe isotopes reflect the extent of benthic Fe redox recycling: evidence from continental shelf and deep-sea sediments. Geology 37, 751–754.

Ingri, J., Malinovsky, D., Rodushkin, I., Baxter, D., Widerlund, A., Andersson, P., Gustafsson, O., Forsling, W., Ohlander, B., 2006. Iron isotope fractionation in river colloidal matter. Earth Planet. Sci. Lett. 245, 792–798.

Jeandel, C., Peucker-Ehrenbrink, B., Jones, M., Pearce, C.R., Oelkers, E., Godderis, Y., Lacan, F., Aumont, O., Arsouze, T., in press. Ocean margins: the missing term for oceanic element budgets? Eos.

Jickells, T., An, Z., Andersen, K., Baker, A., Bergametti, G., Brooks, N., Cao, J., Boyd, P., Duce, R., Hunter, K., Kawahata, H., Kubilay, N., laRoche, J., Liss, P., Mahowald, N., Prospero, J., Ridgwell, A., Tegen, I., Torres, R., 2005. Global iron connections between desert dust, ocean biogeochemistry, and climate. Science 308, 67–71.

John, S., Adkins, J., 2010. Analysis of dissolved iron isotopes in seawater. Mar. Chem. 119, 65–76.

Johnson, K., Gordon, R., Coale, K., 1997. What controls dissolved iron concentrations in the world ocean? Mar. Chem. 57, 137–161.

Johnson, C., Beard, B., Roden, E., 2008. The iron isotope fingerprints of redox and biogeochemical cycling in the modern and ancient Earth. Annu. Rev. Earth Planet. Sci. 36, 457–493.

Jones, M.T., Pearce, C.R., Oelkers, E.H., Jeandel, C., Eiriksdottir, E. and Gislason, S.R., submitted for publication. Suspended river material as key parameter in the global strontium cycle. Earth and Planetary Science Letter.

Kineke, G., Woolfe, K., Kuehl, S., Milliman, J., Dellapenna, T., Purdon, R., 2000. Sediment export from the Sepik River, Papua New Guinea: evidence for a divergent sediment plume. Cont. Shelf Res. 20, 2239–2266.

Kohfeld, K., Le Quere, C., Harrison, S., Anderson, R., 2005. Role of marine biology in glacial–interglacial CO_2 cycles. Science 308, 74–78.

Kuma, K., Nishioka, J., Matsunaga, K., 1996. Controls on iron(III) hydroxide solubility in seawater: the influence of pH and natural organic chelators. Limnol. Oceanogr. 41, 396–407.

Lacan, F., Jeandel, C., 2001. Tracing Papua New Guinea imprint on the central equatorial Pacific Ocean using neodymium isotopic compositions and rare earth element patterns. Earth Planet. Sci. Lett. 186, 497–512.

Lacan, F., Radic, A., Jeandel, C., Poitrasson, F., Sarthou, G., Pradoux, C., Freydier, R., 2008. Measurement of the isotopic composition of dissolved iron in the open ocean. Geophys. Res. Lett. 35.

Lacan, F., Labatut, M., Radic, A., Jeandel, C., in preparation. Chemical composition of suspended particles in the Atlantic sector of the Southern Ocean.

Lacan, F., Radic, A., Jeandel, C., Poitrasson, F., Sarthou, G., Pradoux, C., Freydier, R., chmeleff, J., 2010. High precision determination of the isotopic composition of dissolved iron in iron depleted seawater by double spike MC-ICPMS. Anal. Chem. 82, 7103–7111, doi:10.1021/ac1002504.

Lam, P., Bishop, J., 2008. The continental margin is a key source of iron to the HNLC North Pacific Ocean. Geophys. Res. Lett. 35.

Lam, P., Bishop, J., Henning, C., Marcus, M., Waychunas, G., Fung, I., 2006. Wintertime phytoplankton bloom in the subarctic Pacific supported by continental margin iron. Glob. Biogeochem. Cycles 20.

Lukas, R., Firing, E., 1984. The geostrophic balance of the Pacific equatorial undercurrent. Deep Sea Res. I 31, 61–66.
Mackey, D., O'Sullivan, J., Watson, R., 2002. Iron in the western Pacific: a riverine or hydrothermal source for iron in the equatorial undercurrent? Deep Sea Res. I 49, 877–893.
Maes, C., Gourdeau, L., Couvelard, X., Ganachaud, A., 2007. What are the origins of the Antarctic Intermediate Waters transported by the North Caledonian Jet? Geophys. Res. Lett. 34.
Martin, J., 1990. Glacial-interglacial CO_2 change: the iron hypothesis. Paleoceanography 5, 1–13.
Milliman, J., Syvitski, J., 1992. Geomorphic tectonic control of sediment discharge to the ocean — the importance of small mountainous rivers. J. Geol. 100, 525–544.
Moore, J., Braucher, O., 2008. Sedimentary and mineral dust sources of dissolved iron to the world ocean. Biogeosciences 5, 631–656.
Murray, J., Balistrieri, L., Paul, B., Nelson, B., Laydbak, J., Brunskill, G., 2010. δ^{56}Fe in surface sediments from the northeast margin of Papua New Guinea as a tracer for the origin of iron to the equatorial undercurrent. EOS Trans. Am. Geophys. Union 91 Ocean Sci. Meet. Suppl., Abstract PA35B-03.
Poitrasson, F., 2006. On the iron isotope homogeneity level of the continental crust. Chem. Geol. 235, 195–200.
Rouxel, O., Auro, M., 2010. Iron isotope variations in coastal seawater determined by multicollector ICP-MS. Geostand. Geoanal. Res. 34, 135–144.
Rouxel, O., Shanks, W., Bach, W., Edwards, K., 2008. Integrated Fe- and S-isotope study of seafloor hydrothermal vents at East Pacific rise 9–10 degrees N. Chem. Geol. 252, 214–227.
Rue, E., Bruland, K., 1995. Complexation of Iron(III) by natural organic-ligands in the Central North Pacific as determined by a new competitive ligand equilibration adsorptive cathodic stripping voltammetric method. Mar. Chem. 50, 117–138.
Severmann, S., Johnson, C., Beard, B., McManus, J., 2006. The effect of early diagenesis on the Fe isotope compositions of porewaters and authigenic minerals in continental margin sediments. Geochim. Cosmochim. Acta 70, 2006–2022.
Severmann, S., McManus, J., Berelson, W., Hammond, D., 2010. The continental shelf benthic iron flux and its isotope composition. Geochim. Cosmochim. Acta 74, 3984–4004.
Shank, L., Johansen, A., 2008. Atmospheric trace metal and labile iron deposition fluxes to the equatorial Pacific during EUCFe 2006. Ocean Sci. Meet.
Sharma, M., Polizzotto, M., Anbar, A., 2001. Iron isotopes in hot springs along the Juan de Fuca Ridge. Earth Planet. Sci. Lett. 194, 39–51.
Sholkovitz, E., Elderfield, H., Szymczak, R., Casey, K., 1999. Island weathering: river sources of rare earth elements to the Western Pacific Ocean. Mar. Chem. 68, 39–57.
Slemons, L., Gorgues, T., Aumont, O., Menkes, C., Murray, J.W., 2009. Biogeochemical impact of a model western iron source in the Pacific equatorial undercurrent. Deep Sea Res. I 56, 2115–2128.
Slemons, L., Murray, J., Resing, J., Paul, B., Dutrieux, P., 2010. Western Pacific coastal sources of iron, manganese, and aluminum to the equatorial undercurrent. Glob. Biogeochem. Cycles 24.
Slemons, L., Murray, J.W., Gorgues, T., Aumont, O.,Menkes, C., in press. Retention and loss of upwelled nutrients in the equatorial Pacific Ocean: Nitrate, silicate, and iron cycling in a global biogeochemical model. J. Mar. Res.
Tagliabue, A., Bopp, L., Aumont, O., 2009. Evaluating the importance of atmospheric and sedimentary iron sources to Southern Ocean biogeochemistry. Geophys. Res. Lett. 36.
Tagliabue, A., Bopp, L., Dutay, J., Bowie, A., Chever, F., Jean-Baptiste, P., Bucciarelli, E., Lannuzel, D., Remenyi, T., Sarthou, G., Aumont, O., Gehlen, M., Jeandel, C., 2010. Hydrothermal contribution to the oceanic dissolved iron inventory. Nat. Geosci. 3, 252–256.
Tomczak, M., Godfrey, J.S., 2003. Hydrology of the Pacific Ocean, Regional Oceanography: an Introduction, 2nd improved edition. Daya Publishing House, Delhi, pp. 137–156.
Tsuchiya, M., 1981. The origin of the Pacific equatorial 13°C water. J. Phys. Oceanogr. 11, 794–812.
Tsuchiya, M., 1991. Flow path of the Antarctic Intermediate Water in the western equatorial South-Pacific Ocean. Deep Sea Res. II 38, S273–S279.
Tsuchiya, M., Talley, L., 1996. Water-property distributions along an eastern Pacific hydrographic section at 135 W. J. Mar. Res. 54, 541–564.
Tsuchiya, M., Lukas, R., Fine, R., Firing, E., Lindstrom, E., 1989. Source waters of the Pacific equatorial undercurrent. Prog. Oceanogr. 23, 101–147.
Ussher, S., Achterberg, E., Worsfold, P., 2004. Marine biogeochemistry of iron. Environ. Chem. 1, 67–80.
Waeles, M., Baker, A., Jickells, T., Hoogewerff, J., 2007. Global dust teleconnections: aerosol iron solubility and stable isotope composition. Environ. Chem. 4, 233–237.
Wells, M., Vallis, G., Silver, E., 1999. Tectonic processes in Papua New Guinea and past productivity in the eastern equatorial Pacific Ocean. Nature 398, 601–604.
Wiederhold, J., Kraemer, S., Teutsch, N., Borer, P., Halliday, A., Kretzschmar, R., 2006. Iron isotope fractionation during proton-promoted, ligand-controlled, and reductive dissolution of goethite. Environ. Sci. Technol. 40, 3787–3793.
Wyrtki, K., Kilonsky, B., 1984. Mean water and current structure during the Hawaii-to-Tahiti shuttle experiment. J. Phys. Oceanogr. 14, 242–254.
Yamaguchi, K., Johnson, C., Beard, B., Ohmoto, H., 2005. Biogeochemical cycling of iron in the Archean–Paleoproterozoic Earth: constraints from iron isotope variations in sedimentary rocks from the Kaapvaal and Pilbara Cratons. Chem. Geol. 218, 135–169.

2. Lacan et al 2008. GRL. 1ères mesures de CI de Fe dans l'océan ouvert

Measurement of the isotopic composition of dissolved iron in the open ocean

F. Lacan,[1,2] A. Radic,[1] C. Jeandel,[1,2] F. Poitrasson,[3] G. Sarthou,[4,5] C. Pradoux,[1,2] and R. Freydier[3,6]

Received 28 August 2008; revised 18 November 2008; accepted 24 November 2008; published 31 December 2008.

[1] This work demonstrates for the first time the feasibility of the measurement of the isotopic composition of dissolved iron in seawater for a typical open ocean Fe concentration range (0.1–1 nM). It also presents the first data of this kind. Iron is preconcentrated using a Nitriloacetic Acid Superflow resin and purified using an AG1x4 anion exchange resin. The isotopic ratios are measured with a MC-ICPMS Neptune, coupled with a desolvator (Aridus II), using a ^{57}Fe-^{58}Fe double spike mass bias correction. Measurement precision (0.13‰, 2SD) allows resolving small iron isotopic composition variations within the water column, in the Atlantic sector of the Southern Ocean (from δ^{57}Fe = −0.19 to +0.32‰). Isotopically light iron found in the Upper Circumpolar Deep Water is hypothesized to result from organic matter remineralization. Shallow samples suggest that, if occurring, an iron isotopic fractionation during iron uptake by phytoplankton is characterized by a fractionation factor, such as: $|\Delta^{57}Fe_{(plankton\text{-}seawater)}| < 0.48‰$.
Citation: Lacan, F., A. Radic, C. Jeandel, F. Poitrasson, G. Sarthou, C. Pradoux, and R. Freydier (2008), Measurement of the isotopic composition of dissolved iron in the open ocean, *Geophys. Res. Lett.*, *35*, L24610, doi:10.1029/2008GL035841.

1. Introduction

[2] Iron availability has been shown to be the main limitation factor for phytoplankton growth in wide areas of the world ocean, such as in the so-called High Nutrient Low Chlorophyll (HNLC) areas (Southern Ocean, Subarctic and Equatorial Pacific Ocean; see *Boyd et al.* [2007] for a review). In that respect, the iron oceanic cycle is a component of the global carbon cycle and thus of the climate [*Martin and Fitzwater*, 1988]. Despite this importance, our knowledge of the iron (Fe) oceanic cycle remains partial. In particular, significant uncertainties remain about the iron sources to the open ocean. Whereas dust dissolution is traditionally considered as the dominant source [e.g., *Jickells et al.*, 2005], diagenetic dissolution at the continental margins is proposed to significantly contribute to the Fe content of the open ocean surface waters [*Elrod et al.*, 2004]. Hydrothermal inputs have also been recently hypothesized as significant contributors for the Fe content of the open ocean surface waters [*Boyle and Jenkins*, 2008].

[3] The iron isotopic composition (Fe IC) of these sources are different [*Beard and Johnson*, 2004; *Severmann et al.*, 2006]. Iron isotopes are therefore a very promising tool for the study of the iron sources to the ocean [*Zhu et al.*, 2000; *Beard et al.*, 2003]. Internal oceanic processes, in particular oxydo-reduction and organic complexation processes, have been shown to fractionate iron isotopes [*Bullen et al.*, 2001; *Johnson et al.*, 2002; *Dideriksen et al.*, 2008]. Iron isotopes could therefore also bring new insights into the internal oceanic Fe cycle, such as iron speciation, dissolved/particulate fluxes or biological processes.

[4] This great potential motivated very numerous Fe isotope studies during the last decade in the marine environment and at the ocean boundaries (ferromanganese crusts, plankton tows, aerosols, sediments, pore waters, suspended particles, rivers, estuaries, hydrothermal vents... [*Zhu et al.*, 2000; *Rouxel et al.*, 2003; *Levasseur et al.*, 2004; *Bergquist and Boyle*, 2006; *de Jong et al.*, 2007]). However, the isotopic composition of the iron dissolved in seawater in the open ocean has never been reported so far, because of the analytical difficulty of such measurement, due to the very low seawater Fe content (typically 1 to 0.1 nM) combined to a concentrated salt matrix. Such a measurement is however of the highest importance, because dissolved iron in seawater is the phase which links all the above listed marine phases. It is, for instance, absolutely necessary to fully exploit phytoplankton or ferromanganese Fe IC.

[5] In this paper, we briefly present, for the first time, a protocol allowing the measurement of the isotopic composition of dissolved iron in seawater, for Fe concentrations down to 0.1 nM. We also present the first data of the Fe IC of dissolved iron in the open ocean.

2. Sampling

[6] Four 10 L seawater samples taken during the BONUS/GOODHOPE cruise (Feb–March 2008, RV Marion Dufresne) have been analyzed following the protocol described below. These samples have been taken at station 18 (13°07′E–36°30′S), in the Atlantic sector of the Southern Ocean, north of the subtropical front, from 30 to 4000 m depth. They were collected with acid-cleaned 12-L Go-Flo bottles mounted on a Kevlar wire and tripped by Teflon messengers. The bottles were brought into a trace metal clean container for filtration through 0.4 μm Nuclepore®

[1] LEGOS, Observatoire Midi-Pyrénées, Université de Tolouse, Toulouse, France.
[2] LEGOS, CNRS, Toulouse, France.
[3] LMTG, CNRS, Toulouse, France.
[4] LEMAR, Université Européenne de Bretagne, Rennes, France.
[5] LEMAR, CNRS, Plouzané, France.
[6] Now at Laboratoire HydroSciences Montpellier, Montpellier, France.

0094-8276/08/2008GL035841$05.00

membranes (90 mm), within a few hours of collection. The filtration units were entirely made of PTFE. Samples were then acidified onboard to pH $\approx$ 1.8 (bi-distilled HCl).

3. Chemical Separation

[7] All of the chemical separation procedure is conducted in a trace metal clean lab, equipped with an ISO 4 (class 10) laminar flow hood. Reagents are bi-distilled. All labware is acid cleaned. Blanks of reagents, labware and atmosphere are monitored.

[8] Fe IC measurement in seawater requires its extraction from the sample matrix, with (i) a high yield (because of its low abundance), (ii) low contamination levels, (iii) no isotopic fractionation or a method for correcting for it, and (iv) a sufficient separation of the elements interfering with Fe isotopes during the spectrometric analysis.

[9] Dissolved Fe concentration in open ocean depleted surface waters can be as low as $\sim$0.05 nM [*Croot et al.*, 2004; *Blain et al.*, 2008]. The minimum amount of iron required to perform a precise isotopic analysis is around 20 to 50 ng [*Weyer and Schwieters*, 2003; *Schoenberg and von Blanckenburg*, 2005]. Therefore, analyzing the IC of dissolved Fe in Fe depleted seawater requires the preconcentration of $\sim$10 L samples (10 L of seawater with [Fe] = 0.05 nM contain 28 ng of Fe).

[10] The protocol described here is adapted from *Lohan et al.* [2005], using a commercially available Nitriloacetic Acid (NTA) Superflow resin (Qiagen®). The NTA resin is packed in a PTFE column. The 10L sample, filtered and acidified to pH = 1.75, is stored in a LDPE cubitainer. Such pH quantitatively dissociates the iron complexed to the organic ligands [*Lohan et al.*, 2005]. Hydrogen peroxide is added to the sample before the preconcentration to oxidize Fe^{II} to Fe^{III} ([H_2O_2] = 10 μM). The sample is passed through the resin at about 10 ml.min^{-1}. The resin is then rinsed with deionized water. Iron is eluted with 10 ml 1.5 M HNO_3. The column is then washed with 20 ml 1.5 M HNO_3 and stored at pH = 7. The sample is evaporated and re-dissolved in 6 M HCl for the purification step.

[11] Fe is then purified from the remaining salts using an AG1x4 anionic resin, using a protocol adapted from *Strelow* [1980]. Half a ml of resin is packed in a PTFE column. The sample is loaded onto the resin in 0.5 ml 6 M HCl mixed with 0.001% H_2O_2. Most of the elements are first eluted with 3.5 ml 6 M HCl mixed with 0.001% H_2O_2. Iron is then eluted with 3 ml 1 M HCl mixed with 0.001% H_2O_2. The elements remaining in the resin are washed with 0.1 M HF then 6 M HCl mixed with 0.001% H_2O_2 and 7 M HNO_3.

[12] Briefly, for the whole chemical procedure (preconcentration and purification), the yield for iron is 92 $\pm$ 10%, the Fe blank is 8.0 $\pm$ 2.5 ng and all interfering elements are quantitatively removed. This protocol is simple, since it is composed of a single preconcentration column (that could be carried out on board) and a single purification column.

4. Mass Spectrometric Analysis

[13] A Multi-Collector Inductively Coupled Plasma Mass Spectrometer (MC-ICPMS) Neptune (Thermo Scientific®), coupled with a desolvating nebulizer system (CETAC Aridus II®) is used. The medium mass resolution allows resolving the polyatomic interferences on masses 54 and 56 (e.g., ArN, ArO, ArOH, CaO [*Weyer and Schwieters*, 2003]). The desolvator provides a sensitivity $\sim$3 times higher than the Stable Introduction System (SIS, Elemental Scientific Inc). "X" skimmer cones were also employed to enhance the sensitivity. The very low Fe content of the samples requires the use of such devices. The Collector configuration is indicated in Table 1. This setting allows measuring all stable Fe isotopes as well as monitoring Cr and Ni, which can produce isobaric interferences with Fe.

[14] The mass fractionation occurring within the spectrometer and potentially during the chemical separation are corrected for with a ^{57}Fe-^{58}Fe double spike, assuming that both fractionations are mass dependent and are described by the same fractionation law [*Russel et al.*, 1978; *Siebert et al.*, 2001; *Dideriksen et al.*, 2003]. Data reduction is performed using the iterative approach of *Siebert et al.* [2001] from a single analysis of the sample-spike mixture.

[15] The double spike is added to the acidified sample at least 12 h before the preconcentration to allow the homogenization of the double spike with the sample. After preconcentration and purification, the sample is dissolved in $\sim$0.7 ml 0.3 M HNO_3, for the spectrometric analysis.

[16] Each sample is bracketed with an IRMM-14 certified reference material (mixed with the double spike), relative to which the sample IC is calculated. Each measurement session includes measurements of the ETH (Eidgenössische Technische Hochschule Zürich) in-house hematite standard (named HemSTD hereafter [*Poitrasson and Freydier*, 2005], mixed with the double spike), every 1.5 hours in order to monitor accuracy and precision of the instrument. Instrumental blanks (0.3 M HNO_3), and Cr and Ni interferences are monitored and corrected for. They are most of the time lower than 0.1% (with maximum values reaching 0.5%). The Fe IC is finally corrected for the blank of the overall procedure, which Fe IC is taken to be that of the igneous rocks.

5. Validation

[17] The blank of the whole procedure was determined by applying the above described protocol to 100 ml deionized water in place of a sample. This blank was measured repeatedly at each chemistry session (by isotopic dilution, either on a quadrupole ICPMS, Agilent 7500, with a collision cell in He mode, or on the MC-ICPMS; mass fractionation corrected for by standard bracketing). Its value is 8.0 $\pm$ 2.5 ng (1 SD, n = 5).

[18] The total yield of the chemical Fe preconcentration and purification is determined as follows. A 10 L seawater sample, taken at $\sim$40 m depth at the Dyfamed site (Northwest Mediterranean), is filtered (SUPOR® 47 mm, 0.8 μm), then acidified and spiked with a solution of ^{57}Fe (for the determination of its Fe concentration by isotopic dilution). The sample is then taken through the entire procedure. The resulting Fe is measured on the quadrupole ICPMS, both by the isotopic dilution method and the external calibration method (combined with a sensitivity correction with indium as an internal standard). The former allows determining the initial sample concentration, whereas the latter allows determining the Fe quantity recovered after the purification. Comparison of both quantities allows calculating the total

Table 1. Faraday Cup Configuration and Isotopic Abundances of Fe and Elements That Can Produce Isobaric Interferences With Fe

	Nominal Mass						
	53	54	56	57	58	60	61
Isotope abundance (%)							
Cr	9.5	2.37					
Fe		5.8	91.7	2.2	0.28		
Ni					68.3	26.1	1.13
Collector configuration	L4	L2	L1	H1	H2	H3	H4

yield of the procedure. This has been measured repeatedly, at each chemistry session. Total Fe yield is 92 ± 10% (1SD, n = 5). Achieving a 100% yield is not critical, however, since we add a double spike before the chemical procedure.

[19] The performance of the chemical separation was also assessed by the measurement of the matrix in which the Fe is eluted (after processing of a 10 L seawater sample). Most of the elements (those measurable with the ICPMS technique) were measured on the quadrupole ICPMS. The elements eluted together with Fe, are mostly Ca, Ga and Sb (∼ 90, 30 and 20 ng, respectively). In total, the matrix solid residue weights ∼150 ng and no trace of Cr, Ni or Zn could be detected.

[20] The three ratios δ^{56}Fe, δ^{57}Fe and δ^{58}Fe (usual δ notation, relative to ^{54}Fe) are measured with the same accuracy and the same internal and external precisions per atomic mass unit (see below and Table 2). In the following the Fe IC are reported as δ^{57}Fe, relative to IRMM-14.

[21] Internal precision of the measurements is typically lower than 0.1‰ (δ^{57}Fe; 2 SE = 2 SD/$\sqrt{}$n, where SE and SD stand for standard error and standard deviation, respectively). This is lower than the external precisions reported below.

[22] External precision and accuracy of the Fe IC measurement were tested in different ways. First, the measurement of variable amounts of the HemSTD (relative to IRMM-14) allowed estimating the capabilities of our instrument, configuration and data reduction, for variable Fe consumption. These results are reported in Figure 1. The known Fe IC of HemSTD is δ^{57}Fe(HemSTD) = 0.75 ± 0.14‰ (2 SD, n = 55 unpooled analyses, [*Poitrasson and Freydier*, 2005]). Taking into account all of our measurements, which correspond to Fe consumptions ranging from 200 to 25 ng per analysis, we find: δ^{57}Fe(HemSTD) = 0.79 ± 0.13‰ (2 SD, n = 40, over a period of 4 months). For the measurements with the lowest Fe quantity, corresponding to a Fe consumption of 25 ng, we find δ^{57}Fe(HemSTD) = 0.81 ± 0.16‰ (2 SD, n = 7). The accuracy is estimated from the deviation (absolute value of the difference) of the measurements from the known value. That deviation is on average δ^{57}Fe = 0.06 ± 0.08‰ (2 SD, n = 40), with a maximum value of 0.14‰.

[23] Accuracy and precision were then estimated using natural seawater. Ten liter filtered seawater samples (Dyfamed site, 40 m depth, [Fe] = 5 nM), were processed 3 to 4 times through the NTA column, in order to remove most of their Fe content. The samples were then doped with variable amounts of HemSTD: 550 ng, 165 ng and 55 ng, which correspond to Fe concentrations of 1, 0.3 and 0.1 nM. The samples were allowed to homogenize for 12 hours. Their Fe IC are then measured following the above described protocol. The Fe IC measured is corrected for the contributions of i) the chemistry blank and ii) the Fe remaining in the samples before doping (both are considered having the Fe IC of the igneous rocks). The results are reported in Figure 1. They show that the Fe IC measurements of the doped seawater samples are as precise and accurate as those performed directly on the standard solutions. This validates the overall procedure for seawater samples with Fe concentrations ranging from 1 to 0.1 nM, which represent a typical range found in the open ocean.

[24] Finally, replicate analyses of real seawater samples provide an integrated estimate of the measurement precision. From 3 duplicate analyses, the mean discrepancy between duplicates is found to be 0.04‰ (δ^{57}Fe), with a maximum discrepancy of 0.06‰ (cf. gray symbols in Figure 2). These values are lower than the external precision reported above for HemSTD. Therefore, in the following, the external precision reported above for HemSTD (0.13‰ 2 SD, n = 40) will be considered to best characterize the measurement uncertainty.

6. Fe Concentration

[25] Together with the measurement of the Fe isotopic composition, the double spike method provides precise and accurate determination of the Fe concentration (as shown with a simple spike by *de Jong et al.* [2008]). The detection limit, defined as three times the standard deviation of the blank (7.5 ng, 3 SD, n = 5, cf. section 4), is 13 pM when preconcentrating 10 L of sample. The precision, mostly limited by the blank variability (5 ng 2 SD, n = 5), is 9% for

Table 2. Isotopic Composition of Dissolved Fe From a Seawater Column[a]

Sampling Bottle Number	Depth (m)	[Fe] nM	δ^{56}Fe	2SE	δ^{57}Fe	2SE	δ^{58}Fe	2SE	Fe Consumed per Analysis (ng)
B10	30	0.159	0.06	0.056	0.09	0.084	0.11	0.110	52
B10	30	0.170	0.02	0.108	0.03	0.161	0.04	0.213	22
B6	200	0.282	0.09	0.037	0.14	0.055	0.19	0.072	158
B3	1250	0.577	−0.14	0.035	−0.20	0.053	−0.27	0.070	162
B3	1250	0.577	−0.12	0.056	−0.18	0.083	−0.23	0.110	164
B1	4000	0.539	0.21	0.064	0.32	0.095	0.42	0.126	91
B1[b]	4000	0.550	0.23	0.052	0.34	0.077	0.44	0.102	91
B1[b]	4000	0.550	0.20	0.039	0.30	0.057	0.39	0.076	91

[a]Bonus Goodhope Cruise. February 22nd 2008. Station 18. 13°07′E–36°30′S. Cast GOFLO-8. Each line corresponds to distinct chemical separation and spectrometric measurement, except where noted.
[b]Only the spectrometric measurement was duplicated (the chemical separation was the same).

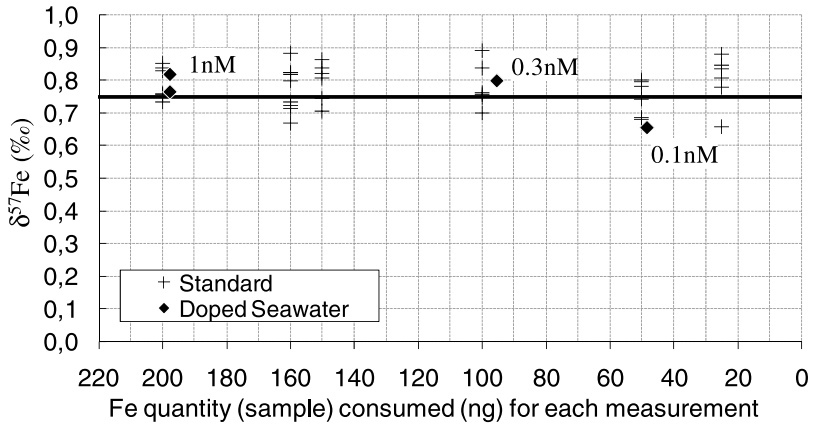

Figure 1. Fe IC of the HemSTD, measured directly (crosses) and after having being mixed to 10 L seawater samples from which most of the iron had been previously removed (diamonds). The thick line represents the known Fe IC of the HemSTD.

seawater samples with [Fe] = 0.1 nM, 2% for [Fe] = 0.5 nM, and lower than 1% for [Fe] > 1 nM.

7. Results and Discussion

[26] Four BONUS/GOODHOPE samples were analyzed following the above described protocol. Once back in the home laboratory, the double spike was added to the samples. Then, 3 of them were split into two duplicates, and analyzed. The results are reported in Table 2 and displayed in Figure 2.

[27] The range of variation is 0.51‰, with values ranging from δ^{57}Fe = −0.19 to +0.32‰. This range is small compared to that found in the environment, of the order of 5‰ [*Beard and Johnson*, 2004]. However, the variations are significant, considering the measurement precision (0.13‰, 2 SD external precision).

[28] The two shallower samples are located at 30 and 200 m depth, in the chlorophyll maximum and just below the euphotic zone, respectively. Their Fe IC (δ^{57}Fe = 0.06 and 0.14‰, respectively) are undistinguishable from the crustal value (δ^{57}Fe = 0.10 ± 0.03‰ 2 SD [*Poitrasson*, 2006]). At 1250 m depth, the sample is located in the core of the Upper Circumpolar Deep Water (UCDW), characterized by an oxygen minimum resulting from organic matter remineralization (see Figure 2). The UCDW Fe IC is δ^{57}Fe = −0.19‰. At 4000 m depth, the sample is located between the cores of the North Atlantic Deep Water (NADW) and of the Antarctic Bottom Water (AABW). Its hydrographic and nutrient properties (in particular its silicate content, not shown here), compared to that of the NADW and AABW allow estimating that it is composed of roughly 80% AABW and 20% NADW (it is identified as mAABW, for modified AABW, in Figure 2). Its Fe IC is δ^{57}Fe = +0.32‰.

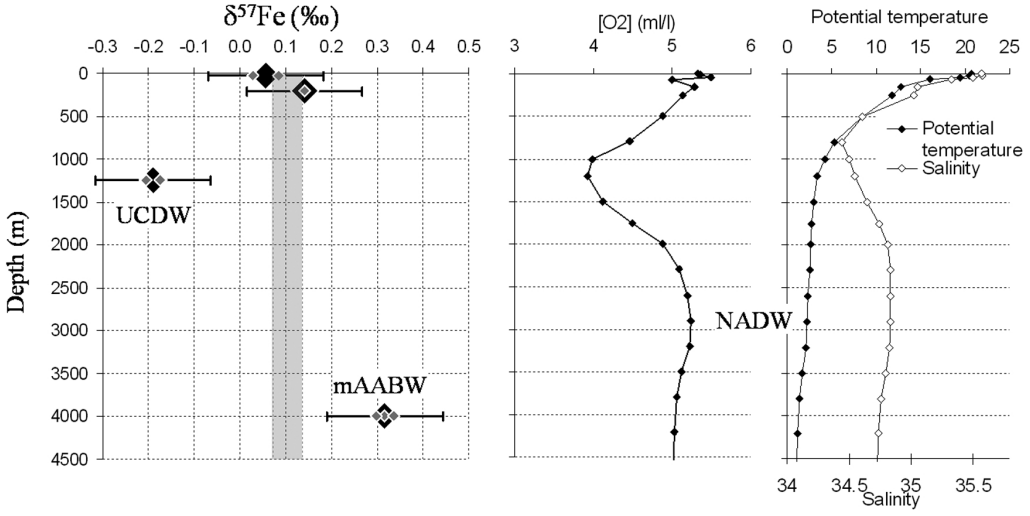

Figure 2. Fe isotopic composition, dissolved oxygen concentration, potential temperature and salinity profiles at station 18 of the Bonus/Goodhope cruise (2008). (left) Gray diamonds represent individual analyses, black diamonds represent the average of the replicate analyses. Error bars are the external precision of the measurements (2 SD = 0.13‰, cf. section Validation). The gray area represents the Fe IC of igneous rocks (±2 SD, [*Poitrasson*, 2006]). (middle and right) Hydrographic data (onboard raw data).

[29] Detailed interpretation of these few data, at a single station, would be premature and speculative. We can however propose hypotheses, which will require to be tested with more data in future works. Plankton tows have been measured at one site in the Equatorial Atlantic (Amazon plume). They are characterized by $\delta^{57}Fe = -0.36‰$ [*Bergquist and Boyle*, 2006]. The isotopically light dissolved Fe found in the UCDW could therefore reflect the remineralization of organic matter (resulting from the degradation of such plankton cells) in this water mass.

[30] Surface (30 m depth) iron depletion relative to subsurface concentrations (200 m depth) is 42%. In the hypothesis of the occurrence of Fe fractionation during Fe uptake by phytoplankton, the present data allow estimating an upper limit for the fractionation factor (according to Rayleigh distillation), above which a Fe IC variation would have been measurable (larger than twice the present data precision, i.e., 0.26‰). If the difference between the Fe IC of phytoplankton and that of seawater in which it grows is equal to ±0.48‰, then a 42% depletion should generate a difference of ±0.26‰ in the seawater relative to the initial value. Since no difference is observed between the 30 and 200 m depth samples, these data could suggest that, if occurring, a potential Fe isotopic fractionation during Fe uptake by phytoplankton could be characterized by a fractionation factor, such as: $|\Delta^{57}Fe_{(plankton\text{-}seawater)}| < 0.48‰$.

[31] Much more data are needed to propose more reliable interpretations of these results. They will be acquired in the framework of GEOTRACES.

[32] **Acknowledgments.** The CNRS (French National Center for Scientific Research) is thanked for its investment in this project. We thank two anonymous reviewers. M. Boye and S. Speich are thanked for having organized the Bonus/GoodHope Project and cruise. We thank the Crew and Captain of R/V Marion Dufresne. We thank the Go-Flo sampling team: J. Bown, M. Boye, E. Bucciarelli, F. Chever and B. Wake. F. Candaudap and J. Chmeleff are thanked for their help with the ICPMS.

References

Beard, B. L., and C. M. Johnson (2004), Fe isotope variations in the modern and ancient earth and other planetary bodies, in *Geochemistry of Non-Traditional Stable Isotopes, Rev. Mineral. Geochem.*, vol. 55, edited by C. M. Johnson, B. L. Beard, and F. Albarède, pp. 319–357, Mineral. Soc. of Am., Washington, D. C.

Beard, B. L., C. M. Johnson, K. L. Von Damm, and R. L. Poulson (2003), Iron isotope constraints on Fe cycling and mass balance in oxygenated Earth oceans, *Geology*, *31*, 629–632.

Bergquist, B. A., and E. A. Boyle (2006), Iron isotopes in the Amazon River system: Weathering and transport signatures, *Earth Planet. Sci. Lett.*, *248*, 54–68.

Blain, S., G. Sarthou, and P. Laan (2008), Distribution of dissolved iron during the natural iron-fertilization experiment KEOPS (Kerguelen Plateau, Southern Ocean), *Deep Sea Res., Part II*, *55*, 594–605.

Boyd, P. W., et al. (2007), Mesoscale iron enrichment experiments 1993–2005: Synthesis and future directions, *Science*, *315*, 612–617.

Boyle, E., and W. J. Jenkins (2008), Hydrothermal iron in the deep western South Pacific, *Geochim. Cosmochim. Acta*, *72*, A107.

Bullen, T. D., A. F. White, C. W. Childs, D. V. Vivit, and M. S. Schulz (2001), Demonstration of significant abiotic iron isotope fractionation in nature, *Geology*, *29*, 699–702.

Croot, P. L., K. Andersson, M. Ozturk, and D. R. Turner (2004), The distribution and specification of iron along 6°E in the Southern Ocean, *Deep Sea Res., Part II*, *51*, 2857–2879.

de Jong, J., et al. (2007), Precise measurement of Fe isotopes in marine samples by multi-collector inductively coupled plasma mass spectrometry (MC-ICP-MS), *Anal. Chim. Acta*, *589*, 105–119.

de Jong, J., V. Schoemann, D. Lannuzel, J. L. Tison, and N. Mattielli (2008), High-accuracy determination of iron in seawater by isotopoe dilution multiple collector inductively coupled plasma mass spectrometry (ID-MC-ICP-MS) using nitrilotriacetic acid chelating resin for preconcentration and matrix separation, *Anal. Chim. Acta*, *623*, 126–139.

Dideriksen, K., J. Baker, S. L. S. Stipp, and H. M. Williams (2003), Fe Isotope analysis by multi-collector inductively coupled plasma mass spectrometry (MC-ICP-MS) using ^{58}Fe-^{54}Fe double spike, *Geophys. Res. Abstr.*, *5*, 06718.

Dideriksen, K., J. A. Baker, and S. L. S. Stipp (2008), Equilibrium Fe isotope fractionation between inorganic aqueous Fe(III) and the siderophore complex, Fe(III)-desferrioxamine B, *Earth Planet. Sci. Lett.*, *269*, 280–290.

Elrod, V. A., W. M. Berelson, K. H. Coale, and K. S. Johnson (2004), The flux of iron from continental shelf sediments: A missing source for global budgets, *Geophys. Res. Lett.*, *31*, L12307, doi:10.1029/2004GL020216.

Jickells, T. D., et al. (2005), Global iron connections between desert dust, ocean biogeochemistry, and climate, *Science*, *308*, 67–71.

Johnson, C. M., J. L. Skulan, B. L. Beard, H. Sun, K. H. Nealson, and P. S. Braterman (2002), Isotopic fractionation between Fe(III) and Fe(II) in aqueous solutions, *Earth Planet. Sci. Lett.*, *195*, 141–153.

Levasseur, S., M. Frank, J. R. Hein, and A. Halliday (2004), The global variation in the iron isotope composition of marine hydrogenetic ferromanganese deposits: Implications for seawater chemistry?, *Earth Planet. Sci. Lett.*, *224*, 91–105.

Lohan, M. C., A. M. Aguilar-Islas, R. P. Franks, and K. W. Bruland (2005), Determination of iron and copper in seawater at pH 1.7 with a new commercially available chelating resin, NTA superflow, *Anal. Chim. Acta*, *530*, 121–129.

Martin, J. H., and S. E. Fitzwater (1988), Iron deficiency limits phytoplancton growth in the north-east Pacific subarctic, *Nature*, *331*, 341–343.

Poitrasson, F. (2006), On the iron isotope homogeneity level of the continental crust, *Chem. Geol.*, *235*, 195–200.

Poitrasson, F., and R. Freydier (2005), Heavy iron isotope composition of granites determined by high resolution MC-ICP-MS, *Chem. Geol.*, *222*, 132–147.

Rouxel, O., N. Dobbek, J. Ludden, and Y. Fouquet (2003), Iron isotope fractionation during oceanic crust alteration, *Chem. Geol.*, *202*, 155–182.

Russel, W. A., D. A. Papanastassiou, and T. A. Tombrello (1978), Ca isotope fractionation on the Earth and other solar system materials, *Geochim. Cosmochim. Acta*, *42*, 1075–1090.

Schoenberg, R., and F. von Blanckenburg (2005), An assessment of the accuracy of stable Fe isotope ratio measurements on samples with organic and inorganic matrices by high-resolution multicollector ICP-MS, *Int. J. Mass Spectrom.*, *242*, 257–272.

Severmann, S., C. M. Johnson, B. L. Beard, and J. McManus (2006), The effect of early diagenesis on the Fe isotope compositions of porewaters and authigenic minerals in continental margin sediments, *Geochim. Cosmochim. Acta*, *70*, 2006–2022, doi:2010.1016/j.gca.2006.2001.2007.

Siebert, C., T. F. Nägler, and J. D. Kramers (2001), Determination of molybdenum isotope fractionation by double-spike multicollector inductively coupled plasma mass spectrometry, *Geochem. Geophys. Geosyst.*, *2*(7), 1032, doi:10.1029/2000GC000124.

Strelow, F. W. E. (1980), Improved separation of iron from copper and other elements by anion-exchange chromatography on a 4% cross-linked resin with high concentrations of hydrochloric acid, *Talanta*, *27*, 727–732.

Weyer, S., and J. B. Schwieters (2003), High precision Fe isotope measurements with high mass resolution MC-ICPMS, *Int. J. Mass Spectrom.*, *226*, 355–368.

Zhu, X.-K., R. K. O'Nions, Y. Guo, and B. C. Reynolds (2000), Secular variation of iron isotopes in North Atlantic Deep Water, *Science*, *287*, 2000–2002.

R. Freydier, Laboratoire HydroSciences Montpellier, F-34095 Montpellier CEDEX 5, France.

C. Jeandel, F. Lacan, C. Pradoux, and A. Radic, LEGOS, Observatoire Midi-Pyrénées, Université de Tolouse, 14, avenue Edouard Belin, F-31400 Toulouse, France. (francois.lacan@legos.obs-mip.fr)

F. Poitrasson, LMTG, CNRS, 14–16, avenue Edouard Belin, F-31400 Toulouse, France.

G. Sarthou, LEMAR, CNRS, Place Nicolas Copernic, F-29280 Plouzané, France.

3. Lacan et al 2006. GCA 1ères mesures de CI de Cd dans l'océan et en cultures

Available online at www.sciencedirect.com
ScienceDirect
Geochimica et Cosmochimica Acta 70 (2006) 5104–5118
Geochimica
www.elsevier.com/locate/gca

Cadmium isotopic composition in the ocean

Francois Lacan [a,*,1], Roger Francois [a,2], Yongcheng Ji [b], Robert M. Sherrell [b]

[a] *Woods Hole Oceanographic Institution, Department of Marine chemistry and Geochemistry, Woods Hole, MA 02543, USA*
[b] *Institute of Marine and Coastal Sciences and Department of Geological Sciences, Rutgers University, 71 Dudley Road, New Brunswick, NJ 08901-8521, USA*

Received 21 December 2005; accepted in revised form 27 July 2006

Abstract

The oceanic cycle of cadmium is still poorly understood, despite its importance for phytoplankton growth and paleoceanographic applications. As for other elements that are biologically recycled, variations in isotopic composition may bring unique insights. This article presents (i) a protocol for the measurement of cadmium isotopic composition (Cd IC) in seawater and in phytoplankton cells; (ii) the first Cd IC data in seawater, from two full depth stations, in the northwest Pacific and the northwest Mediterranean Sea; (iii) the first Cd IC data in phytoplankton cells, cultured in vitro. The Cd IC variation range in seawater found at these stations is not greater than 1.5 $\varepsilon_{Cd/amu}$ units, only slightly larger than the mean uncertainty of measurement (0.8 $\varepsilon_{Cd/amu}$). Nevertheless, systematic variations of the Cd IC and concentration in the upper 300 m of the northwest Pacific suggest the occurrence of Cd isotopic fractionation by phytoplankton uptake, with a fractionation factor of 1.6 ± 1.4 $\varepsilon_{Cd/amu}$ units. This result is supported by the culture experiment data suggesting that freshwater phytoplankton (*Chlamydomonas reinhardtii* and *Chlorella* sp.) preferentially take up light Cd isotopes, with a fractionation factor of 3.4 ± 1.4 $\varepsilon_{Cd/amu}$ units. Systematic variations of the Cd IC and hydrographic data between 300 and 700 m in the northwest Pacific have been tentatively attributed to the mixing of the mesothermal (temperature maximum) water ($\varepsilon_{Cd/amu} = -0.9 \pm 0.8$) with the North Pacific Intermediate Water ($\varepsilon_{Cd/amu} = 0.5 \pm 0.8$). In contrast, no significant Cd IC variation is found in the northwest Mediterranean Sea. This observation was attributed to the small surface Cd depletion by phytoplankton uptake and the similar Cd IC of the different water masses found at this site. Overall, these data suggest that (i) phytoplankton uptake fractionates Cd isotopic composition to a measurable degree (fractionation factors of 1.6 and 3.4 $\varepsilon_{Cd/amu}$ units, for the in situ and culture experiment data, respectively), (ii) an open ocean profile of Cd IC shows upper water column variations consistent with preferential uptake and regeneration of light Cd isotopes, and (iii) different water masses may have different Cd IC. This isotopic system could therefore provide information on phytoplankton Cd uptake and on water mass trajectories and mixing in some areas of the ocean. However, the very small Cd IC variations found in this study indicate that applications of Cd isotopic composition to reveal aspects of the present or past Cd oceanic cycle will be very challenging and may require further analytical improvements. Better precision could possibly be obtained with larger seawater samples, a better chemical separation of tin and a more accurate mass bias correction through the use of the double spiking technique.

1. Introduction

Although cadmium can be a toxic element at high concentrations, it is taken up by phytoplankton at the lower concentrations found in ocean surface waters, and may play a role in phytoplankton nutrition. The vertical oceanic distribution of dissolved Cd is typical of that of a nutrient, with a surface depletion, a maximum associated with organic matter remineralization and relatively constant values at depth. Dissolved Cd distribution in the ocean is closely correlated to that of phosphate (Boyle et al., 1976; Bruland et al., 1978).

* Corresponding author. Fax: +33 5 61 25 32 05.
E-mail address: francois.lacan@legos.cnes.fr (F. Lacan).
[1] Present address: CNRS, LEGOS, UMR5566, CNRS-CNES-IRD-UPS, Observatoire Midi-Pyrenees, 18, Av. E. Belin, 31400 Toulouse, France.
[2] Present address: Department of Earth and Ocean Sciences, The University of British Columbia, 6339 Stores Road, Vancouver, BC, Canada V6T 1Z4.

0016-7037/$ - see front matter © 2006 Elsevier Inc. All rights reserved.
doi:10.1016/j.gca.2006.07.036

The Cd/Ca ratio recorded in foraminiferal tests has been exploited to reconstruct past oceanic PO_4 distributions and infer past oceanic circulation and nutrient concentrations in the context of long-term climate variations (Boyle, 1988; Elderfield and Rickaby, 2000). However, although the Cd versus P relationship is very consistent in deep waters, substantial deviations have been documented in surface waters, in particular in high nutrient low chlorophyll (HNLC) areas of the Subarctic Pacific (e.g., Martin et al., 1989) and Southern Oceans (e.g., Frew and Hunter, 1992). Although these deviations can be accounted for by empirical models based on the modern Cd and P distributions (e.g., Elderfield and Rickaby, 2000; Sunda and Huntsman, 2000), the mechanisms yielding these deviations have only begun to be explored (Cullen et al., 2003; Cullen, 2006).

It has been shown that Cd can substitute for Zn in Zn-carbonic-anhydrase (an enzyme involved in inorganic carbon acquisition); (Price and Morel, 1990; Morel et al., 1994) or used directly in a Cd-specific form of the enzyme (Cullen et al., 1999; Lane et al., 2005). However, the factors controlling Cd concentration is seawater are still poorly understood. Zinc concentration (Price and Morel, 1990), CO_2 partial pressure (Cullen et al., 1999), growth rate and Fe or Mn availability (Sunda and Huntsman, 2000; Frew et al., 2001; Cullen et al., 2003) are all factors that could substantially influence Cd uptake by phytoplankton.

These recent findings underscore the need for a better understanding of the oceanic cadmium cycle. Owing to the large mass range of the Cd isotopic system (from ^{106}Cd to ^{116}Cd), biological uptake, adsorptive scavenging and remineralization of organic matter could produce Cd isotopic fractionations. Cadmium isotopic data may therefore provide new insight into these processes. In particular, biologically mediated Cd isotopic fractionation could be significant. In such a case, for areas in which surface water Cd depletion is partial (as in N-limited or HNLC areas, where excess phosphate is found), the Cd isotopic composition (Cd IC) of surface waters and in turn that of the exported organic matter could vary according to Rayleigh fractionation. Cd isotopic measurements in seawater or exported organic matter could therefore allow quantification of the extent of Cd utilization. If significant Cd isotopic fractionations occur in the environment, this parameter could also help to trace different Cd sources and transports in the ocean.

As a first step towards elucidating the systematics of Cd isotopic fractionation in the environment, we present the first cadmium isotope measurements in seawater (northwest Pacific and northwest Mediterranean), and in phytoplankton (cultured freshwater green algae, *Chlamydomonas reinhardtii* sp. and *Chlorella* sp.).

2. Samples

The seawater samples were taken from the northwest Pacific (Cruise MR02-K05 Leg2, 16/10/2002, Station K1, 51.28°N, 165.2°E, 5140 m depth) and at the DYFAMED site in the Mediterranean Sea (Cruise Barmed 5, 25/06/2003, 43.4°N, 7.9°E, 2350 m depth) (Fig. 1). These two sites represent very different oceanic regimes with distinct Cd and nutrient distributions. Cadmium and P concentrations are approximately an order of magnitude higher at station K1 than at DYFAMED (Fig. 2). There is near complete surface phosphate depletion at DYFAMED, which is not the case at K1. The Cd cycle in the Mediterranean is unique. Surface Cd concentrations are much higher than in nutrient-depleted waters of the open ocean (Boyle et al.,

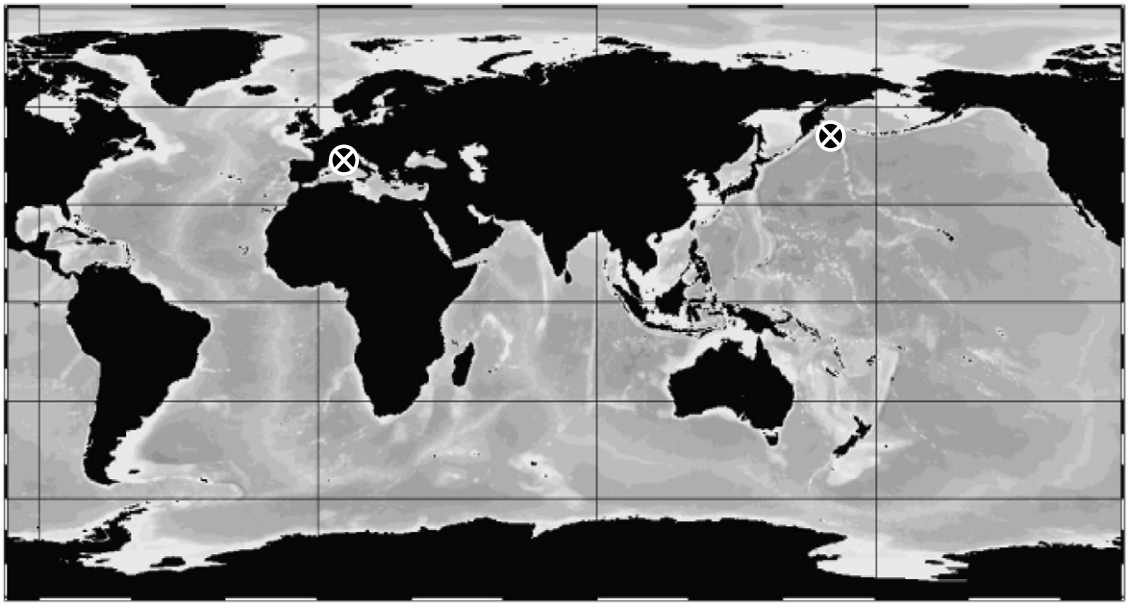

Fig. 1. The locations of the two sampling sites, shown by crosses.

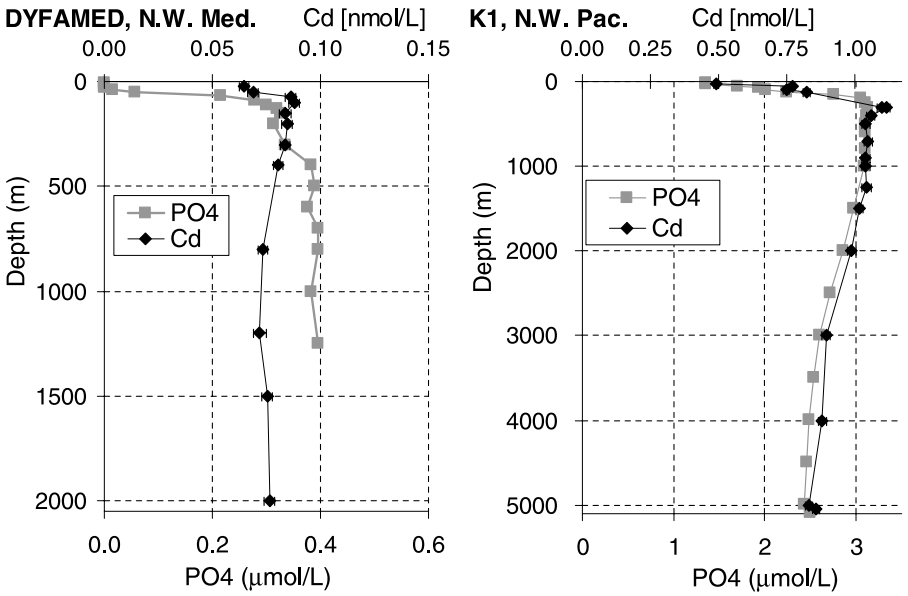

Fig. 2. Cd and phosphate profiles at the two sites. The nutrient concentrations at DYFAMED were measured on 10/07/2003, 2 weeks after the Cd sampling. The Cd error bars correspond to the internal precision (~3% at DYFAMED and 1.5% at K1, $2\sigma_n$), found to be similar to the reproducibility (2%).

1985; van Geen et al., 1991). This enrichment could have various natural or anthropogenic origins, such as advection with river waters, aeolian inputs or shelf sediment remobilization (Riso et al., 2004 and references therein).

Depending on the sampling site, 250 (North Pacific) to 1000 mL (Mediterranean) of unfiltered seawater were acidified with trace metal clean HCl to pH <2. Subsequent sample handling was conducted under stringent trace metal clean conditions. Whereas it is commonly accepted that particulate Cd is a negligible fraction of dissolved at depth, this is not necessarily the case for surface waters. There are few studies reporting both dissolved and particulate Cd concentration in seawater. In the Atlantic Ocean surface water (40°N to 20°S), particulate Cd concentrations amount to ~3.3% of total Cd (values ranging from 0.7 to 9%. Helmers, 1996). In the northeast Pacific, Sherrell (1989) reports particulate Cd concentration decreasing from about 4 pmol L^{-1} at 30 m to 0.10–0.15 pmol L^{-1} at 2000–3000 m, whereas surface dissolved Cd content in this area were found around 60 pmol L^{-1} (Bruland, 1980). Taken together, these two studies suggest that particulate Cd amounts to ~6% of total Cd in the surface waters of the northeast Pacific and to much less at depth. Finally, dissolved Cd data from the surface waters of the northwest Pacific are identical to our total Cd data (when comparing samples at similar depths and similar hydrographical properties. Abe, 2002), suggesting negligible particulate Cd content at this site. We therefore assume that the Cd concentrations and isotopic compositions measured in this study (in unfiltered samples) characterize primarily dissolved Cd.

Two species of freshwater phytoplankton were selected in this study: *Chlamydomonas reinhardtii* sp. and *Chlorella* sp. The algae were grown in vitro (Institute of Marine and Coastal Sciences, Rutgers University) in acid-washed 1 L polycarbonate bottles under 100 µmol quanta m^{-2} s^{-1} light illumination with 12:12 h light:dark cycle at 19 ± 1 °C. Bacterial biomass was controlled to negligible levels by microwave heating of the media to near 100 °C prior to phytoplankton inoculation. Replicate culture bottles (4 per species) were grown in low-metal nutrient replete freshwater media (pH ~7.0), in which the trace metals were buffered by 5 µM EDTA. The total metal concentration in the culture media was: Fe: 116 nM; Mn: 13 nM; Zn: 27.2 nM; Cu: 44.3 nM; Co: 4 nM; Cd: 17.3 nM, and Ni: 3520 nM. Buffered by 5 µM EDTA, these total metal concentrations correspond to equilibrium Me′ (the concentration of free metal ions plus labile dissolved inorganic species) of: Fe, 40 pM; Mn, 2 nM; Zn, 20 pM; Cu, 0.14 pM; Co, 2 pM; Cd, 7.9 pM and Ni, 20 pM (calculated using the chemical speciation program MINEQL+, version 5.0). Cadmium was added to the concentrated mixed metal stock solution as $CdCl_2$ (Aldrich Chem Co., >99.99%), and less than 1% of total Cd in the media was removed by phytoplankton uptake during the incubation. Accordingly, we assume that the Cd isotopic composition of the media did not change during phytoplankton growth.

The phytoplankton were acclimated to the experimental media for several generations and inoculated into fresh media to initiate the incubation from which isotope fractionation was determined. Cells were harvested at mid-exponential growth stage (cell density ~ 200,000 cells mL^{-1}) by centrifugation at 6500 rpm (3000*g*) (Eppendorf model 5403) using six 50 mL polycarbonate centrifuge tubes for 15 min at 19 °C. After centrifugation, cell pellets were rinsed twice with 50 mL Milli-Q deionized H_2O to wash away any residual media (>99.99% removal), thus eliminating the contribution of metals from residual media to the cell pellet. Each sample represents combined cell pellets

from 2 culture bottles. The pooled pellets were concentrated to a <0.5 mL suspension, which was transferred into 15 mL screw-cap Teflon vials for digestion in 1 mL of 16 N trace metal clean HNO_3 (Baseline, SeaStar Chemical) at 120 °C for 4 h on a hotplate. Digest solutions were then dried on a hotplate (60 °C) and redissolved in 1.2 N HCl (Baseline, SeaStar Chemical). All handling steps were carried out in a HEPA Class 100 clean bench. Once in 1.2 N HCl, the samples were processed and measured following the analytical protocol described below. In addition, samples of $CdCl_2$ powder, mixed-metal stock solution, and post-harvest media supernatant were retained for isotopic analysis to characterize thoroughly the isotopic composition of the source Cd.

3. Analytical procedures

The measurement of the Cd isotopic composition (Cd IC) in seawater and plankton cells requires its extraction from the sample matrix, with (i) a high yield (because of its low abundance), (ii) low contamination levels, (iii) no isotopic fractionation and (iv) a sufficient separation of the elements interfering with the Cd isotopes during the spectrometric analysis (mainly Pd, In and Sn, cf. Table 1 and Section 3.2.1. for further details).

3.1. Chemical separation

Whereas Cd extraction from seawater requires a preconcentration procedure due to its low abundance, this step is useless for plankton samples. Seawater samples were therefore processed through a Chelex and AGMP1 resins, as described below, whereas plankton samples were processed through the AGMP1 resin only.

3.1.1. Transition metals separation from seawater matrix

This protocol is adapted from Kingston et al. (1978). The pH of the acidified seawater samples was raised to ~5.5 by adding concentrated NH_4OH and buffering with maleic acid/ammonium hydroxide (pH 5.8. Pai et al., 1990). Two milliliters of Biorad® Chelex 100 resin (in 2 N HNO_3), 100–200 mesh, were packed in a Biorad® polyprep column (bed volume: 2 mL, conical, 0.8 cm mean internal diameter, 4 cm height; 10 mL reservoir). The resin was converted to its ammonia form with 6 mL of 2 N NH_4OH and rinsed with 6 mL of MQ water. The samples were pumped through the resin with a peristaltic pump at a flow rate less than 1 mL min^{-1} (acid cleaned Tygon® tubing was used). The major seawater cations were eluted with 30 mL of 1 N NH_4Ac at pH 5. After rinsing with 6 mL of MQ water, the transition metals were eluted with 9 mL of 2 N HNO_3. The eluates were then evaporated and redissolved in 1 mL of 1.2 N HCl for the next separation. The resin and tubing were cleaned with 20 mL of 2 N HNO_3 and rinsed for future use.

3.1.2. Cadmium separation

The following protocol is based on a personal communication by C. Cloquet (CRPG, Nancy, France). Two milliliters of Biorad® AGMP1 resin were packed in a Biorad® polyprep column. The resin was first cleaned following the sequence: 10 mL of 6 N HCl, 10 mL water, 10 mL of 0.5 N HNO_3, 10 mL water, 10 mL of 8 N HF + 2 N HCl, 10 mL water, 10 mL of 0.5 N HNO_3 and 10 mL water. The resin was then conditioned with 10 mL of 1.2 N HCl and the sample loaded in 1 mL of 1.2 N HCl. The elution was done following the sequence: 4 mL of 1.2 N HCl (elution of the matrix), 15 mL of 0.3 N HCl (elution of Pb, Sn), 17 mL of 0.012 N HCl (elution of Pb, Sn, Zn) and 16 mL of 0.0012 N HCl to elute the Cd. The Cd eluates were then evaporated and redissolved in 0.6 mL of 0.5 N HNO_3 for spectrometric analysis.

3.2. Spectrometric analysis

All results are reported as $\varepsilon^{i/j}_{Cd/amu}$ which is the deviation of the Cd isotope composition of a sample relative to a reference material in parts per 10,000, normalized to a mass difference of one atomic mass unit (amu):

$$\varepsilon^{i/j}_{Cd/amu} = \left(\frac{\left(\frac{^{i}Cd}{^{j}Cd}\right)_{Sample}}{\left(\frac{^{i}Cd}{^{j}Cd}\right)_{Reference}} - 1 \right) \times \frac{10,000}{m_i - m_j} \quad (1)$$

where i and j refer to the isotopes of mass m_i and m_j. The "/amu" notation facilitates the comparison of data obtained from different isotope ratios. Increasing values of $\varepsilon^{i/j}_{Cd/amu}$ reflect enrichment in heavy Cd isotopes, whatever i and j values are used. Rigorously, such comparison should take into account the mass fractionation law that describes the isotope fractionation process. However, considering the range of variation of our data set (<0.5‰ amu^{-1}), the discrepancies between this rigorous approach and the simple mass difference normalization used here are negligible (Wombacher and Rehkämper,

Table 1
Faraday cup configuration and isotopic abundances of Cd and of the elements that can produce isobaric interferences with Cd

Nominal mass		105	106	107	108	109	110	111	112	113	114	115	116	117
Isotope abundance (%)	Pd	22.3	27.3		26.5		11.7							
	Ag			51.8		48.2								
	Cd		1.2		0.89		12.5	12.8	24.1	12.2	28.7		7.49	
	In									4.3		95.7		
	Sn								0.97		0.65	0.36	14.5	7.68
Collector configuration				L_4	L_3	L_2	L_1	C	H_1		H_2		H_3	H_4

2004). The reference material used in this work is the JMC standard solution (Wombacher et al., 2003).

Cadmium isotopic ratios were measured on a Thermo-Finnigan Neptune multiple collector inductively coupled plasma mass spectrometer (MC-ICPMS, WHOI). The instrument parameters are summarized in Table 2. Samples were introduced with a desolvating nebulizer (CETAC Aridus System) to maximize the efficiency of sample introduction into the plasma and to reduce oxide formation and interferences.

Isotopic ratios measured with a MC-ICPMS must be corrected for (i) a relatively large, but steady, instrumental mass fractionation, (ii) spectral interferences and (iii) matrix effects (discussed in Section 3.3.).

3.2.1. Interference corrections

Tin (Sn), indium (In) and palladium (Pd) can produce isobaric interferences with Cd (Table 1). Therefore, the abundances of ^{117}Sn, ^{105}Pd and ^{115}In are measured in addition to Cd isotopes. The Faraday cup configuration is shown in Table 1. The method first measures the isotopic ratios of Cd and Ag (used for instrumental mass fractionation correction, see below) and ^{117}Sn. Subsequently, the magnetic field is shifted twice in order to successively and quickly measure ^{105}In and ^{115}Pd. In and Pd were always found at insignificant levels, so that these two steps were only systematic verifications of their non-occurrence. Significant levels of Sn were observed, however, which required correcting for this interference. Molecular interferences (e.g., molybdenum oxides and zinc argides) were found to be insignificant (cf. Section 3.3.).

Table 2
MC-ICPMS Cd operation parameters

ThermoFinnigan Neptune at the Woods Hole Oceanographic Institution	
Standard conditions for Cd analysis	
RF power	1200 W
Acceleration voltage	10 kV
Mass analyzer pressure	5×10^{-9} mbar
Nebulizer	ESI PFA 50[a]
Spray chamber	ESI SIS (Stable Introduction System)[a]
Sample uptake rate	~60 μL/min
Extraction lens	−2000 V
Typical signal intensity	~2.3 nA/ppmCd[b]
Transmission efficiency	~0.04%
Mass Discrimination	~1.4% per amu
Desolvating Sample Introduction System (Cetac® Aridus)	
Nebulizer	ESI PFA 50[a]
Spray chamber	ESI PFA Teflon upgrade[a]
Spray chamber temperature	100 °C
Desolvating membrane temperature	70 °C
Sample uptake rate	~60 μL/min
Argon sweep gas flow	~6 L/min (optimized for max. signal)
Nitrogen additional gas	~10 mL/min (optimized for sensitivity)

[a] ESI, Elemental Scientific Inc., Omaha, NB, USA.
[b] Based on 0.6 volt ^{110}Cd per 20 ppb total Cd; 10^{11} Ω resistor.

Tin produces interferences on ^{112}Cd, ^{114}Cd and ^{116}Cd. To a first approximation, one could estimate the ^{112}Sn, ^{114}Sn and ^{116}Sn abundances from the measured ^{117}Sn peak intensity and the mean natural isotopic abundance for Sn. With MC-ICP-MS, however, instrumental fractionation of isotopes during measurements is substantial (up to 100's epsilon units) and much larger than the small natural fractionation that we are trying to measure (a few epsilon units). In order to estimate accurately the Sn isobaric interferences, we thus need to correct for Sn instrumental mass fractionation. Mass fractionation is traditionally modeled by linear, power or exponential laws (Russel et al., 1978). Marechal et al. (1999) suggested that the exponential law provide a more consistent correction than the linear and the power laws. Wombacher et al. (2003) also preferred the exponential law for describing Cd fractionation by MC-ICPMS. We will show in Section 3.2.2. that the exponential law was also the most suitable for Cd fractionation corrections. This law is therefore used here for Sn interference corrections.

Let M_{iX} and M_{jX} be the masses of ^{i}X and ^{j}X, two isotopes of the same element, with $\Delta M_{i,jX} = M_{jX} - M_{iX}$. Let $R_{i,jX}$ and $r_{i,jX}$ be the true and instrumentally fractionated abundance ratios of isotope ^{j}X relative to isotope ^{i}X. In the absence of interferences, $r_{i,jX}$ is the parameter measured with the spectrometer: $r_{i,jX} = I_{jX}/I_{iX}$, where I_α is the beam intensity produced by isotope α (note that in the presence of interferences, I_α is not directly measured and therefore neither is $r_{i,jX}$). The exponential law postulates that the logarithmic fractionation $\ln(r_{i,jX}/R_{i,jX})$ is, to the first order, proportional to the mass logarithm difference $\Delta \ln M_{i,jX} = \ln M_{jX} - \ln M_{iX}$ (Marechal et al., 1999):

$$\ln\left(\frac{r_{i,jX}}{R_{i,jX}}\right) \approx f \times \Delta \ln M_{i,jX} \tag{2}$$

where f is the mass independent exponential law mass fractionation coefficient. Eq. (2) is equivalent to:

$$r_{i,jX} \approx R_{i,jX}\left(\frac{M_{jX}}{M_{iX}}\right)^{f} \tag{3}$$

Given ^{k}X and ^{l}X two other isotopes of the same element, (2) implies:

$$\ln(r_{k,lX}) \approx \frac{\Delta \ln M_{k,lX}}{\Delta \ln M_{i,jX}} \times \ln(r_{i,jX}) - \frac{\Delta \ln M_{k,lX}}{\Delta \ln M_{i,jX}} \times \ln(R_{i,jX}) + \ln(R_{k,lX}) \tag{4}$$

Eq. (4) is equivalent to:

$$R_{k,lX} \approx r_{k,lX} \times \left(\frac{R_{i,jX}}{r_{i,jX}}\right)^{\left(\ln\frac{M_{lX}}{M_{kX}}/\ln\frac{M_{jX}}{M_{iX}}\right)} \tag{5}$$

If we were to measure the ratio of two Sn isotopes free of significant interferences (e.g., ^{117}Sn and ^{118}Sn) and compare the results to an accepted "mean" natural abundance (Rosman and Taylor, 1998), the difference would mainly reflect

the relatively larger instrumental fractionation, albeit with a small, variable and unknown contribution from natural fractionation in the samples. Applying Eq. (2) using measured (r) and accepted (R) ratios would thus provide a good approximation for f:

$$f = \ln\left(\frac{r_{117,118Sn}}{R_{117,118Sn}}\right) \times \frac{1}{\ln(M_{118Sn}) - \ln(M_{117Sn})} \quad (6)$$

This value could then be used to estimate Sn contributions to the measured beam intensity for masses 112, 114 and 116, according to Eq. (3), e.g., for ^{112}Sn :

$$I_{112Sn} = I_{117Sn} \times R_{117,112Sn} \times \left(\frac{M_{112Sn}}{M_{117Sn}}\right)^{f} \quad (7)$$

Note that I_{112Sn} is defined as the beam intensity produced by ^{112}Sn, which is different from the beam intensity measured for mass 112, I_{112}, which includes contributions from different isotopes to the beam (here Sn and Cd). On the other hand, since no significant interference occurs for ^{117}Sn, I_{117Sn} is equal to I_{117}.

These interferences ($I_{112Sn}, I_{114Sn}, I_{116Sn}$) could then be corrected, by subtracting the Sn contributions from the beam intensities measured for masses 112, 114 and 116 (which are the sum of Cd and Sn contributions), e.g., for ^{112}Sn:

$$I_{112Cd} = I_{112} - I_{112Sn} \quad (8)$$

However, the collector configuration that we chose did not allow direct estimation of Sn mass fractionation, as doing so would have required longer analyses and therefore larger samples. Instead, we estimated f using two Cd isotopes free of isobaric interference (^{110}Cd and ^{111}Cd) and assumed that f calculated for Cd holds for Sn (as previously done by Wombacher et al., 2003). There is some level of circularity in this procedure, since our ultimate goal is to measure small natural variations in Cd isotopic composition and here we assume that there is no natural Cd isotopic fractionation. However, the latter (a few epsilon units) is approximately two orders of magnitude smaller than the instrumental fractionation (up to 100's epsilons units). Therefore the error on the Sn mass fractionation estimation is only on the order of a few percent. Since ^{112}Sn and ^{114}Sn interferences were always lower than 1% and 0.5% of the Cd signals, respectively, the method yielded small errors on the interference corrections and provided meaningful Cd isotopic ratios (although, this procedure was less suitable for ^{116}Cd, due to the much larger ^{116}Sn contribution on mass 116). This was further verified by estimating f using two Ag isotopes (^{107}Ag and ^{109}Ag), which yielded similar results.

The validity of the Sn interference correction was assessed following the method proposed by Wombacher et al. (2003). Cadmium isotopic ratios corrected for Sn interferences were normalized using the exponential law to a "true" Cd ratio. Such normalization should (if Cd obeys this fractionation law) remove simultaneously the instrumental and natural fractionations. Thus, if the interferences were accurately corrected, all samples should display the same Cd isotopic ratios. Results of this test are shown in Fig. 3. Whereas the uncorrected $\varepsilon^{114/111}_{Cd/amu}$ data display significant anomalies (up to 3.7 units), the Sn interference corrected anomalies are restricted to the range $[-0.3, +0.5]$. In the case of ^{112}Cd, the Sn uncorrected $\varepsilon^{112/111}_{Cd/amu}$ display anomalies up to 19 units, which are restricted to the range $[-0.5, +0.7]$ after correction. In the case of ^{116}Cd (results not shown for clarity purposes), the Sn uncorrected $\varepsilon^{116/111}_{Cd/amu}$ display anomalies up to 179 units, which are restricted to the range $[-0.5, +0.9]$ after correction. These results show that Sn interference corrections are adequate (reducing the interferences by a factor larger than 300, in some cases). However, for isotopes with larger interferences (notably ^{116}Cd) Sn interference corrections can sometimes be too uncertain to produce useful Cd isotopic data.

3.2.2. Instrumental mass fractionation

After correcting for isobaric interferences, the Cd instrumental mass fractionation must be considered. Several methods are available to estimate instrumental mass fractionation. The standard bracketing method consists in bracketing each sample by reference standard measurements. The average isotopic ratio from each two bracketing standard measurements is then taken as the reference ratio to calculate epsilon of the sample as per Eq. (1). However this method assumes a linear variation of the instrumental mass fractionation with time between standard measurements, which is not always the case, as shown by the sharp variation of the unnormalized data in Fig. 4.

A better approach consists in using the isotopic composition of a standard of a different element, in our case silver (Ag), added to the sample prior to the spectrometric analysis, to estimate instrumental mass fractionation. The main advantage of this method lies in the fact that the instrumental mass fractionation is monitored during the sample measurement. This method, called internal inter-element normalization, assumes that the Cd and Ag isotope fractionations are related according to a known law. The exponential law, described above in the case of a single element, was shown to be appropriate for this purpose in several studies (e.g., Marechal et al., 1999; Wombacher et al., 2003). The correction was performed using Eq. (5), in which a pair of silver isotopes is substituted for a pair of Cd isotopes. The exponential normalization to Ag considerably reduced the dispersion of the standard $\varepsilon^{114/111}_{Cd/amu}$ values (which should all be equal to zero), the largest deviation from the mean being of 0.8 $\varepsilon_{Cd/amu}$ unit (Fig. 4). This results indicates that the logarithm of the measured ratio of two Cd isotopes ($\ln(r_{k,lCd})$) must be a linear function of the logarithm of the measured ratio of two Ag isotopes ($\ln(r_{i,jAg})$), with a proportionality factor equal to $\frac{\Delta \ln M_{k,lCd}}{\Delta \ln M_{i,jAg}}$ (Eq. (4)). In other words, the data plotted in Fig. 5 should lie on a line with a slope of $\frac{\ln(M_{110\ Cd}/M_{114Cd})}{\ln(M_{107\ Ag}/M_{109Ag})} = 1.9292$. When

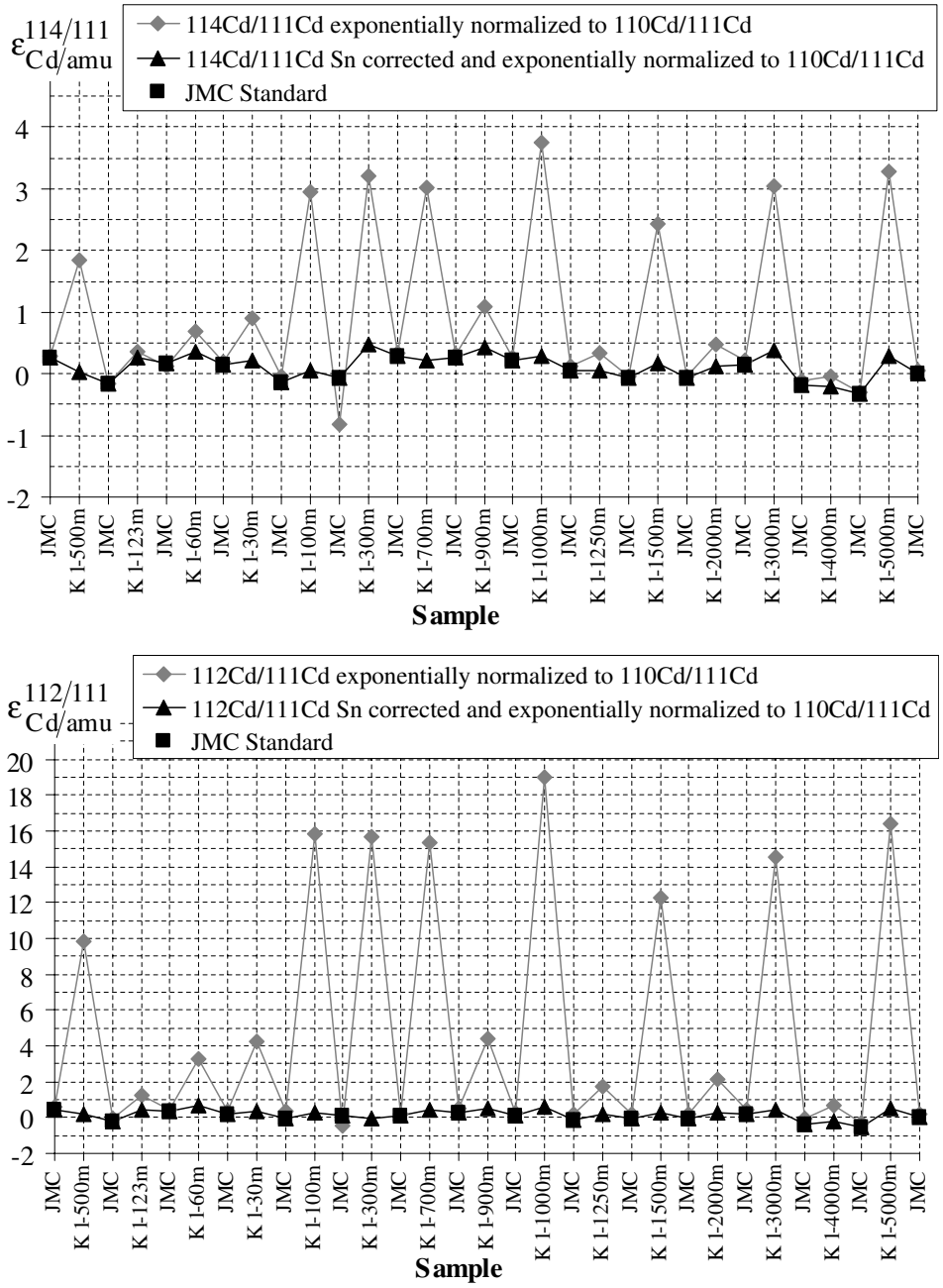

Fig. 3. Tin interference corrected and uncorrected data during one measurement session. The $\varepsilon_{Cd/amu}$ values are calculated relative to the mean JMC standard Cd ratios.

looking at the whole dataset, this slope is found to be 1.9295 ± 0.02 (1σ), in good agreement with the theoretical value. This agreement was found to be equally good for other Cd ratios (not shown here).

However, Fig. 5 also shows that the slope of the linear regression significantly varies between the different measurement sessions. Therefore, a variant of the exponential normalization method, which uses the measured correlation between the Cd and Ag fractionation, can be used. This method, called the empirical normalization (described by Marechal et al., 1999), consists in using the slope measured during a specific measurement session as shown in Fig. 5 instead of that predicted by the exponential law, following Eq. (9).

$$R_{k,l_{Cd}} \approx r_{k,l_{Cd}} \times \left(\frac{R_{i,j_{Ag}}}{r_{i,j_{Ag}}}\right)^{s} \tag{9}$$

where s is the measured slope of the linear regression of $\ln(r_{k,l_{Cd}})$ versus $\ln(r_{i,j_{Ag}})$.

The results of the corrections obtained with the empirical method are shown in Fig. 4. The standard $\varepsilon^{114/111}_{Cd/\ amu}$ values are all very close to 0, the largest deviation from the mean being of 0.2 $\varepsilon_{Cd/amu}$ unit. These results are slightly better than those obtained with the exponential normalization.

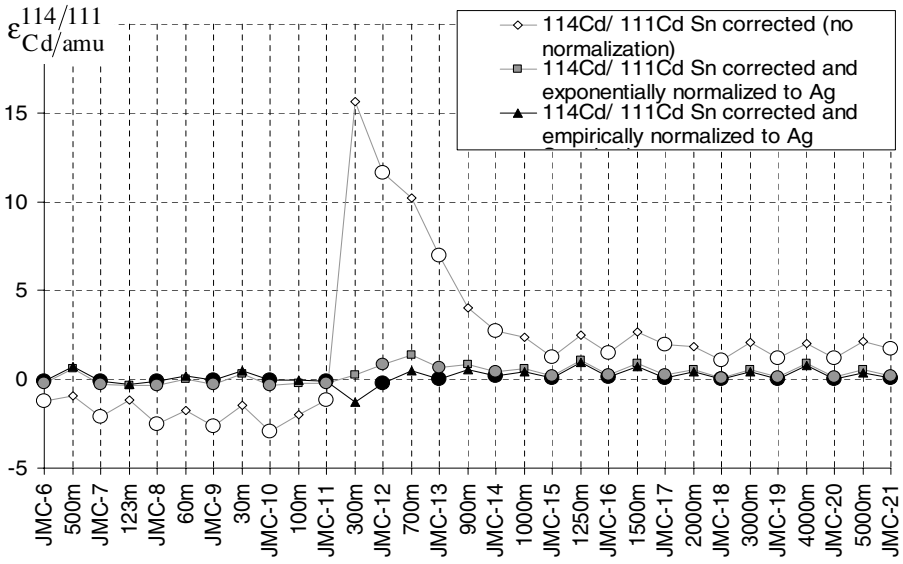

Fig. 4. Instrumental mass fractionation corrections. Standard samples are indicated by large circles. The $\varepsilon_{Cd/amu}$ values are calculated relative to the mean JMC standard Cd ratios.

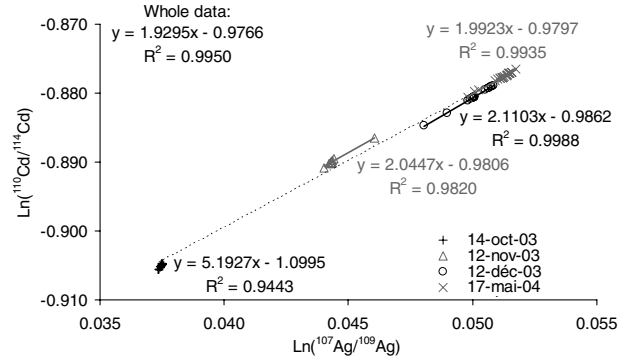

Fig. 5. Cadmium versus silver instrumental mass fractionation. Linear regressions for each measurement session, as well as for the whole data set are reported.

The empirical method was thus used to correct for instrumental fractionation in our samples.

For both the exponential and empirical method, the standard reference value used to calculate epsilon (Eq. (1)) can either be chosen as the average of the two standard measurements bracketing the sample, or as the average of the all standard measurements made within the measurement session. The latter option is used in this work, since it is more consistent with the normalization methods, which should theoretically lead to constant standard values; the variations observed reflecting the internal precision of the measurement.

3.3. Validation

3.3.1. Blanks

Total procedural blanks were estimated as follows: 250 mL of coastal seawater (Nantucket Sound, Mass. USA) were passed through three consecutive Chelex columns (following the procedure described above, Section 3.1.1.). Assuming a repetitive yield of ~93% (see below), this procedure should have removed 99.97% of the Cd initially present. This "Cd-free" seawater was then analyzed following the chemical procedure described above. This procedure simulates as accurately as possible the procedural blank, since the amount and matrix of the Cd-free samples used are similar to those of a real sample. The resulting Cd content was then measured by isotope dilution (by addition of a ^{108}Cd spike and measurement of the ^{108}Cd/^{111}Cd ratio, free of Sn interference) and found to be 0.6 10^{-12} mol $\pm$ 4% (1σ). This represents less than 1% of our smallest sample and ~0.5% on average. This blank was therefore neglected.

3.3.2. Yields

The yield of the total procedure was estimated by subdividing a coastal seawater sample (Nantucket Sound, Mass. USA) into three pairs of samples of 250, 400 and 1000 mL. One sample of each pair was spiked with ^{108}Cd. The samples were then run through the entire column separation procedure. The unspiked samples were spiked after column separation. The Cd content of each sample was determined by isotope dilution, thereby providing the Cd concentration before and after the chemical procedure. The total yield was found to be ~86% $\pm$ 1% and was independent of sample size. A similar technique was applied to the second AGMP1 column, only using a standard solution instead of a seawater sample to determine yield, found to be ~93%. The yield of the first Chelex column was thus estimated at ~93% (this yield could not be determined directly because the salt content of the Chelex column seawater eluate is still too high for direct ICPMS measurement).

3.3.3. Isotopic fractionation during column separation

Because the total yield of the chemical separation was lower than 100%, isotopic fractionation during column separation had to be assessed. This was done by addition of 10^{-7} g of the JMC Cd standard to 250 mL Cd-free seawater samples (prepared as described above), which were then analyzed following the normal procedure. The isotopic fractionation for the whole two-column method was found to be $\varepsilon^{110/114}_{Cd/amu} = -0.2 \pm 0.2$. The isotopic fractionation of the second AGMP1 column alone was measured separately by running a standard solution through the resin and was found to be $\varepsilon^{110/114}_{Cd/amu} = -0.3 \pm 0.2$. These results indicate that neither the Chelex nor the AGMP1 column fractionate significantly. The isotopic composition of the Cd-free seawater samples spiked with a realistic amount of Cd standard also shows that matrix effects are negligible.

3.3.4. Precision and accuracy

3.3.4.1. Internal precision. The internal precision (i.e. counting statistics) of the measurements, expressed as twice the standard error of the mean ($2\sigma_n$) were 0.4, 0.3 and 0.2 $\varepsilon_{Cd/amu}$ unit on average for the $^{110}Cd/^{111}Cd$, $^{112}Cd/^{111}Cd$ and $^{114}Cd/^{111}Cd$ ratios respectively (with maximum values of 0.9, 0.6 and 0.3 $\varepsilon_{Cd/amu}$ unit respectively, for the smallest sample).

3.3.4.2. External precision and reproducibility. The external precisions were estimated from the measurement of 30 JMC standard and found to be: 1.2 $\varepsilon_{Cd/amu}$ units (2σ) for the $^{110}Cd/^{111}Cd$ ratio by standard bracketing; 0.2, 0.1 and 0.4 $\varepsilon_{Cd/amu}$ unit (2σ) for the $^{110}Cd/^{111}Cd$, $^{112}Cd/^{111}Cd$ and $^{114}Cd/^{111}Cd$ ratios respectively by exponential normalization; 0.1, 0.1 and 0.2 $\varepsilon_{Cd/amu}$ unit (2σ) for the $^{110}Cd/^{111}Cd$, $^{112}Cd/^{111}Cd$ and $^{114}Cd/^{111}Cd$ ratios respectively by empirical normalization. These results confirm the good performances of the exponential and especially empirical normalizations. However, standard reproducibility does not account for variabilities due to matrix effects or interferences. Therefore, seven seawater duplicates from the North Pacific (Fig. 6a) were also measured and yielded a mean reproducibility of: 0.8 $\varepsilon_{Cd/amu}$ unit (empirical normalization), with a maximum discrepancy of 1.5 $\varepsilon_{Cd/amu}$ units (for $^{110}Cd/^{111}Cd$, $^{112}Cd/^{111}Cd$ and $^{114}Cd/^{111}Cd$ ratios). This reproducibility (0.8 $\varepsilon_{Cd/amu}$ unit) is the best assessment of the measurement precision, as it includes variations due to sample processing.

3.3.4.3. Accuracy. The fractionated "Münster" standard (Wombacher and Rehkämper, 2004), was measured three times and found to have an isotopic composition of $\varepsilon^{110/111}_{Cd/amu} = +11.1 \pm 0.5$ and $\varepsilon^{114/111}_{Cd/amu} = +11.3 \pm 0.5$. These results are identical to the only other reported measurement (Wombacher and Rehkämper, 2004; measured by C. Cloquet in Nancy, +45 $\varepsilon^{114/110}Cd$.)

3.3.4.4. Inter-isotope consistency. In the case of the North Pacific station, different isotope ratios measured concurrently on seawater samples give results that are identical

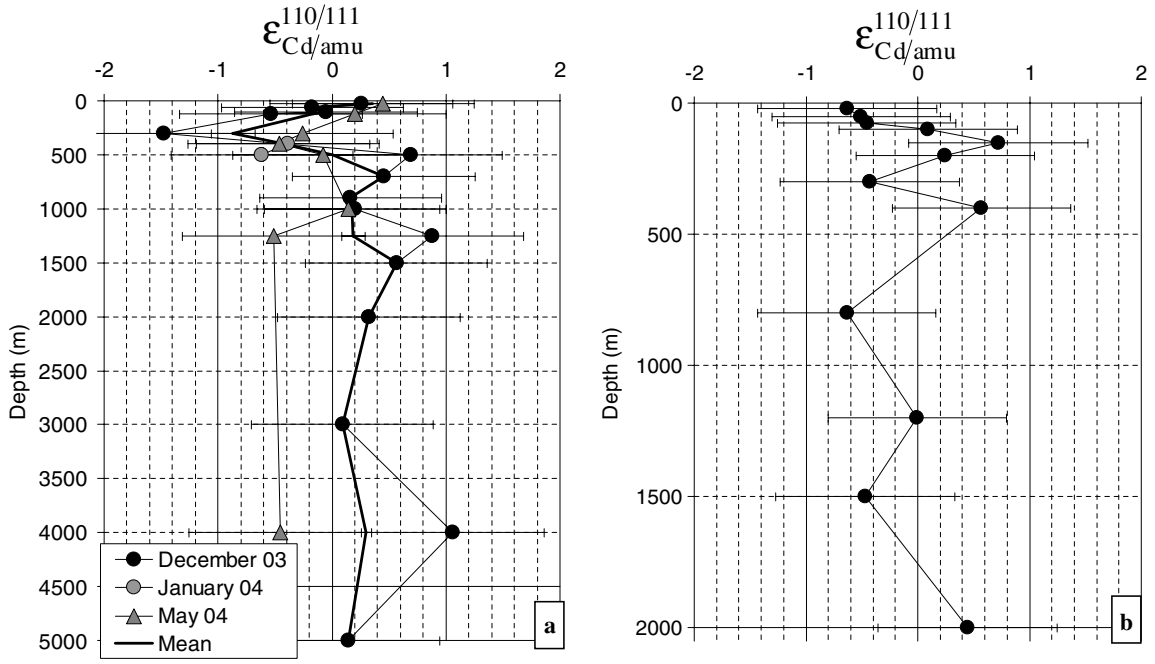

Fig. 6. Cd isotopic composition profiles at station K1 (N.W. Pacific, a) and DYFAMED (N.W. Mediterranean Sea, b). Error bars represent the mean discrepancy between replicates (0.8 $\varepsilon_{Cd/amu}$ unit). (Left) The different data series correspond to different measurement sessions (the mean profile is also displayed). Comparisons of these replicates allowed the determination of the reproducibility of the Cd IC measurement. The mean discrepancy between the duplicates is 0.8 $\varepsilon_{Cd/amu}$ unit, with a maximum discrepancy of 1.5 $\varepsilon_{Cd/amu}$ units (1250 m depth). Note that, because of the "/amu" notation, increasing values of $\varepsilon^{110/111}_{Cd/amu}$ reflect enrichment in heavy Cd isotopes.

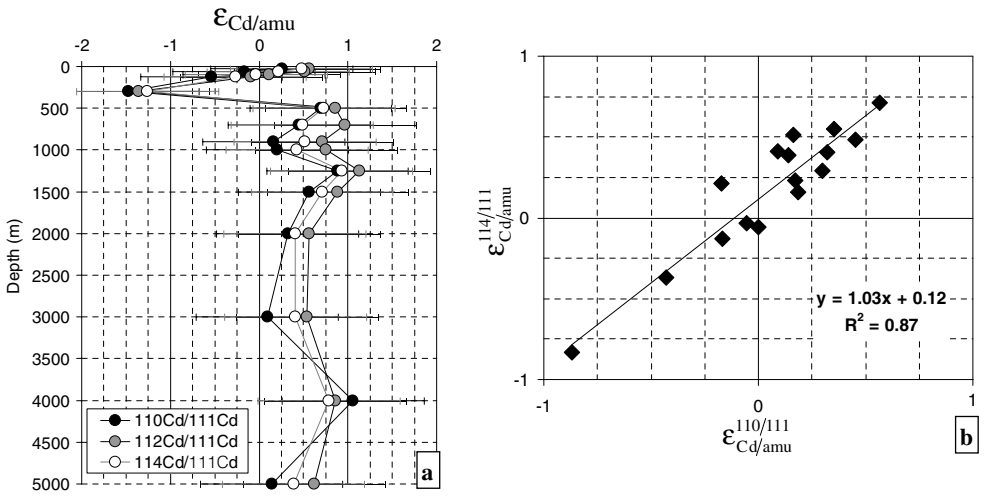

Fig. 7. Comparison of the isotopic compositions derived from different Cd isotope ratios at station K1 (N.W. Pacific). All isotopes were measured simultaneously. Error bars represent the mean discrepancy between replicates (0.8 $\varepsilon_{Cd/amu}$ unit). Note that the data from station DYFAMED (not shown for clarity purpose) do not show such inter isotope consistencies (because of unsatisfactory Sn interference corrections).

within measurement error (Fig. 7). The linear relationship between $\varepsilon^{110/111}_{Cd/amu}$ and $\varepsilon^{114/111}_{Cd/amu}$ (Fig. 7b) indicates that Cd isotope fractionation is mass dependant, which validates the analytical and measurement protocol. A similar linear relationship (although not as good, $R^2 = 0.79$, not shown here for clarity purposes) is found between $\varepsilon^{110/111}_{Cd/\ amu}$ and $\varepsilon^{112/111}_{Cd/amu}$, but not between $\varepsilon^{110/111}_{Cd/amu}$ and $\varepsilon^{116/111}_{Cd/amu}$. This shows that, in the case of the North Pacific samples, Sn interferences on ^{114}Cd and ^{112}Cd are satisfactorily corrected (with better corrections for ^{114}Cd) but interference on ^{116}Cd is not. These results validate the ^{110}Cd/^{111}Cd, ^{112}Cd/^{111}Cd and ^{114}Cd/^{111}Cd data, at the North Pacific station. The ^{114}Cd/^{111}Cd ratio is preferred to the ^{112}Cd/^{111}Cd ratio at this station, given the better interference correction on ^{114}Cd than on ^{112}Cd. Such a linear relationship is not found at the DYFAMED station (neither for ^{112}Cd, nor for ^{114}Cd, nor for ^{116}Cd). This suggests that Sn interferences are unsatisfactorily corrected for all Cd isotopes, which very likely results from the lower Cd content of these samples (6 to 8.5 ng, compared to 12–25 ng for the North Pacific samples), resulting in significantly higher Sn interferences at DYFAMED than at the North Pacific station. The ^{112}Cd, ^{114}Cd and ^{116}Cd data from this station are thus very likely incorrect. On the other hand, owing to the fact that the ^{110}Cd/^{111}Cd ratio is free of interference and that all the other aspects of the protocol are validated, this single ratio allows determination of the Cd IC at this site.

3.4. Measurement of Cd concentrations

To determine Cd concentrations in the seawater samples, 3 mL of unfiltered seawater was spiked with ^{108}Cd, evaporated, loaded onto the AGMP1 column and eluted following the protocol described above (Section 3.1.2.). The Cd concentrations were then determined by isotopic dilution on a ThermoFinnigan Element II inductively coupled plasma mass spectrometer (ICPMS, WHOI). The total procedural blank was $\sim 23 \pm 3$ pg (1σ). Blank variability sets the detection limit to 9 pg (defined as three times the blank standard deviation), which is less than a third of the Cd content of the most depleted sample. Duplicate analyses of seawater samples yielded an external reproducibility of 2% (2σ), equivalent to the internal precision of $\sim$1.5% ($2\sigma_n$). The concentrations measured in the northwest Pacific and in the Mediterranean Sea were in very good agreement with Cd profiles measured earlier in neighboring areas (Bruland, 1980; Laumond et al., 1984).

4. Results and discussion

4.1. Seawater Cd isotopic data

$\varepsilon^{110/111}_{Cd/amu}$ profiles at station K1 and DYFAMED (Fig. 6) vary between -0.8 and $+0.7$ (similar values are found for the other ratios at K1). This range is more than one order of magnitude smaller than the variability found for light elements such as C, N and Si. It is similar to those reported in the single study published so far about Cu and Zn isotopes in seawater (northeast Pacific), $\sim$0.15‰ and $\sim$0.25‰ for δ^{66}Zn and δ^{65}Cu per atomic mass unit, respectively (Bermin et al., 2006). Apparent enrichment of the light isotopes of both Cd and Zn in biogenic particulate matter suggests qualitatively similar biochemical control and is consistent with the close association of these metals in living organisms, while the opposite fractionation for Cu suggests removal dominated by non-physiological scavenging processes. Although the measured Cd isotopic variability is barely larger than the mean uncertainty of measurement (0.8 $\varepsilon_{Cd/amu}$), there are hints of oceanographically consistent features in the seawater profiles, which can be tentatively interpreted.

4.1.1. Upper 300 m of the northwest Pacific station

The progressive $\varepsilon_{Cd/amu}$ decrease from the surface to 300 m depth at station K1 is associated with a Cd concentration increase (Fig. 2), suggesting that the Cd isotopic ratios in the upper water column may be controlled by Rayleigh fractionation, driven by preferential uptake and removal of isotopically light Cd by phytoplankton:

$$(\varepsilon_{Cd/amu})^{f}_{SW} = (\varepsilon_{Cd/amu})^{f=1}_{SW} - \alpha \ln(f) \quad (10)$$

$$(\varepsilon_{Cd/amu})^{f}_{I-Pkt} = (\varepsilon_{Cd/amu})^{f}_{SW} - \alpha \quad (11)$$

$$(\varepsilon_{Cd/amu})^{f}_{A-Pkt} = (\varepsilon_{Cd/amu})^{f=1}_{SW} + \alpha \frac{f \times \ln(f)}{1-f} \quad (12)$$

where f is the fraction of dissolved Cd remaining in solution and α is the fractionation factor per amu. The term $(\varepsilon_{Cd/amu})^{f}_{X}$ is the $\varepsilon_{Cd/amu}$ value of media X for a given value of f. The subscripts SW, I-Pkt and A-Pkt subscript refer to seawater, instantaneous (I) and accumulated (A) phytoplankton products, respectively.

Rearranging Eq. (10) indicates that, in the case of Rayleigh distillation, there should be a linear relationship between the logarithm of the Cd concentration in seawater ($[Cd]^{f}_{SW}$) and its isotopic ratios, with the slope of the relationship equal to $-\alpha$:

$$(\varepsilon_{Cd/amu})^{f}_{SW} = (\varepsilon_{Cd/amu})^{f=1}_{SW} + \alpha \ln[Cd]^{f=1}_{SW} - \alpha \ln[Cd]^{f}_{SW} \quad (13)$$

The Cd depletion in K1 surface water (30 m depth) reaches ~56% relative to the subsurface Cd concentration maximum (300 m depth). Despite large uncertainties, we find a linear relationship between Cd IC and the logarithm of Cd concentration (Fig. 8). These results suggest that the Cd isotopic variation measured between the surface and 300 m depth may be due to Rayleigh distillation induced by phytoplankton uptake and sinking, following presumed Cd input events, for example through upwelling or winter mixing. The fractionation factor estimated from the linear regression of the data is $\alpha = 1.6 \pm 1.4$ $\varepsilon_{Cd/amu}$ units for $\varepsilon^{110/111}_{Cd/amu}$ and $\alpha = 1.5 \pm 1.4$ for $\varepsilon^{114/111}_{Cd/amu}$, ignoring the 2% uncertainty of the concentration data, and taking a Cd IC uncertainty of 0.8 $\varepsilon_{Cd/amu}$ unit.

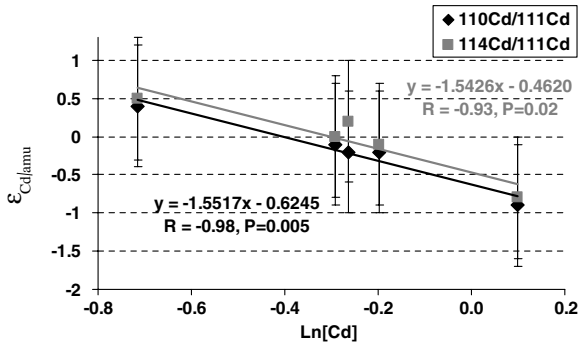

Fig. 8. Cd isotopic composition versus the logarithm of the Cd concentration (nmol/L) in the surface layer of station K1 (upper 300 m), for two Cd isotopic ratios ($^{110}Cd/^{111}Cd$ and $^{114}Cd/^{111}Cd$). Error bars correspond to 0.8 $\varepsilon_{Cd/amu}$ unit. Linear regressions are plotted. Their slopes (corresponding to the opposite of the Rayleigh fractionation factors, cf. Eq. (13)), correlation coefficients (R) and significance levels (P) are reported. Note: the lower $\varepsilon_{Cd/amu}$ values correspond to lighter Cd.

4.1.2. 300–700 m layer of the northwest Pacific station

Below the upper 300-m layer, there is a progressive $\varepsilon_{Cd/amu}$ increase from $\varepsilon^{110/111}_{Cd/amu} = -0.9 \pm 0.8$ (300 m depth) to $\varepsilon^{110/111}_{Cd/amu} = 0.5 \pm 0.8$ at 700 m depth. This increase is not associated with significant Cd concentration variations (cf. Fig. 2 and Table 3).

The potential temperature profile (Fig. 9) documents a maximum at ~300 m depth, corresponding to the mesothermal water (Uda, 1963), which originates from the area east of Japan (Ueno and Yasuda, 2000, 2003). Below this water mass, a well developed oxygen minimum and nitrate maximum, centered around 600 m (Fig. 9), clearly identifies the North Pacific Intermediate Water. A silicate maximum centered at 2000 m depth identifies the North Pacific Deep Water. The $\varepsilon_{Cd/amu}$ increase from 300 to 700 m depth could therefore reflect the mixing between the mesothermal water and the North Pacific Intermediate Water. In such a case, the product of $\varepsilon^{110/111}_{Cd/amu}$ and the Cd concentration should behave conservatively within this depth range. Fig. 10 displays this quantity versus salinity. Despite the large uncertainties of these data, their mean values are strongly linearly correlated between 300 and 700 m depth (correlation coefficient $R = 0.99$, significance level $P < 0.001$), which suggests that $\varepsilon^{110/111}_{Cd/amu} \times [Cd]$ behaves conservatively within this depth range (similar relationships, not shown here for clarity purpose, are found for $\varepsilon^{110/111}_{Cd/\ amu} \times [Cd]$ versus potential temperature and nitrate, phosphate and silicate concentrations, with ($R = -0.96$, $P = 0.04$), ($R = -0.99$, $P = 0.01$), ($R = -0.99$, $P = 0.01$), and ($R = 0.99$ and $P = 0.004$), respectively). Again, despite the large uncertainties of the Cd isotopic data, this observation suggests that the Cd isotopic composition variation observed between the core of the mesothermal water (300 m depth) and the core of the North Pacific Intermediate Water (700 m depth) is the result of water mass mixing.

Below this depth, no significant Cd isotopic composition variation is found; in particular, no distinctive signature is associated with the North Pacific Deep Water.

4.1.3. Northwest mediterranean station

The range of variation at this site (1.3 $\varepsilon_{Cd/amu}$ unit; Fig. 6b) is comparable to that found in the North Pacific. However, in contrast to the North Pacific, we could not find statistically significant relationships between the Cd IC and any of the following parameters: Cd concentration (which could have supported the hypothesis of a Rayleigh distillation), the conservative tracers (θ and S, which could have supported the hypothesis of a water mass mixing), the nutrient and dissolved oxygen concentrations.

The lack of measurable Cd isotopic fractionation due to Rayleigh distillation is not surprising considering the relatively small Cd depletion at the surface (~27% depletion relative to the subsurface maximum, located at 100 m

Table 3
Temperature, salinity, potential density, dissolved oxygen, nutrient and cadmium concentrations, and cadmium isotopic compositions of seawater samples from K1 (northwest Pacific) and DYFAMED (northwest Mediterranean—The nutrient concentrations at DYFAMED were measured on 10/07/2003, 2 weeks after the Cd sampling) stations

Sample	θ (°C)	S	σ_θ (kg/m^3)	O_2 (μmol/kg)	NO_3 (μmol/kg)	$Si(OH)_4$ (μmol/kg)	PO_4 (μmol/kg)	Cd (nmol/L)	$\varepsilon^{110/111}_{Cd/amu}$	$\varepsilon^{112/111}_{Cd/amu}$	$\varepsilon^{114/111}_{Cd/amu}$
K1 - 30 m[a]	8.04	32.88	25.60	293.33	15.0	28.7	1.35	0.489	0.4	0.7	0.5
K1 - 60 m	2.19	33.09	26.42	318.43	*22.0*	*37.3*	*1.81*	0.768	−0.2	0.5	0.2
K1 - 100 m	1.32	33.14	26.53	308.61	26.2	43.3	2.01	0.747	−0.1	0.1	0.0
K1 - 123 m[a]	1.50	33.28	26.63	264.70	29.9	53.8	2.24	0.821	−0.2	0.0	−0.1
K1 - 300 m[a]	3.49	34.02	27.06	27.07	44.4	107.8	3.13	1.105	−0.9	−0.8	−0.8
K1 - 400 m[a]	3.41	34.13	27.15	22.74	44.2	117.4	3.11	1.057	−0.4	−0.8	−0.4
K1 - 500 m[a]	3.25	34.22	27.24	20.97	44.0	124.8	3.10	1.038	0.0	−0.2	−0.1
K1 - 700 m	2.95	34.31	27.34	20.64	*43.9*	*137.0*	*3.09*	1.046	0.5	1.0	0.5
K1 - 900 m	2.65	34.39	27.43	23.58	*43.8*	*147.9*	*3.09*	1.037	0.2	0.7	0.5
K1 - 1000 m	2.51	34.43	27.47	24.98	43.8	153.2	3.09	1.038	0.2	0.5	0.2
K1 - 1250 m[a]	2.23	34.49	27.55	34.50	*43.1*	*158.9*	*3.03*	1.041	0.2	0.3	0.2
K1 - 1500 m	2.01	34.54	27.60	47.11	42.4	165.1	2.98	1.016	0.6	0.9	0.7
K1 - 2000 m	1.70	34.60	27.68	73.94	40.6	167.1	2.85	0.985	0.3	0.6	0.4
K1 - 3000 m	1.33	34.66	27.75	121.37	37.6	157.8	2.61	0.893	0.1	0.5	0.4
K1 - 4000 m[a]	1.15	34.68	27.78	144.30	36.2	150.5	2.48	0.879	0.3	0.5	0.3
K1 - 5000 m	1.09	34.69	27.79	152.28	35.6	150.3	2.44	0.831	0.1	0.6	0.4
DYF - 20 m	15.90	38.27	28.29	259.85	0.00	0.63	0.00	0.065	−0.6	—	—
DYF - 50 m	13.32	38.30	28.89	254.43	3.47	1.46	0.06	0.069	−0.5	—	—
DYF - 75 m	13.21	38.35	28.95	199.04	*6.34*	*2.75*	*0.23*	0.086	−0.5	—	—
DYF - 100 m	13.21	38.40	28.98	194.99	*7.13*	*3.34*	*0.29*	0.088	0.1	—	—
DYF - 150 m	13.35	38.49	29.03	179.63	7.65	4.11	0.33	0.084	0.7	—	—
DYF - 200 m	13.39	38.53	29.05	174.09	8.03	5.89	0.31	0.085	0.2	—	—
DYF - 300 m	13.44	38.58	29.08	164.96	8.99	6.75	0.33	0.084	−0.4	—	—
DYF - 400 m	13.38	38.58	29.09	165.98	8.99	7.73	0.38	0.081	0.6	—	—
DYF - 800 m	13.17	38.54	29.10	177.47	8.35	8.04	0.40	0.073	−0.6	—	—
DYF - 1200 m	12.97	38.49	29.10	183.38	*8.34*	*7.82*	*0.39*	0.072	0.0	—	—
DYF - 1500 m	12.87	38.46	29.10	187.63	5.54	4.91	0.24	0.075	−0.5	—	—
DYF - 2000 m	12.82	38.45	29.11	190.72	5.15	5.22	0.24	0.076	0.4	—	—

A few nutrient concentrations reported in italic are linear interpolation of nearby data.
[a] Samples for which replicate have been measured. In that case, the mean $\varepsilon_{Cd/amu}$ values are reported. Note that the DYFAMED $^{110}Cd/^{111}Cd$ data could not be validated by other Cd isotopic ratios (due to unsatisfactorily Sn interference corrections) and need therefore to be considered very cautiously.

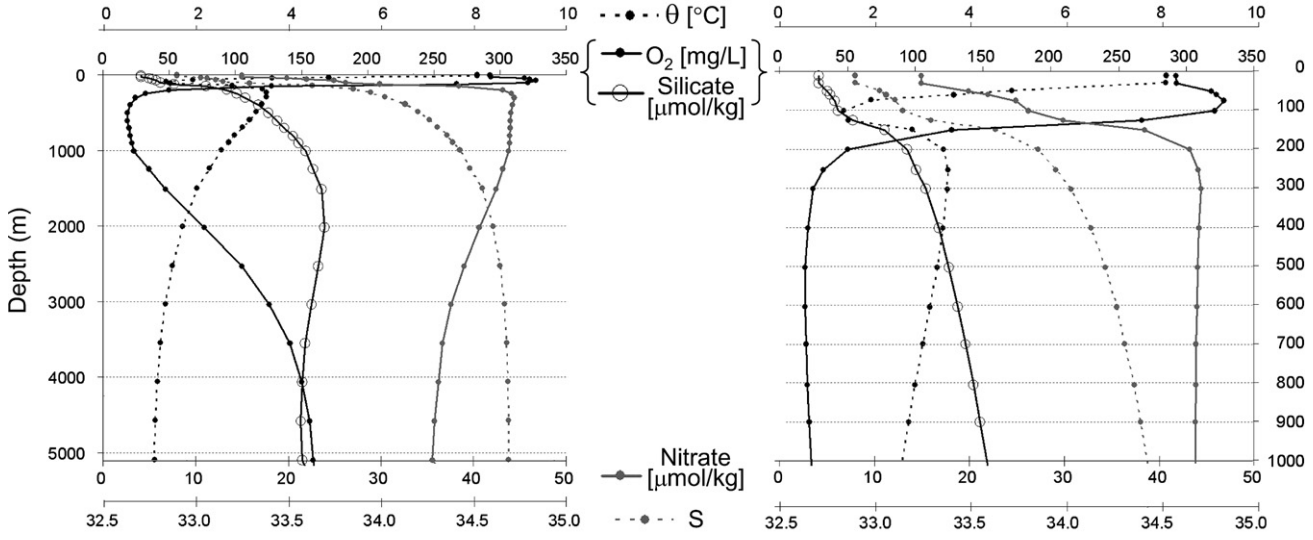

Fig. 9. Potential temperature, dissolved oxygen, nitrate and silicate concentrations and salinity at station K1. A detail of the upper 1000 m is displayed in the right.

depth, at the base of the seasonal thermocline). Using the fractionation factor calculated in the North Pacific surface waters ($\alpha = 1.6$), the DYFAMED surface depletion would result in a Cd IC increase of 0.5 $\varepsilon_{Cd/amu}$ unit ($-1.6 \times \ln(0.73) = 0.5$, cf. Eq. (10)), which is within measurement uncertainty.

There are three distinct water masses at the DYFAMED site: Modified Atlantic Water, Levantine Intermediate Water (θ and S local maximum around 300–400 m depth) originating from the Eastern Mediterranean Sea, and Western Mediterranean Deep Water ($\theta \approx 12.8$ °C and $S \approx 38.45$) (Millot, 1999). Between 400 and 2000 m depth, a linear relationship between θ and S ($R^2 = 0.99$, not shown, cf. Table 3) clearly indicates mixing between the Levantine Intermediate Water and Western Mediterranean Deep Water. Therefore, the DYFAMED water column is clearly composed of water masses from different origins that mix together. The lack of measurable Cd isotopic variation associated to this hydrographic setting therefore suggests that these three water masses have similar Cd IC (within the measurement uncertainty). This homogeneity could result from deep water formation processes in the Mediterranean Sea. This hypothesis is supported by Boyle et al. (1985), who suggested that comparable trace metal (including Cd) levels found in deep Mediterranean waters and in surface waters in regions of Mediterranean deep water formation imply a minimal role for trace metal transport by biological activity relative to deep water formation processes.

4.2. Culture experiment

Cadmium isotopic data from the phytoplankton culture experiment are reported in Table 4. Sn interference corrections (cf. Section 3.2.1) were too large for accurate measurements of ^{116}Cd and ^{112}Cd. Interference correction anomalies (as defined in Section 3.2.1.) for ^{114}Cd were lower than or equal to 1.1 $\varepsilon_{Cd/amu}$ unit. The ^{114}Cd/^{111}Cd ratio of the phytoplankton samples will thus be cautiously used in the following, in addition to the interference-free ^{110}Cd/^{111}Cd ratio. The ^{114}Cd/^{111}Cd and ^{110}Cd/^{111}Cd ratio data (Fig. 11) are in excellent agreement for the Cd powder, stock-solution and cultured-solution samples, for which the Sn interferences were low, and in fairly good agreement for the phytoplankton samples (subject to larger Sn interferences).

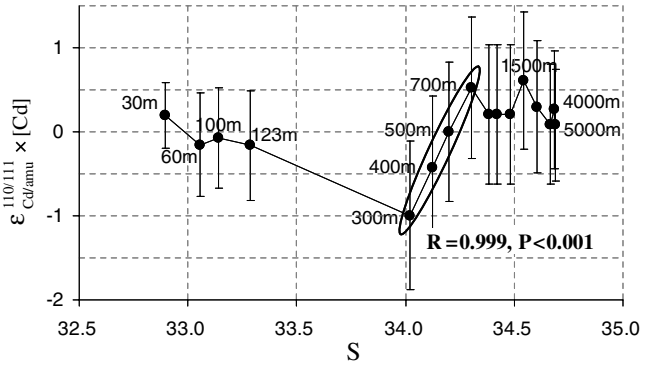

Fig. 10. Cd isotopic composition ($\varepsilon^{110/111}_{Cd/amu}$) times Cd concentration (nmol/L) versus salinity. The ellipse shows the linear relationship found between 300 and 700 m depth. The corresponding regression coefficient (R) and significance level (P) are indicated, as are some sampling depths. Errors bars are calculated by propagating the 0.8 $\varepsilon_{Cd/amu}$ unit uncertainty characterizing the Cd isotopic composition data (the 2% uncertainty of the concentration data are ignored).

Table 4
Cadmium isotopic composition of different phases involved in the phytoplankton culture experiment (cf. Fig. 11 caption for sample descriptions)

Sample	$\varepsilon^{110/111}_{Cd/amu}$	$\varepsilon^{112/111}_{Cd/amu}$	$\varepsilon^{114/111}_{Cd/amu}$
Cd powder	−2.5	−3.2	−3.1
Stock solution	−2.0	−2.3	−2.3
Cultured solution	−3.1	−2.7	−2.7
Chlamydomonas-1	−6.6	—	−5.7[a]
Chlamydomonas-2	−5.7	—	−4.7[a]
Chlorella-1	−5.2	—	−4.4[a]
Chlorella-2	−5.2	—	−3.8[a]

Some $\varepsilon^{112/111}_{Cd/amu}$ data are not reported due to unsatisfactory Sn interference correction on ^{112}Cd.

[a] These data need to be used cautiously because of imperfect Sn interference corrections (see text for more details).

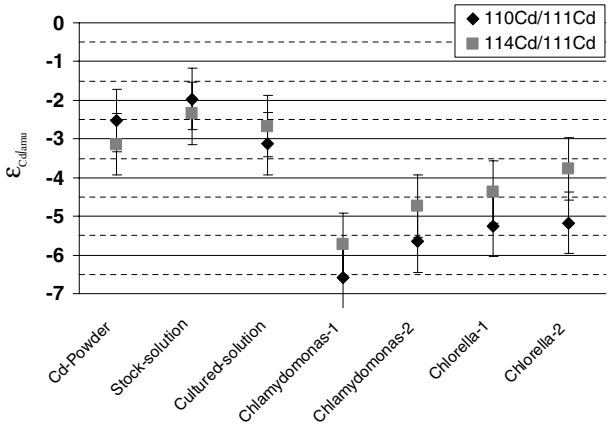

Fig. 11. Cadmium isotopic compositions (measured from ^{110}Cd/^{111}Cd and ^{114}Cd/^{111}Cd ratios) of different phases involved in the phytoplankton culture experiment. Cd powder: Cd used to make the Stock-solution; Stock-solution: initial solution used to grow the phytoplankton; Cultured-solution: growth media after culturing *Chlamydomonas* cells; Chlamydomonas 1 and 2: duplicate samples of *Chlamydomonas* cells; Chlorella 1 and 2: duplicate samples of *Chlorella* cells. Error bars correspond to 0.8 $\varepsilon_{Cd/amu}$ unit. Note: the lower $\varepsilon_{Cd/amu}$ values correspond to lighter Cd. Note also that ^{114}Cd/^{111}Cd ratios of the phytoplankton samples are imperfectly corrected for Sn interferences (see text for more details).

Since less than 1% of total Cd in the media was removed by phytoplankton uptake during the incubation, we assume that the Cd IC of the media did not change during phytoplankton growth. The initial Cd isotopic composition of the culture media before the growth experiment could therefore equally be determined from the Cd powder, stock solution or cultured solution samples (cf. Fig. 11). These three samples have similar Cd IC (cf. Fig. 11 and Table 4). However, the initial Cd isotopic composition of the culture media was determined as the mean value of the Cd powder and stock solution samples, because these samples are more concentrated than the cultured solution sample, and therefore provide a more reliable measurement:

$\varepsilon^{110/111}_{Cd/\ amu} = -2.3 \pm 0.8$ (2σ); $\varepsilon^{114/111}_{Cd/amu} = -2.7 \pm 1.1$. The phytoplankton samples have a mean value of $\varepsilon^{110/111}_{Cd/amu} = -5.7 \pm 1.2$ (2σ; $\varepsilon^{114/111}_{Cd/amu} = -4.7 \pm 1.5$). The significant difference between the initial Cd IC of the culture media and that of the phytoplankton suggest that the phytoplankton preferentially take up light Cd isotopes. Less than 1% Cd was taken up from the culture media by the cells. Neglecting this depletion, Eq. (11) (instantaneous product) yields a fractionation factor $\alpha = 3.4 \pm 1.4$ $\varepsilon_{Cd/amu}$ units (2σ, from the $^{110}Cd/^{111}Cd$ ratios; $\alpha = 2.0 \pm 1.9$ $\varepsilon_{Cd/amu}$ units from the $^{114}Cd/^{111}Cd$ ratios; using Eq. (12) with $f = 0.99$ gives the same results). These values are comparable (given the uncertainties) to those derived from the northwest Pacific seawater samples ($\alpha = 1.6 \pm 1.4$ $\varepsilon_{Cd/amu}$ units). The difference between the phytoplankton uptake fractionation factor and that derived from the water column distributions may be the result of a number of factors including non-representative phytoplankton species or growth rate, Cd scavenging in the water column by particle adsorption in addition to biological uptake, inappropriate assumptions in application of the Rayleigh fractionation model, or IC measurement uncertainty. Further research will be required to further constrain the processes leading to Cd isotope variations in the oceanic water column.

5. Summary and concluding remarks

The range of cadmium isotopic composition (Cd IC) in seawater from the northwest Pacific and the northwest Mediterranean is not greater than 1.5 $\varepsilon_{Cd/amu}$ units. It is only slightly larger than the mean uncertainty of measurement using the method described here (0.8 $\varepsilon_{Cd/amu}$) and more than one order of magnitude smaller than the variability found for light elements such as C, N and Si. On the other hand, it is very similar to those reported in the single study published so far about Cu and Zn isotopes in seawater (northeast Pacific. Bermin et al., 2006).

In the northwest Pacific station, despite error bars approaching the measured isotopic variability, we find systematic relationships between the Cd IC and Cd concentration in the upper 300 m, and between Cd IC and hydrographic data between 300 and 700 m. These results suggest that (i) the variation observed within the upper 300 m layer may be due to Cd isotopic fractionation by phytoplankton uptake, with a fractionation factor of 1.6 ± 1.4 $\varepsilon_{Cd/amu}$ units; (ii) the variation observed between 300 and 700 m depth, may be due to the mixing of the mesothermal water ($\varepsilon^{110/111}_{Cd/\ amu} = -0.9 \pm 0.8$) with the North Pacific Intermediate Water ($\varepsilon^{110/111}_{Cd/amu} = 0.5 \pm 0.8$).

On the other hand, at the DYFAMED site (Mediterranean), we cannot find similar correlations between Cd IC and Cd concentration nor between the Cd IC and hydrographic data. We suggest that this lack of systematic Cd IC variation is due to (i) insufficient surface Cd depletion by phytoplankton uptake in the surface waters and (ii) similar Cd IC of the different water masses found at this site, possibly linked to deep water formation processes.

Culture experiments suggest that freshwater phytoplankton (*Chlamydomonas reinhardtii* and *Chlorella*) preferentially take up light Cd isotopes, with a fractionation factor of 3.4 ± 1.4 $\varepsilon_{Cd/amu}$ units (similar fractionation is found for both species). This observation supports the conclusion based on the NW Pacific data that biological uptake of Cd by phytoplankton results in a small preferential uptake of the lighter Cd isotopes.

The North Pacific data suggest that different water masses may have different Cd IC, notably the mesothermal water with $\varepsilon^{110/111}_{Cd/amu} \sim -1$ compared to $\sim$0.3 for deeper waters. The present data set is insufficient to establish the origin of this signature but suggests that Cd isotopes could provide information on water mass trajectory and mixing in some areas of the ocean.

Future studies aimed at quantifying specific Cd isotopic fractionations associated with various aspects of biological uptake, adsorptive scavenging and remineralization of organic matter may provide new insight into these processes. Understanding controls on the mean Cd isotope composition of the ocean will require measurements of the mean river input Cd IC and of fractionations associated with ultimate Cd removal in organic-rich and reducing sediments. Investigations of Cd isotope distributions and mean IC in the past ocean, while technically difficult, may help to quantify past changes in the oceanic budget, internal cycling, and advective transport of this element, augmenting the current paleoceanographic utility of cadmium. The small variations in Cd isotopic composition found in this study indicate that applications of this parameter for studying the present or past Cd oceanic cycle will be challenging. This will likely require further analytical improvements. Better precision could likely be obtained with larger seawater samples, a better chemical separation of tin and a more accurate mass bias correction through the use of the double spiking technique.

Acknowledgments

We thank K. Bruland for his advice about chemical procedures. We acknowledge O. Rouxel and C. Cloquet for their help with the chromatography. We are grateful to L. Ball for his help with the MC-ICPMS. C. Jeandel is acknowledged for providing the Mediterranean seawater samples, and P. van Beek and M. Kienast for carrying out the sampling of the Pacific samples. We thank H. de Baar and two anonymous reviewers for very helpful comments that improved this manuscript.

Associate editor: David W. Lea

References

Abe, K., 2002. Preformed Cd and PO4 and the relationship between the two elements in the northwestern Pacific and the Okhotsk Sea. *Mar. Chem.* **79**, 27–36.

Bermin, J., Vance, D., Archer, C., Statham, P.J., 2006. The determination of the isotopic composition of Cu and Zn in seawater. *Chem. Geol.* **226** (3–4), 280–297.

Boyle, E.A., 1988. Cadmium: chemical tracer of deepwater paleoceanography. *Paleoceanography* **3**, 471–489.

Boyle, E.A., Chapnick, S.D., Bai, X.X., Spivack, A., Huested, S.S., 1985. Trace metal enrichments in the Mediterranean Sea. *Earth Planet. Sci. Lett.* **74**, 405–419.

Boyle, E.A., Sclater, F., Edmond, J.M., 1976. On the marine geochemistry of cadmium. *Nature* **263**, 42–44.

Bruland, K., 1980. Oceanographic distributions of cadmium, zinc, nickel, and copper in the North Pacific. *Earth Planet. Sci. Lett.* **47**, 176–198.

Bruland, K.W., Knauer, G.A., Martin, J.H., 1978. Cadmium in northeast Pacific waters. *Limnol. Oceanogr.* **23**, 618–625.

Cullen, J.T., 2006. On the nonlinear relationship between dissolved cadmium and phosphate in the modern global ocean: could chronic iron limitation of phytoplankton growth cause the kink? *Limnol. Oceanogr.* **51** (3), 1369–1380.

Cullen, J.T., Chase, Z., Coale, K.H., Fitzwater, S.E., Sherrell, R.M., 2003. Effect of iron limitation on the cadmium to phosphorus ratio of natural phytoplankton assemblages from the Southern Ocean. *Limnol. Oceanogr.* **48** (3), 1079–1087.

Cullen, J.T., Lane, T.W., Morel, F.M.M., Sherrell, R.M., 1999. Modulation of cadmium uptake in phytoplankton by seawater CO_2 concentration. *Nature* **402**, 165–167.

Elderfield, H., Rickaby, R.E.M., 2000. Oceanic Cd/P ratio and nutrient utilization in the glacial Southern Ocean. *Nature* **405**, 305–310.

Frew, R., Bowie, A., Croot, P., Pickmere, S., 2001. Macronutrient and trace-metal geochemistry of an in situ iron-induced Southern Ocean bloom. *Deep Sea Res. II* **48** (11–12), 2467.

Frew, R.D., Hunter, K.A., 1992. Influence of Southern Ocean waters on the Cd-phosphate properties of the global ocean. *Nature* **360**, 144–146.

Helmers, E., 1996. Trace metals insuspended particulate matter of Atlantic Ocean surface water (40°N to 20°S). *Mar. Chem.* **53**, 51–67.

Kingston, H.M., Barnes, I.L., Brady, T.J., Rains, T.C., 1978. Separation of eight transition elements from alkali and alkaline earth elements in estuarine and seawater with chelating resin and their determination by graphite furnace atomic adsorption spectrometry. *Anal. Chem.* **50**, 2064–2070.

Lane, T.W., Saito, M.A., George, G.N., Pickering, I.J., Prince, R.C., Morel, F.M.M., 2005. A cadmium enzyme from a marine diatom. *Nature* **435**, 42.

Laumond, F., Copin-Montegut, G., Courau, P., Nicolas, E., 1984. Cadmium, copper and lead in the Western Mediterranean Sea. *Mar. Chem.* **15**, 251–261.

Marechal, C.N., Telouk, P., Albarede, F., 1999. Precise analysis of copper and zinc isotopic compositions by plasma-source mass spectrometry. *Chem. Geol.* **156**, 251–273.

Martin, J.H., Gordon, R.M., Fitzwater, S., Broenkow, W.W., 1989. VERTEX: phytoplankton/iron studies in the Gulf of Alaska. *Deep Sea Res.* **36**, 649–680.

Millot, C., 1999. Circulation in the Western Mediterranean Sea. *J. Mar. Syst.* **20**, 432–442.

Morel, F.M.M., Reinfelder, J.R., Roberts, S.B., Chamberlain, C.P., Lee, J.G., Yee, D., 1994. Zinc and carbon co-limitation of marine phytoplankton. *Nature* **369**, 740–742.

Pai, S.C., Chen, T.C., Wong, G.T.F., Hung, C.C., 1990. Maleic acid/ammonium hydroxide buffer system for preconcentration of trace metals from seawater. *Anal. Chem.* **62** (7), 774–777.

Price, N.M., Morel, F.M.M., 1990. Cadmium and cobalt substitution for zinc in a marine diatom. *Nature* **344**, 658–660.

Riso, R.D., Le Corre, P., L'Helguen, S., Morin, P., 2004. On the presence of a cadmium-rich subsurface water mass in the western Mediterranean and its influence on the distribution of cadmium in the surface waters. *Mar. Chem.* **87** (1–2), 15–22.

Rosman, K.J.R., Taylor, P.D.P., 1998. Isotopic compositions of the elements 1997. *Pure Appl. Chem.* **70** (1), 217–235.

Russel, W.A., Papanastassiou, D.A., Tombrello, T.A., 1978. Ca isotope fractionation on the Earth and other solar system materials. *Geochim. Cosmochim. Acta* **42**, 1075–1090.

Sherrell, R.M, 1989. The trace metal geochemistry of suspended oceanic particulate matter. Ph.D. Thesis, MIT-WHOI (USA), 211 p.

Sunda, W.G., Huntsman, S.A., 2000. Effect of Zn, Mn, and Fe on Cd accumulation in phytoplankton: implications for oceanic Cd cycling. *Limnol. Oceanogr.* **45**, 1501–1516.

Uda, M., 1963. Oceanography of the subarctic Pacific Ocean. *J. Fish. Res. Board Can.* **20**, 119–179.

Ueno, H., Yasuda, I., 2000. Distribution and formation of the mesothermal structure (temperature inversions)in the North Pacific subarctic region. *J. Geophys. Res.* **105** (C7), 16885–16897.

Ueno, H., Yasuda, I., 2003. Intermediate water circulation in the North Pacific subarctic and northern subtropical regions. *J. Geophys. Res.* **108** (C11). doi:10.1029/2002JC00137.

van Geen, A., Boyle, E.A., Moore, W.S., 1991. Trace metal enrichments in the waters of the Gulf of Cadiz. *Geochim. Cosmochim. Acta* **55**, 2173–2191.

Wombacher, F., Rehkämper, M., 2004. Problems and suggestions concerning the notation of cadmium stable isotope compositions and the use of reference materials. *Geostand. Geoanal. Res.* **28** (1).

Wombacher, F., Rehkamper, M., Mezger, K., Munker, C., 2003. Stable isotope compositions of cadmium in geological materials and meteorites determined by multiple-collector ICPMS. *Geochim. Cosmochim. Acta* **67** (23), 4639–4654.

4. Lacan et Jeandel 2005. EPSL. Proposition du concept de Boundary Exchange.

Available online at www.sciencedirect.com

SCIENCE DIRECT®

Earth and Planetary Science Letters 232 (2005) 245–257

EPSL

www.elsevier.com/locate/epsl

Neodymium isotopes as a new tool for quantifying exchange fluxes at the continent–ocean interface

Francois Lacan*, Catherine Jeandel[1]

LEGOS, Observatoire Midi-Pyrénées, 14, Av. E. Belin, 31400 Toulouse, France

Received 27 September 2004; received in revised form 29 December 2004; accepted 4 January 2005
Available online 19 March 2005
Editor: E. Bard

Abstract

Continental margins are, via river sediment discharges, the major source of a number of elements to the ocean. They are also, for several reactive elements, sites of preferential removal from the water column, due to enhanced scavenging [1] [M.P. Bacon, Tracers of chemical scavenging in the ocean: Boundary effects and large-scale chemical fractionation, Philos. Trans. R. Soc. Lond., A 325 (1988) 147–160.]. They can therefore be understood as sources of elements for the ocean, sinks or both. Although exchanges of matter are suspected to occur at the continent/ocean interface [2] [P.H. Santschi, L. Guo, I.D. Walsh, M.S. Quigley, M. Baskaran, Boundary exchange and scavenging of radionuclides in continental margin waters of the Middle Atlantic Bight: implications for organic carbon fluxes, Cont. Shelf Res. 19 (1999) 609–636.] and despite their probable importance for the ocean chemistry, closed budgets have still yet to be determined. Here, based on neodymium isotopic composition data obtained during the past 6 yr, we document and quantify significant neodymium exchange at ocean boundaries, in areas covering a large spectra of hydrographical, biological and geochemical characteristics : Eastern Indian Ocean, Western Equatorial Pacific, Western Tropical Pacific and Northwestern Atlantic, with neodymium removal fluxes accounting for 74±23%, 100±38%, 62±54% and 84±45% of the neodymium input fluxes, respectively. Recognition of boundary exchange and its potential globalization have important implications for (1) our understanding of margin/ocean interactions and their influence on the oceanic isotopic chemistry, and (2) geochemical cycling of reactive elements (including pollutants) at ocean margins.

Keywords: boundary exchange; neodymium isotopic composition; continent ocean interactions; margins; water masses

1. Introduction

Continental margins occupy less than 20% of the surface area of the world ocean. However, they are regions of enhanced biological production and thus were estimated to be as important as the open ocean in

* Corresponding author. Now at Laboratoire des Sciences du Climat et de l'Environnement (LSCE), L'Orme des Merisiers, Bat. 712, 91191 Gif-sur-Yvette Cedex, France. Tel.: +33 1 69 08 39 73; fax: +33 1 69 08 77 16.
E-mail addresses: Francois.Lacan@cea.fr (F. Lacan), Catherine.Jeandel@cnes.fr (C. Jeandel).
[1] Tel.: +33 5 61 33 29 33; fax: +33 5 61 25 32 05.

0012-821X/$ - see front matter © 2005 Elsevier B.V. All rights reserved.
doi:10.1016/j.epsl.2005.01.004

the carbon and nitrogen cycles [3]. Whereas upwelling waters seem to provide 90% of the nitrate required to sustain primary production above the margins, river inputs are the main sources of silica and phosphate into the ocean [3–5]. In addition, the strong diffusive and advective fluxes characterizing these areas yield water mass exchanges between the shelve/slope and open ocean [6,7] as well as resuspension of sediments on continental shelves and export of resuspended sediments to deeper waters [8,9]. These processes may have two inverse effects: (1) river inputs being the source of most of the elements in the ocean (essentially the lithogenic and anthropogenic ones), water mass mixing and lateral transport of resuspended sediments may enhance the continent to ocean transfer of these elements, (2) on the opposite, the continent/ocean interface is often understood as a sink for a number of elements. Particle fluxes being much greater in ocean-margins than in the open ocean, they yield more efficient removal of the reactive elements from the water column in these areas. Depending on their residence time (i.e. their sensitivity to scavenging), some reactive elements remain under the dissolved form sufficiently long to be transported by lateral mixing from the center of a gyre to areas as continental margins, where strong particle fluxes will remove them actively towards the sediment. The combination of lateral mixing of ocean waters and lateral gradients in particle fluxes leading to enhanced deposition together with fractionation of particle-reactive substances is called boundary scavenging [1,8,10,11]).

Therefore, continental margins can be understood either as a source of elements for the ocean or as a sink, or both. Santschi et al. [2] showed that strong scavenging affects the whole water column of the Middle Atlantic Bight continental slope leading to the inshore transport of dissolved species, followed by their removal and the offshore transport of particulate species, including carbon. Simultaneously, their $^{228}Ra/^{226}Ra$ data suggest that exchanges affect the benthic boundary layer water mass composition.

Although exchanges of water, chemical species and matter are suspected to occur at the continent/ocean interface, and despite the importance of these processes for the biogeochemical cycles, closed budgets have still yet to be determined and quantifications of these processes are scarce. Estimation of long term particle and dissolved export rates on large scales by direct observations is difficult because of the episodic nature of the processes, the different nature/behavior of the already studied margins and the need of long time series of data [12]. Indirect approaches are possible by the use of tracers that allow following long term fate of particles and their bound substances. Such an approach was developed by Bacon et al. [12] using ^{210}Pb.

The neodymium isotopic composition (Nd IC) is expressed as ε_{Nd}, defined by:

$$\varepsilon_{Nd} = \left(\frac{\left(\frac{^{143}Nd}{^{144}Nd}\right)_{Sample}}{\left(\frac{^{143}Nd}{^{144}Nd}\right)_{CHUR}} - 1 \right) \times 10^4 \quad (1)$$

Where CHUR stands for Chondritic Uniform Reservoir and represents a present day average earth value; $(^{143}Nd/^{144}Nd)_{CHUR}=0.512638$ [13]. The Nd IC of the continents is heterogeneous, varying from −45 in old granitic cratons to +12 in recent mid oceanic ridge basalts [14]. Nd ICs of marine lithogenic particles are therefore used to follow their pathways [15,16]. In the ocean, Nd is a trace element (concentrations of the order of 10^{-12} g g^{-1}), predominantly found in the dissolved form (90–95% [17]). Its residence time is around 500 to 1000 yr [14]. The oceanic Nd IC distribution is heterogeneous, as shown on the compilation of 544 ε_{Nd} data (Fig. 1), varying from −25 in the extreme North West Atlantic to 0 in the North Pacific. On first order, this variation reflects the dominant imprint of the surrounding continent of each oceanic basin [18]. In the absence of lithogenic input, ε_{Nd} behaves conservatively in the ocean and since variations have been observed between the different water masses of the same water column, it is used as a water mass tracer [18–21]. On the other hand, in the presence of lithogenic inputs (aeolian, riverine or derived from the sediments), this tracer is no more conservative. The processes by which water masses acquire their Nd signatures remain unclear. Previous studies underlined the role of sediment/water mass interactions in this acquisition ([22–24] and references therein). Remobilization of Rare Earth Elements (REE) during early diagenesis has already been suggested as a potential source to the overlying seawater [25–29], but precise quantifications are still lacking. This work exploits a compilation of Nd IC data obtained at continent/ocean boundaries allowing (1) evidencing that significant dissolved/partic-

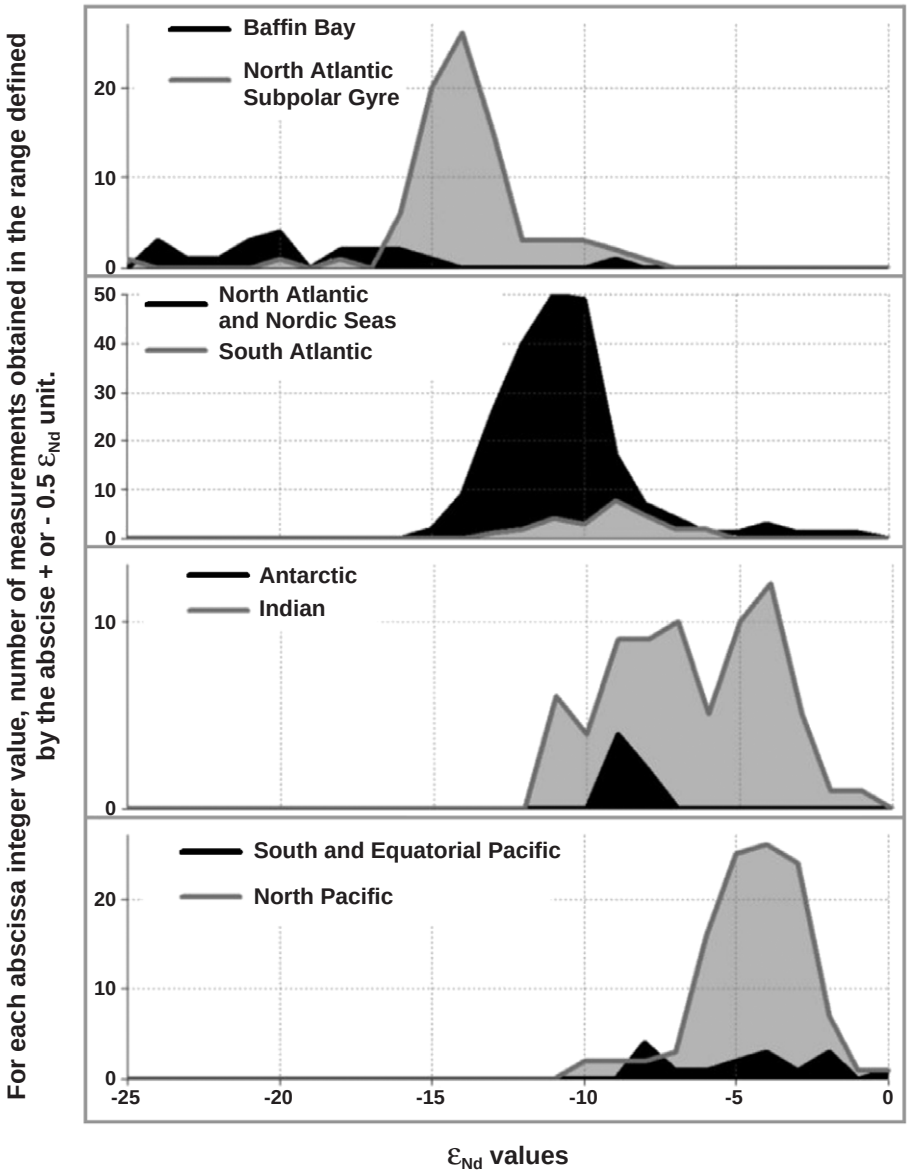

Fig. 1. Nd isotopic composition distribution among the different oceanic basins. All the data available in the literature are plotted (546 data of which 274 were added in comparison with the previous similar compilation, [18–21,24,30–32,34,37,47–50]; Tachikawa, 2003 #1622 and references therein). The abscissa scale was however restricted to values greater than −25 for clarity, as only two measurements were found lower than that value (in the Baffin Bay and the Labrador Basin [37,47]). Note that the "North Atlantic" curve excludes data from the North Atlantic Subpolar Gyre (which are plotted on the top panel). A progressive increase of ε_{Nd} values, from the Northwest Atlantic to the North Pacific, associated with the global thermohaline circulation, appears clearly.

ulate exchange occurs at the ocean boundaries and (2) quantifying this exchange. Two set of the data discussed here have been published in works using ε_{Nd} as a tracer of water mass origin and mixing, both restricted to intermediate waters along equatorial basaltic margins [20,21]. Data from a third work focused on water mass pathways in the North West Pacific are also used in the present article,

since they were never discussed in term of exchange at the margin [30]. Finally, a new set of data describing Nd IC modifications affecting the North West Atlantic Bottom Water along South Greenland is also presented and discussed. Comparison of these different data sets shows for the first time that exchange is occurring along granitic as well as basaltic margins, under different latitudes, depths, hydrodynamical forcings, erosion regimes and productivity conditions. These results have further reaching implications about (1) our understanding of margin/ocean interactions and their influence on the oceanic isotopic chemistry, and (2) geochemical cycling of reactive elements at ocean margins.

2. Analytical procedures

The analytical procedures corresponding to the published data used in this work can be found in [20,21,31–33]. Concerning the new data set, briefly, for Nd IC measurements: (1) 10 L seawater samples were preconcentrated on a C_{18} cartridge loaded with a REE complexant (HDEHP/H2MEHP); (2) REE were separated from the remaining seawater matrix by a cationic exchange chromatography; (3) Nd was separated from the other REE by anionic exchange chromatography. Samples were then measured by thermal ionization mass spectrometry (Thermo Finnigan MAT 261, at the Observatoire Midi Pyrénées, Toulouse, France; in static mode, Nd was analyzed as Nd+). The national Rennes Nd standard gave $^{143}Nd/^{144}Nd=0.511962\pm20$ (2σ, 160 runs), which corresponds to a La Jolla value of 0.511849 [33]. No corrections were applied to measured isotopic ratios. External reproducibility measured on seawater samples was ±0.4 ε_{Nd} unit. Blank values were ≤700 pg (3.5% of the most depleted sample and 2% on average, which allows neglecting them). Concerning the Nd concentration measurements, REE were extracted from 500 mL seawater samples by iron oxide co-precipitation. The iron was then removed by anionic exchange chromatography. Nd concentrations were determined by isotopic dilution on ICPMS (Perkin Elmer Elan 6000, in the same laboratory). Reproducibility of the Nd concentration measurements was better than 5%. Blanks values were lower than 3%. Internal precision (2σ) lower than 0.2 ppt (part per trillion, i.e. 10^{-12} g g^{-1}).

3. Results

Fig. 2 and Table 1 display Nd ICs and concentrations for 4 different water masses, upstream and downstream of a continental contact area. As discussed below these sites cover a significant range of hydrographical and biogeochemical properties.

3.1. Data compilation

The sampling sites are displayed in Fig. 2. The data reported in Table 1, in the "Initial, before mixing corrections" and "Final" columns, were compiled as follows: Concerning the North Indian Intermediate Water (NIIW), the upstream and downstream values correspond to one measurement and the average of four measurements, respectively. These samples were taken along the same isopycnal and display very close hydrographical properties ($S\approx34.7$, $\theta\approx8$ °C at depths ranging from 500 to 800 m along the Java margin, and by $S\approx34.8$, $\theta\approx8$ °C at depths ranging from 600 to 800 m in the South Somali Basin) [20,31]. Concerning the Antarctic Intermediate Water (AAIW) in the Pacific Ocean, the upstream and downstream values correspond to one measurement and the average of two measurements, respectively. The samples, collected along the same isopycnal, display similar hydrographical properties ($S\approx34.54$, $\theta\approx5.3$ °C at 835 m depth). Concerning the North Pacific Tropical Water (NPTW) the upstream and downstream values correspond to the average of three and two measurements, respectively [19,30,32]. The NPTW is characterized by a vertical salinity maximum (S>34.8) around 250 m depth within the Kuroshio (downstream samples). Since this water mass is believed to be formed by subduction of surface water in the Western Subtropical North Pacific, the upstream samples were taken at the surface and subsurface in the source water region [30]. Hydrographical features of NIIW, AAIW and NPTW are discussed in more details in [20,21,30], respectively. Finally, concerning the North West Atlantic Bottom Water

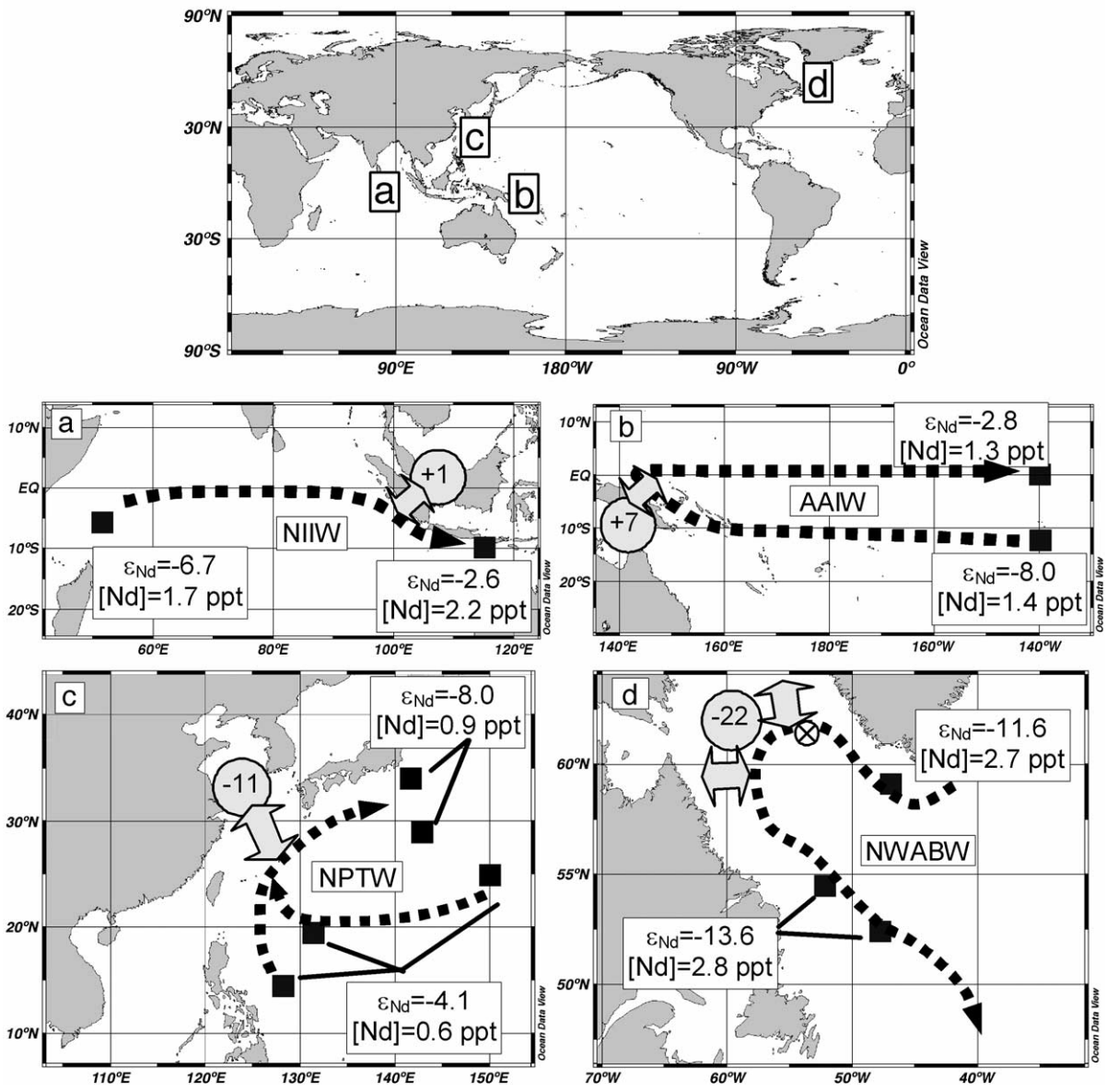

Fig. 2. Variations of the Nd isotopic composition and concentration within a water mass due to continent/ocean interactions. 1 ppt (part per trillion)=10^{-12} g g^{-1}. Left panel shows the location of the other panels. (a) NIIW, (b) AAIW, (c) NPTW and (d) NWABW (acronyms defined in Table 1). The sample locations are shown by the black squares, water mass pathways are schematized by the dotted arrows and the Nd isotopic composition of the interacting sediments are shown on gray circles [16,20,21,41]. The double arrows schematize boundary exchange. In panel (d) the cross indicates the location of the station used to quantify the mixing and evidence the occurrence of external inputs.

(NWABW), the upstream and downstream values correspond to one measurement and the average of two measurements, respectively. These samples were collected at the bottom of the water columns, characterized by local vertical salinity minima and dissolved oxygen maxima ([18] and the Signature/GINS cruise, R/V Marion Dufresne, Institut Paul Emile Victor, August 1999). Since NWABW data are published for the first time here, further details on this hydrography are given below.

Table 1
Neodymium property variations associated with margin/water mass interactions, and related fluxes

Water mass	Flow depth (m)	Initial, before mixing corrections		Significance of mixing	Initial		Final		ε_{Nd} margin	Flow magnitude ($10^6 m^3/s$)	$F_{Nd}^{Addition}$ ton (Nd)/yr	$F_{Nd}^{Removal}$ ton (Nd)/yr	$F_{Nd}^{Removal}/F_{Nd}^{Addition}$ (%)	Nd sediment discharge (*) ton (Nd)/yr	Contact area
		ε_{Nd}	Conc. (ppt)		ε_{Nd}	Conc. (ppt)	ε_{Nd}	Conc. (ppt)							
NIIW	700	−6.7[a]	1.7[a]	nil	−6.7[a]	1.7[a]	−2.6[b]	2.2[b]	1[a]	6[a]	366±233	272±246	74±23	1635	Java Slope (Indonesia)
AAIW	800	−8.0[c]	1.4[c]	nil	−8.0[c]	1.4[c]	−2.8[c]	1.4[c]	7[c]	3[c]	70±21	70±39	100±38	7740	Vitiaz Strait (Papua New Guinea)
NPTW	250	−4.1[d]	0.6[d]	nil	−4.1[d]	0.6[d]	−8.0[d]	0.9[d]	−11[e]	12[f]	295±240	181±289	62±54	57,354	East China Sea Shelf
NWABW	2600	−10.5[g]	2.8[g]	cf. text	−11.6[g]	2.7[g]	−13.6[h]	2.8[h]	−22[i]	6[j]	122±57	103±84	84±45	–	West Greenland and Labrador Slopes

Isotopic compositions (IC) and concentrations for several water masses (NIIW: North Indian Intermediate Water, AAIW: Antarctic Intermediate Water, NPTW: North Pacific Tropical Water and NWABW: North West Atlantic Bottom Water), upstream and downstream of a continental margin contact area (specified). 1 ppt (part per trillion)=10^{-12} g g^{-1}. When hydrographical properties showed the occurrence of water mass mixing (significant only in the case of the NWABW), the latter was taken into account, so that the Nd property variations displayed in the "Initial" and "Final" columns reflect interactions with external sources only (The "Initial before mixing corrections" column display the measured values upstream of the margin; see the Result section). The Nd IC of the input matter is given. $F_{Nd}^{Addition}$ and $F_{Nd}^{Removal}$ are defined in the text; their relative magnitude is given. The water mass and margin Nd IC and concentration uncertainties were determined as follows: (i) when a single data is available, the uncertainty is the standard deviation of the measurement; (ii) when several data are averaged, the uncertainty is the average deviation from the mean. However, to simplify the calculations and increase the result robustness, these uncertainties were set to their maximum values calculated in the four different cases; those are: 0.5 and 2 ε_{Nd} units, and 0.2×10^{-12} g/g for the water mass and margin Nd IC and concentration, respectively. Uncertainties for the other parameters were calculated propagating those values.

[a] [31].
[b] [20].
[c] [21].
[d] [30].
[e] [41].
[f] Estimation based on geostrophic calculation using data from WOCE section P24 1995, with a 2000 m deep reference level, for water with salinity greater than 34.75.
[g] This work.
[h] [18].
[i] [14,16].
[j] [46].

* Nd sediment discharges to the specified margin, calculated as the product of the sediment discharges, 109, 860 and 1738×10^{-6} tons, with the sediment Nd concentrations, 15, 9 and 33×10^{-6} g/g, for the NIIW, AAIW and NPTW, respectively [21,41,43–45] (no data were found concerning the sediment flux likely to interact with NWABW, in particular because of the large depth at which the latter flows).

3.2. Need of external inputs to account for the Nd IC variations

The four water masses display large Nd IC variations (cf. Table 1). Concerning the first 3 water masses (NIIW, AAIW and NPTW), combined hydrodynamical and geochemical studies suggest that the proportion of the Nd property variations which can be attributed to water mass mixing is insignificant [20,21,30]. This results either (1) from the fact that the hydrographical properties within the same water mass remain almost constant and therefore suggest almost no water mass mixing [21], or (2) from the fact that, even when significant mixing could occur, the Nd IC of the surrounding water masses (potentially involved in the mixing) cannot induce the observed variations. Either these Nd IC are similar to that of the studied water mass and are therefore unable to significantly modify it, or they are significantly different, but their isotopic values would lead to a reverse variation than the observed one, which rule out the hypothesis of any mixing effect [20,30]. In the following, we will illustrate this reasoning in the case of the NWABW.

The NWABW (which constitutes the precursor of the lower layer of the North Atlantic Deep Water), flows within the deep western boundary current along the Labrador Sea continental margin (see Fig. 2d). At the southern tip of Greenland, its characteristics are: θ=1.29 °C, S=34.838, [O_2]=9.82 mg/L, ε_{Nd}=−10.5 and [Nd]=2.8 ppt (R/V Marion Dufresne, cruise FI3519992, station 2, 2800 m, July 1999). Downstream of this current, in the North of the Labrador Sea, its characteristics are: θ=1.85, S=34.87, [O_2]=9.445 mg/L, ε_{Nd}=−14.9 and [Nd] is unknown (same cruise, station 3, 2430 m, indicated by a cross in Fig. 2d). The hydrographical property variations suggest a significant mixing with the overlying water mass, the North East Atlantic Deep Water (NEADW), characterized by θ=2.10 °C, S=34.885, [O_2]=9.26 mg/L, ε_{Nd}=−12.1 and [Nd]=2.6 ppt (same cruise, station 2, core of the NEADW, 2550 m, July 1999). Salinity, potential temperature and dissolved oxygen concentration imply mixing proportions of 68%, 69% and 66% of NEADW, respectively. The similarity of these results definitely confirms the hypothesis of a water mass mixing. However, considering these mixing proportions and the Nd characteristics of the two end members, the resulting water mass (the one sampled at station 3) should have an ε_{Nd} of −11.6 and a concentration of 2.7 ppt (value reported in Table 1 as the initial value). This value is 3.3 ε_{Nd} units larger than the one measured (−14.9). Therefore, even though water mass mixing cannot be neglected in this case, this calculation shows that a large ε_{Nd} decrease can not be explained by water mass mixing and is therefore the result of external inputs.

3.3. Need of exchange fluxes to reconcile the Nd IC and concentration balances

For the four water masses, large Nd IC variations imply the occurrence of external inputs. These variations occur with little or no concentration changes (cf. Table 1). Exchange fluxes (i.e., fluxes from the water mass to the margin in addition to fluxes from the margin to the water mass) are therefore required to explain the data. The goal of the following calculation is only to quantify the fluxes required to balance the data. In particular it does not intent to resolve the processes involved in these exchanges (those could include sediment resuspension, remineralization, dissolution, desorption, scavenging, precipitation, etc.). Therefore we estimated the fluxes using the box model schematized in Fig. 3. Steady state and mass conservation imply the following equations (quantities defined in Fig. 3).

$$F_W \times [Nd]^{Final} = F_W \times [Nd]^{Initial} + F_{Nd}^{Addition} - F_{Nd}^{Removal} \quad (2)$$

$$F_W \times [Nd]^{Final} \times \varepsilon_{Nd}^{Final} = F_W \times [Nd]^{Initial} \times \varepsilon_{Nd}^{Initial} + F_{Nd}^{Addition} \times \varepsilon_{Nd}^{Addition} - F_{Nd}^{Removal} \times \varepsilon_{Nd}^{Final} \quad (3)$$

From which we draw:

$$F_{Nd}^{Addition} = F_W \times [Nd]^{Initial} \times \frac{\varepsilon_{Nd}^{Final} - \varepsilon_{Nd}^{Initial}}{\varepsilon_{Nd}^{Addition} - \varepsilon_{Nd}^{Final}} \quad (4)$$

$$F_{Nd}^{Removal} = F_W \times \frac{[Nd]^{Final} \times \left(\varepsilon_{Nd}^{Final} - \varepsilon_{Nd}^{Addition}\right) - [Nd]^{initial} \times \left(\varepsilon_{Nd}^{Initial} - \varepsilon_{Nd}^{Addition}\right)}{\varepsilon_{Nd}^{Addition} - \varepsilon_{Nd}^{Final}} \quad (5)$$

The lack of time series prevents us to assess the reliability of the steady-state hypothesis. Due to the

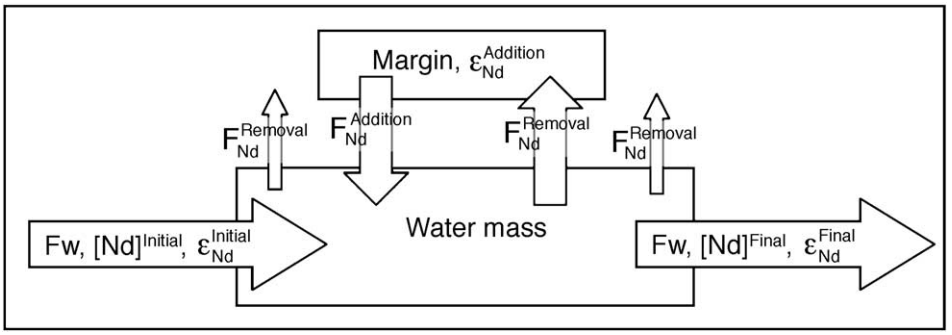

Fig. 3. Box model used to calculate Nd fluxes at the margin/water mass interface. *Initial* and *Final* refer to measurements, within the water mass, upstream and downstream of the margin contact area, respectively. F_w and F_{Nd} stand for water mass and Nd fluxes, respectively. *Addition* and *Removal* refer to fluxes from the margin to the water mass and leaving the water mass, respectively. The different arrows labeled $F_{Nd}^{Removal}$ indicate that the removal fluxes can occur upstream and downstream of the margin area, as well as at the margin (the values calculated for $F_{Nd}^{Removal}$, reported in Table 1, correspond to the sum of all removal fluxes occurring between the location of the initial and final measurements. Note that this model only aims at estimating the fluxes required to explain the data and does not intent to resolve the processes involved.

variability that could affect the hydrography and surface productivity along these boundaries, the studied systems could not be at steady state, implying different fluxes than those calculated below (which could be either greater or smaller). However, the few data available in other areas submitted to hydrographical variability, e.g. the Denmark Strait and the Faroe Shetland Channel, show remarkably constant values in the course of time, arguing in favor of the steady state hypothesis (for samples taken in 1981 and 1999, respectively: Denmark Strait Overflow Water: ε_{Nd}=−8.4 and −8.6 and [Nd]=3.2 and 3.0 ppt; Iceland Scotland Overflow Water: ε_{Nd}−8.2 and −7.7 and [Nd]=3.1 and 3.1 ppt [18,23,24]).

The fluxes, calculated for the 4 studied water masses, according to the above equations, are reported in Table 1. $F_{Nd}^{Removal}$ represents 62±54% of $F_{Nd}^{Additional}$ for the NPTW flowing along the East China Sea shelf; in other words, for 100 g of Nd supplied by the margin to the water mass, 62±54 g are scavenged from the water mass to the margin (cf. Table 1 legend for uncertainty calculations). Concerning the NWABW, flowing along the Labrador Sea continental margin, our data yielded a ratio ($F_{Nd}^{Removal}/F_{Nd}^{Additional}$) of 84±45%. Finally, we estimated this ratio to be 74±23% and 100±38% for the NIIW and the AAIW, respectively, definitely confirming our former hypothesis that exchange processes could occur along the Java and Papua New Guinea margins [20,21].

4. Discussion

Although the above uncertainties remain significant, the present data set seems to constitute a robust evidence of the occurrence of processes that yield exchange fluxes between margins and water masses. In the following, we will name this process “boundary exchange”. The nature, time and space scales of the processes involved are not precisely known and will need further investigations.

The four sites presented here are characterized by contrasting geographical, lithological, and dynamical properties. They range from 250 to 2500 m depth. They are located in contrasting climatic areas, which implies notably different (i) sedimentary sources and fluxes, including various erosion products (river borne and aeolian particles, from different lithologies), and (ii) types of organic matter with different export rates. The water masses overlying these margins also display different dissolved oxygen content. Thus, the reactions within these sediments, which are highly dependent on the organic carbon accumulation rates and the dissolved oxygen contents of the overlying water masses, are likely different among these four margins. Therefore, the following discussion does not intent to draw a unique picture of the boundary exchange, but to summarize the potential processes that could yield such exchange and which relative importance may greatly vary from a site to another. Note also that all types of margins are not represented in our study, in

particular significant upwelling and oxygen minimum zones are not documented.

4.1. Sources of the external inputs

For all of the water masses reported in Table 1, we suggest that the most likely Nd source is the remobilization–which includes dissolution as well as particle resuspension–of the margin deposited sediments (shelf or slope or both). The following arguments are put forward. (1) Aeolian particles settling within the water column have been shown to enrich surface water REE content without significant influence on deeper layers [25,34]. On the other hand, although REE aeolian inputs can rapidly reach deep waters [17,35], no significant influence on deep water dissolved REE budgets have been evidenced so far [19,36]. Similarly, dissolved riverine and groundwater inputs (having low densities) would also preferentially enrich surface waters. Since all the water masses considered here flow deeper than 250 m and since the corresponding surface waters do not display such enrichment, another source has to be invoked. These water masses flowing along continental margins, sediment/water mass interactions is a good candidate. (2) Above all, sediment remobilization is the only source that is large enough to provide the calculated fluxes, the other sources being orders of magnitudes too low. For instance, dissolved riverine input from the northeastern coast of Papua New Guinea could not account for more than 5% of the AAIW Nd property variations [21], whereas 1% remobilization of the fluvial sediment discharge in that area would be sufficient (cf. Table 1 for sediment discharge data). Similarly, aeolian fluxes along the west Greenland coast of the Labrador Sea could account for only 1% of the flux required to explain the NWABW Nd property variations [37].

4.2. Processes involved

Precise mechanisms yielding sediment/water Nd fluxes at the margins are still poorly documented. Studies in the early eighties already suggested that bottom water REE enrichments in the North East Atlantic could be due to diffusion from pores waters of REE released during early diagenesis and that the magnitude of these fluxes should be considerable [25]. REE concentration measurements have been conducted in pore waters of margin sediments under various diagenetic conditions (oxic, suboxic and anoxic) [26–29] and references therein. All these works show that these sediments are significant sources of REE to the pore waters, under both oxic and anoxic conditions, leading to pore water REE concentrations up to 50 times typical seawater values. Some of these works also show the occurrence of significant dissolved REE fluxes from the pore waters to the overlying seawater, under contrasting diagenetic conditions, notably with oxic surface layers ranging from 1 mm to 6 cm [25,29]. However, quantifications of such fluxes are still scarce. For instance, Elderfield et al. [26] estimated them to be of similar importance as the dissolved REE input rates from local rivers, in a case study of reducing nearshore sediments.

Although all these works involve diagenesis, the precise processes remain unclear. Most of the studies suggest that REE sources mainly include reduction of iron oxyhydroxides and degradation of organic matter (as well as Ce-oxide reduction in the case of Ce). However, whereas reduction of manganese oxides was traditionally though to be a potential REE source, Haley et al. [29] recently suggested that these are not significant REE carriers. Pore water REE sinks are also uncertain. Whereas REE uptake by phosphate minerals does occur in an oxic deep sea environment [38], we still do not know if it is the case within pore waters. Iron precipitation is well known to effectively scavenge REE. Finally barite formation has also been suggested as a REE sink in pore waters [29].

Despite the complexity of the REE cycling within the sediment/pore water environments, it appears that larger pore water REE concentrations are found in anoxic conditions associated with iron oxyhydroxides reduction (with pore water Nd concentration as high as 170 ppt), whereas much smaller concentrations are found in oxic/suboxic conditions. Moreover, Sholkovitz et al. [27] observed an excellent correlation between the seasonal cycles of REE and Fe in the bottom water of Chesapeake Bay (North West Atlantic), with release of REE into bottom waters during the transition from oxic/suboxic to anoxic conditions. Therefore, one could expect larger REE fluxes from anoxic margins than from oxic/suboxic ones. The reducing character of a margin is notably

enhanced by (i) significant fluxes of organic matter towards the sediments, which itself is favored by large export productions and shallow water columns, and (ii) old water masses having low dissolved oxygen concentration. Moreover, diagenetic reactions are enhanced by high temperature. Therefore, REE fluxes from the sediments to the overlying waters are expected, and have been showed [27], to be subject to large seasonal cycles.

According to Jahnke [39], the four presented margins display benthic oxygen fluxes (which reflect organic matter remineralization), ranging from ca. 0.1 (Papua New Guinea) to ca. 0.3 mol m^{-2} yr^{-1} (South Greenland). However, this range is relatively small compared to values of the order of 0.8 mol m^{-2} yr^{-1} above the most reducing margins (notably in the Eastern Pacific and North Indian oceans). These latter sites need therefore to be documented, since the above discussion suggests that they could yield significantly larger Nd fluxes than those estimated here.

Within the water column, REE scavenging by settling particles and their subsequent burial within the sediments has been widely documented and is likely to play a major role in the Nd removal at the margin ocean interface [17,25,31,35,40]. However most of these studies were conducted in the open ocean and little is known about the specific behavior of REE relative to scavenging near the sediment/seawater interface. Nevertheless, the large particulate fluxes occurring in margin environments (due to large biological and terrigeneous particulate fluxes) and the remobilization of the sediments deposited on the margin by dynamic flows are likely to enhance scavenging processes along this interface. Assuming that scavenging is the main process responsible for the Nd subtraction fluxes evidenced above, we can speculate that this sink is more diffuse than the input fluxes associated with sediment remobilization, since scavenging can occur: (1) throughout the entire water mass thickness (in contrast with sediment remobilization restricted to the interface), (2) not only above the margins, but also upstream and downstream of them (i.e. in the open ocean).

4.3. Role of the hydrodynamical forcing

Boundary exchange could be enhanced by high hydrodynamic conditions. All the margin/water mass interactions reported in Table 1 are located within western boundary currents or straits. Although this does not imply that such processes could not take place elsewhere, we suspect that the high dynamic conditions (strong vertical mixing, internal waves, intensified contour and boundary currents and turbulences etc.) found in such areas could enhance the remobilization of sediment and its dissolution. Moreover, it seems that a high contact area/water mass volume ratio enhances those fluxes. The horizontal dimension being roughly three orders of magnitude larger than the vertical one in the ocean, contact areas involving horizontal parts such as straits or shelves should constitute preferential sites for sediment/water mass interaction.

4.4. Remark about the lithology

Sediment/water mass interactions could also depend on sediment lithology. In this study, we present the first evidences of exchange fluxes along granitic margins. Fig. 1 shows the progressive Nd IC increase, associated with the global thermohaline circulation, from ≈ -13 in the North Atlantic Ocean, to ≈ -4 in the North Pacific Ocean. In the present work, we suggest that this evolution takes place mainly along continental margins. However, there is a wide predominance of unradiogenic river sources surrounding the oceans (Amazon $\varepsilon_{Nd}=-9.2$; Ganges $\varepsilon_{Nd}=-15.4$; Yellow River $\varepsilon_{Nd}=-12.6$; etc. [41]). In particular, the fraction of the Pacific Ocean drainage basins composed of acid volcanic rocks and basalts (that are radiogenic enough to yield the North Pacific mean Nd IC) is only $\approx 13\%$ [42]. Therefore, we suspect that sediments derived from those type of rocks are more efficient in modifying water mass Nd IC than other types of sediment. This hypothesis is supported by the fact that acid volcanic rocks and basalts are more rapidly weathered than granites and gneisses [42].

4.5. Globalization

The dataset presented here is still too small to directly extrapolate our conclusions to the global scale. However, the new evidences presented here, along the East China Sea shelf and Labrador Sea margin, in addition to the previous results from the

Indonesian volcanic arc (Java and Papua New Guinea), show that boundary exchange occurs in widely diverse area, characterized by very different lithologies (granitic versus basaltic), latitudes and therefore climates and weathering regimes (equatorial, sub-tropical, subpolar), nature and intensity of primary productivities, water dynamics and depths. This allows expecting that boundary exchange could occur in other areas.

Modeling studies are required to explore the global significance of boundary exchange. The global Nd IC and concentration distributions have been studied with a ten-box ocean model [14]. The authors estimate that aeolian and riverine inputs are insufficient to account for the Nd IC and concentration variations observed among the different oceanic basins. They suggest that continental margins could supply the missing Nd to the ocean. Our data and the necessary reconciliation between Nd IC and concentration variations within a given water mass are a strong evidence that supports their hypothesis.

In order to explore the significance of boundary exchange in the control of the global oceanic cycle of the Nd IC relative to the other fluxes, a parameterization of the Nd boundary exchange has been implemented in an oceanic global circulation model (OPA-ORCA, LSCE France). This ongoing work will be published elsewhere. However preliminary results suggest that boundary exchange could have a similar or even greater importance than net terrigeneous inputs on the global scale.

5. Conclusion

In summary, we showed that particulate/dissolved exchange processes along continental margins are necessary to explain the Nd IC of several water masses in the three oceans and along geologically different margins. It is stipulated for the first time that such processes occur along granitic as well as basaltic margins and in subpolar and subtropical as well as equatorial regions. The diversity of the studied sites suggests that boundary exchange could occur in other areas, opening the way to further investigations. We also showed that Nd IC allows quantifying these processes. Modeling approaches suggest that Nd exchange fluxes could be of the same order of magnitude or larger than net terrigeneous inputs on a global scale. Therefore, instead of considering margins as scavenging boundaries, they could be considered as exchange boundaries for several elements (in other words, both sources and sinks) and we suggest naming this process *boundary exchange*. It could play a significant role in the oceanic chemistry of many reactive elements and could be an important factor in interpreting sedimentary records. However, we know very little about its spatial and temporal variability, and still need to investigate the precise processes involved. Early diagenesis and scavenging processes are likely key factors controlling Nd sources and sinks, respectively, at the margin/seawater interface. However, we also suggest that the lithology of the material eroded towards the margin and the dynamic of the flow could play an important role. In situ (including sediment, pore water and seawater samples) multi-tracer approaches (Nd, Th, Ra, Pb and Fe isotopes, and Mn content) and modeling studies should help better understanding the precise processes involved and the global significance, respectively, of boundary exchange.

Acknowledgements

We thank R. Francois, four anonymous reviewers and the editor (E.B.) for their advices and comments on the manuscript. This work was supported by the PNEDC/INSU program “Signatures” (France) and the IPEV (Institut Paul Emile Victor).

References

[1] M.P. Bacon, Tracers of chemical scavenging in the ocean: boundary effects and large-scale chemical fractionation, Philos. Trans. R. Soc. Lond., A 325 (1988) 147–160.

[2] P.H. Santschi, L. Guo, I.D. Walsh, M.S. Quigley, M. Baskaran, Boundary exchange and scavenging of radionuclides in continental margin waters of the Middle Atlantic Bight: implications for organic carbon fluxes, Cont. Shelf Res. 19 (1999) 609–636.

[3] J.J. Walsh, Importance of continental margins in the marine biogeochemical cycling of carbon and nitrogen, Nature 350 (1991) 53–55.

[4] P. Tréguer, G. Jacques, Dynamics of nutrient and phytoplankton and cycles of carbon, nitrogen and silicon in the Southern Ocean: a review, Polar Biol. 12 (1992) 149–162.

[5] W.S. Broecker, T.H. Peng, Tracers in the Sea, Eldigio Press, Palisades, NY, 1982, 690 pp.
[6] R.W. Houghton, C.N. Flagg, L.J. Pietrafesa, Shelf-slope water frontal structure, motion and eddy heat-flux in the southern Middle Atlantic Bight, Deep-Sea Res. II 41 (1994) 273–306.
[7] J.M. Huthnance, H.M. Van Aken, M. White, E.D. Barton, B. Le Cann, E.F. Coelho, E.A. Fanjul, P. Miller, J. Vitorino, Ocean margin exchange—water flux estimates, J. Mar. Syst. 32 (2002) 107–137.
[8] R.F. Anderson, M.Q. Fleisher, P.E. Biscaye, N. Kumar, B. Dittrich, P. Kubik, M. Suter, Anomalous boundary scavenging in the Middle Atlantic Bight: evidence from ^{230}Th, ^{231}Pa, ^{10}Be and ^{210}Pb, Deep-Sea Res. II 41 (1994) 537–561.
[9] P.E. Biscaye, C.N. Flagg, P.G. Falkowski, The shelf edge exchange processes experiment, SEEP-II: an introduction to hypotheses, results and conclusions, Deep-Sea Res. II 41 (1994) 231–255.
[10] D.W. Spencer, M.P. Bacon, P.G. Brewer, Models of the distribution of ^{210}Pb in a section across the north equatorial Atlantic Ocean, J. Mar. Res. 39 (1981) 119–138.
[11] R.F. Anderson, Y. Lao, W.S. Broecker, S.E. Trumbore, H.J. Hofmann, W. Wolfli, Boundary scavenging in the Pacific Ocean: a comparison of ^{10}Be and ^{231}Pa, Earth Planet. Sci. Lett. 96 (1990) 287–304.
[12] M.P. Bacon, R.A. Belastock, M.H. Bothner, ^{210}Pb balance and implications for particle transport on the continental shelf, U.S. Middle Atlantic Bight, Deep-Sea Res. II 41 (1994) 511–535.
[13] S.B. Jacobsen, G.J. Wasserburg, Sm–Nd isotopic evolution of chondrites, Earth Planet. Sci. Lett. 50 (1980) 139–155.
[14] K. Tachikawa, V. Athias, C. Jeandel, Neodymium budget in the modern ocean and paleoceanographic implications, J. Geophys. Res. 108 (2003) 3254 doi:10.1029/1999JC000285.
[15] F.E. Grousset, P.E. Biscaye, A. Zindler, J. Prospero, R. Chester, Neodymium isotopes as tracers in marine sediments and aerosols: North Atlantic, Earth Planet. Sci. Lett. 87 (1988) 367–378.
[16] C. Innocent, N. Fagel, R. Stevenson, C. Hillaire-Marcel, Sm–Nd signature of modern and late quaternary sediments from the northwest North Atlantic: implications for deep current changes since the last glacial maximum, Earth Planet. Sci. Lett. 146 (1997) 607–625.
[17] C. Jeandel, J.K. Bishop, A. Zindler, Exchange of Nd and its isotopes between seawater small and large particles in the Sargasso Sea, Geochim. Cosmochim. Acta 59 (1995) 535–547.
[18] D.J. Piepgras, G.J. Wasserburg, Rare earth element transport in the western North Atlantic inferred from isotopic observations, Geochim. Cosmochim. Acta 51 (1987) 1257–1271.
[19] D.J. Piepgras, S.B. Jacobsen, The isotopic composition of neodymium in the North Pacific, Geochim. Cosmochim. Acta 52 (1988) 1373–1381.
[20] C. Jeandel, D. Thouron, M. Fieux, Concentrations and isotopic compositions of Nd in the Eastern Indian Ocean and Indonesian Straits, Geochim. Cosmochim. Acta 62 (1998) 2597–2607.
[21] F. Lacan, C. Jeandel, Tracing Papua New Guinea imprint on the central Equatorial Pacific Ocean using neodymium isotopic compositions and Rare Earth Element patterns, Earth Planet. Sci. Lett. 186 (2001) 497–512.
[22] K. Tachikawa, M. Roy-Barman, A. Michard, D. Thouron, D. Yeghicheyan, C. Jeandel, Neodymium isotopes in the Mediterranean Sea: comparison between seawater and sediment signals, Geochim. Cosmochim. Acta 68 (2004) 3095–3106.
[23] F. Lacan, C. Jeandel, Denmark Strait water circulation traced by heterogeneity in neodymium isotopic compositions, Deep-Sea Res. I 51 (2004) 71–82.
[24] F. Lacan, C. Jeandel, Neodymium isotopic composition and rare earth element concentrations in the deep and intermediate Nordic Seas: constraints on the Iceland Scotland Overflow Water signature, Geochem. Geophys. Geosyst. 5 (2004) Q11006 doi:10.1029/2004GC000742.
[25] H. Elderfield, M.J. Greaves, The rare earth elements in seawater, Nature 296 (1982) 214–219.
[26] H. Elderfield, E.R. Sholkovitz, Rare earth elements in the pore waters of reducing nearshore sediments, Earth Planet. Sci. Lett. 82 (1987) 280–288.
[27] E.R. Sholkovitz, T.J. Shaw, D.L. Schneider, The geochemistry of rare earth elements in the seasonally anoxic water column and porewaters of Chesapeake Bay, Geochim. Cosmochim. Acta 56 (1992) 3389–3402.
[28] E.R. Sholkovitz, D.J. Piepgras, S.B. Jacobsen, The pore water chemistry of rare earth elements in Buzzards Bay sediments, Geochim. Cosmochim. Acta 53 (1989) 2847–2856.
[29] B.A. Haley, G.P. Klinkhammer, J. McManus, Rare earth elements in pore waters of marine sediments, Geochim. Cosmochim. Acta 68 (2004) 1265–1279.
[30] H. Amakawa, Y. Nozaki, D.S. Alibo, J. Zhang, K. Fukugawa, H. Nagai, Neodymium isotopic variations in Northwest Pacific waters, Geochim. Cosmochim. Acta 68 (2004) 715–727.
[31] C.J. Bertram, H. Elderfield, The geochemical balance of the rare earth elements and Nd isotopes in the oceans, Geochim. Cosmochim. Acta 57 (1993) 1957–1986.
[32] H. Amakawa, D.S. Alibo, Y. Nozaki, Nd isotopic and REE pattern in the surface waters of the eastern Indian Ocean and its adjacent seas, Geochim. Cosmochim. Acta 64 (2000) 1715–1727.
[33] F. Lacan, C. Jeandel, Subpolar mode water formation traced by neodymium isotopic composition, Geophys. Res. Lett. 31 (2004) doi:10.1029/2004GL019747.
[34] K. Tachikawa, C. Jeandel, M. Roy-Barman, A new approach to Nd residence time in the ocean: the role of atmospheric inputs, Earth Planet. Sci. Lett. 170 (1999) 433–446.
[35] K. Tachikawa, C. Jeandel, B. Dupré, Distribution of rare earth elements and neodymium isotopes in settling particulate material of the tropical Atlantic Ocean (EUMELI site), Deep-Sea Res. 44 (1997) 1769–1792.
[36] S. Nakai, A.N. Halliday, D.K. Rea, Provenance of dust in the Pacific Ocean, Earth Planet. Sci. Lett. 119 (1993) 143–157.
[37] F. Lacan, Masses d'eau des Mers Nordiques et de l'Atlantique Subarctique tracées par les isotopes du néodyme, PhD thesis, Toulouse III University, France. Available at http://francois.lacan.free.fr/job.htm (2002).

[38] H.F. Shaw, G.J. Wasserburg, Sm–Nd in marine carbonates and phosphates: implications for Nd isotopes in seawater and crustal ages, Geochim. Cosmochim. Acta 49 (1985) 503–518.
[39] R.A. Jahnke, Benthic oxygen fluxes, JGOFS Report, vol. 38, 2003, p. 17.
[40] H. Elderfield, The oceanic chemistry of the rare earth elements, Philos. Trans. R. Soc. Lond. 325 (1988) 105–106.
[41] S.L. Goldstein, R.K. O'Nions, P.J. Hamilton, A Sm–Nd study of atmospheric dusts and particulates from major river systems, Earth Planet. Sci. Lett. 70 (1984) 221–236.
[42] P. Amiotte Suchet, J.-L. Probst, W. Ludwig, Worldwide distribution of continental rock lithology: implications for the atmospheric/soil CO_2 uptake by continental weathering and alkalinity river transport to the oceans, Glob. Biogeochem. Cycles 17 (2003) 1038 doi:10.1029/2002GB001891.
[43] J.D. Milliman, K.L. Farnsworth, C.S. Albertin, Flux and fate of fluvial sediments leaving large islands in the East Indies, J. Sea Res. 41 (1999) 97–107.
[44] J.D. Milliman, R.H. Meade, World-wide delivery of river sediment to the oceans, J. Geol. 91 (1983) 1–21.
[45] D. Ben Othman, W.M. White, J. Patchett, The geochemistry of marine sediments, island arc magma genesis, and crust–mantle recycling, Earth Planet. Sci. Lett. 94 (1989) 1–21.
[46] W.J.J. Schmitz, On the World Ocean circulation: Volume I, Wood Hole Oceanog. Instit. Tech. Rept. WHOI-96-03, 1996, p. 141.
[47] M.C. Stordal, G.J. Wasserburg, Neodymium isotopic study of Baffin Bay water: sources of REE from very old terranes, Earth Planet. Sci. Lett. 77 (1986) 259–272.
[48] A.J. Spivack, G.J. Wasserburg, Neodymium isotopic composition of the Mediterranean outflow and the eastern North Atlantic, Geochim. Cosmochim. Acta 52 (1988) 2762–2773.
[49] F. Henry, C. Jeandel, B. Dupre, J.-F. Minster, Particulate and dissolved Nd in the Western Mediterranean Sea: sources, fates and budget, Mar. Chem. 45 (1994) 283–305.
[50] C. Jeandel, Concentration and isotopic composition of neodymium in the South Atlantic Ocean, Earth Planet. Sci. Lett. 117 (1993) 581–591.

5. Lacan et Jeandel 2001. EPSL. L'impact des sources côtières au large.

ELSEVIER

Earth and Planetary Science Letters 186 (2001) 497–512

EPSL

www.elsevier.com/locate/epsl

Tracing Papua New Guinea imprint on the central Equatorial Pacific Ocean using neodymium isotopic compositions and Rare Earth Element patterns

F. Lacan, C. Jeandel *

LEGOS (CNRS/CNES/UPS), Observatoire Midi-Pyrénées, 14, Ave E. Belin, F-31400 Toulouse, France

Received 29 September 2000; received in revised form 29 January 2001; accepted 4 February 2001

Abstract

The Nd isotopic composition (IC) and Rare Earth patterns of hydrodynamic structures of the Equatorial Pacific Ocean were characterized along 140°W. The Nd IC of Antarctic Intermediate Water (AAIW) and of the lower layer of the Equatorial Undercurrent (EUC) at 140°W (13°C Water) are much more radiogenic at the equator than at their origin in the South Equatorial Current (12°S), revealing that these water masses have been in contact with the highly radiogenic Papua New Guinea (PNG) slope. In both cases, only a small fraction (less than 9%) of the sediment deposited on the PNG slope is required to be exchanged or dissolved to explain these Nd IC variations, whereas the hydrographic properties of the same water masses remain unchanged. This confirms the usefulness of this tracer to identify pathways of water masses. These results emphasize the importance of jets in transporting lithogenic material into the subsurface layers of remote areas, where aeolian inputs are particularly weak and corroborate the previous results on Fe and Al maximum in this area [M.L. Wells, G.K. Vallis, E.A. Silver, Nature 398 (1999) 601–604]. The Nd IC of the upper layer of the EUC contrasts strongly to that of the subpycnocline layer, indicating that the equatorial upwelling only affects the surface waters and is not effective between 120 and 150 m. We calculate that the Nd imprint of the PNG input is likely to vanish from this surface layer as it traverses the basin, due to the replacement of upwelled waters by non-radiogenic ones.

Keywords: neodymium; isotopic composition; rare earths; sea water; geochemical indicators; Papua New Guinea

1. Introduction

Since the eighties, the neodymium isotopic composition (Nd IC) of sea water has been recognized as a tracer in marine geochemistry. The Nd IC corresponds to the $^{143}Nd/^{144}Nd$ ratio. It is expressed as ε_{Nd} which is the deviation of this ratio from its average value in the earth:

$$\varepsilon_{Nd} \left(\frac{\left(\frac{^{143}Nd}{^{144}Nd}\right)_{measured}}{\left(\frac{^{143}Nd}{^{144}Nd}\right)_{CHUR}} - 1 \right) \times 10^4$$

The present-day $^{143}Nd/^{144}Nd$ ratio in the CHUR (Chondritic Uniform Reservoir) taken as reference is 0.512638 [2]. In the ocean, dissolved

E-mail: francois.lacan@cnes.fr
* Corresponding author. Tel.: +33-5-6133-29033; Fax: +33-5-6125-3205; E-mail: catherine.jeandel@cnes.fr

0012-821X/01/$ – see front matter
PII: S0012-821X(01)00263-1

ε_{Nd} values allow the pathways and mixing of water masses on the oceanic basin scale to be traced [3–7]. In contrast to many circulation tracers, the sea water Nd IC is not affected by evaporation or any subtraction processes: the ε_{Nd} of any given water mass will only be modified when it receives an input of Nd with a different isotopic signal. Therefore, modification of the isotopic signature of a water body implies mixing with other water bodies and/or contact and exchange with continental inputs [7–9]. The Nd IC is also a powerful tracer of the sources and fates of marine particles: as Nd is a lithogenic element, it is brought to the sea by continental inputs. The distribution of ε_{Nd} in the solid earth is heterogeneous, varying from −36 for old granitic cratons to more than +10 for recent Mid Ocean Ridge Basalts (see the compilation in the data bank www.earthref.org). Therefore, pathways of particles between their sampling location and their source can be reconstructed and transformation processes through the water column can also be studied using ε_{Nd} ([10,11] and references therein, [12,13]).

In addition to its isotopic properties, Nd belongs to the geochemical group of the Rare Earth Elements (REE). In the ocean, the dissolved REE distribution is determined by the competition between soluble carbonate–REE(III) complexes and the removal of REE(III) by particle scavenging [14]. This competition causes fractionation between light and heavy REE (LREE and HREE). Moreover, cerium, which is oxidized to insoluble Ce(IV) , is removed more effectively than its REE neighbors. These fractionations are represented by the REE pattern, that is all the REE concentrations measured in a sample normalized using the REE data of a reference material. This is a useful tool to identify which marine process could have modified the distribution of the REE in sea water (adsorption, desorption, redox process..., [14–16] and references therein). The simultaneous use of both the Nd IC and REE patterns is a fruitful approach for analyzing the dissolved/particulate exchanges and pathways of particles in sea water [13,17].

Despite the interest for this tracer, ε_{Nd} sea water data are scarce, especially in the Pacific Ocean [5,18]. This is one of the reasons why the oceanic balance of Nd is not completely understood: the exact way according to which water masses change their Nd IC is still unclear, although exchanges with particulate material at the ocean margins and along the coasts are suspected to be likely candidates [7,8].

Coale et al. [46] reported Fe and Al maximum at the equator at 140°W in the Pacific Equatorial Undercurrent (EUC), between 100 and 250 m. As aeolian inputs are low in this area [19], Coale et al. [46] deduced that the iron found in the surface waters is supplied from the enriched subsurface layer by the equatorial upwelling. This input of iron could control the primary production in this region. These authors suggested that this iron may originate from the Papua New Guinea (PNG) shelf (or upper slope), and be advected within the EUC. Wells et al. [1] speculate that past variations in the tectonic activity of PNG (mostly during the late Miocene) could have induced variations of iron inputs into the EUC source waters and subsequently caused variations in the Central Equatorial Pacific primary production. It is therefore important to assess clearly the origin of the iron enrichment of the subsurface waters. The Nd isotopic signature of the PNG slope ($\varepsilon_{Nd} = +7$, [20]) is much more radiogenic (high ε_{Nd}) than the surrounding waters ($-9 < \varepsilon_{Nd} < 0$; [5]). Therefore, we expect that the Nd IC of the uppermost 1000 m in the Central Equatorial Pacific could help test whether the lithogenic enrichments measured by Coale et al. [46] indeed originate from the PNG.

2. Hydrological context and sampling

Within the framework of the EqPac cruise (*R.V. Thomson*, November 1992), 17 samples were collected at three stations, between the surface and 850 m depth, along a north–south transect (2°N to 12°S) around 140°W. Conductivity, temperature, depth (CTD) measurements were also carried out at those stations, as well as at intermediate stations.

The major features of the circulation of the surface Central Pacific Ocean are (i) two large anti-

cyclonic gyres with axes along 20°N and 20°S and (ii) the equatorial current system (Fig. 1a). The northern limb of the southern anticyclonic gyre flows westwards and forms the South Equatorial Current (SEC), that extends from 5°N to 20°S at the surface. Below 100 m, the current shifts to the south and is found between 6°S and 25°S penetrating to depths greater than 1000 m [21] (Fig. 1b).

Along the equator, underneath the SEC, the EUC flows eastwards. This current originates north of PNG at ~200 m depth and rises gently along its 14 000 km pathway across the basin. It is located between 2°N and 2°S, is ~200 m thick, and has a mean speed of 0.4 m s^{-1} with a maximum around 1 m s^{-1} ([22,23] and compilation of current meter and ADCP (Acoustic Doppler Current Profiles) data from the TAO (Tropical Atmosphere Ocean) moorings (PMEL, US; JAMSTEC, Japan; IRD, France); Gourdeau, personal communication, 2000). It is mainly formed out of four undercurrents merging off the PNG coast (Fig. 1c). Three of them are coastal currents entraining waters of southern origin: the New Guinea Coastal Undercurrent (NGCU), the Saint Georges Undercurrent (SGU) and the New Ireland Coastal Undercurrent (NICU). The fourth one entrains waters of northern origin [24,25]. A strong pycnocline divides the EUC into two main layers: at 140°W, the upper one lies between 50 and 150 m and the lower one between 150 and 250 m. The upper layer includes the core of maximum velocity for the EUC. This layer contains Tropical Water originating from the high salinity cell centered around the tropic of Capricorn between 170°W and 120°W, where convective sinking of surface water takes place (Fig. 1a). This Tropical Water is entrained westwards in the SEC and then brought to the EUC by the coastal undercurrents described above. A large fraction of this water may be lost to the surface circulation as it flows eastwards [24]. The water that forms the subpycnocline layer of the EUC is described by Tsuchiya [26] as the Equatorial 13°C Water. Originating from the Tasman Sea, it flows eastwards to reach the southern limb of the south subtropical gyre, then it follows the course of this gyre, joining the SEC that brings it to the Coral Sea. Finally, it flows northwards to the Solomon Sea and enters the Bismarck Sea through the Vitiaz Strait in the NGCU from which it feeds the EUC [26] (Fig. 1a,c).

Underneath the EUC, the Equatorial Intermediate Current (EIC) flows westwards between ~3°N and ~2°S [22] and from about 300 to more than 500 m depth (Fig. 1b). Underneath the EIC the flow direction is eastwards again. The boundary between this eastwards flow and the EIC is uncertain but situated between 500 and 800 m depth [21]. On both sides of the EIC eastwards flows are found, the North and South Subsurface Countercurrents (NSCC and SSCC), about 5° wide each (Fig. 1b).

The intermediate water mass found at 135°W between 10°S and 6.5°N is described by Tsuchiya and Talley [34] as the Antarctic Intermediate Water (AAIW) of the 'equatorial type'. These authors suggest that it originates from the AAIW of the 'subtropical type' found between 33°S and 17°S. Following these authors, the AAIW of the subtropical type would be carried to the west by the SEC and then northwards to the equatorial zone by the western boundary undercurrents in the PNG region. Equatorial flows would then spread the water mass into the interior of the equatorial region. The region between 17°S and 10°S is an AAIW transition zone.

The samples collected during the EqPac cruise allow us to document some of these hydrographic structures along 140°W (Fig. 1b and Table 1 for hydrographical characteristics). At 12°S we have sampled at 120 and 150 m the tongue of Tropical Water formed by convective sinking ($S = 36.5$ and 36.4, respectively). At 200 m the sample is located around the path of the 13°C Equatorial Water. At 835 m, we have sampled in the transition zone for AAIW, adjacent to the equatorial type AAIW. At 0°, there are two samples in the core of the EUC: 120 and 150 m, one sample in the core of the EIC: 350 m, one in the bottom end of the EIC: 545 m and one sample of AAIW of the equatorial type at 835 m. The 2°N station is located at the northern limit of the equatorial upwelling. We collected a sample at 15 m in the SEC, a sample around the northern boundary of the EUC at

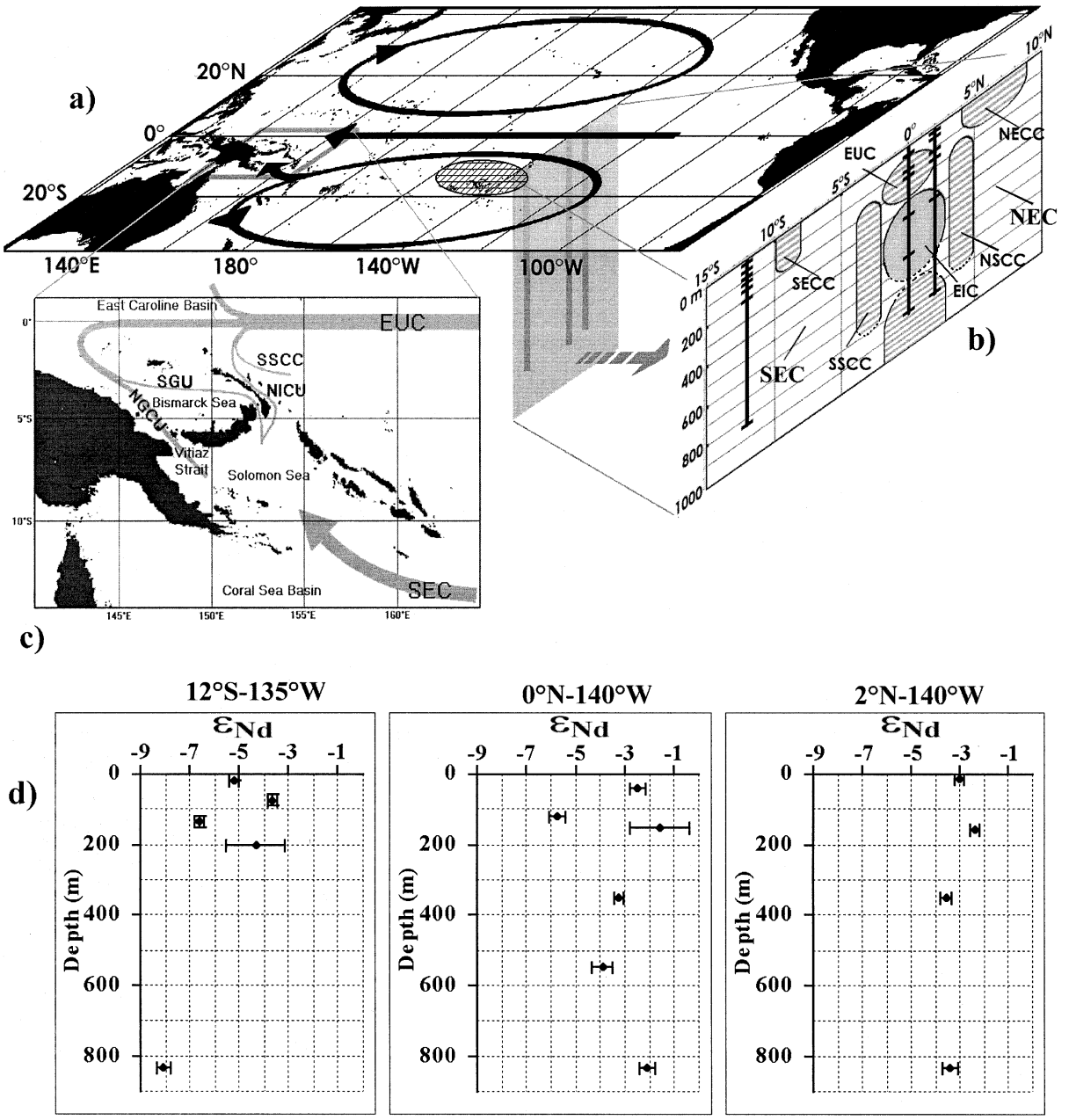

Fig. 1. (a) Map of the Central Pacific. The main structures of the surface circulation are represented by black arrows, the squared area schematizes the high salinity cell where the Tropical Water is formed. The gray plane represents the 140°W section where the three Nd stations are shown by vertical lines. (b) Details of the 140°W section, modified from a 170°W section from Tomczak and Godfrey [47]. The three stations are represented by the vertical black lines, on which the sample locations are shown by horizontal segments. The main zonal currents are schematized. Unfilled and gray tint areas are westward flows: the SEC, the North Equatorial Current (NEC), and the EIC. Striped areas are eastwards flows: the South Equatorial Counter Current (SECC), the North Equatorial Counter Current (NECC), the Southern Subsurface Counter Current (SSCC), the Northern Subsurface Counter Current (NSCC) and the EUC. Note that the bottom extensions of the SSCC, NSCC and EIC are not well defined in the literature (it is represented by a dotted line). (c) Zoom on the PNG region showing in detail the currents that form the EUC: The NGCU, the SGU, the NICU and the SSCC. (d) ε_{Nd} profiles at the three stations.

Table 1
Nd ICs, Ce anomalies and hydrological properties of the samples analyzed in this work

Station location	Depth (m)	θ (°C)	Salinity (psu)	σ_θ	Ce/Ce*	$^{143}Nd/^{144}Nd$[a]	ε_{Nd}
2°N–140°W	15	26.246	34.582	22.643	0.51 ± 0.06	0.512484 ± 11	−3.0 ± 0.2
	40	26.239	34.582	22.645	0.36 ± 0.06	–	–
	110	22.817	34.730	23.783	0.37 ± 0.07	–	–
	155	13.978	34.910	26.123	0.17 ± 0.02	0.512516 ± 11	−2.3 ± 0.2
	350	11.011	34.776	26.599	0.32 ± 0.03	0.512455 ± 11	−3.5 ± 0.2
	835	5.401	34.548	27.270	0.23 ± 0.03	0.512463 ± 17	−3.4 ± 0.3
0°–140°W	40	24.598	34.954	23.430	0.34 ± 0.06	0.512511 ± 13	−2.4 ± 0.3
	120	19.674	35.134	24.950	0.33 ± 0.05	0.512343 ± 13	−5.7 ± 0.3
	150	17.236	35.174	25.593	0.26 ± 0.04	0.512556 ± 66	−1.6 ± 1.2
	350	10.847	34.783	26.635	0.21 ± 0.03	0.512471 ± 11	−3.2 ± 0.2
	545	7.823	34.620	27.002	0.54 ± 0.05	0.512437 ± 20	−3.9 ± 0.4
	835	4.341	34.549	27.278	0.22 ± 0.02	0.512530 ± 15	−2.1 ± 0.3
12°S–135°W	20	27.270	35.922	23.328	0.70 ± 0.07	0.512371 ± 11	−5.2 ± 0.2
	60	26.666	36.212	23.739	0.44 ± 0.06	–	–
	75 ± 15	26.269	36.345	23.966	–	0.512450 ± 11	−3.6 ± 0.2
	90	25.937	36.455	24.153	0.41 ± 0.08	–	–
	120	24.949	36.490	24.485	0.60 ± 0.07	–	–
	135 ± 15	24.124	36.467	24.717	–	0.512300 ± 11	−6.6 ± 0.2
	150	23.489	36.399	24.854	0.85 ± 0.10	–	–
	200	21.352	36.080	25.221	0.37 ± 0.06	0.512417 ± 66	−4.3 ± 1.2
	835	5.180	34.523	27.276	0.59 ± 0.05	0.512224 ± 16	−8.0 ± 0.3

–: not measured.
[a]Absolute errors of $^{143}Nd/^{144}Nd$ have to be multiplied by 10^{-6}.

155 m, a sample in the EIC at 350 m and a sample of AAIW of the equatorial type at 835 m.

3. Analytical procedures

3.1. Nd IC

The analytical procedure used to purify Nd from the sea water comprises three steps. First, 10 l of sea water were preconcentrated using C18 cartridges loaded with a REE complexant (HDEHP/H_2MEHP). The REE were subsequently eluted with 6 N HCl, which efficiently separated them from most sea water ions. This procedure is described in detail by Jeandel et al. [7]. Second, this solution is dried and dissolved in 2.5 N HCl for the separation of the REE from the remaining ions (traces of Ca, Sr, Ba, Mg...). This second extraction was a chromatography using a cationic resin [27]. The REE were eluted with 9 ml of 6 N HCl. This solution was dried and dissolved again in 0.3 N HCl for the final extraction of Nd. This last step is based on a reversed phase chromatography (anionic exchange; [6,28]).

Mass spectrometric analyses were carried out on a Finnigan MAT 261 mass spectrometer (static mode). Sample size for mass spectrometric analysis was typically 6–30 ng and Nd was analyzed as Nd . The $^{146}Nd/^{144}Nd$ ratio of 0.7219 is used to correct the mass fractionation. An international standard (La Jolla, $^{143}Nd/^{144}Nd = 0.511850 \pm 20 \times 10^{-6}$; Lugmair, personal communication, 2001) was analyzed daily ($n = 24$) to monitor instrumental drift. The averaged result was within the certified range of the La Jolla value, so that no instrumental bias had to be taken into account. The standard deviation of this average is 11×10^{-6} (2σ), that is 0.2 ε_{Nd} unit: this external precision was applied to all the results having a better counting statistic.

Blank values range between 120 and 300 pg, that is 2–5% of the signal. Our limited sampling did not allow us to split or duplicate any sample analyzed in this work: concentrations were too low and only one sample per depth was collected.

However, the procedure used here is exactly the same as the Jeandel et al. [7] procedure. We therefore expect a similar reproducibility, which is within the 2σ error of the counting statistics.

3.2. REE concentrations

REE concentrations were measured on a Perkin Elmer Elan 6000 Inductively Coupled Plasma Mass Spectrometer (ICP-MS), following the procedure established in our laboratory [17], which coupled an internal standard and an isotopic dilution analysis. First, REE concentrations were evaluated by comparing the machine responses for the sample and a standard solution. Then, isotopic dilution was applied to Nd and Yb only. This last method is independent of the analytical recovery. The comparison of the results obtained for Nd and Yb concentrations by both methods allows us to estimate the experiment recovery of these two elements in each sample (range of values: 77–100% and 87–100% for Nd and Yb, respectively). Efficiencies of the protocol for the other REE are calculated by linear interpolation; finally, their concentrations measured by the internal standard method were corrected. The weight of the samples was approximately known, inducing an uncertainty of about 20% on absolute concentration values. Nevertheless, this has no effect on the LREE/HREE ratio within a given sample, nor its Ce anomaly. Absolute values used in the discussion are from Zhang and Nozaki [15].

REE were extracted from sea water by iron oxide co-precipitation. A 0.5 l aliquot, first acidified to pH = 2, was spiked with ^{150}Nd (97.84%) and ^{172}Yb (94.9%). Then 1 ml of 1 N HNO_3 containing 0.5% Fe was added. After equilibration, the pH was increased to 7–8 by addition of NH_4OH, and co-precipitation took place. The REE–Fe precipitate was extracted by successive centrifugations. It was redissolved in 1 ml of 6 N HCl and loaded on an anion exchange column to remove Fe (0.8 cm in diameter, 4 cm in length, containing 2 ml Bio-Rad AG1×8 resin). REE were eluted with 9 ml of 6 N HCl. This solution was evaporated and the residue was redissolved in 9 ml of 0.3 N HNO_3 for ICP-MS measurement.

Concentrations were reproducible within 0.9% for LREE and 4% for HREE, the worse reproducibility corresponding to the smallest samples. Blank values were smaller than 40 pg for abundant LREE and 3 pg for HREE.

4. Results

4.1. Nd IC

The sea water Nd IC are reported in Table 1. Vertical profiles of ε_{Nd} are plotted on Fig. 1d.

4.1.1. 2°N–140°W

Vertical variations of ε_{Nd} values are quite small. ε_{Nd} values range from −3.5 to −2.3. The mean value is -3.1 ± 0.5. The AAIW sample (835 m) has a value of −3.4.

4.1.2. 0°–140°W

ε_{Nd} variations are much larger, ε_{Nd} values range from −5.7 to −1.6. The mean value is -3.2 ± 1.5. There is a very important difference (3.9 ε_{Nd} units) between the two samples of the EUC, only 30 m apart (120 and 150 m), but situated in two distinct layers of the undercurrent. The deepest one (150 m) has an isotopic value comparable to that observed for the same depth at 2°N. Measurements in the EIC gave values of −3.2 and −3.9, in the same range as that observed at 2°N for this current ($\varepsilon_{Nd} = -3.5$). The intermediate water sample at 835 m is relatively radiogenic, with a value of −2.1.

4.1.3. 12°S–135°W

Vertical variations of ε_{Nd} values are also significant, especially within the first 200 m. ε_{Nd} values are between −8.0 and −3.6. The average value is -5.5 ± 1.8, this is the least radiogenic station observed in this work. Because of the insufficient amount of Nd in some samples, we had to mix some of them to make one out of two. The 60 m and 90 m samples were mixed as well as the 120 m and 150 m ones, producing data at 75 ± 15 m and 135 ± 15 m, respectively. At 135 m, in the tongue of Tropical Water, ε_{Nd} is −6.6, whereas it is −4.3 at 200 m in the path of the Equatorial

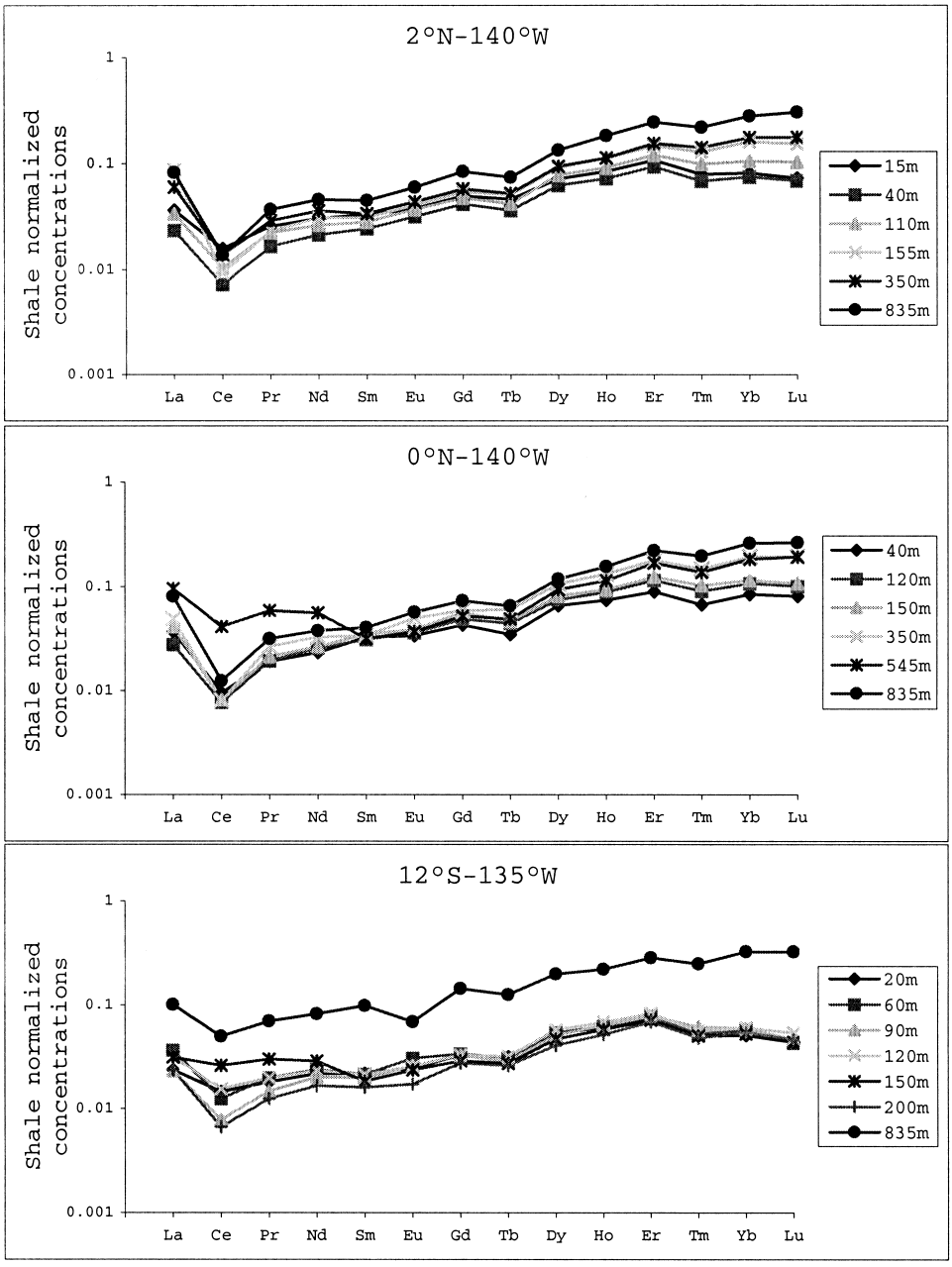

Fig. 2. Shale normalized REE concentrations of sea water samples collected during the EqPac cruise in November 1992. Due to the uncertainty affecting absolute concentrations of each sample (see the text), the shapes of the REE patterns are mostly used in this work.

13°C Water. The AAIW shows a value of −8.0, considerably less radiogenic than the intermediate waters of the two northernmost stations.

4.2. REE concentrations

REE patterns are shown in Fig. 2. Measured concentrations have been normalized to the aver-

age REE concentrations of North American, European and Russian shales ([16] and references therein). Patterns have marine properties, i.e. a negative cerium anomaly and a LREE/HREE fractionation. These characteristics reflect the particle activity and/or the aging during water mass transport: in general, the older (deeper) the water mass, the larger are the Ce anomaly and the HREE enrichment (e.g. [29]). In agreement with recent observations [19,30] surface waters do not reflect any influence of aeolian input at this remote longitude. Ce anomalies, Ce/Ce*, were calculated using the equation:

$$\frac{Ce}{Ce^{*}} \quad \frac{Ce \times 2}{La \quad Pr}$$

where Ce, La and Pr are the shale normalized concentrations (values close to 0 correspond to large anomalies whereas values close to 1 correspond to weak ones). Calculated anomalies are reported in Table 1. The most relevant features are the Ce anomalies of the three AAIW samples, which are 0.23 at 2°N, 0.22 at 0° and 0.59 at 12°S.

5. Discussion

Measured ε_{Nd} and REE concentrations are in good agreement with previous studies for the Pacific Ocean [3,5,18,29,31]. The average Nd IC of the whole Pacific basin is not significantly modified by our results ($\varepsilon_{Nd} = -4.3 \pm 1.8$ before our measurements to -4.2 ± 1.8 after). Similarly, the average ε_{Nd} shifts from -4.1 ± 1.5 to -4.0 ± 1.5 for the North Pacific and from -5.7 ± 3.7 to -5.6 ± 2.7 for the South Pacific. The measured value for AAIW at 12°S also compares well with preceding data [3,6,29], contrasting with the northernmost intermediate waters ('equatorial' AAIW) with its more radiogenic ε_{Nd} (Table 1, Fig. 1d). As a general rule, the 12°S station has a less radiogenic signature than the two others. This contrast can be related to the origins of the collected waters, the South Pacific being characterized by a less radiogenic signature than the North Pacific [5,18,32].

In the following, we will first discuss the Nd IC of the equatorial intermediate water (0° and 2°N), then that of the lower part of the EUC (0°, 150 m) and finally that of its upper part (0°, 120 m). In the three cases the results will be compared to the 12°S station results, since the latter can be considered as the origin of the waters found at the equator, as described by Tsuchiya ([24, 26,31]) and Tsuchiya and Talley [34] and represented on Fig. 1. The general picture is that part of the water entrained in the SEC (where the 12°S station is located) turns northwestwards towards PNG, and reaches the Central Equatorial Pacific (where the 0° and 2°N stations are located) entrained by equatorial flows. As the SEC is active to depths greater than 1000 m, it entrains the three layers studied here. The AAIW found at the equator comes from the South Subtropical Gyre by the way of western boundary undercurrents such as the NGCU, that flows northwestwards through the Vitiaz Strait and along the north coast of PNG [33,34]. The water found in the lower part of the EUC, originating from the Tasman Sea, flows around the South Subtropical Gyre before entering the NGCU, and finally reaches the EUC. The depth of the isopycnal characterizing this water ($\sigma_\theta = 26.4$) around the 12°S station is roughly 300 m [26]. At its source in the PNG region, the upper part of the EUC is mainly composed of waters originating on the high salinity cell centered around the tropic of Capricorn [24]. This tongue of high salinity was sampled at 135 m depth at the 12°S station. Note that all these trajectories involve western boundary coastal undercurrents of the PNG region.

5.1. Intermediate waters

Samples of intermediate waters at 2°N, 0° and 12°S show very similar hydrological properties ($\theta = 5.40$, 5.34 and 5.18°C, $S = 34.55$, 34.55 and 34.52 psu, $\sigma_\theta = 27.27$, 27.28 and 27.28 at 2°N, 0° and 12°S respectively, see Fig. 3). This indicates that they likely have a common origin, that is AAIW [34]. On the contrary, the measured Nd IC (Fig. 1d), and REE patterns (Fig. 2) are very similar at 2°N and 0° but there are large differences between these two stations and the 12°S one: ε_{Nd} increases from -8 ± 0.3 at 12°S,

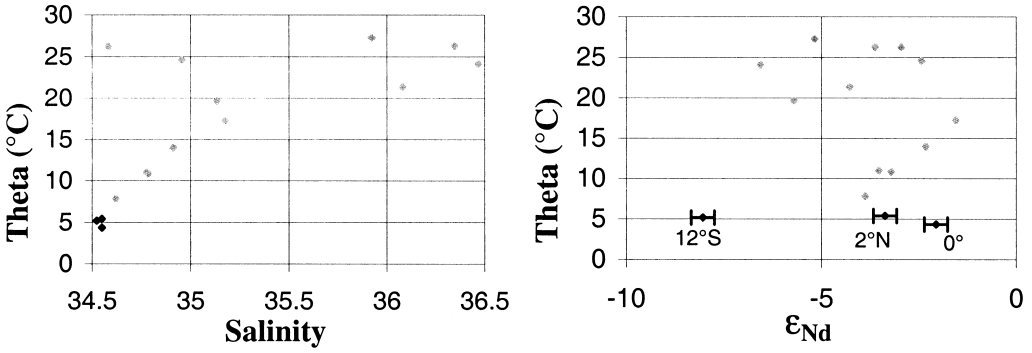

Fig. 3. θ-S and θ–ε_{Nd} diagrams of the analyzed samples. Black symbols represent AAIW samples. On the θ-S diagram AAIW show very similar characteristics, whereas they are clearly distinguishable on the θ–ε_{Nd} diagram.

to -2.1 ± 0.3 and -3.4 ± 0.3 at 0° and 2°N respectively. These significant ε_{Nd} variations contrast with the similar hydrographic properties, as illustrated in Fig. 3. Given that the Nd IC at 2°N and 0° are similar, we will consider only their average ($\varepsilon_{Nd} = -2.8 \pm 0.7$) in the following. As outlined above, such a radiogenic value in the northern part of the EqPac section requires that the AAIW found at 0°/2°N has been modified by an input of radiogenic Nd ($\varepsilon_{Nd} > -2.1$). The AAIW trajectory between 12°S and the equator through the PNG region (see above) offer one viable explanation for the ε_{Nd} variation from -8 in the 'southern' AAIW to -2.8 in the equatorial AAIW. Any ε_{Nd} change requires an input of Nd from a source with a different IC. Hydrography shows no mixing of water masses [34], which implies that the Nd input is of lithogenic origin. PNG (and adjacent volcanic islands) is the only land mass on the possible pathways of AAIW from the South Subtropical Gyre to the Equator. Its northeastern coast (together with the New Britain one, on the other side of the Vitiaz Strait) is characterized by $\varepsilon_{Nd\,PNG} \approx +7$ [20], a value radiogenic enough to allow the observed increase. In support of this, Jeandel et al. [7] suggested that the Nd isotopic signature of water masses is likely to be modified in areas where intense dissolved/particulate exchange occurs. This could happen in the vicinity of coasts, along continental slopes or within straits, where the hydrodynamics would enhance re-suspension of deposited sediment. The Vitiaz Strait is particularly narrow (less than 30 km width at 800 m depth) and is a likely place for changes in Nd IC in the waters flowing through it to occur. For these reasons we conclude that the AAIW isotopic signature is likely to be modified as it flows along the northern coast of PNG.

We now estimate the Nd fluxes required to achieve the observed ε_{Nd} variation through the Vitiaz Strait. The AAIW flows at about 2–4 Sv ([33]; 1 Sv = 10^6 m^3 s^{-1}); we take here the average value ($F_1 = 3$ Sv). It flows at about 800 m depth, so that the Nd input might come from the PNG slope. The Nd concentrations measured in waters having AAIW properties (at 795 m in the Coral Sea, upstream from PNG and at 991 m in the Caroline Sea, downstream of PNG) are respectively $C_{up} = 10$ pmol kg^{-1} and $C_{down} = 9.3$ pmol kg^{-1} [15]. Neglecting the minor decrease, we assume that the Nd concentration is constant in this water mass as it flows along the coast of PNG. We assumed the upstream Nd IC to be that measured at 12°S ($\varepsilon_{Nd\,up} = -8$) and the downstream value to be the average of those measured at 2°N and 0° ($\varepsilon_{Nd\,down} = -2.8$). Constant concentrations combined with a varying ε_{Nd} requires an *exchange* of Nd between the slope of PNG and the AAIW. If E is the average flux of Nd exchanged and $\varepsilon_{Nd\,result}$ the Nd IC resulting from this process, then:

$$\varepsilon_{Nd\,result} \quad \frac{C_{up} \times F_1 - E \times \varepsilon_{Nd\,up} \quad E \times \varepsilon_{Nd\,PNG}}{C_{down} \times F_1} \qquad 1$$

Taking $\varepsilon_{Nd\ PNG} \approx +7$ [20], we find $E = 4.9 \times 10^7$ g(Nd) y^{-1}. The possible process causing this exchange of Nd between the slope of PNG and sea water will be discussed in detail in Section 5.2. However, we can estimate the amount of solid material that would be required to release the Nd contained in its lattice to obtain such fluxes, whatever the process. The Nd concentration in the volcanic PNG material is approximately 9 ppm [20], the percentage of dissolution of Nd from marine particles or sediments in sea water is between 3 and 20% [17,35,36]. Assuming an average of 10% dissolution, the amount of PNG material needed for this Nd exchange is 5.4×10^7 t y^{-1}, that is 9% of the fluvial sediment discharge from PNG to the ocean [37]. Milliman [37] demonstrated that this sediment discharged to an active margin directly reached the deep sea. The steepness of the slope likely induces re-suspension of the deposited material and favors solution/particles contact. The residence time of AAIW in the Vitiaz Strait is around 6 days; it reaches a maximum of 2 months when assuming that it flows along the whole slope of PNG in the NICU. This means an efficient modification of the water mass Nd signature in such an oceanographic context (strong hydrodynamics, high dissolved/particulate exchanges). These results are consistent with the more pronounced Ce anomaly in the 'equatorial type' AAIW: adsorption/desorption processes promote larger anomalies [17]. These results indicate that AAIW is modified from the 'southern type' to the 'equatorial type' by flowing along the PNG coast. They also confirm that the Nd isotope signature helps reconstruct the present-day pathways of a water mass even though its hydrographical properties are not strongly modified along its path (see Fig. 3 and [7]).

5.2. EUC

Two samples were analyzed in the core of the EUC at the equator. Despite their small difference in water depths, their Nd IC differ significantly ($\varepsilon_{Nd} = -5.7 \pm 0.3$ at 120 m and $\varepsilon_{Nd} = -1.6 \pm 1.2$ at 150 m). This indicates that the boundary between the two layers of the EUC is between those depths. The large vertical ε_{Nd} gradient also indicates that the two layers do not influence each other significantly. In other words, the upwelling does not seem to affect the subpycnocline layer of the EUC.

5.2.1. Lower part of the EUC

The lower part of the EUC comprises the 13°C Water. It is a thick and homogeneous layer, not directly involved in the Ekman flow [24] so that, to a first approximation, we assume that its Nd IC remains constant between the source of the EUC and the 140°W section ($\varepsilon_{Nd} = -1.6 \pm 1.2$). The Nd IC of the 13°C Water entering the NGCU was chosen to be that of our 12°S sample having the closest density to that characterizing the 13°C Water ($\varepsilon_{Nd} = -4.3 \pm 1.2$, 200 m). These hypotheses suggest an increase from $\varepsilon_{Nd} = -4.3$ to $\varepsilon_{Nd} = -1.6$ while the water flows in the NGCU. The concentrations measured by Zhang and Nozaki [15] in the Coral and Caroline Sea for the layer with the density of the 13°C Water ($\sigma_\theta = 26.4$) show a slight increase: $C_{up} = 4.9$ pmol kg^{-1} and $C_{down} = 6.6$ pmol kg^{-1} respectively. The flux of the 13°C Water is estimated at $F_2 = 3$ Sv from data given by Lindstrom et al. [38]. The concentration increase (1.7 pmol l^{-1}) in this layer requires an input of Nd from PNG of 2.3×10^7 g(Nd) y^{-1}. With the 13°C Waters flowing around 300 m depth, Nd inputs are likely to be provided by the PNG the upper slope. This input modifies ε_{Nd} as follows:

$$\varepsilon_{Nd\ result} \quad \frac{C_{up} \times F_2 \times \varepsilon_{Nd\ up} \quad C_{down} - C_{up} \times F_2 \times \varepsilon_{Nd\ PNG}}{C_{down} \times F_2} \qquad (2)$$

The resulting Nd IC is $\varepsilon_{Nd\ result} = -1.4$, very close to the measured value of -1.6. No exchange is required this time to reconcile the concentration and isotopic signal variations. This input of Nd roughly corresponds to the remobilization of 2.6×10^7 t y^{-1} of PNG material, that is 4% of the total fluvial load [37]. This small proportion is of the same order as above, and makes our explanation conceivable.

The fact that exchange processes are required

to explain the variations observed in the AAIW and not in the 13°C layer can be related to (1) different speciations of Nd in the different input sources or (2) velocity differences between the currents entraining the 13°C Water and the AAIW (about 70 cm s^{-1} and 12 cm s^{-1}, respectively [33,38]). However this difference of behavior could not be significant because we initially assumed no ε_{Nd} variation within the EUC. However, the salinity at 0° 150 m is 35.17 whereas the same isopycnal leaves the PNG region with a value 35.5. This slight freshening could reflect the merging of waters originating from the Northern Pacific into the EUC, although the precise dynamic of this input is not yet understood [24]. From the literature [5] and this work, the Nd IC of these waters is likely below −1.6. If this input occurs, it would therefore induce a decrease of ε_{Nd} between PNG and 140°W, implying that waters would leave the PNG with a more radiogenic value than that assumed here ($\varepsilon_{Nd} = -1.6$). In that case, the ε_{Nd} increase in the NGCU could no longer be explained by a sole input, an exchange would become necessary. The lack of ε_{Nd} data in the PNG region does not allow us to conclude firmly on that point, the hypothesis of a sole input remaining the most probable hypothesis regarding our data set.

Three kinds of sources can be considered to explain the input: (1) Hydrothermal inputs seem unlikely since it has been demonstrated that the influence of hydrothermalism is not significant for the local and global REE budget in the ocean [39]. (2) Dissolved riverine inputs: following Sholkovitz et al. [16], the europium weathered from PNG as dissolved load explains 20% of the excess of the Eu observed in the upper layers of the Caroline Sea. Using their data, we estimated that about 1.9×10^6 g y^{-1} of dissolved riverine Nd are brought to the upper Caroline Sea, that is less than 10% of the amount required to explain the Nd enrichment and the isotopic variation. In addition, Sholkovitz (personal communication, 2000) provided us with the only dissolved Nd IC measured in the SEPIK river. Its ε_{Nd} is −3.1, definitely more negative than the volcanic material outcropping on the eastern coast (about +7; [20]). Finally, Sholkovitz et al. [16] suggested that the dissolved riverine REE inputs from PNG can be traced in the surface layers of the Caroline Sea by a mid-REE enrichment when the samples are normalized to a composite reference, deduced from the Coral Sea data of Zhang and Nozaki [15]. We applied this normalization to all our REE patterns, and did not observe any mid-REE enrichment between the southern and northern stations of the section. Hence, we suspect that direct input of riverine dissolved Nd plays a minor role in the variations observed. (3) The best candidate is the dissolution of solid material at the continent/ocean interface (shelf, slope...). This process can yield the two types of behaviors, exchange or net input, but does not give a hint which one to favor. This third hypothesis is also invoked to explain 80% of the Eu excess observed in the upper layers of the Caroline Sea, the excess which is not balanced by dissolved riverine [16]. This 'exchange' hypothesis has previously been proposed to reconcile the variations of Nd concentration and Nd IC on a basin scale [6,7] and on a global scale [9,29]. Although it would be useful to quantify this process here, we demonstrated above that our data do not allow to solve that point here. However, the Nd isotope signal does demonstrate what was suspected [40]: that lithogenic elements are transported across the Pacific Ocean within the subpycnocline layer of the EUC and that they originate from PNG.

This westward advection of lithogenic material is supported by the high ^{228}Ra signal observed in subsurface waters collected at the same location as this study, but earlier in the year (spring 1992; [41]). The strong ^{228}Ra gradient also supports the idea that the equatorial upwelling does not affect the 13°C layer. Ku et al. [41] suggested that the source of ^{228}Ra is the nearby western American coast. We do not agree with this interpretation as (1) the ε_{Nd} of Californian inputs is expected to be around −5 [42], which is too low to explain the equatorial ε_{Nd} values and (2) the hydrographic literature clearly states that advection is eastwards for these waters.

5.2.2. Upper part of the EUC

The upper part of the EUC, containing Trop-

ical Waters, is affected by equatorial upwelling and lateral advection. Thus, a large part of its water is renewed on its way from the PNG coast to 140°W [24]. Wells et al. [1] proposed a simple model of this layer to explain the dissolved Fe concentrations measured at 140°W in the EUC: 0.1 nmol kg^{-1} in the upper part and 0.35 nmol kg^{-1} in the lower part. These authors assumed that both layers have the same iron concentration (0.35 nmol kg^{-1}) when leaving the PNG coast, the lower layer remaining unchanged all the way to 140°W. On the contrary, the upper part loses Fe by upwelling, while no enrichment occurs by lateral advection since the surrounding waters are Fe-depleted. This results in an exponential decrease of the dissolved Fe concentration from 0.35 to 0.1 nmol kg^{-1} at 140°W [1]. This model was modified to reconstruct the variation of the Nd IC along the upper layer of the EUC. First, we took into account lateral inputs, since surrounding waters are not Nd-depleted. In addition we considered that the horizontal velocity of the EUC is 0.4 m s^{-1} instead of the 1 m s^{-1} taken by Wells et al. [1]. The former estimate was made for the period of about 6 months that effectively corresponds to the transport of the water that was sampled at 140°W in November 1992. Four different sources of data converge towards this lower value: (1) The TAO ADCP and current meter data at the equator, at 165°E, 170°W and 140°W gave velocities between 0.4 and 0.8 m s^{-1}; but these values overestimate the average EUC current speed since they sample its maximum velocity. (2) Wyrtki and Kilonsky [22] give the mean transport and area of the EUC measured during the Hawaii-to-Tahiti Shuttle Experiment (1979–1980, around 155°W) from which we calculated a mean velocity of 0.4 m s^{-1}. (3) From a depth profile of a modeled zonal velocity averaged over the period from 1992 to 1997 at 0°–140°W [43], we calculated a mean velocity of 0.6 m s^{-1}, likely to be overestimated because centered on the equator, as for the TAO data. (4) Finally, Gourdeau (personal communication, 2000), using the model from Gent and Cane [44], gave us the zonal velocity averaged between 2.2°N and 2.2°S, for the 6 months preceding the sampling. From those simulations we extracted a mean zonal velocity of 0.4 m s^{-1} in the EUC. We therefore adopted 0.4 m s^{-1}.

Then, we estimated the Nd IC in the upper EUC layer at its source. As it has neither the same origin, nor the same volume as the underlying 13°C layer, we cannot assume that it has the same Nd signal when leaving PNG. In its formation region it is characterized by $\varepsilon_{Nd\ up} = -6.6$ (12°S, 135 m). We assumed then that this Tropical Water flowing through the Vitiaz Strait interacts with the PNG upper slope in a similar way to the 13°C Water, i.e. that there is no Nd exchange, only inputs. This assumption is based on the facts that these two water masses are flowing on top of each other in the NGCU (150–200 m and 220–360 m for the Tropical Water and the 13°C Water, respectively); therefore they should interact with similar layers along the slope; in addition, their speeds are close to each other (around 90 cm s^{-1} and 70 cm s^{-1} respectively). The flux of Tropical Water through the Vitiaz Strait is estimated to be 2 Sv [38]. The concentrations upstream and downstream of PNG are those of Zhang and Nozaki [15] in the Coral and Caroline Sea, $C_{up} = 3.5$ pmol kg^{-1} and $C_{down} = 4.25$ pmol kg^{-1} respectively. The values are chosen at $\sigma_\theta = 24.95$, which is the density of the Tropical Water in that area. Applying Eq. 2 to these data, we find $\varepsilon_{Nd\ down} = -4.2$. This value will be used as the starting value in the following model.

The model is sketched on Fig. 4. The upper layer of the EUC is represented as a rectangular box, 8333 km long (from 145°E to 140°W) and 100 m thick (50–150 m). The horizontal velocity is constant and set to 0.4 m s^{-1}, the vertical velocity is also constant and set to 1.23 m day^{-1} [45]. This implies a water renewal of approximately 95% between the source of the EUC and 140°W. This renewal corresponds to a loss from the top due to upwelling and to a gain from the side due to lateral advection. The proportions of water advected from the northern and southern sides of the box are constrained by the salinity budget (Fig. 4). Salinity values used for lateral inputs were those measured during the campaign at 2°N and 2°S at 120 m depth (34.8 and 35.2 respectively). The original salinity value of the Tropical Water in the region of formation of the

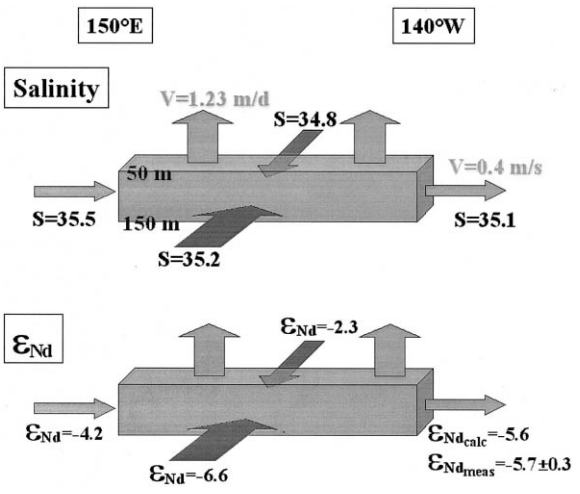

Fig. 4. Model of the upper layer of the EUC, between 150°E and 140°W. The velocity of the westward flow is set to 0.4 m s^{-1}, the one of the upwelling to 1.23 m day^{-1}. Lateral advection is constrained by salinity. The model is then used to calculate ε_{Nd} at 140°W from ε_{Nd} values at the source (150°E) and in the advected waters.

EUC is that given by Tsuchiya et al. ([24]; $S = 35.5$). This constraint implies that out of the 95% of water renewal, 74% came from the south and 21% from the north. We assumed a constant and equal Nd concentration inside and outside the box (this work). The Nd IC for the water advected from the south is set at $\varepsilon_{Nd\ south} = -6.6$ because this is the value of the Tropical Water measured at 12°S. The Nd IC for the water advected from the north is set to $\varepsilon_{Nd\ north} = -2.3$, as measured at the level corresponding to the upper layer of the EUC at 2°N, that is 155 m. The output of the model gives a Nd IC at 140°W in the upper layer of the EUC of −5.6, perfectly consistent with the measured value of -5.7 ± 0.3 for this layer. Owing to the hypothesis made for the ε_{Nd} value for the upper EUC waters at their origin, this agreement has to be considered with caution. Nevertheless, the good agreement between measured and calculated values also holds when a horizontal velocity of 1 m s^{-1} is applied to this model [1]: this corresponds to a renewal of 70% of the water, and yields a calculated ε_{Nd} value of −5, only slightly below the measured one. We also tested the sensitivity of our calculation to the original ε_{Nd} value taken at 12°S: assuming that it is of −3.6, as measured at 12°S, 75 m, the ε_{Nd} value after the PNG would be −1.7 and the resulting ε_{Nd} value after the renewal of waters at 140°W would be −5.5. In any case, the original value of the Tropical water is not crucial for the remaining calculation: the renewal of waters due to the active equatorial upwelling suppresses any PNG contribution on these surface waters. On the other hand, applying a velocity of 0.4 m s^{-1} to calculate the iron concentration variations leads to the total depletion of iron in the surface layer of 140°W, with a calculated value of 0.02 pmol l^{-1}, far below the measured one [46].

Wells et al. [1] suggest that paleo-variations in primary production in the eastern Equatorial Pacific could reflect variations in the tectonic activity of PNG. Such activity would imply variations in the Fe enrichment of the source waters of the EUC and therefore variations of the Fe content of the surface waters of the eastern Equatorial Pacific. Primary production being limited by Fe in this area [46], this would result in variations in the primary production. Our results contradict this hypothesis, as the important renewal of the upper layer of the EUC (due to upwelling) seems to completely eliminate the PNG imprint, as shown by the depletion of the Nd signal in this layer. This would have a similar effect on iron. On the other hand, neither the Fe nor the ε_{Nd} of this water is known at its source today (both are estimated in [1] and this work). In addition, all these hypotheses assume that the mean upwelling conditions today were the same as those in the past, which are not known. Higher Fe contents and/or more radiogenic ε_{Nd} values could yield a remaining signal at 140°W, even after water renewal: ε_{Nd} measurements of sediments deposited during higher productivity events would certainly help to solve these questions.

6. Conclusion

We characterized the Nd IC of hydrodynamic structures in the Equatorial Pacific Ocean at 140°W: Intermediate Water at 12°S: $\varepsilon_{Nd} = -8.0 \pm 0.3$; Intermediate Water of the equatorial

type: $\varepsilon_{Nd} = -2.8 \pm 0.7$; Upper layer of the EUC: $\varepsilon_{Nd} = -5.7 \pm 0.3$; Subpycnocline layer of the EUC: $\varepsilon_{Nd} = -1.6 \pm 1.2$; EIC: $\varepsilon_{Nd} = -3.5 \pm 0.4$; Tropical Water formed in the high salinity cell of the Tropic of Capricorn: $\varepsilon_{Nd} = -6.6 \pm 0.2$

The Nd IC of the three Intermediate Water samples confirm the hypothesis proposed by Tsuchiya and Talley [34]: the Intermediate Water found at 140°W in the equatorial region is a 'modified AAIW' and comes from the South Subtropical Gyre by the way of the western boundary undercurrents. Whereas its hydrological properties remain unchanged, its Nd signature is strongly modified by the contact with the PNG slope, confirming the usefulness of this tracer to identify the pathway of water masses.

The Nd IC measured in the subpycnocline layer of the EUC at 140°W ($\varepsilon_{Nd} = -1.6 \pm 1.2$, 150 m) also reflects the influence of PNG lithogenic inputs on the Central Equatorial Pacific. This emphasizes the importance of jets to transport lithogenic material into the subsurface layers of basin centers, where aeolian inputs are particularly weak. This corroborates the preceding results on Fe and Al maxima in this area [1].

The Nd IC of the upper layer of the EUC ($\varepsilon_{Nd} = -5.7 \pm 0.3$, 120 m) is very different from that of the subpycnocline layer ($\varepsilon_{Nd} = -1.6 \pm 1.2$, 150 m) indicating that upwelling was not active between 150 and 120 m at the place and time of the sampling. A simple model of the upper layer of the EUC, with an average velocity lowered to 60% from the Wells value, shows that the radiogenic Nd enrichment originating from PNG (and therefore Fe enrichment) likely disappears from this layer as it traverses the basin. For these two reasons we suspect that PNG lithogenic inputs were not able to affect the surface water of the Central Equatorial Pacific, as suggested by Wells et al. [1]. However, this contradiction may be due to (i) the simplicity of both Wells' and our models, (ii) the lack of ε_{Nd} and Fe data in the source of EUC (PNG area) and therefore uncertainties on these supposed values.

Our best candidate to explain REE inputs in intermediate and subsurface waters in this area is the dissolution of volcanogenic material, supplied by erosion, caused by boundary undercurrents flowing against the PNG slope. This process is the same as the one suggested by Wells et al. [1] for the iron inputs. Therefore, we suppose that Fe and REE enrichments are tightly linked. This is why, if measurements of traditional paleo-primary production tracers are made in the sediment of the Central Equatorial Pacific to identify past input variations, it would be essential to measure also the authigenic Nd isotopic signatures imprinted in the sediments.

Acknowledgements

Marty Fleisher is deeply thanked for having collected the samples during the EqPac cruise of November 1992. We acknowledge also Margaret Leinen, chief scientist, for having accepted this additional sampling during the cruise, as well as the captain and the crew of the *R.V. Thomson*. We also thank D. Yeghicheyan, K. Tachikawa, M. Roy-Barman, F. Candaudap, M. Souhaut, P. Brunet, M. Valladon and B. Reynier for their analytical and technical support during F. Lacan's master training period. Comments of M. Rutgers Van der Loeff, V. Athias and R. Morrow, as well as the constructive reviews of D. Vance, M. Frank and an anonymous reviewer, considerably helped to improve this manuscript. ***[AH]***

References

[1] M.L. Wells, G.K. Vallis, E.A. Silver, Tectonic processes in Papua New Guinea and past productivity in the eastern Equatorial Pacific Ocean, Nature 398 (1999) 601–604.
[2] S.B. Jacobsen, G.J. Wasserburg, Sm–Nd isotopic evolution of chondrites, Earth Planet. Sci. Lett. 50 (1980) 139–155.
[3] D.J. Piepgras, G.J. Wasserburg, Isotopic composition of neodymium in waters from the Drake Passage, Science 217 (1982) 207–217.
[4] D.J. Piepgras, G.J. Wasserburg, Rare Earth Element transport in the western North Atlantic inferred from isotopic observations, Geochim. Cosmochim. Acta 51 (1987) 1257–1271.
[5] D.J. Piepgras, S.B. Jacobsen, The isotopic composition of neodymium in the North Pacific, Geochim. Cosmochim. Acta 52 (1988) 1373–1381.

[6] C. Jeandel, Concentration and isotopic composition of neodymium in the South Atlantic Ocean, Earth Planet. Sci. Lett. 117 (1993) 581–591.
[7] C. Jeandel, D. Thouron, M. Fieux, Concentrations and Isotopic compositions of Nd in the Eastern Indian Ocean and Indonesian Straits, Geochim. Cosmochim. Acta 62 (1998) 2597–2607.
[8] H. Amakawa, D.S. Alibo, Y. Nozaki, Nd isotopic and REE pattern in the surface waters of the eastern Indian Ocean and its adjacent seas, Geochim. Cosmochim. Acta 64 (2000) 1715–1727.
[9] K. Tachikawa, V. Athias, C. Jeandel, The Neodymium paradox in the ocean, J. Geophys. Res., submitted.
[10] C. Jeandel, J.K. Bishop, A. Zindler, Exchange of Nd and its isotopes between seawater small and large particles in the Sargasso Sea, Geochim. Cosmochim. Acta 59 (1995) 535–547.
[11] F.E. Grousset, M. Parra, A. Bory, P. Martinez, P. Bertrand, G. Shimmield, R.M. Ellam, Saharan wind regimes traced by the Sr–Nd isotopic compositions of the subtropical Atlantic sediments: last glacial maximum vs. today, Q. Sci. Rev. 17 (1998) 395–409.
[12] F. Henry, C. Jeandel, J.-F. Minster, Particulate and dissolved Nd in the Western Mediterranean Sea: sources, fates and budget, Mar. Chem. 45 (1994) 283–305.
[13] K. Tachikawa, C. Jeandel, A. Vangriesheim, B. Dupré, Distribution of Rare Earth Elements and neodymium isotopes in suspended particles of the tropical Atlantic Ocean (EUMELI site), Deep-Sea Res. 46 (1999) 733–756.
[14] H. Elderfield, The oceanic chemistry of the Rare Earth Elements, Phil. Trans. R. Soc. Lond. 325 (1988) 105–106.
[15] J. Zhang, Y. Nozaki, Rare Earth Elements and yttrium in seawater: ICP-MS determinations in the East Caroline, Coral Sea and South Fiji basins of the western south Pacific Ocean, Geochim. Cosmochim. Acta 60 (1996) 4631–4644.
[16] E.R. Sholkovitz, H. Elderfield, R. Szymczak, K. Casey, Island weathering: river sources of Rare Earth Elements to the Western Pacific Ocean, Mar. Chem. 68 (1999) 39–57.
[17] K. Tachikawa, C. Jeandel, M. Roy-Barman, A new approach to Nd residence time in the ocean: the role of atmospheric inputs, Earth Planet. Sci. Lett. 170 (1999) 433–446.
[18] H. Shimizu, K. Tachikawa, A. Masuda, Y. Nozaki, Cerium and neodymium ratios and REE patterns in seawater from the North Pacific Ocean, Geochim. Cosmochim. Acta 58 (1994) 323–333.
[19] R.A. Duce, P.S. Liss, J.T. Merrill, E.L. Atlas, P. Buat-Ménard, B.B. Hicks, J.M. Miller, J.M. Prospero, R. Arimoto, T.M. Church, W. Ellis, J.N. Galloway, L. Hansen, T.D. Jickells, A.H. Knap, K.H. Reinhardt, B. Schneider, A. Soudine, J.J. Tokos, S. Tsunogai, R. Wollast, M. Zhou, The atmospheric input of trace species to the world ocean, Glob. Biogeochem. Cycles 5 (1991) 193–259.
[20] J.B. Gill, J.D. Morris, R.W. Johnson, Timescale for producing the geochemical signature of island arc magmas: U–Th–Po and Be–B systematics in recent Papua New Guinea lavas, Geochim. Cosmochim. Acta 57 (1993) 4269–4283.
[21] J.L. Reid, On the total geostrophic circulation of the pacific ocean: flow patterns, tracers, and transports, Prog. Oceanogr. 39 (1997) 236–352.
[22] K. Wyrtki, B. Kilonsky, Mean water and current structure during the Hawaii-to-Tahiti shuttle experiment, J. Phys. Oceanogr. 14 (1984) 242–254.
[23] R. Lukas, E. Firing, The geostrophic balance of the Pacific Equatorial Undercurrent, Deep-Sea Res. 31 (1984) 61–66.
[24] M. Tsuchiya, R. Lukas, R.A. Fine, Source Waters of the Pacific Equatorial Undercurrent, Prog. Oceanogr. 23 (1989) 101–147.
[25] J. Butt, E. Lindstrom, Currents off the east coast of New Ireland, Papua New Guinea, and their relevance to regional undercurrents in the Western Equatorial Pacific Ocean, J. Geophys. Res. 99 (1999) 12503–12514.
[26] M. Tsuchiya, The Origin of the Pacific Equatorial 13°C Water, J. Phys. Oceanogr. 11 (1981) 794–812.
[27] M. Loubet, Géochimie des Terres Rares dans les massifs de péridotites dits de 'haute température'. Evolution du manteau terrestre, Ph.D., Paris VII, 1976.
[28] P. Richard, N. Shimizu, C.J. Allègre, $^{143}Nd/^{146}Nd$, a natural tracer: an application to oceanic basalts, Earth Planet. Sci. Lett. 31 (1976) 269–278.
[29] C.J. Bertram, H. Elderfield, The geochemical balance of the Rare Earth Elements and Nd isotopes in the oceans, Geochim. Cosmochim. Acta 57 (1993) 1957–1986.
[30] M.J. Greaves, H. Elderfield, E.R. Sholkovitz, Aeolian sources of Rare Earth Elements to the Western Pacific Ocean, Mar. Chem. 68 (1999) 31–38.
[31] D.J. Piepgras, G.J. Wasserburg, E.G. Dasch, The isotopic composition of Nd in different ocean masses, Earth Planet. Sci. Lett. 45 (1979) 223–236.
[32] A. Aplin, A. Michard, F. Albarede, $^{143}Nd/^{144}Nd$ in Pacific ferromanganese incrustations and nodules, Earth Planet. Sci. Lett. 81 (1986) 7–14.
[33] M. Tsuchiya, Flow path of the Antarctic Intermediate Water in the western equatorial South Pacific Ocean, Deep-Sea Res. 38 (Suppl. 1) (1991) S273–S279.
[34] M. Tsuchiya, L.D. Talley, Water-property distributions along an eastern Pacific hydrographic section at 135°W, J. Mar. Res. 54 (1996) 541–564.
[35] R. Arraes-Mescoff, L. Coppola, M. Roy-Barman, M. Souhaut, K. Tachikawa, C. Jeandel, R. Sempéré, C. Yoro, The behavior of Al, Mn, Ba, Sr, REE and Th isotopes during in vitro bacterial degradation of large marine particles, Mar. Chem., in press.
[36] M.J. Greaves, P.J. Statham, H. Elderfield, Rare Earth Element mobilization from marine atmospheric dust into seawater, Mar. Chem. 46 (1994) 255–260.
[37] J.D. Milliman, Sediment discharge to the ocean from mountainous rivers: the New Guinea example, Geo-Mar. Lett. 15 (1995) 127–133.
[38] E. Lindstrom, J. Butt, R. Lukas, S. Godfrey, The flow

through Vitiaz Strait and St. George's channel, Papua New Guinea, The physical Oceanography of Sea Straits, 1990, pp. 171–189.
[39] A. Michard, F. Albarède, G. Michard, J.F. Minster, J.L. Charlou, Rare Earth Elements and uranium in high-temperature solutions from East Pacific Rise hydrothermal vent field (13°N), Nature 303 (1983) 795–797.
[40] A.L. Gordon, H.W. Taylor, D.T. Georgi, Antarctic oceanographic zonation, in: Polar Oceans Conference, M.J. Dunbar, 1977, pp. 45–76.
[41] T.L. Ku, S. Luo, M. Kusakabe, J.K.B. Bishop, ^{228}Ra-derived nutrient budgets in the upper Equatorial Pacific and the role of 'new' silicate in limiting productivity, Deep-Sea Res. 42 (1995) 479–497.
[42] S.L. Goldstein, S.B. Jacobsen, The Nd and Sr isotopic systematics of river-water dissolved material: implications for the sources of Nd and Sr in the seawater, Chem. Geol. Isot. Geosc. Sect. 66 (1987) 245–272.
[43] H.F. Seidel, B.S. Giese, Equatorial currents in the Pacific Ocean 1992–1997, J. Geophys. Res. 104 (1999) 7849–7863.
[44] P.R. Gent, M.A. Cane, A reduced gravity primitive equation model of the upper equatorial ocean, J. Comput. Phys. 81 (1989) 444–480.
[45] H.L. Bryden, E.C. Brady, Diagnostic model of the three-dimensional circulation in the upper Equatorial Pacific Ocean, J. Phys. Oceanogr. 15 (1985) 1255–1273.
[46] K.H. Coale, S.E. Fitzwater, R.M. Gordon, K.S. Johnson, R.T. Barber, Control of community growth and export production by upwelled iron in the Equatorial Pacific Ocean, Nature 379 (1996) 621–624.
[47] M. Tomczak, J.S. Godfrey, Regional Oceanography: An Introduction, Pergamon, Oxford, 1994, 422 pp.

IV. Références

Abouchami, W., S. J. G. Galer, H. J. W. de Baar, A. C. Alderkamp, R. Middag, P. Laan, H. Feldmann, et M. O. Andreae (2011), Modulation of the Southern Ocean cadmium isotope signature by ocean circulation and primary productivity, *Earth and Planetary Science Letters*, *305*(1–2), 83‑91, doi:10.1016/j.epsl.2011.02.044.

Alibo, D. S., et Y. Nozaki (1999), Rare earth elements in seawater: particle association, shale-normalization, and Ce oxidation, *Geochimica et Cosmochimica Acta*, *63*(3-4), 363‑372, doi:16/S0016-7037(98)00279-8.

Arsouze, T., J. C. Dutay, M. Kageyama, F. Lacan, R. Alkama, O. Marti, et C. Jeandel (2008), A modeling sensitivity study of the influence of the Atlantic meridional overturning circulation on neodymium isotopic composition at the Last Glacial Maximum, *Climate of the Past*, *4*(3), 191‑203.

Arsouze, T., J. C. Dutay, F. Lacan, et C. Jeandel (2007), Modeling the neodymium isotopic composition with a global ocean circulation model, *Chemical Geology*, *239*(1-2), 165‑177.

Arsouze, T., J. Dutay, F. Lacan, et C. Jeandel (2009), Reconstructing the Nd oceanic cycle using a coupled dynamical - biogeochemical model, *Biogeosciences*, *6*(12), 2829‑2846.

Arsouze, T., A. Treguier, S. Peronne, J. Dutay, F. Lacan, et C. Jeandel (2010), Modeling the Nd isotopic composition in the North Atlantic basin using an eddy-permitting model, *OCEAN SCIENCE*, *6*(3), 789‑797, doi:10.5194/os-6-789-2010.

Aumont, O., et L. Bopp (2006), Globalizing results from ocean in situ iron fertilization studies, *Global Biogeochemical Cycles*, *20*(2), doi:10.1029/2005GB002591.

Aumont, O., E. Maier-Reimer, S. Blain, et P. Monfray (2003), An ecosystem model of the global ocean including Fe, Si, P co-limitation, *Global Biogeochemical Cycles*, *17*, doi:10.1029/2001GB001745.

De Barr, H. J. W., et J. T. M. de Jong (2001), Distributions, Sources and Sinks of Iron in Seawater, in *The Biogeochemistry of Iron in Seawater*, p. 123‑253.

Beard, B., C. Johnson, J. Skulan, K. Nealson, L. Cox, et H. Sun (2003a), Application of Fe isotopes to tracing the geochemical and biological cycling of Fe, *Chemical Geology*, *195*, 87‑ 117.

Beard, B. L., C. M. Johnson, L. Cox, H. Sun, K. H. Nealson, et C. Aguilar (1999), Iron isotope biosignatures, *Science*, *285*(5435), 1889‑1892.

Beard, B. L., C. M. Johnson, K. L. Von Damm, et R. L. Poulson (2003b), Iron isotope constraints on Fe cycling and mass balance in oxygenated Earth oceans, *Geology*, *31*, 629–632.

Bennett, S. A., E. P. Achterberg, D. P. Connelly, P. J. Statham, G. R. Fones, et C. R. German (2008), The distribution and stabilisation of dissolved Fe in deep-sea hydrothermal plumes, *Earth and Planetary Science Letters*, *270*(3-4), 157‑167, doi:10.1016/j.epsl.2008.01.048.

Bergquist, B. A., et E. A. Boyle (2006), Iron isotopes in the Amazon River system: Weathering and transport signatures, *Earth and Planetary Science Letters*, *248*(1-2), 54‑68.

Blain, S., G. Sarthou, et P. Laan (2008), Distribution of dissolved iron during the natural iron-fertilization experiment KEOPS (Kerguelen Plateau, Southern Ocean), *Deep Sea Research Part II: Topical Studies in Oceanography*, *55*(5-7), 594‑605.

Von Blanckenburg, F., et T. F. Nagler (2001), Weathering versus circulation-controlled changes in radiogenic isotope tracer composition of the Labrador Sea and North Atlantic Deep Water, *Paleoceanography*, *16*(4), 424‑434.

Bown, J., M. Boye, A. Baker, E. Duvieilbourg, F. Lacan, F. Le Moigne, F. Planchon, S. Speich, et D. M. Nelson (2011), The biogeochemical cycle of dissolved cobalt in the Atlantic and the Southern Ocean south off the coast of South Africa, *Marine Chemistry*, *126*(1–4), 193‑206, doi:10.1016/j.marchem.2011.03.008.

Boyd, P. W. et al. (2007), Mesoscale iron enrichment experiments 1993-2005: Synthesis and future directions, *Science*, *315*(5812), 612‑617.

Boyd, P. W., et M. J. Ellwood (2010), The biogeochemical cycle of iron in the ocean, *Nature Geoscience*, *3*(10), 675‑682, doi:10.1038/ngeo964.

Boyle, E. A. (1988), Cadmium: chemical tracer of deepwater paleoceanography, *Paleoceanography*, *3*, 471‑489.

Boyle, E. A., S. John, W. Abouchami, J. F. Adkins, Y. Echegoyen-Sanz, M. Ellwood, A. R. Flegal, K. Fornace, C. Gallon, et S. Galer (2012), GEOTRACES IC1 (BATS) contamination-prone trace element isotopes Cd, Fe, Pb, Zn, Cu, and Mo intercalibration, *Limnology and Oceanography: Methods*, *10*, 653‑665, doi:10.4319/lom.2012.10.653.

De Brauwere, A., C. Jeandel, F. Lacan, P. van Beek, C. Venchiarutti, et F. Fripiat (2012), Putting the pieces together: _A multi-tracer model for the Kerguelen Plateau, San Francisco USA.

Bullen, T. D., A. F. White, C. W. Childs, D. V. Vivit, et M. S. Schulz (2001), Demonstration of significant abiotic iron isotope fractionation in nature, *Geology*, *29*, 699–702.

Chase, Z., R. F. Anderson, M. Q. Fleisher, et P. W. Kubik (2002), The influence of particle composition and particle flux on scavenging of Th, Pa and Be in the ocean, *Earth and Planetary Science Letters*, *204*(1-2), 215‑229.

Chen, M., R. C. . Dei, W.-X. Wang, et L. Guo (2003), Marine diatom uptake of iron bound with natural colloids of different origins, *Marine Chemistry*, *81*(3-4), 177‑189, doi:10.1016/S0304-4203(03)00032-X.

Coale, K. H., S. E. Fitzwater, R. M. Gordon, K. S. Johnson, et R. T. Barber (1996), Control of community growth and export production by upwelled iron in the equatorial Pacific Ocean, *Nature*, *379*, 621‑624.

Croot, P. L., et M. Johansson (2000), Determination of Iron Speciation by Cathodic Stripping Voltammetry in Seawater Using the Competing Ligand 2-(2-Thiazolylazo)-p-cresol (TAC), *Electroanalysis*, *12*(8), 565–576.

Cullen, J. T., T. W. Lane, F. M. M. Morel, et R. M. Sherrell (1999), Modulation of cadmium uptake in phytoplankton by seawater CO2 concentration, *Nature*, *402*, 165‑167.

Deshayes, J., C. Frankignoul, et H. Drange (2007), Formation and export of deep water in the Labrador and Irminger Seas in a GCM, *Deep-Sea Res. Part I-Oceanogr. Res. Pap.*, *54*(4), 510‑532, doi:10.1016/j.dsr.2006.12.014.

Dutay, J. C., F. Lacan, M. Roy-Barman, et L. Bopp (2009), Influence of particle size and type on Pa-231 and Th-230 simulation with a global coupled biogeochemical-ocean general circulation model: A first approach, *Geochemistry Geophysics Geosystems*, *10*.

Elderfield, H., et R. E. M. Rickaby (2000), Oceanic Cd/P ratio and nutrient utilization in the glacial Southern Ocean, *Nature*, *405*, 305‑310.

Elrod, V. A., W. M. Berelson, K. H. Coale, et K. S. Johnson (2004), The flux of iron from continental shelf sediments: A missing source for global budgets, *Geophysical Research Letters*, *31*, doi:10.1029/2004GL020216.

Escoube, R., O. J. Rouxel, E. Sholkovitz, et O. F. X. Donard (2009), Iron isotope systematics in estuaries: The case of North River, Massachusetts (USA), *Geochimica et Cosmochimica Acta*, *73*(14), 4045‑4059, doi:10.1016/j.gca.2009.04.026.

Fitzsimmons, N., W. J. Jenkins, J. M. Lee, R. A. Kayser, et E. A. Boyle (2012), Distal transport of hydrothermal iron in the deep Eastern South Pacific Ocean,

Van de Flierdt, T., K. Pahnke, H. Amakawa, P. Andersson, C. Basak, B. Coles, C. Colin, K. Crocket, M. Frank, et N. Frank (2012), GEOTRACES intercalibration of neodymium isotopes and rare earth element concentrations in seawater and suspended particles. Part 1: reproducibility of results for the international intercomparison, *Limnology and Oceanography: Methods*, *10*, 234‑251, doi:10.4319/lom.2012.10.234.

Garcia-Solsona, E., C. Jeandel, M. Labatut, F. Lacan, D. Vance, et V. Chavagnac (Submitted), Rare Earth Elements and Nd isotopes tracing water mass mixing and particle-seawater interactions in the SE Atlantic...Garcia-Solsona, E., Jeandel, C., Lacan, F., Labatut, M., Vance, D. and Chavagnac, V., *Geochimica et Cosmochimica Acta*.

Gherardi, J.-M., L. Labeyrie, S. Nave, R. Francois, J. F. McManus, et E. Cortijo (2009), Glacial-interglacial circulation changes inferred from Pa-231/Th-230 sedimentary record in the North Atlantic region, *Paleoceanography*, *24*, doi:10.1029/2008PA001696.

Goldstein, S. L., et S. R. Hemming (2003), Long lived Isotopic Tracers in Oceanography, Paleoceanography, and Ice sheet dynamics, in *Treatise on Geochemistry*, p. chapter 6.17, Elsevier Pergamon press, Amsterdam.

Grenier, M., C. Jeandel, F. Lacan, D. Vance, C. Venchiarutti, A. Cros, et S. Cravatte (2012), From the subtropics to the central equatorial Pacific Ocean: Neodymium isotopic composition and rare earth element concentration variations, *Journal of Geophysical Research*, doi:10.1029/2012JC008239.

Homoky, W., S. Severmann, R. Mills, P. Statham, et G. Fones (2009), Pore-fluid Fe isotopes reflect the extent of benthic Fe redox recycling: Evidence from continental shelf and deep-sea sediments, *Geology*, *37*(8), 751‑754, doi:10.1130/G25731A.1.

Van Hulten, M. M. P., A. Sterl, A. Tagliabue, J.-C. Dutay, M. Gehlen, H. J. W. de Baar, et R. Middag (2012), Aluminium in an ocean general circulation model compared with the West Atlantic Geotraces cruises, *Journal of Marine Systems*, (0), doi:10.1016/j.jmarsys.2012.05.005.

Ingri, J., D. Malinovsky, I. Rodushkin, D. C. Baxter, A. Widerlund, P. Andersson, Ö. Gustafsson, W. Forsling, et B. Öhlander (2006), Iron isotope fractionation in river colloidal matter, *Earth and Planetary Science Letters*, *245*(3–4), 792‑798, doi:10.1016/j.epsl.2006.03.031.

Jacobsen, S. B., et G. J. Wasserburg (1980), Sm-Nd isotopic evolution of chondrites, *Earth and Planetary Science Letters*, *50*, 139‑155.

Jeandel, C., T. Arsouze, F. Lacan, P. Techine, et J. C. Dutay (2007), Isotopic Nd compositions and concentrations of the lithogenic inputs into the ocean: A compilation, with an emphasis on the margins, *Chemical Geology*, *239*(1-2), 156‑164.

Jeandel, C., J. K. Bishop, et A. Zindler (1995), Exchange of Nd and its isotopes between seawater small and large particles in the Sargasso Sea, *Geochimica et Cosmochimica Acta*, *59*, 535‑547.

Jeandel, C., H. Delattre, M. Grenier, C. Pradoux, et F. Lacan (2013), Rare earth element concentrations and Nd isotopes in the South East Pacific Ocean, *Geochemistry Geophysics Geosystems*, doi:10.1029/2012GC004309.

Jeandel, C., B. Peucker-Ehrenbrink, M. T. Jones, C. R. Pearce, E. H. Oelkers, Y. Godderis, F. Lacan, O. Aumont, et T. Arsouze (2011a), Ocean margins: The missing term in oceanic element budgets?, *Eos, Transactions American Geophysical Union*, *92*(26), 217–218, doi:10.1029/2011EO260001.

Jeandel, C., D. Thouron, et M. Fieux (1998), Concentrations and Isotopic compositions of Nd in the Eastern Indian Ocean and Indonesian Straits, *Geochimica et Cosmochimica Acta*, *62*, 2597‑2607.

Jeandel, C., C. Venchiarutti, M. Bourquin, C. Pradoux, F. Lacan, P. van Beek, et J. Riotte (2011b), Single Column Sequential Extraction of Ra, Nd, Th, Pa and U from a Natural Sample, *Geostandards and Geoanalytical Research*, *35*(4), 449–459, doi:10.1111/j.1751-908X.2010.00087.x.

Jickells, T. D. et al. (2005), Global iron connections between desert dust, ocean biogeochemistry, and climate, *Science*, *308*(5718), 67‑71.

John, S., et J. Adkins (2010), Analysis of dissolved iron isotopes in seawater, *Marine Chemistry*, *119*(1-4), 65‑76, doi:10.1016/j.marchem.2010.01.001.

John, S. G., J. Mendez, J. Moffett, et J. Adkins (2012), The flux of iron and iron isotopes from San Pedro Basin sediments, *Geochimica et Cosmochimica Acta*, *93*, 14 ‑ 29, doi:10.1016/j.gca.2012.06.003.

Johnson, C. M., B. L. Beard, et E. E. Roden (2008), The iron isotope fingerprints of redox and biogeochemical cycling in the modern and ancient Earth, *Annual Review of Earth and Planetary Sciences*, *36*, 457‑493.

Johnson, C. M., E. E. Roden, S. A. Welch, et B. L. Beard (2005), Experimental constraints on Fe isotope fractionation during magnetite and Fe carbonate formation coupled to dissimilatory hydrous ferric oxide reduction, *Geochimica et Cosmochimica Acta*, *69*(4), 963 ‑ 993, doi:10.1016/j.gca.2004.06.043.

Johnson, K. S., R. M. Gordon, et K. H. Coale (1997), What controls dissolved iron concentrations in the world ocean?, *Marine Chemistry*, *57*, 137‑161.

Jones, M. T., C. R. Pearce, C. Jeandel, S. R. Gislason, E. S. Eiriksdottir, V. Mavromatis, et E. H. Oelkers (2012a), Riverine particulate material dissolution as a significant flux of strontium to the oceans, *Earth and Planetary Science Letters*, *355–356*, 51‑59, doi:10.1016/j.epsl.2012.08.040.

Jones, M. T., C. R. Pearce, et E. H. Oelkers (2012b), An experimental study of the interaction of basaltic riverine particulate material and seawater, *Geochimica et Cosmochimica Acta*, *77*, 108‑120, doi:10.1016/j.gca.2011.10.044.

De Jong, J., V. Schoemann, J. L. Tison, S. Becquevort, F. Masson, D. Lannuzel, J. Petit, L. Chou, D. Weis, et N. Mattielli (2007), Precise measurement of Fe isotopes in marine samples by multi-collector inductively coupled plasma mass spectrometry (MC-ICP-MS), *Analytica Chimica Acta*, *589*(1), 105‑119.

Lacan, F. (2002), Masses d'eau des Mers Nordiques et de l'Atlantique Subarctique tracées par les isotopes du néodyme, PhD thesis, Toulouse III University, France. [en ligne] Available from: http://tel.archives-ouvertes.fr/tel-00118162

Lacan, F., R. Francois, Y. C. Ji, et R. M. Sherrell (2006), Cadmium isotopic composition in the ocean, *Geochimica Et Cosmochimica Acta*, *70*(20), 5104‑5118.

Lacan, F., et C. Jeandel (2001), Tracing Papua New Guinea imprint on the central Equatorial Pacific Ocean using neodymium isotopic compositions and Rare Earth Element patterns, *Earth and Planetary Science Letters*, *186*(3-4), 497‑512.

Lacan, F., et C. Jeandel (2004a), Denmark Strait water circulation traced by heterogeneity in neodymium isotopic compositions, *Deep-Sea Research Part I-Oceanographic Research Papers*, *51*(1), 71‑82, doi:10.1016/j.dsr.2003.09.006.

Lacan, F., et C. Jeandel (2004b), Neodymium isotopic composition and rare earth element concentrations in the deep and intermediate Nordic Seas: Constraints on the Iceland Scotland Overflow Water signature, *Geochemistry Geophysics Geosystems*, *5*, doi:10.1029/2004GC000742.

Lacan, F., et C. Jeandel (2004c), Subpolar Mode Water formation traced by neodymium isotopic composition, *Geophysical Research Letters*, *31*(14), doi:10.1029/2004GL019747.

Lacan, F., et C. Jeandel (2005a), Acquisition of the neodymium isotopic composition of the North Atlantic Deep Water, *Geochemistry Geophysics Geosystems*, *6*, doi:10.1029/2005GC000956.

Lacan, F., et C. Jeandel (2005b), Neodymium isotopes as a new tool for quantifying exchange fluxes at the continent-ocean interface, *Earth and Planetary Science Letters*, *232*(3-4), 245‑257, doi:10.1016/j.epsl.2005.01.004.

Lacan, F., A. Radic, C. Jeandel, F. Poitrasson, G. Sarthou, C. Pradoux, et R. Freydier (2008), Measurement of the isotopic composition of dissolved iron in the open ocean, *Geophysical Research Letters*, *35*(24).

Lacan, F., A. Radic, M. Labatut, C. Jeandel, F. Poitrasson, G. Sarthou, C. Pradoux, J. Chmeleff, et R. Freydier (2010), High-Precision Determination of the Isotopic Composition of Dissolved Iron in Iron Depleted Seawater by Double Spike Multicollector-ICPMS, *Analytical Chemistry*, *82*(17), 7103‑7111, doi:10.1021/ac1002504.

Lacan, F., K. Tachikawa, et C. Jeandel (2012), Neodymium isotopic composition of the oceans: A compilation of seawater data, *Chemical Geology*, *300–301*(0), 177 - 184, doi:10.1016/j.chemgeo.2012.01.019.

Mackey, D. J., J. E. O'Sullivan, et R. J. Watson (2002), Iron in the western Pacific: a riverine or hydrothermal source for iron in the Equatorial Undercurrent?, *Deep-Sea Research Part I-Oceanographic Research Papers*, *49*(5), 877‑893.

Martin, J. H. (1990), Glacial-Interglacial CO2 Change: The Iron Hypothesis, *Paleoceanography*, *5*, 1‑13.

Martin, J. H., et S. E. Fitzwater (1988), Iron deficiency limits phytoplancton growth in the north-east Pacific subarctic., *Nature*, *331*, 341‑343.

Martin, J. H., et R. M. Gordon (1988), Northeast Pacific iron distribution in relation to phytoplancton productivity, *Deep-Sea Research*, *35*, 177‑196.

McManus, J. F., R. Francois, J.-M. Gherardi, L. D. Keigwin, et S. Brown-Leger (2004), Collapse and rapid resumption of Atlantic meridional circulation linked to deglacial climate changes, *Nature*, *428*, 834‑837.

Milliman, J. D. (1995), Sediment discharge to the ocean from mountainous rivers: the New Guinea example, *Geo-Mar. Lett.*, *15*, 127‑133.

Moore, J. K., et O. Braucher (2008), Sedimentary and mineral dust sources of dissolved iron to the world ocean, *Biogeosciences*, *5*(3), 631‑656.

Moore, J. K., S. C. Doney, et K. Lindsay (2004), Upper ocean ecosystem dynamics and iron cycling in a global three-dimensional model, *Global Biogeochemical Cycles*, *18*(4), n/a–n/a, doi:10.1029/2004GB002220.

Morel, F. M. M., et N. M. Price (2003), The Biogeochemical Cycles of Trace Metals in the Oceans, *Science*, *300*, 944‑947.

Morel, F. M. M., J. R. Reinfelder, S. B. Roberts, C. P. Chamberlain, J. G. Lee, et D. Yee (1994), Zinc and carbon co-limitation of marine phytoplankton, *Nature*, *369*, 740‑742.

Negre, C., R. Zahn, A. L. Thomas, P. Masqué, G. M. Henderson, G. Martínez-Méndez, I. R. Hall, et J. L. Mas (2010), Reversed flow of Atlantic deep water during the Last Glacial Maximum, *Nature*, *468*(7320), 84‑88, doi:10.1038/nature09508.

Nozaki, Y. (1997), A fresh look at element distribution in the North Pacific Ocean, *Eos Trans. AGU*, *78*(21), 221‑221, doi:10.1029/97EO00148.

Paulmier, A., et D. Ruiz-Pino (2009), Oxygen minimum zones (OMZs) in the modern ocean, *Progress in Oceanography*, *80*(3–4), 113‑128, doi:10.1016/j.pocean.2008.08.001.

Piepgras, D. J., et G. J. Wasserburg (1987), Rare earth element transport in the western North Atlantic inferred from isotopic observations, *Geochimica et Cosmochimica Acta*, *51*, 1257‑1271.

Piotrowski, A. M., S. L. Goldstein, H. R., R. G. Fairbanks, et D. R. Zylberberg (2008), Oscillating glacial northern and southern deep water formation from combined neodymium and carbon isotopes, *Earth and Planetary Science Letters*, *272*(1-2), 394‑405, doi:16/j.epsl.2008.05.011.

Poitrasson, F. (2006), On the iron isotope homogeneity level of the continental crust, *Chemical Geology*, *235*(1-2), 195‑200.

Radic, A., F. Lacan, et J. W. Murray (2011), Isotopic composition of dissolved iron in the equatorial Pacific Ocean: new constraints for the oceanic iron cycle, *Earth And Planetary Science Letters*, *306*, 1‑10, doi:10.1016/j.epsl.2011.03.015.

Raiswell, R., L. G. Benning, M. Tranter, et S. Tulaczyk (2008), Bioavailable iron in the Southern Ocean: the significance of the iceberg conveyor belt, *Geochemical Transactions*, *9*(1), 7, doi:10.1186/1467-4866-9-7.

Revels, B. N., et J. G. John (2012), Chemical leaching methods and measurements of marine labile particulate Fe,

Ripperger, S., M. Rehkämper, D. Porcelli, et A. N. Halliday (2007), Cadmium isotope fractionation in seawater — A signature of biological activity, *Earth and Planetary Science Letters*, *261*(3–4), 670‑684, doi:10.1016/j.epsl.2007.07.034.

Rousseau, T. C. C., J. E. Sonke, J. Chmeleff, F. Candaudap, F. Lacan, G. Boaventura, P. Seyler, et C. Jeandel (2013), Rare earth element analysis in natural waters by multiple isotope dilution – sector field ICP-MS, *J. Anal. At. Spectrom.*, doi:10.1039/C3JA30332B.

Rouxel, O. J., et M. Auro (2010), Iron Isotope Variations in Coastal Seawater Determined by Multicollector ICP-MS, *Geostandards and Geoanalytical Research*, *34*(2), 135–144, doi:10.1111/j.1751-908X.2010.00063.x.

Rouxel, O., W. C. Shanks III, W. Bach, et K. J. Edwards (2008), Integrated Fe- and S-isotope study of seafloor hydrothermal vents at East Pacific Rise 9–10°N, *Chemical Geology*, *252*(3–4), 214‑227, doi:10.1016/j.chemgeo.2008.03.009.

Sarthou, G. et al. (2003), Atmospheric iron deposition and sea-surface dissolved iron concentrations in the eastern Atlantic Ocean, *Deep-Sea Research Part I-Oceanographic Research Papers*, *50*(10-11), 1339‑1352.

Sarthou, G., E. Bucciarelli, F. Chever, S. P. Hansard, M. González-Dávila, J. M. Santana-Casiano, F. Planchon, et S. Speich (2011), Labile Fe(II) concentrations in the Atlantic sector of the Southern Ocean along a transect from the subtropical domain to the Weddell Sea Gyre, *Biogeosciences*, *8*(9), 2461‑2479, doi:10.5194/bg-8-2461-2011.

Saunier, G., G. S. Pokrovski, et F. Poitrasson (2011), First experimental determination of iron isotope fractionation between hematite and aqueous solution at hydrothermal conditions, *Geochim. Cosmochim. Acta*, *75*(21), 6629‑6654, doi:10.1016/j.gca.2011.08.028.

Severmann, S., C. M. Johnson, B. L. Beard, et J. McManus (2006), The effect of early diagenesis on the Fe isotope compositions of porewaters and authigenic minerals in continental margin sediments, *Geochimica et Cosmochimica Acta*, *70*, 2006‑2022. doi:10.1016/j.gca.2006.01.007.

Severmann, S., T. W. Lyons, A. Anbar, J. McManus, et G. Gordon (2008), Modern iron isotope perspective on the benthic iron shuttle and the redox evolution of ancient oceans, *Geology*, *36*(6), 487.

Severmann, S., J. McManus, W. M. Berelson, et D. E. Hammond (2010), The continental shelf benthic iron flux and its isotope composition, *Geochimica et Cosmochimica Acta*.

Severmann, S., J. McManus, C. M. Johnson, et B. L. Beard (2004), Iron Isotope Geochemistry in California Margin Sediments and Porewaters, in *Ocean Science Meeting*, Portland, OR. (USA).

Sharma, M., M. Polizzotto, et A. D. Anbar (2001), Iron isotopes in hot springs along the Juan de Fuca Ridge, *Earth and Planetary Science Letters*, *194*(1-2), 39‑51.

Sholkovitz, E. R., W. M. Landing, et B. L. Lewis (1994), Ocean particle chemistry: The fractionation of rare earth elements between suspended particles and seawater., *Geochemica Cosmochemica Acta*, *58*, 1567‑1579.

Slemons, L. O., J. W. Murray, J. Resing, B. Paul, et P. Dutrieux (2010), Western Pacific coastal sources of iron, manganese, and aluminum to the Equatorial Undercurrent, *Glob. Biogeochem. Cycle*, *24*, doi:10.1029/2009GB003693.

Tachikawa, K., V. Athias, et C. Jeandel (2003), Neodymium budget in the modern ocean and paleoceanographic implications, *Journal of Geophysical Research*, *108*(C8), 3254, doi:10.1029/1999JC000285.

Tachikawa, K., T. Toyofuku, I. Basile-Doelsch, et T. Delhaye (2013), Microscale neodymium distribution in sedimentary planktonic foraminiferal tests and associated mineral phases, *Geochimica et Cosmochimica Acta*, *100*, doi:10.1016/j.gca.2012.10.010.

Tagliabue, A. et al. (2010), Hydrothermal contribution to the oceanic dissolved iron inventory, *Nature Geoscience*, *3*(4), 252‑256, doi:10.1038/ngeo818.

Waeles, M., A. R. Baker, T. Jickells, et J. Hoogewerff (2007), Global dust teleconnections: aerosol iron solubility and stable isotope composition, *Environmental Chemistry*, *4*(4), 233‑237.

Watson, A. J., D. C. E. Bakker, A. J. Ridgwell, P. W. Boyd, et C. S. Law (2000), Effect of iron supply on Southern Ocean CO2 uptake and implications for glacial atmospheric CO2, *Nature*, *407*(6805), 730‑733, doi:10.1038/35037561.

Welch, S. A., B. L. Beard, C. M. Johnson, et P. S. Braterman (2003), Kinetic and equilibrium Fe isotope fractionation between aqueous Fe(II) and Fe(III), *Geochimica et Cosmochimica Acta*, *67*(22), 4231‑4250, doi:10.1016/S0016-7037(03)00266-7.

Wells, M. L., G. K. Vallis, et E. A. Silver (1999), Tectonic processes in Papua New Guinea and past productivity in the eastern equatorial Pacific Ocean, *Nature*, *398*, 601‑604.

Wu, J. F., E. A. Boyle, W. Sunda, et L. S. Wen (2001), Soluble and colloidal iron in the oligotrophic North Atlantic and North Pacific, *Science*, *293*, 847‑849.

Wu, L., B. L. Beard, E. E. Roden, et C. M. Johnson (2011), Stable Iron Isotope Fractionation Between Aqueous Fe(II) and Hydrous Ferric Oxide, *Environ. Sci. Technol.*, *45*(5), 1847 ‑ 1852, doi:10.1021/es103171x.

Yeghicheyan, D. et al. (2013), A compilation of silicon, rare earth element and twenty one other trace element concentrations in the natural river water standard SLRS-5 (NRC-CNRC), *Geostandards and Geoanalytical Research*, *in press*.

Yu, E.-F., R. Francois, et M. Bacon (1996), Similar rates of modern and last-glacial ocean thermohaline circulation inferred from radiochemical data, *Nature*, *379*, 679‑680.

Zhang, Y., F. Lacan, et C. Jeandel (2008), Dissolved rare earth elements tracing lithogenic inputs over the Kerguelen Plateau (Southern Ocean), *DEEP-SEA RESEARCH PART II-TOPICAL STUDIES IN OCEANOGRAPHY*, *55*(5-7), 638‑652, doi:10.1016/j.dsr2.2007.12.029.